

5th

BBBB International Conference

From Drug Discovery and Formulation Strategies

(design-synthesis, natural products and preclinical testing, delivery systems, nanotechnology, biopharmaceuticals, biosimilars, BCS, BDDCS, generics-bioequivalence)

To Pharmacokinetics-Pharmacodynamics

(metabolism, transporters, pharmacogenomics, biomarkers, drug therapy, individualized therapy, biotherapeutics, PK/PD modeling)

▶ **26-28 September 2013**
Athens-Greece

▶ Metropolitan Hotel

Book of abstracts

SPEAKERS ABSTRACTS

**MULTILIGAND/MULTIFUNCTIONAL NANOLIPOSOMES FOR BRAIN TARGETING:
POTENTIAL FOR TARGETING ALZHEIMER DISEASE RELATED PATHOLOGIES**

S. G. Antimisiaris^{1,2}, E. Markoutsas¹, K. Papadia¹, A. Giannou³, M. Spella³ and G.T. Stathopoulos³

¹Department of Pharmacy, University of Patras, Rio 26510, Greece

²FORTH /ICES, Rio 26504 Patras, Greece

³Laboratory for Molecular Respiratory Carcinogenesis, Faculty of Medicine, University of Patras, Rio 26510, Greece

For brain targeting, anti-transferrin receptor MAb (TfRMAB)-decorated liposomes (LIP) were formulated [1] and evaluated for BBB targeting in vitro (hCMEC/D3 cells/monolayers), in vivo (live-animal imaging), and ex-vivo (explanted organs). In vitro, in vivo and ex vivo results prove that immunoliposomes target the brain at substantially higher amounts compared to control liposomes; however, in vitro and in vivo results are contradictory, especially for dually targeted LIP on which a peptide to target the BBB LDLr [2] was additionally immobilized. Interestingly, when in vivo studies were modified and performed in presence of increasing amount of serum proteins their results were correlated with the in vivo ones [3].

For A β targeting, anti-A β MAb (A β MAB)-decorated LIP, and dually-decorated ones (ddLIP) with TfRMAB and A β MAB were constructed [4]. A β MAB-LIP uptake was higher than control PEGylated liposomes, and increased significantly when cells were pre-incubated with A β 1-42 peptides; while transcytosis of A β MAB-LIP through monolayers was also increased (by 2.5 times) after pre-incubated with A β 1-42 peptides. After blocking RAGE (receptor for advanced glycation end-products, known to regulate transcytosis of A β peptides across the BBB [5]), it was proved that the A β peptide-induced increase in binding of A β MAB-decorated LIP-types is regulated by RAGE receptor for A β 1-42 peptides. This finding may have serious implications for nanosystems constructed to target A β species in the brain or in the blood.

Acknowledgement: LDLr peptide was from Mario Negri Institute, Italy; A β MAB was developed by STAB VIDA, Portugal. Funding from EU-FP7/ grant n° 212043 (to SGA) and 260524 (to GTS).

References:

- [1]. E. Markoutsas, G. Pampalakis, A. Niarakis, et al. EJPB 77 (2011) 265-274.
- [2]. F. Re, I. Cambianica, C. Zona, et al. Nanomedicine: Nanotechnology, Biology, and Medicine 7 (2011) 551-559.
- [3]. A. Salvati, A.S. Pitek, M.P. Monopoli, et al. Nature Nanotechnology 8 (2013) 137-143.
- [4]. E. Markoutsas, K. Papadia, C. Clemente, et al. EJPB 81 (2012) 49-56.

PHARMACOGENOMICS AND PERSONALIZED MEDICINE

Gyorgy Bagdy 1,2 and Gabriella Juhasz 1,2,3

1 Department of Pharmacodynamics, Semmelweis University, Budapest, Hungary

2 MTA-SE, Neuropsychopharmacology and Neurochemistry Research Group, Budapest, Hungary

3 Neuroscience and Psychiatry Unit, The University of Manchester, Manchester, UK

Prescription of personalized medication is based on a wide variety of personal, environmental and genetic variables. Among those, genomics has gained major impetus from recent technological advances, which raised high expectations for the near future. In addition, it became clear that the blockbuster era had come to the end raising the hope for the application of biomarkers including pharmacogenomics for selection of patients and treatments. Currently, pharmacogenomic (PG) tests are either available or suggested by the FDA for the prediction of therapeutic or adverse effects of more than 100 drugs marketed in the USA. The majority of these drugs belong to two therapeutic categories representing about 30-30% of all pharmacogenomic tests each. The first group is anticancer drugs, e.g., kinase inhibitors, the application of which increasingly depends on these tests. The second main category comprises certain drugs used in psychiatry. In this talk, principles and examples regarding personalized drug selection and personalized dosing will be highlighted. In addition to general factors, such as age or racial group, personalized drug selection depends also on genetic alterations. These include the widely known variations of drug-metabolizing enzymes leading to pharmacokinetic diversity on one hand, and polymorphisms associated with pharmacodynamics on the other. It is generally known that pharmacogenomics is used to predict ADME processes, e.g. CYP2D6 poor metabolizers may need half the usual dosage of certain tricyclic antidepressants. New discoveries shed light also on the role of pharmacodynamic processes, e.g., variable expression of the drug target molecules and molecules involved in pathomechanisms, such as. HER2 positivity in the indication of trastuzumab treatment, or EML4-ALK fusion gene mutation for crizotinib. In addition, HLA-B*1502 genotyping is necessary in carbamazepine treatment, since it may reveal a serious adverse reaction to this drug. Although medications used for the treatment of several somatic illnesses, including anticancer, antimicrobial, immunomodulatory, neurological and hormonal therapies, may have serious negative effect on mood, this fact didn't receive adequate attention until the withdrawal of rimonabant. Rimonabant is an effective CB1 receptor antagonist antiobesity agent that was withdrawn from the market in 2008 due to its psychiatric side effects including anxiety, depression, insomnia and suicide attempts. The discovery of the functional gene x gene interaction of the serotonin transporter and the CB1 receptor provided a new possibility for personalized therapy and a tool for the prediction of these psychiatric side effects (Lazary et al., 2011). Despite the high expectations, we have to keep in mind, that the use of pharmacogenomics will moderately proceed also in the future, regarding that, first, the effect of a single polymorphism on the phenotype is limited in most cases, and thus, a large array of SNP-s have to be genotyped, second, other personal or environmental factors (e.g. age, exposure to UV light, viral infection, country living, smoking) confound the effects of the genes, called gene x environment interactions, third, different polymorphisms in different genes may result in similar phenotypic alterations, symptoms or variations in drug effects (Bagdy and Juhasz 2013). Therefore, especially for complex disorders and their treatments, a large array of personal data, environmental factors, biomarkers, intermediate- and endophenotypes will be used in addition to pharmacogenomics in the future.

1. Lazary J, Juhasz G, Hunyady L and Bagdy G: Personalized medicine can pave the way for the safe use of CB1 receptor antagonists. *Trends Pharmacol Sci*, 2011, 32: 270-80.

2. Bagdy, G and Juhasz, G: Biomarkers for personalized treatment in psychiatric disease. *Expert Opinion in Medical Diagnostics*, 2013

(doi:10.1517/17530059.2013.821979)

in press.

INVESTIGATION OF POLYMER MOLECULAR STRUCTURE ENABLES UNDERSTANDING OF DOSAGE FORM DRUG DELIVERY

S. Baumgartner¹, U. Mikac², A. Sepe², P. Kocbek¹, M. Bešter-Rogač³, R. Rošic¹, J. Pelipenko¹, J. Kristl¹

1. University of Ljubljana, Faculty of Pharmacy, Ljubljana Slovenia

2. Jožef Stefan Institute, Ljubljana, Slovenia

3. University of Ljubljana, Faculty of Chemistry and Chemical Technology, Ljubljana Slovenia

To elucidate how the structure of polymers (namely xanthan (XAN) and poly(vinyl alcohol) (PVA)) on molecular level influences the drug release from different dosage forms.

XAN ($M_w = 2 \times 10^6$) and pentoxifylline (PF) were mixed in ratio 1:1 and compressed into tablets (700 mg, 100 N). The drug release from tablets was performed using USP II apparatus in water and HCl medium. The gel layer thickness during tablet swelling was measured by combination of different MRI techniques¹.

On the other hand, sodium naproxenate (SN) PVA solutions were prepared by adding various amounts of SN to 8% aqueous PVA (Mowiol® 20-98, $M_w = 125,000$) solution. The obtained samples were investigated by different physico-chemical methods² to reveal the polymer structure in the solution. Further, the solutions were electrospun (applied voltage 15 kV, needle-to-collector distance 15 cm, flow rate 0.707 ml/h) and PVA-SN nanofibers were characterized (SEM, drug release).

In the case of complex anionic polyelectrolyte like XAN; the polymer structure in aqueous environment is dependent mostly on medium characteristics, whereas in the case of simple nonionic PVA the structure or polymer organization is influenced mostly by polymer and drug concentration. XAN adopts single chain conformation in water, whereas at pH 1.2 rigid double stranded structures are formed³ resulting in formation of thinner gel layer in the HCl medium. MRI analysis showed that incorporated PF does not influence the hydrogel thickness formed in water, whereas in low pH medium the presence of the drug in the XAN tablet results in thinner hydrogel formation due to different positions of erosion and penetration fronts. The drug release studies revealed faster drug release from tablets in pH 1.2 medium compared to water, even though the XAN molecular structure was more rigid. The diffusion barrier was thinner and, therefore, the release faster compared to water medium.

The organization of PVA within the colloid solution has a great impact on nanofiber formation. The smooth nanofibers can be produced only, when PVA molecules form properly firm internal structures in solution, which can be oriented in the direction of applied electric field, enabling complete polymer elongation during electrospinning. The addition of SN influences some PVA solution characteristics (density, conductivity, kinematic viscosity) in concentration dependent manner, meaning bigger changes with higher drug concentration. However, SAXS analysis did not show any differences. The PVA-SN nanofibers were produced using the same process parameters as plain PVA nanofibers, therefore, it can be concluded that SN in concentration up to 10% does not change significantly the PVA structure in solution and does not influence the nanofiber formation. The drug release from nanofibers was almost immediate regardless to the ratio between PVA and SN in nanofibers.

The influence of polymer structure on drug release from tablets was proved for XAN, whereas in the case of PVA nanofibers the relation is not so straight forward.

Literature Reference

1. U. Mikac, A. Sepe, J. Kristl, and S. Baumgartner, *J. Control Release*, 145 (2010) 247.
2. R. Rošic, J. Pelipenko, J. Kristl, P. Kocbek, M. Bešter-Rogač, S. Baumgartner, *Eur Polym J*, 49 (2013) 290.
3. B. Govedarica, T. Sovány, K. Pintye-Hódi, M. Škarabot, et al., *Eur J Pharm Biopharm*, 80 (2012)

CONTRIBUTION OF MODERN PHARMACOLOGY TO PRACTICAL MANAGEMENT OF RESISTANT EPILEPSY

Professor Meir Bialer, Institute of Drug Research, School of Pharmacy, Faculty of Medicine, The Hebrew University of Jerusalem 91120, Jerusalem, Israel

Modern pharmacology has led to the design and development fifteen new antiepileptic drugs (AEDs) approved in the last two decades by regulatory bodies in Europe and the US (most AEDs). These AEDs offer appreciable advantages in terms of their favorable pharmacokinetics (PK), improved tolerability and lower potential for drug interactions. In addition, the availability of old and new AEDs with various activity spectra and different tolerability profiles enables clinicians to better tailor drug choice to the characteristics of individual patients. However, in spite of the large therapeutic arsenal of old and new AEDs about 30% of patients with epilepsy are still not seizure-free and thus, there is a substantial unmet need to develop new AEDs.

These fifteen new AEDs as well as the AEDs currently in development were discovered by three strategies: a) empirical animal-based screening of newly designed compounds with diverse chemical structures that might have CNS potential. b) follow-up or second-generation compounds of existing AEDs that circumvent problems associated with the mother compound. c) mechanism-based or target-based or hypothesis-driven drug design. The new AEDs can be divided into two categories: a) Compounds with completely new chemical structures developed mainly through the empirical approach such as retigabine (Trobalt®, approved in 2011 but its use has been restricted since 5/2013) and perampnel (Fycompa®, approved in 2012); b) Follow-up compounds of existing AEDs such as: eslicarbazepine acetate (ESL or Zebinex®, an oxcarbazepine derivative), valnoctamide [valproic acid (VPA) derivative], or brivaracetam (a levetiracetam derivative). ESL is a prodrug to (S)-licarbazepine the monohydroxy derivative and the active entity of oxcarbazepine. The development of brivaracetam stemmed from the recognition of the unique pharmacological profile of levetiracetam which correlates with a novel mechanism of action (MOA). Valnoctamide and its one-carbon homologue SPD have the potential to be non-teratogenic, more potent VPA derivatives with unique activity against status epilepticus (SE) and organophosphate neuronal damage.

From a pharmacodynamic (PD) perspective new AEDs should be: a) better than existing AEDs in efficacy, safety, broad utilization and/or disease modification; b) active in refractory animal models where existing AEDs are inactive (e.g. benzodiazepine resistant-SE); c) active in animal models of other non-epileptic CNS disorders since epilepsy alone is not commercially attractive in 2013. From a PK perspective new AEDs should have: a) complete oral absorption (>80%); b) linear and not-highly variable PK; c) minimal drug interaction potential; d) minimal transporters' involvement in their oral absorption and brain penetration; e) a wide therapeutic range; and f) no or minimal need for dose titration.

A new MOA is an incentive if it is the drug's only (or major) MOA and does not cause MOA-related adverse reactions (AE) not shared by AEDs with multiple MOAs. Target-based drug design or Targephilia's mantra of: "one gene, one protein, one function" is useful in developing HMG CoA reductase inhibitors (statins), HIV protease inhibitors or antibiotics but is not useful in the development of antiepileptics or CNS drugs. This is because all successful AEDs have multiple MOAs and the two single-mechanism AEDs developed by target-based design are not widely used due to AE related to their single MOA. In addition, CNS drugs with multiple MOAs have a better probability of being efficacious in refractory epilepsies and other CNS disorders. PK-based design can increase potency and minimize toxicity (e.g. teratogenicity) of existing AEDs. Small chemical changes "do big" (e.g. brivaracetam, eslicarbazepine acetate, valnoctamide). However PK is secondary to PD namely, efficacy and safety as can be learned from retigabine's recent AE that were unpredictable.

References

1. M. Bialer, S.J. Johannessen, R.H. Levy, E. Perucca, T. Tomson, H.S. White. Progress report on new antiepileptic drugs: A summary of the Eleventh Eilat Conference (EILAT XI). *Epilepsy Res.*103:2-30 (2013).
2. M. Bialer, H.S. White. Key factors in the discovery and development of new antiepileptic drugs (AEDs). *Nature Rev Drug Discov.*9:68-83 (2010).
3. M. Bialer. Chemical properties of antiepileptic drugs (AEDs). *Adv. Drug Deliv. Rev.* 64:887-895 (2012).
- 4.M. Bialer. Why antiepileptic drugs (AEDs) are used for non-epileptic conditions? *Epilepsia*, 53 (Suppl. 7): 26-33 (2012).
- 5.. Enna SJ, Williams M. Challenges is the search for drugs to treat central be nervous system. *J. Pharmacol. Exp. Ther* 329:404-411 (2009).
6. W. Loscher, H. Klitgaard, R. E. Twyman, D. Schmidt. New avenues for antiepileptic drug discovery and development. *Nature Rev. Drug Discov.*, in press (2013)
- 7.T. Shekh-Ahmad, N. Hen, J. H. McDonough, B. Yagen, M. Bialer. Valnoctamide and sec-butyl-propylacetamide (SPD) for acute seizures and status epilepticus. *Epilepsia.*, 54 (Suppl. 5):98-101 (2013).

NEW ANTIPLATELET AGENTS TARGETING THE PLATELET INTEGRIN α IIB β 3 AND PAR-4 RECEPTORS

Vasileios G. Chantzichristos, Iraklis C. Moschonas, Alexandros D. Tselepis
 Laboratory of Biochemistry Department of Chemistry, Atherothrombosis Research Centre, University of Ioannina, 45510 Ioannina, Greece

The platelet integrin-receptor α IIB β 3 (Glycoprotein IIb/IIIa; GPIIb/IIIa) is composed of two noncovalently associated subunits the α IIB and β 3, each of which exhibit an extracellular and an intracellular domain. On unstimulated platelets α IIB β 3 is present in a closed conformation that prevents ligand binding. Upon platelet activation, α IIB β 3 undergoes conformational changes leading to the exposure of various binding sites primarily for fibrinogen (1,2). Fibrinogen binding to the activated α IIB β 3 results in cross-linking of adjacent platelets and to platelet aggregation. Furthermore, it activates a series of intracellular events through an outside-in signaling mechanism (1,3). Since α IIB β 3 is involved in the final pathway for platelet aggregation, regardless of the platelet stimulus, α IIB β 3 receptor antagonists provide a wider range of protection against thrombosis compared to the other antiplatelet agents (1,2). All antagonists used up to date in the clinical practice, are effective inhibitors of platelet aggregation. However, the clinical use of these agents has been limited, due to major side effects (1,2). Over the last years our research interest has been focused on the development of novel potent antagonists of α IIB β 3 that do not have the above drawbacks. In this regard, we have synthesized a series of peptide analogues of the intracellular and extracellular domains of both α IIB β 3 subunits. In this regard, we have identified a 20/peptide, modelled from the extracellular domain of the α IIB subunit (313YMESRADRKLAEVGRVYFL332), which potently inhibits platelet aggregation and secretion (4). We have also demonstrated that 8/peptide analogues containing the ESRAD motif maintained the inhibitory properties exhibited by the original 20/peptide. Of interest is our finding that these peptides fail to induce an outside-in signaling through α IIB β 3 (5). Furthermore, the 8/peptide YMESRADR significantly reduces experimentally-induced thrombus formation in rabbits (6). Furthermore, a series of peptide analogues of the intracellular domains of α IIB and β 3 subunits were synthesized and tested for antiplatelet activity. Among them, the peptide analogue of α IIB 997RPPLEED1003 (in its palmitoylated form) and the peptide analogue of β 3 755TNITYRGT762 (containing the Tat-Cys-NH₂ signaling sequence: GRKKRRQRRPPQC-NH₂) exhibited a potent inhibitory effect on platelet aggregation (7). Such peptides may provide a valuable basis for the development of a new generation of potent antiplatelet and antithrombotic drugs useful for the treatment of acute coronary syndromes.

Currently, we perform research work aiming to discover potent antagonists of the platelet protease-activated receptor-4 (PAR-4). Human platelets express two types of

PARs, ie PAR-1 and PAR-4 (8). To date, only PAR-1 antagonists have been developed and 2 of them (atopaxar and vorapaxar) have been studied in large clinical trials. Thus, our aim is to develop specific PAR-4 antagonists in an effort to further shed light on the potential role of this receptor in platelet pathophysiology. Preliminary results on new PAR-4 antagonists will be presented and discussed.

References

- Goudevenos JA, Tselepis AD. *Curr Opin Invest Drugs*. 2001; 2: 244-249.
Kalantzi KI, Tsoumani ME, Goudevenos IA, Tselepis AD. *Expert Rev Clin Pharmacol*. 2012; 5: 319-336.
Shattil SJ. *Thromb Haemost*. 1999; 82: 318-325.
Biris N, et al. *Eur J Biochem*. 2003; 270: 3760-3767.
Mitsios JV, et al. *Eur J Biochem*. 2004; 271: 855-862.
Papamichael ND, et al. *J Pharmacol Exp Ther*. 2009; 329: 634-640.
Dimitriou AA, et al. *Platelets*. 2009; 20: 539-547.
Shah R, et al. *Am Heart J*. 2009; 157: 253-262.

BIO-INSPIRED DRUG DELIVERY NANO SYSTEMS : A FRACTAL ANALYSIS OF THEIR AGGREGATES

Costas Demetzos

Department of Pharmaceutical Technology, Faculty of Pharmacy, University of Athens, University Campus Zografou, 15784 Athens, Greece.

fax: 00302107274027; e-mail: demetzos@pharm.uoa.gr

The aggregation process of nanoparticles and their fractal dimensionality are of paramount importance due to their applications as drug delivery systems[1,2]. The goal of this study is to evaluate the aggregation process of bio-inspired chimeric liposomal carriers (chi-DDnSs) composed of 1DPPC, DPPC:cholesterol (9:1 molar ratio), DPPC:PAMAM 2 (9:1 molar ratio) and DPPC:MPOx i (9:1 molar ratio) by comparing their R_h (hydrodynamic Radius) with their d_f (fractal dimension), which could be correlated to their morphological quantification, in aqueous (HPLC-grade water) and biological medium (Fetal Bovine Serum, FBS). The physicochemical, morphological characteristics and the aggregation kinetics of the chimeric liposomal nanosystems are presented in Table 1. In all cases, the fractal dimensions fell in the range from 2.5 to 1.8, corresponding to two regimes: diffusion-limited aggregation (DLA) and reaction-limited cluster aggregation (RLCA). Focusing on the evolution of the size of the liposomal clusters, DPPC liposomes showed a clear transition from the RLCA to the DLA regime depending on the dispersion medium. On the contrary, DPPC:PAMAM G4 liposomes displayed an unexpected behaviour since the aggregation was limited because the incorporation of PAMAM G4 in DPPC liposomes caused a structural rearrangement of the liposomal bilayers (Table 1). These topological constraints did not observe for the DPPC:MPOx system. This concurs with the concept that hydration forces are responsible for the existence of the secondary minima in the interaction potential (extended DLVO theory). In conclusion, the fractal dimensionality of nanoparticles' aggregates would be the tool to evaluate the functionality of bio-inspired chimeric Drug Delivery nano Systems (aDDnSs).

References: 1. Pippa N, Pispas S, Demetzos C, 2012. *Int. J. Pharm.* 430(1-2):65-73. 2. Demetzos C., *Advances in drug delivery systems (DDSs)*, Greece, 2010.

Acknowledgements: To Dr. Stergios Pispas Senior Researcher, National Hellenic Research Foundation and Natassa Pippa, PhD candidate for their valuable contribution to this work.

INFLUENCE OF CLINICAL PHARMACIST-LED EDUCATION ON THERAPEUTIC DRUG MONITORING SKILLS OF PHYSICIANS

Assoc. Prof. Kutay Demirkan, Pharm.D.

Hacettepe University Faculty of Pharmacy, Department of Clinical Pharmacy, Ankara-TURKEY

Therapeutic drug monitoring (TDM) of certain medications is essential to obtain the desired therapeutic effect and to reduce toxic effects. However TDM is frequently performed without a proper indication and samples are often improperly collected or interpreted by physicians. The aim of this study is to determine the role of a clinical pharmacist on TDM, such as education of the physicians, drug toxicity, and the reduction of unnecessary or improperly sampled drug levels in the intensive care unit setting (ICU).

Data collection was conducted for 3 months before and 3 months after the clinical pharmacist initiated therapeutic drug monitoring education to physicians at Hacettepe University Hospital, Adult ICU, Ankara-Turkey. Data was collected on serum levels of amikacin, vancomycin, phenytoin, digoxin, and theophylline. The data was evaluated separately if the intervention performed by the clinical pharmacist for potential/documented toxicity or lack of efficacy.

Results: Total of 110 and 90 drug serum levels were analyzed during the pre- and post-education periods, respectively. Overall, the number of drug levels sampled improperly and obtained without any indications were significantly decreased after education (35,5% and 16,7% respectively, $p < 0,0001$). Also, the number of pharmacist intervention decreased significantly at post-educational period (32,7% and 4,4% respectively, $p < 0,0001$). However, drug levels inappropriately interpreted by physicians were similar (14,6% and 15,6% respectively, $p=0,85$).

This study demonstrated that clinical pharmacist initiated physicians' education on TDM has a significant impact on reducing the number of unnecessary drawn drug levels in ICU setting. Also, accurate and meaningful drug concentrations can only be obtained by collaboration between pharmacists and clinicians. In addition, clinical pharmacist should involve in TDM to minimize drug adverse effects and toxicities.

CROSS-LINKING OF GELATIN CAPSULES AND ITS RELEVANCE TO THEIR IN VITRO AND IN VIVO PERFORMANCE

George A. Digenis, Ph.D.

Mechanistic rationalizations in connection with the occurrence of gelatin cross-linking under "stress" as well as storage conditions will be provided. These will include high humidity and temperature conditions. In addition, possible chemical interactions between the interior surface of gelatin capsules and the formulation constituents they encapsulate will be discussed. The effects of the chemical cross-linking of gelatin capsules to their in vitro and in vivo dissolution will be discussed. It is suggested that in vitro dissolution tests of gelatin capsule dosage forms be conducted in two stages, one in a dissolution medium without enzymes and secondly in dissolution media containing enzymes (pepsin at pH 1.2 or pancreatin at pH 7.2).

Examples of reduced bioavailability of drugs due to cross-linking of gelatin capsules will be presented.

THE CHANGING FACE OF THE RATE CONCEPT IN BIOPHARMACEUTICAL SCIENCES: FROM CLASSICAL TO FRACTAL AND FINALLY TO FRACTIONAL

A. Dokoumetzidis

School of Pharmacy, University of Athens, Athens, Greece

Diffusion is one of the main mechanisms of various processes in living organisms and plays an important role in the course of drugs in the body. Processes such as membrane permeation, dissolution of solids and dispersion in cellular matrices are governed by diffusion. Diffusion is classically described by Fick's law, which gives rise to exponential drug concentration vs time curves. However in the last few decades, strong experimental evidence has suggested that diffusional processes may deviate from this law. Specifically in pharmacokinetics, power-law concentration time series have been observed. While the classic representations of rate are applicable under homogeneous conditions where classic diffusion dominates, in heterogeneous confined topologies, fractal concepts need to be introduced to account for anomalous diffusion and memory effects. These effectively introduce time-varying properties for the system. A more elaborate and appealing way to represent these non-classic rates is by fractional calculus, where the phenomena of anomalous diffusion are described naturally, as fractional generalizations of classic laws, without introducing explicit time dependence. In this presentation the changing face of the rate concept in Biopharmaceutical Sciences will be discussed with emphasis on the latest developments in methodology and applications of fractional calculus in pharmacokinetics.

NOVEL THERAPEUTIC APPROACHES IN OSTEOPOROSIS THROUGH RANKL INHIBITION

Eleni Douni^{1,2}

¹Laboratory of Genetics, Department of Biotechnology, Agricultural University of Athens, Greece, douni@aua.gr

²Biomedical Sciences Research Center "Alexander Fleming", Vari, Greece

Receptor activator of nuclear factor- κ B ligand (RANKL) is a central regulator of bone remodeling by mediating osteoclast-induced bone resorption. Overproduction of RANKL is implicated in a variety of degenerative bone diseases such as osteoporosis and its specific inhibition effectively reduces the incidence of fractures in postmenopausal women. We have recently generated transgenic mice (TghuRANKL) carrying the human RANKL (huRANKL) genomic region and achieved a physiological relevant pattern of RANKL overexpression in order to establish novel genetic models of RANKL-mediated pathologies. TghuRANKL mice of both sexes developed early-onset bone loss, and the levels of huRANKL expression were correlated with bone resorption and disease severity. Low copy Tg5516 mice expressing huRANKL at low levels displayed a mild osteoporotic phenotype as shown by trabecular bone loss and reduced biomechanical properties. Notably, overexpression of huRANKL, in the medium copy Tg5519 line, resulted in severe early-onset osteoporosis characterized by lack of trabecular bone, destruction of the growth plate, increased osteoclastogenesis, bone marrow adiposity, increased bone remodeling and severe cortical bone porosity accompanied by decreased bone strength. Model validation was further established by evidence that known RANKL inhibitors, fully corrected the hyper-resorptive and osteoporotic phenotypes of Tg5519 mice.

Our recent efforts have been focused on the identification and evaluation of novel small molecule inhibitors of huRANKL, designed to dissociate RANKL trimers. Lately, we identified that SPD304, a promising but toxic TNF antagonist that promotes the dissociation of TNF trimers, inhibits also human RANKL activity. Of the 72 SPD304-like derivatives synthesized and tested, we identified 13 as potent inhibitors of human RANKL function with less cytotoxicity compared to SPD304. Our novel TghuRANKL models of osteoporosis represent a unique tool for the preclinical evaluation of such novel RANKL inhibitors and for understanding the molecular mechanisms underlying RANKL-induced pathologies such as osteoporosis.

CAN ALL DRUGS BE CLASSIFIED BY BCS OR BDDCS?

Zeev Elkoshi

The binary nature of the biopharmaceutical classification system is problematic. The amount of drug dissolved or absorbed is a continuous function of kt (k is a first order dissolution or absorption constant and t is the time), and cannot be divided into two clearly separated phases. Therefore, the division of all drugs into "high" or "low" solubility or permeability drugs is questionable. Upper and lower limits for solubility or permeability should be set, as proposed by Rinaki et al. (Pharm. Res. 2003; 20(12):1917-25). Only drugs presenting solubility or permeability values above the upper limit can be classified as high solubility or high permeability drugs. Similarly, only drugs presenting solubility or permeability values below the lower limit can be classified as a low solubility or a low permeability drugs. Drugs in the middle zone (between limits) cannot be classified since this group is not homogenous in either solubility, permeability or both. For this reason it is inappropriate to predict the disposition of drugs in the middle zone by their BCS/BDDCS classification. This rule was ignored by authors since it was originally set eleven years ago, leading to a lower predictability power of food effect or bioequivalence studies success rate by BCS and BDDCS. Class 1 is an exception as it does not contain "middle zone" drugs. Hence, predicting the disposition or granting biowaivers for members of Class 1, as a group, is possible.

CONTROLLED RELEASE OF 5-FLUOROURACIL FROM MICROPORES ZEOLITES

Dimitrios Fatouros

Zeolite particles with different pore diameter and particle size were loaded with the model anticancer drug 5-fluorouracil. The loaded zeolites were characterized by means of SEM, XRD, DSC, XPS, N₂ physisorption and FT-IR. Higher loading of 5-FU was observed for NaX-FAU than BEA. Release studies were carried out in simulated gastric fluid. Release of 5-FU from NaX-FAU showed exponential-type behaviour with the drug fully released within 10 min. In the case of BEA, the kinetics of 5-FU shows a multi-step profile with prolonged release over time. Molecular dynamics simulations showed that diffusion of the drug molecule through the BEA framework is lower than for NaX-FAU due to increased van der Waals interaction between the drug and the framework. The effect of zeolitic particles on the viability of Caco-2 monolayers

FLAVONOIDS SUPPRESS TUMOUR ANGIOGENESIS BY INHIBITING VEGF SIGNALLING

Bellou, S¹, Bagli, E¹, Karali, E¹, Murphy, C¹ and Fotsis^{1,2}

¹ *Foundation for Research and Technology-Hellas, Institute of Molecular Biology & Biotechnology – Division of Biomedical Research, University Campus, 45110 Ioannina, Greece*

² *Laboratory of Biological Chemistry, Medical School, University of Ioannina, 45110 Ioannina, Greece*

Flavonoids are phenolic compounds that are ingested via a plant-rich diet exerting an abundance of positive biological health effects on humans. One of the targets of flavonoids is inhibition of tumour angiogenesis, a process that is critical for the local and metastatic expansion of tumours. Recently, we have screened a set of hitherto untested isoflavonoid metabolites concerning their anti-angiogenic effect. A novel metabolite, 6-methoxyequol (6-ME), inhibited VEGF-induced proliferation of human umbilical vein endothelial cells (HUVEC) and VEGF-induced phosphorylation of ERK1/2 MAPK, the key cascade responsible for VEGF-induced proliferation of endothelial cells. Moreover, 6-ME inhibited in a dose dependent manner the phosphorylation of MEK1/2, the only known upstream activator of ERK1/2. 6-ME did not alter VEGF-induced phosphorylation of p38

MAPK or AKT, compatible with the lack of effect on VEGF-induced migration and survival of endothelial cells. Peri-tumour injection of 6-ME in A-431 xenograft tumors resulted in reduced tumour growth with suppressed neovascularization compared to vehicle controls (Bellou et al. *Mol. Cancer* 2012; 11: 35 (11 p.)). The inhibitory mechanism of 6-ME on VEGF signalling was different than that of the isomeric flavonoids. We have shown that luteolin did not affect VEGF-induced phosphorylation of ERK1/2 MAPKs. Surprisingly, inhibition of PI3K activity was responsible for both the antimitotic and apoptotic effects of the compound. Survival was affected via inhibition of the PI3K/Akt pathway, whereas proliferation was affected via the PI3K/p70 S6K pathway. Importantly, luteolin was active in vivo inhibiting tumor growth and angiogenesis in a murine xenograft model and VEGF-induced angiogenesis in the rabbit corneal assay (Bagli et al. *Cancer Res.* 2004; 64: 7936-7946). The differential mechanism of flavonoids and isoflavonoids on VEGF signalling will be discussed and the status of contemporary anti-angiogenic cancer therapy will be outlined.

MODIFICATIONS ON THE CARBOXYLIC FUNCTION OF KYNURENIC ACID

Ferenc Fülöp

Institute of Pharmaceutical Chemistry and Research Group for Stereochemistry, Hungarian Academy of Sciences, University of Szeged, H-6720 Szeged, Eotvos u. 6, Hungary

E-mail: fulop@pharm.u-szeged.hu

Kynurenic acid (4-hydroxyquinoline-2-carboxylic acid, KYNA) is an endogenous product of the tryptophan (TRP) metabolism. In this metabolic pathway, which is responsible for the production of nicotinamide adenine dinucleotide (NAD⁺) and NAD phosphate (NADP⁺), TRP is converted into various compounds, including L-kynurenine, which can be metabolized in two separate ways, one branch furnishing KYNA, and the other 3-hydroxykynurenine and quinolinic acid, the precursors of NAD. Most metabolites of the kynurenine pathway are neuroactive and have essential roles in the regulation of NMDA (N-methyl-D-aspartate) receptor function and free radical production.

Present lecture will focus on the chemistry of KYNA, where a number of transformations were performed earlier. In our work the KYNA amides were designed with regard to the following structural properties: 1) the presence of a water-soluble side-chain; 2) the inclusion of a new cationic centre; and 3) side-chain substitution to facilitate brain penetration. In several cases we have found robust neuroprotective effects.

F. Fülöp, I. Szatmári, E. Vámos, D. Zádori, J. Toldi, L. Vécsei, Syntheses, transformations and pharmaceutical applications of kynurenic acid derivatives *Curr. Med. Chem.*, 16, 4828-4842 (2009)

L. Vécsei, L. Szalárdy, F. Fülöp, J. Toldi, Kynurenines in the CNS: recent advances and new questions *Nature Rev. Drug Disc.* 12, 64-82 (2013)

L. Vécsei, D. Zádori, P. Klivényi, F. Fülöp, I. Szatmári, J. Toldi, T. Freund, G. Nyíri, A. Szőnyi, Use of [kynurenic acid amide derivatives for the treatment of Huntington's disease](#). *PCT Int. Appl.* (2012), WO 2012/001438 A1

showed that the NaX-FAU particles cause a reduction of cell viability in a more pronounced way compared with the BEA particles.

PANCREATIC ISLET CELL TRANSPLANTATION: AN UPDATE

Dimitrios T. Hatzivramidis

School of Chemical Engineering, National Technical University of Athens, Athens 15780, GR

Transplantation of pancreatic islets, as a therapeutic modality for type 1 diabetes mellitus (T1DM), at this stage of its development, is reserved for patients with severe glycemic

variability, progressive diabetic complications, and life threatening hypoglycemia unawareness, regardless of intensive insulin management. Up to now, islet transplantation followed by an immunosuppressive drug regimen has not succeeded to become the method of choice for treating T1DM because, in addition to immunosuppression risks, it suffers from limited supply and suboptimal yields of procurement and isolation of islets, graft failure, and relatively high requirements, i.e., at least 10,000 functional Islet Equivalents (IE) per kg of patient weight, to achieve prolonged insulin independence and glucose stability. Encapsulation of islets in selectively permeable membranes of biocompatible polymers, prior to transplantation, removes the burden of an immunosuppressive regimen but adds new requirements on the procedure. Past efforts aimed at making islet transplantation a competitive alternative to exogenous insulin injections for treating T1DM have focused on improving the for longevity and functionality of islet cells. In order for transplantation of encapsulated islets to succeed, these efforts need to be complemented by others to optimize the rate and efficiency of encapsulation.

DEVELOPMENT AND REGULATORY ASPECTS OF NEW PHARMACEUTICAL EXCIPIENTS

Jyrki Heinämäki

Department of Pharmacy, Faculty of Medicine, University of Tartu, Nooruse 1, 50411 Tartu, Estonia

Email: jyrki.heinamaki@ut.ee

Pharmaceutical excipients are chemical substances apart from the active substance and they are designed to be therapeutically inert. Excipients are known as “pharmaceutical necessities” that have various important functions in a medicine. Today, new and specialized areas of drug delivery (e.g. nanoparticles, dendrimers, drug impregnated adhesives and coatings, tissue repair products, etc.) provide opportunity and necessitate the novel use of excipients and/or the development of new excipients.

Novel excipient is defined as an excipient which is used for the first time in a drug product (European Medicines Agency, EMA, 2008). It may be a new chemical entity or a well established one which has not yet been used for human administration and/or particular route (pathway) of administration in the EU and/or outside the EU. Today, novel excipients are reviewed and approved with the drug product marketing authorisation (MA) approval. No Drug Master File (DMF) -type system has been established for excipients. Novel excipients require a thorough characterisation and documentation in the MA dossier with regard to their functionality, physicochemistry and safety like a new active substance (EMA, 2008; Koo and Varia, 2011). General toxicity studies with a novel excipient need to be provided in non-clinical part of the MA dossier.

This lecture will review development of new pharmaceutical excipients and regulatory actions to approve these excipients. Multiple roles of pharmaceutical excipients will be described. The differences of EMA and US Food and Drug Administration (FDA) guidances on quality and safety testing of new excipients will be compared and discussed. Moreover, the regulation perspectives on selection of excipients for pediatric formulations will be shortly given. Three case studies will be presented as examples of development and implementation of new excipients including a new chemical excipient (polyoxyl 15 hydroxystearate), a new graft co-polymer (polyvinyl caprolactam-poly-vinyl acetate-PEG), and a new co-processed excipient (silicified microcrystalline cellulose). Potential toxicological concerns for impurity safety of new excipients will be also discussed with a special reference set impurity safe limits.

Literature references

EMA, 2008. EMEA/CHMP/QWP/396951/2006. Guideline on excipients in the dossier for application for marketing authorisation of a medicinal product, January 2008, 1-12.

Koo, M.Y., Varia, S.A., 2011. Case studies with new excipients: development, implementation and regulatory approval. *Ther. Deliv.* 2 (7), 949-956.

A NEW METHOD FOR THE MEASUREMENT OF THE SPATIAL DISTRIBUTION OF SUPER-PARAMAGNETIC NANOPARTICLES IN THE BODY

E. Hristoforou

National TU of Athens, Zografou Campus, Athens 15780, Greece

An innovative magnetic method promises the measurement of the super-paramagnetic nanoparticle (SPAN) distribution in the body. The method is based on magnetic polarization and superconducting magnetometry, allowing for a few minutes fast body scanning. Alternatively, the method can offer detailed analysis of SPAN distribution with less than 10 μm^3 volume sensitivity. An advantage of the method is that the determined tumor cells can be exploded due to high current inductive heating: the increase of temperature in healthy cells is kept in a minimum ($\Delta T < 2\text{K}$), while explosion of cancer cells is due to their large and fast temperature increase ($\Delta T > 50\text{K}$).

KINETICS IN DRUG DISCOVERY. A CASE FOR G PROTEIN-COUPLED RECEPTORS.

Ad P. IJzerman*, Dong Guo, Laura H. Heitman.

Leiden Academic Centre for Drug Research, Division of Medicinal Chemistry, Leiden University, PO Box 9502, 2300RA Leiden, The Netherlands, ijzerman@lacdr.leidenuniv.nl

In early drug discovery one strives to optimize the properties of drug candidates for a given therapeutic target, usually focusing on standard pharmacological parameters of affinity, potency and intrinsic activity. There is mounting evidence, however, that the often ignored kinetic aspects of the interaction between a drug and its target in the body are highly relevant for in vivo efficacy and clinical success. This ignorance may be one of the reasons for the high attrition rates in drug discovery, as it has been analyzed that quite a few recently marketed drugs had indeed improved kinetic profiles.

G protein-coupled receptors (GPCRs) are attractive drug targets, and a few examples of FDA- or EMA-approved drugs acting on GPCRs indicate that their beneficial effects in patients may result from prolonged receptor occupancy, i.e. a long residence time. Such retrospective observations, however, provide neither a theoretical nor a technological framework for the 'titration' of this novel design criterion into new chemical entities. To make this happen it seems imperative to understand the molecular mechanisms of kinetic action better, to come up with suitable 'off-the-shelf' assays, and to make the translational effort from early in vitro screening to in vivo profiling of new lead candidates.

In this presentation we will provide an overview of our own recent efforts in this respect, while addressing the GPCR protein superfamily. We will first briefly introduce some concepts of receptor kinetics, then move towards the development of higher-throughput assays, and finally study the possible link between residence time and other pharmacological parameters such as affinity and intrinsic efficacy. Ultimately our efforts may lead to a better understanding of structure - kinetics relationships (SKR) to be used in the design of kinetically appealing molecules.

DRUG-FOOD, ALCOHOL AND SMOKING INTERACTIONS AND THEIR CLINICAL RELEVANCE

I. Klebovich

Semmelweis University, Department of Pharmaceutics, H-1092 Budapest, Hógyes E. St. 7., Hungary

Within the wide area of drug interactions, drug-food, alcohol and smoking interactions, as a new, dynamic discipline of pharmacokinetics and pharmacodynamics, are of special impact both in the original and the generic/supergeneric drug development which is confirmed by several new regulatory requirements.

The high sensitivity and selectivity of different LC-MS and LC-MS/MS, Headspace-GC, GC-MS, furthermore HPTLC/OPLC-ESI-MS applications are of high importance in the pharmaceutical food-drug and food-alcohol and smoking interaction research. Bioanalytical methods play an important role in the original and generic/supergeneric drug development in the interaction studies. The primary aim of the present lecture is to give a comprehensive view about the tracking possibilities of drug-food, -alcohol and -smoking interactions with the possible novel bioanalytical techniques.

The presentation summarizes additionally the obligatory interaction tests in the course of the drug research and the possible changes of drugs in the body due to the drug-food, -alcohol and -smoking interactions.

The most important drug-alcohol and drug-smoking interactions of different therapeutic areas having clinical significance will be presented with several shocking and not widely known examples in the second part of the lecture.

The different effects of acute and chronic alcohol consumption on various drug interactions and the effect of smoking, raising civilization problems, on the bioavailability and pharmacokinetic parameters of drugs will be presented, as well.

The study of the various interaction types offers new directions in the modern drug research as well as promising perspectives in the every day therapy.

Literature:

1. Imre Klebovich: Food, Alcohol and Smoking Interactions, In: Imre Klebovich, Vinod P. Shah (Eds.): Moving Forward – Advancing Regulatory Sciences Towards International Standards for Bioequivalence, Hungarian Society for Separation Sciences, Pécs, OOK-Press Ltd., Veszprém, Hungary, p. 143 – 152 (2012), ISBN 978-963-89335-1-5I.
2. Karen Baxter (Ed.): Stockley's Drug Interactions 2011, Pharmaceutical Press, London, UK, (2011).

STABILITY AND DISSOLUTION BEHAVIOR OF AMORPHOUS SOLID DISPERSIONS

K. Kogermann 1,*¹, A. Lust 1, U. Paaver 1, A. Penkina 1, J. Kozlova 1, J. Rantanen 2, K. Kirsimäe 1, P. Veski 1, J. Heinämäki 1, K. Naelapää 2,3
*1University of Tartu, Tartu, Estonia; *kkogermann@gmail.com; targeted financing project no SF0180042s09, ETF grant project no ETF7980; 2University of Copenhagen, Copenhagen, Denmark; 3Current institution: Novo Nordisk A/S, Maaloev, Denmark*

The purpose of the study was to investigate the stability and dissolution behavior of amorphous solid dispersions (ASDs) prepared by three different methods, namely solvent evaporation, electrospinning, and co-milling either at low (LT) or room (RT) temperature. The model API, piroxicam form I (PRXAH), was obtained from Lianyangang Ruidong Int. Co., Ltd (China) and/or Letco Medical, Inc. (USA). PRX monohydrate (PRXMH) was prepared by recrystallization from hot aqueous solution. Polyvinylpyrrolidone (PVP) in two different grades, PVP 25 and PVP 90 (BASF SE, Germany) were used as received. Polyvinyl caprolactam - polyvinyl acetate - polyethylene glycol graft copolymer, PVCL-PVAc-PEG, Soluplus® (BASF SE, Germany) was pre-milled for 1 h. PRXAH and PVCL-PVAc-PEG were dissolved in acetone for the preparation of ASDs by solvent evaporation. For electrospinning, PRXAH was dissolved in a 0.8-% solution of hydroxypropyl methylcellulose, HPMC (Methocel K100M premium CR grade) and 1,1,1,3,3,3-hexafluoro-2-propanol. All solid state forms were characterized using XRPD, Raman spectroscopy and the morphology of the samples was investigated by SEM. In-line Raman spectroscopy and polarized light microscopy (PLM) were used to monitor the recrystallization of amorphous piroxicam (aPRX) from ASDs in a simulated gastric fluid without pepsin (SGF, pH 1.2) during modified dissolution testing. Conventional dissolution testing (basket method) was performed with hard gelatine capsules (USP 33 NF 28, n=3) in SGF. All three investigated ASD preparation methods enabled to produce aPRX. The stability of aPRX in ASDs was significantly improved by the polymers. Depending on the method of preparation and the polymer used, together

with its polymer/API ratio, the stability upon storage at RT (0% RH) varied. Raman spectroscopy and PLM revealed the conversion of aPRX to PRXMH after few minutes of modified dissolution testing with all ASDs. Different polymers showed different stabilizing properties most likely due to the formation of physically different diffusion layers around the ASD particles. These results were also reflected in the varying dissolution performance of ASDs (Fig. 1). All co-milled and solvent evaporated ASDs showed higher total amount of PRX dissolved compared to the crystalline PRX forms. Interestingly, the dissolution profile of the electrospun ASD showed zero order kinetics most likely due to the HPMC that was used in the electrospun ASDs and/or capsule/polymer interactions.

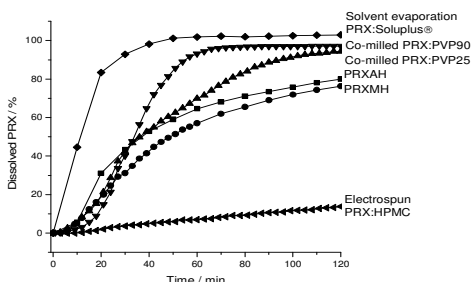


Fig. 1. Dissolution behavior of PRX from ASDs during conventional dissolution testing in SGF ($n = 3$) compared to crystalline PRXAH and PRXMH: co-milled ASDs with PVP25 1:2, co-milled ASDs with PVP90 1:2, electrospun ASD with HPMC 1:1 and ASD prepared by solvent evaporation method with PVCL-PVAc-PEG (Soluplus®) 1:4. The standard deviation is not shown due to clarity purposes.

EXPLORING FLEXIBILITY AND MOLECULAR RECOGNITION IN THE HUMAN CYTOCHROME P450S

Christina Hayes, Daniel Ansbro, Brittany Schuchman, Phil Kilver, and Maria Kontoyianni
Department of Pharmaceutical Sciences, Southern Illinois University Edwardsville, Edwardsville, Illinois 62026, United States

The human cytochrome P450 enzymes (CYPs) are heme-protein mono-oxygenases, which catalyze oxidative and reductive reactions of a broad spectrum of substrates. Consequently, they play a critical role in the metabolism of xenobiotics, such as drugs and carcinogens. These enzymes can also have their activity altered when exposed to various inducers or inhibitors. Bioavailability and toxicity, both of which can be related to CYPs, continue to pose problems in the development of new drugs. The isoform that metabolizes over one third of drugs, CYP 3A4, was investigated employing ensemble-docking experiments of 200-substrate and 54-inhibitor libraries with Glide and GOLD docking algorithms and a number of scoring functions. Enzyme conformations included three currently available crystal 3A4 structures. All docking experiments were performed in duplicates with and without inclusion of crystallographic waters. Resultant substrate poses were assessed based on accuracy of site of metabolism prediction, while inhibitors were evaluated in terms of feasibility of the drug-3A4 generated complexes. Analyses of the docked solutions pertaining to ranking efficacy, ligand molecular properties, stabilizing interactions, metabolic reactions, and energetics will be discussed.

NANOCARRIER-AIDED MUCOSAL DELIVERY OF MACROMOLECULES

C. Kiparissides 1,2, O. Kammona 2

1Department of Chemical Engineering, Aristotle University of Thessaloniki, P.O. Box 472, 54124 Thessaloniki, Greece, cypress@cperi.certh.gr

2Chemical Process & Energy Resources Institute, Center for Research and Technology Hellas, P.O. Box 60361, 57001 Thessaloniki, Greece

Macromolecular drugs (e.g., peptides, proteins, etc.) have the unique ability to tackle challenging diseases but their structure, physicochemical properties, stability, pharmacodynamics, and pharmacokinetics place stringent demands on the way they are delivered to a specific site/tissue in the body. Additionally, they do not easily cross mucosal surfaces and biological membranes. They are susceptible to loss of their native structure, through cleavage of peptide bonds and destruction of amino acid residues (e.g., proteolysis, oxidation, deamidation, and b-elimination) and conformation due to disruption of noncovalent interactions (e.g., aggregation, precipitation, and adsorption). Moreover, they are prone to rapid clearance in the liver and other non-specific tissues and require precise dosing. At present, protein drugs and antigens are usually administered parenterally (i.e., by subcutaneous or intramuscular injections as well as intravenous infusions), but this route is less desirable and also poses problems of oscillating blood drug concentrations. Moreover, their short biological half-lives, usually in the range of few hours, necessitate in some cases multiple injections per week causing considerable discomfort to the patients, especially when long term or chronic treatment is necessary. Carrier-based drug delivery systems (DDS) can diminish the toxicity of macromolecules, improve their bioavailability and make possible their administration via less-invasive routes (e.g., oral, nasal, pulmonary, etc.). Thus, the development of functionalized nanocarriers for the delivery of macromolecular drugs is considered an important scientific challenge and at the same time a business breakthrough for the biopharmaceutical industry. In order to be translated to the clinic, a nanocarrier-based DDS needs to be biocompatible, biodegradable, non toxic and non immunogenic, to cross the designated mucosal barrier, to protect its sensitive payload and deliver it to the specific target site in a controlled manner, thus increasing significantly its bioavailability and efficacy. To date, polymeric nanocarriers (e.g., chitosan (CS) (Fig. 1), poly(lactic acid) (PLA), poly(lactic-co-glycolic acid) (PLGA), poly(ϵ -caprolactone) (PCL), polyacrylic acid (PAA), poly(methacrylic acid) (PMAA), polyalkyl cyanoacrylates (PACA), starch, dextran, alginate, etc), liposomes, solid lipid nanoparticles (SLNs) and self-nanoemulsifying drug delivery systems (SNEDDS) have been employed for the mucosal delivery of macromolecular therapeutics and antigens (Table 1). Concerning the polymer based nanocarriers, the use of various polymeric materials and formulation processes facilitates the modulation of their physicochemical properties (e.g., surface charge and mucoadhesiveness), drug loading, drug release profile and biological behaviour. Liposomes are considered an interesting alternative for administration of macromolecules through various mucosal surfaces, since they are versatile, tend to be relatively innocuous and permit the encapsulation of both hydrophilic and lipophilic drugs. Drug loaded SNEDDS can rapidly disperse in gastrointestinal fluids resulting in the formation of drug containing nanodroplets capable of diffusing through the mucus gel layer. However, despite the promising *in vivo* and in some cases clinical results, further understanding of the mechanisms related to the crossing of the mucosal barriers (e.g., mucus gel layer, epithelium) as well as of those related to the stimulation of the mucosal immune system and correlation of these mechanisms with the characteristics of the nanocarriers could result in improved drug delivery systems, tailor-made for specific applications.

Table 1. Nanocarriers for mucosal delivery / vaccination (adapted from Kammona and Kiparissides 2012).

Carrier	Macromolecular Therapeutic / Antigen
Mucosal Delivery	
CS, CS derivatives, CS/polymer, PLA- CS, PLA copolymers, PLGA, PAA,	Insulin, plasmid DNA, melatonin, nuclear factor kappa B decoy oligonucleotide, thymopentin,

PMAA, starch, dextran, lipid/chitosan NPs complexes, liposomes, lipid nanoparticles, SLNs, SNEDDS, etc	helodermin, thyroglobulin, concanavalin A, myoglobin, calcitonin, β -lactamase, siRNA, heparin, vasoactive intestinal peptide, anti-VEGF intrareceptor (Flt23k) plasmid, etc
Mucosal Vaccination CS, CS derivatives, CS/polymer, alginate, dextran, PLA, modified PLA, PLA-PEG, PLGA, PLGA copolymers, PLGA/polymer, PCL, modified PCL, polypropylene sulphide, dendrimers, liposomes, liposomes/CS, niosomes/CS, lipid particles, etc	group C meningococcal conjugated vaccine, ovalbumin, tetanus toxoid, plasmid DNA encoding hepatitis B surface antigen, bovine serum albumin, hepatitis B surface antigen, monovalent influenza subunit vaccine, <i>S. equi</i> antigens, diphtheria toxoid, beta-galactosidase encoding gene, etc

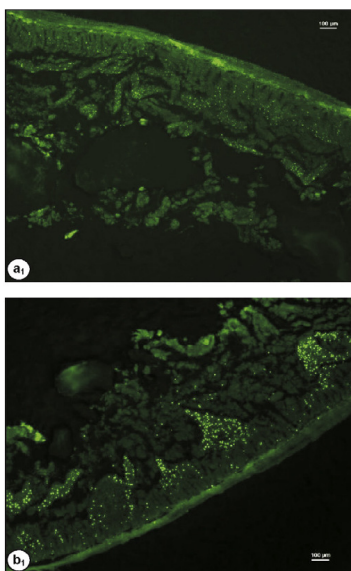


Fig. 1. Microscopic images (40 \times) of intestinal tissue segments taken after 2 h incubation with 100 μ l (0.5%, w/v) of (a) CS and (b) CS-2-iminothiolane nanoparticles labelled with the fluorescent hydrophilic dye (AF 488) (adapted from Dünnhaupt et al., 2011).

References

- Dünnhaupt, S, Barthelmes, J, Hombach, J, Sakloetsakun, D, Arkhipova, V, Bernkop-Schnürch, A, 2011. Distribution of thiolated mucoadhesive nanoparticles on intestinal mucosa. *Int. J. Pharm.* 408, 191-199.
- Kammona, O., Kiparissides, C., 2012. Recent advances in nanocarrier-based mucosal delivery of biomolecules. *J. Control. Release* 161, 781-794.

PHARMACOLOGICAL EVALUATION OF AN APOLIPOPROTEIN-E BASED LEAD COMPOUND FOR THE TREATMENT OF DYSLIPIDEMIA

Kyriakos E. Kypreos

Department of Medicine, Pharmacology Unit, University of Patras Medical School, Rio, TK. 26500, Greece.

Physiological levels of wild-type (wt) apolipoprotein E (apoE) in plasma mediate the clearance of cholesterol-rich atherogenic lipoprotein remnants while higher than normal plasma apoE concentrations fail to do so and trigger hypertriglyceridemia. This property of wt apoE reduces significantly its therapeutic value as a lead biological for the treatment of dyslipidemia. Recently, we reported the generation of a recombinant apoE variant, apoE4 [L261A, W264A, F265A, L268A, V269A] (apoE4mut1) with improved biological functions. Specifically, in apoE-deficient (apoE^{-/-}) mice this variant can normalize high plasma cholesterol levels without triggering hypertriglyceridemia, even at

supraphysiological levels of expression. Preliminary data also indicate that treatment of atherosclerosis prone mice with proteoliposomes containing this apoE variant results in the effective reduction of atherosclerosis progression. Pharmacodynamic and pharmacokinetic analysis of apoE4mut1 in experimental mice revealed some interesting features of the protein that will be useful in its future development as a drug. Using adenovirus-mediated gene transfer in LDL receptor deficient (LDLr^{-/-}) mice, we show that the cholesterol lowering potential of apoE4mut1 is dependent on the expression of a functional classical LDLr. Bolus infusion of apoE4mut1-containing proteoliposomes in apoE^{-/-} mice fed western-type diet for 6 weeks indicated that exogenously synthesized apoE4mut1 maintains intact its ability to normalize the high cholesterol levels of these mice with a maximum pharmacological effect obtained at 10 hours post-treatment. Interestingly, plasma cholesterol levels remained significantly reduced up to 24 hours following intravenous administration of apoE4mut1 proteoliposomes. Measurements of plasma apoE levels indicated that apoE4mut1 in the form of proteoliposomes used in the study has a half-life of 15.8 h. Our data suggest that purified apoE4mut1 may be an attractive new candidate for the acute correction of hypercholesterolemia in subjects expressing functional LDL receptor.

PHARMACOPHORE-BASED ACTIVITY PROFILING IN LEAD IDENTIFICATION AND OPTIMIZATION

T. Langer

Prestwick Chemical SAS, 220 Blvd Gonthier d'Andernach, 67000 Strasbourg-Illkirch, France

Pharmacophore-based virtual screening and activity profiling has become one of the most popular in silico techniques for supporting medicinal chemists in their hit finding, hit expansion, hit to lead, and lead optimization programs. (1)

At Inte:Ligand GmbH, the program LigandScout (2) was developed as a software containing rapid and efficient tools for automatic interpretation of ligand-protein interactions and subsequent transformation of this information into 3D chemical feature-based pharmacophore models. Additionally, algorithms were developed for ligand-based pharmacophore modeling in the absence of a target structure, as well as for accurate virtual screening. As an extension of this approach, parallel pharmacophore-based screening has been introduced as an innovative in silico method to predict the potential biological activities of compounds by screening them with a multitude of pharmacophore models.

In the presentation, Prof. Langer will give an overview of this technology and will present the results of several success stories: Examples range from proof of concept studies employing a set of antiviral compounds that were submitted to in silico activity profiling using a subset (3) of the Inte:Ligand Pharmacophore Database (4) to in silico fragment-based discovery of novel enzyme inhibitors. Additionally, several medicinal chemistry application examples yielding clinical candidates will be highlighted.

REFERENCES

- (1) Langer, T., Pharmacophores in Drug Research, Mol. Inf. 2010, 29, 470-475.
- (2) Wolber, G., Langer, T.; LigandScout: 3D Pharmacophores Derived from Protein-Bound Ligands and their Use as Virtual Screening Filters, J. Chem. Inf. Model. 2005, 45, 160-169.
- (2) Gennaro, A. R. Remington's Pharmaceutical Sciences, XXII. Mack Publishing Company, Easton, PA, 1990.
- (3) Steindl, T. M., Schuster, D., Laggner, C., Langer, T.; Parallel Screening: A Novel Concept in Pharmacophore Modelling and Virtual Screening, J. Chem. Inf. Model. 2006, 46, 2146-2157.
- (4) The Inte:Ligand Pharmacophore Database is available from Inte:Ligand GmbH, Vienna, Austria (<http://www.inteligand.com>)

THE DENDRIMER SPACE CONCEPT FOR INNOVATIVE NANOMEDICINE

Prof. J.P. Majoral

Laboratoire Chimie de Coordination, CNRS, 205 route de Narbonne, 31077 Toulouse, France.

The emergence of nanotechnology has a significant impact on the drug-delivery field with many applications such as in clinical medicine and pharmaceutical researches. Dendrimer nanostructures represent outstanding nano-carriers in nanomedicine, and they have often been referred to as the "Polymers of the 21st century". The main potential advantages of dendrimers in medicinal chemistry can be well defined within a new concept. Thus, we proposed the dendrimer space concept, per analogy with the chemistry and biology space concepts which are extensively used in pharmaceutical industry to develop new drugs. This new concept represents a powerful exploration tool for chemists (e.g. visualization, mapping and traveling) of both the vast chemical and biological spaces to find new biologically active compounds and then to develop original drugs. Based on several and selected success stories, the boundaries of the dendrimer space can be summarized as the main following dendrimer's propensities:

Enhance the therapeutic potency, the pharmacokinetic and pharmacodynamic behaviors of the plain drug
Reduce toxicity versus activity
Deliver drugs in designated place of supply
Use possibly both active and passive drug targeting
Overcome low oral bioavailability
Allow non-classical routes of administration (trans-dermal, trans-nasal, ocular delivery system, etc.)

Permit the development of a theranostic nanomedicine directed to a personalized medicine Etc.

These non exhaustive dendrimer characteristics defining the dendrimer space will be illustrated with several examples such as for instance of classical and non classical routes of administration of a drug complexed with dendrimers. In the way to use dendrimers in the theranostic approach for nanomedicine, the design of non toxic, biocompatible, efficient organic dendritic nanodots for diagnosis will be also presented.

Finally, in the course of the search of safe and effective drug delivery systems based on dendrimers, we will see how modifications of known drugs to link to dendrimers allow the discovery of new fascinating active antitumoral reagents.

ORIGINAL MULTIVALENT COPPER(II)-CONJUGATED PHOSPHORUS-DENDRIMERS WITH POTENT ANTI-TUMORAL ACTIVITIES*

Serge Mignani

Formerly Head of Medicinal Chemistry Department and Scientific Director (Sanofi)

Université Paris Descartes, PRES Sorbonne Paris Cité, CNRS UMR 860, Laboratoire de Chimie et de Biochimie pharmacologiques et toxicologique, 45, rue des Saints Pères, 75006 Paris, France

Corresponding author: serge.mignani@parisdescartes.fr

* This work was done in collaboration with Prof. J-P. Majoral (Laboratoire de Chimie de Coordination du CNRS, Toulouse, France)

This presentation focuses on the design of novel biocompatible multivalent copper(II)-conjugated phosphorus-dendrimers bearing a cyclotriphosphazene core and their corresponding mononuclear copper(II) complexes as anti-proliferative nanodevices.

The respective role of three factors, the structural feature of the coordination ligands, the dendrimer generation (G_n) and the presence or not of copper(II) on the surface was explored through the expected cytotoxicity activities on human cell lines.

Selected copper-ligands were grafted on the surface of phosphorus dendrimers of generation G_n (n = 1 to 3): N-(pyridin-2-ylmethylene)ethanamine (series 1) for dendrimers 1G_n, N-(di(pyridin-2-yl)methylene)ethanamine (series 2) for dendrimers 2G_n and 2-(2-methylenehydrazinyl)pyridine (series 3) for dendrimers 3G_n. Dendrimer synthesis was accomplished by a straightforward synthetic pathway.

The results indicated that the most potent derivatives - against solid and liquid tumor cancer cell lines - are 1Gn and 1Gn-Cu versus 2Gn, 2Gn-Cu, and 3Gn, 3Gn-Cu. A direct relationship between the growth inhibitory effect and the number of terminal moieties or the amount of copper complexed to the dendrimer was observed in copper-complexed 1 series and non-complexed 1

series. These data clearly suggested that cytotoxicity increased with the number of terminal moieties available and interestingly was boosted by the presence of complexed Cu atoms. Importantly, no cytotoxic effect was observed with CuCl₂ at the same concentrations.

1G3 and 1G3-Cu have been selected for anti-proliferative studies against a panel of tumor cell lines: 1G3 and 1G3-Cu demonstrated potent anti-proliferative activities with IC₅₀ values ranging 0.3-1.6 μM. Interestingly, the complexation of the terminal ligands of 1G3 dendrimers by copper (II) metal strongly increased the IC₅₀ values in non-cancer cells lines referred as "safety" cell lines.

Finally, the first investigations in the search of the mechanism of action of both copper-complexed series and non-complexed series will be also analyzed.

DENDRIMERS AS NANOVECTORS FOR RNA DELIVERY IN GENE THERAPY

Ling PENG

Centre d'Interdisciplinaire de Nanoscience de Marseille, CINaM CNRS UMR 7325, Aix-Marseille University, Campus Luminy, 13288 Marseille, France

With the spectacular advance of nanotechnology in medical science to improve healthcare, there is fuelled interest to develop conceptionally new dendrimer nanocarriers for drug delivery to satisfy clinical demand. We have specifically developed structurally flexible¹ and amphiphilic dendrimers² as nanocarriers for nucleic acid delivery. Some of them are exceptionally effective in delivery of RNA therapeutics in vitro in various cells including cancer, suspension, primary and stem cells and in vivo in mice models with potent anticancer activity against various cancer forms and antiviral activity against HIV infection.¹⁻² We will present our recent results in this direction and discuss their structure/activity relationship analysis for further design of more efficacious and safer dendrimer nanovectors for nucleic acid delivery to treat various diseases.

Wu, J.; Zhou, J.; Qu, F.; Bao, P.; Zhang, Y.; Peng, L. *Chem. Commun.* 2005, 313-315; Zhou, J.; Wu, J.; Hafdi, N.; Behr, J. P.; Erbacher, P.; Peng, L. *Chem. Commun.* 2006, 2362-2364; Liu, X.; Wu, J.; Yammine, M.; Zhou, J.; Posocco, P.; Viel, S.; Liu, C.; Ziarelli, F.; Fermeglia, M.; Pricl, S.; Victorero, G.; Nguyen, C.; Erbacher, P.; Behr, J. P.; Peng, L. *Bioconjugate Chem.* 2011, 22, 2461-2473; Liu, X. X.; Rocchi, P.; Qu, F. Q.; Zheng, S. Q.; Liang, Z. C.; Gleave, M.; Iovanna, J.; Peng, L. *ChemMedChem* 2009, 4, 1302-1310; Liu, X.; Liu, C.; Laurini, E.; Posocco, P.; Pricl, S.; Qu, F.; Rocchi, P.; Peng, L. *Mol. Pharmaceutics* 2012, 9, 470-481; Zhou, J.; Neff, C. P.; Liu, X.; Zhang, J.; Li, H.; Smith, D. D.; Swiderski, P.; Aboellail, T.; Huang, Y.; Du, Q.; Liang, Z.; Peng, L.; Akkina, R.; Rossi, J. J. *Mol. Ther.* 2011, 19, 2228-2238; Lang, M. F.; Yang, S.; Zhao, C.; Sun, G.; Murai, K.; Wu, X.; Wang, J.; Gao, H.; Brown, C. E.; Liu, X.; Zhou, J.; Peng, L.; Rossi, J. J.; Shi, Y. *PLoS One* 2012, 7, e36248; Posocco, P.; Liu, X.; Laurini, E.; Marson, D.; Chen, C.; Liu, C.; Fermeglia, M.; Rocchi, P.; Pricl, S.; Peng, L. *Mol. Pharmaceutics* 2013, Doi:10.1021/mp400329g.

Yu, T.; Liu, X.; Bolcato-Bellemin, A-L.; Liu, C.; Wang, Y.; Erbacher, P.; Qu, F.; Rocchi, P.; Behr, J-P.; Peng, L. *Angew. Chem. Int. Ed.* 2012, 51, 8478-8484.

TOPOGRAPHIC ANALYSIS OF ELECTROSPUN DRUG-LOADED NANOFIBROUS MATS WITHOUT SAMPLE PREPARATION

U. Paaver¹, J. Heinämäki¹, I. Kassamakov², E. Hæggström², T. Ylitalo², A. Nolvi², J. Kozlova¹, I. Laidmäe¹, K. Kogermann¹, P. Veski¹

1. University of Tartu, Tartu, Estonia

2. University of Helsinki, Helsinki, Finland

Scanning white light interferometry (SWLI) is a non-destructive, non-contacting, method employed e.g. in microelectronics and optics to examine miniature elements, micro-fluidic devices, and micro-electro mechanical systems [1,2]. To our knowledge, SWLI has not been applied to determine geometric properties and surface topography of polymeric nanofibers and nanofibrous mats intended for pharmaceutical or biomedical applications. We therefore investigated SWLI as a technique for determining geometry (i.e. fiber diameter, diameter distribution, orientation, and morphology) and surface topography of pharmaceutical polymer nanofibers and nanofibrous mats.

The nanofibers of a poorly water-soluble piroxicam (PRX) and hydroxypropyl methylcellulose (HPMC) were prepared by electrospinning (ES). A high-resolution scanning electron microscopy (SEM) device equipped with a measurement program was used as a reference method. In fabricating the ES drug containing nanofibers and nanomats, a carrier polymer HPMC combined with PRX at ratios of 1:1, 1:2 or 1:4 was used. SWLI 3D images featuring 29 nm by 29 nm active pixel size were obtained of a 55 x 40 μm^2 area.

The thickness of the drug-loaded nanomats was uniform, ranging from 2.0 μm to 3.0 μm (SWLI), and independent of the ratio between HPMC and PRX. The 3D topographical maps obtained by SWLI showed deep porous structures in the non-woven drug-loaded nanomats. The average SEM diameters ($n = 100$) for drug-loaded nanofibers were 387 ± 125 nm (HPMC and PRX 1:1), 407 ± 144 nm (HPMC and PRX 1:2), and 290 ± 100 nm (HPMC and PRX 1:4).

We found advantages and limitations in both SWLI and SEM techniques. SWLI permits rapid non-contacting and non-destructive characterization of layer orientation, layer thickness, porosity, and surface morphology of drug-loaded nanofibers and nanomats. Such analysis is important because the surface topography affects the performance of nanomats in pharmaceutical and biomedical applications.

Acknowledgements: This work is part of the targeted financing project no SF0180042s09 and ETF grant project no ETF7980. This research was also supported by the European Social Fund's Doctoral Studies and Internationalization Program DoRa.

References:

- [1] Kassamakov, I. V., Seppänen, H.O., Oinonen, M.J., Hæggström, E.O., Österberg, J.M., Aaltonen, J.P., Saarikko, H., Radivojevic, Z.P., 2007. Scanning white light interferometry in quality control of single-point tape automated bonding. *Microelectron. Eng.* 84, 114-123.
- [2] Kassamakov, I., Hanhijärvi, K., Abbadi, I., Aaltonen, J., Ludvigsen, H., Hæggström, E., 2009. Scanning white-light interferometry with a supercontinuum source. *Opt. Lett.* 34 (10), 1582-1584.

urve.paaver@ut.ee

POLYMER BASED NANOSTRUCTURES AS CARRIERS FOR DRUGS, PROTEINS AND NUCLEIC ACIDS

S. Pispas

Theoretical and Physical Chemistry Institute, National Hellenic Research Foundation, 48 Vassileos Constantinou Ave., 11635 Athens, Greece

Polymeric nanomedicine has seen a considerable blooming during the last years. Polymer based nanostructures has been widely utilized for the encapsulation and delivery of a large gamut of pharmaceutically important compounds, including hydrophobic drugs, therapeutic proteins and peptides, and nucleic acids.

In our group we developed a series of amphiphilic block copolymers and block polyelectrolytes with designed macromolecular architecture and chemical functionality, using controlled polymerization methodologies. These macromolecules self-organize in aqueous media in a variety of nanostructures, like core-shell micelles and polyelectrolyte complexes, through complexation with oppositely charged proteins, DNA and RNA. The properties of the chimeric nanostructures have been studied by light scattering,

fluorescence spectroscopy and AFM techniques. Their ability to encapsulate and electrostatically bind with low and high molecular weight drugs respectively has been tested.

Results: Several amphiphilic block copolymers based on poly(ethylene oxide) (PEO) and blocks of varying hydrophobicity have been synthesized. These block copolymers were found to successfully encapsulate hydrophobic low molecular weight drugs, like curcumin and indomethacin. Block polyelectrolytes with a biomimetic anionic block were utilized for the complexation of lysozyme. Lysozyme was found to be released from the complexes in a sustainable way. Block polyelectrolytes with a cationic block and a PEO block were used in complex formation with DNA and RNA. The binding affinity was observed to be dependent on the nature of the nucleic acid. Novel gradient block copolymer architectures were also implemented in different encapsulation protocols demonstrating promise for utilization in polymeric nanomedicine.

Advances in contemporary polymer chemistry allow the synthesis of a variety of tailor-made macromolecules, which are able to perform as nanocarriers for pharmaceutical compounds by virtue of their self-assembly properties and their ability to complex with macromolecular biological (macro)molecules.

The author acknowledges partial financial support of the work by the NANOMACRO 1129 project which is implemented in the framework of the Operational Program "Education and Life-long Learning" of the National Strategic Reference Program-NSRF (Action "ARISTEIA I") and it is co-funded by the European Union (European Social Fund-ESF).

BIORELEVANT PERFORMANCE TESTING OF ORALLY ADMINISTERED DRUG PRODUCTS: RATIONALE AND CURRENT REGULATORY STATUS

C. Reppas

National and Kapodistrian University of Athens

Performance of orally administered dosage forms can be evaluated with in vivo studies indirectly (e.g. plasma levels) or directly (e.g. imaging techniques, sampling from the lumen), and with in-vitro studies. In-vitro studies are free from ethical issues, comparatively less expensive, and easier to perform. An in-vitro performance test is termed biorelevant when it mimics intraluminal performance of the dosage form. This presentation is divided into three parts. Firstly, the ability of current in-vitro performance tests to predict in-vivo performance and generate successful in-vitro and in-vivo correlations for oral dosage forms will be reviewed. In the second part, key efforts to improve predictability of biorelevant tests will be presented. In the third part, a summary on the regulatory status will be made. Currently, the most desirable approach for regulators globally in order to explore and establish clinically relevant dosage form specifications requires the development of a validated in-vivo in-vitro correlation model to predict the clinical impact of changes without the need for additional in-vivo studies. Perhaps the difference compared with 1-2 decades ago is that a mechanistic understanding of drug release through risk analysis, design of experiments and development of appropriate design space and control space is strongly encouraged as it ensures in-vivo dosage form performance. However, certain differences among regulators do exist: In the US, there are no official regulatory definitions or requirements for use of biorelevant media in in-vitro release testing; only guidances. For European regulators, the term biorelevance is supposed to reflect the in-vivo dissolution behaviour (European Medicines Agency, Guideline on investigation of bioequivalence, CPMP/QWP/EWP/1401/98Rev12010, Appendix I), hence in-vitro dissolution should have a relation to in-vivo data.

PRINTABLE FORMULATIONS IN DRUG DELIVERY

N. Sandler 1

1 Åbo Akademi University, Turku, Finland

Printing technologies such as inkjet and flexographic printing, offer possibilities in the flexible production of more medicines. The purpose of this talk is to give an overview of

printing technologies and give examples of their use in fabrication of drug-delivery systems.

The main advantage of inkjet printing includes their ability to dispense uniform droplets in the picoliter range with a high degree of accuracy. The droplet formation and 3D placement can be digitally controlled by a personal computer. The ink formulation has to be designed with respect to its viscosity and surface tension to guarantee continuous printing and high reproducibility of the forming droplets. Recently this technology has opened new perspectives when designing individual dosage forms [1-2]. Inkjet printing to directly deposit drug solutions or suspensions containing API and excipients onto carrier materials such as porous substrates and biodegradable films, offers a way for fabrication of oral solid dosage forms with controlled materials properties. In this presentation the use of riboflavin sodium phosphate (RSP) and propranolol hydrochloride (PH) as water-soluble model drugs are demonstrated. Three different types substrates were used as porous model carriers for drug delivery. APIs containing solutions were printed onto 1 cm × 1 cm substrate areas using an inkjet printer. The printed APIs were coated with water insoluble ethylcellulose (EC) films of different thickness using flexographic printing. Immediate release behavior was shown by the printed drug substances without any polymer coating. The EC layers printed using flexographic printing resulted in sustained drug release with increasing amount of layers as anticipated. The release profiles were different for the different substrates used. The results indicate that the drug release is therefore influenced both by the properties of the substrates in and polymer layering. In conclusion, the use of combined printing technologies to deposit drug substances onto porous cellulose substrates is a promising approach in the production of solid medicines with distinct characteristics and tailored release behavior.

Literature References

- [1] Sandler et al., 2011. J. Pharm. Sci. 100, 3386-3395.
[2] Genina et al., 2012. Eur. J. Pharm. Sci. 47, 615-623.

GREEN SEA URCHINS AS A SOURCE OF NATURAL PRODUCTS

A.N. Shikov, O.N. Pozharitskaya, I.N. Urakova, V.G. Makarov, M.N. Makarova
Saint-Petersburg Institute of Pharmacy, St-Petersburg, Russia

Marine species shows approximately half of biodiversity and sea has been classified as the largest remaining reservoir of natural molecules to be evaluated for drug activity.

Green sea urchin (*Strongylocentrotus droebachiensis*) is major consumers in the shallow waters of the world. They are consumed primarily because valuable gonads known as highly priced sushi foodstuff "Uni" in Japanese traditional food. Sea urchin by-products, as such as coelomic fluid, digestive tract, shell, discarded gonads that do not meet commercial needs in colour, texture and taste, may represent up to 80%. Research and development of value-added items from biological wastes becomes crucial to discover their chemical composition, pharmacological activity and to find their medicinal applications.

Green sea urchins were harvested from the Barents Sea and were separated in shells, coelomic fluid, digestive tract, and gonads. Each part was subject of special processing. In result, five products were received and subjected for pharmacological tests.

Sea urchin pigments, namely spinochromes B and D, anhydroethylidene-6,6-bis(2,3,7-trihydroxynaphthazarin and its isomer ethylidene-6,6-bis(2,3,7-trihydroxynaphthazarin) has been showed potent antiradical activity which exceeds that of well known echinochrome A. An antihistaminic action of pigments on H1-receptor was studied *ex vivo*. Sea urchin pigments have significantly and dose-dependently inhibited histamine-induced contraction of the isolated guinea pig ileum. Molecular docking confirmed that spinochromes B and D were able bind to H1-receptor, although dimers have higher

affinities. In experimental pre-clinical study on mice, for the first time it was established that the complex polyhydroxylated naphthoquinone pigments and minerals from shells of sea urchins decrease concentration of glucose, and stimulates synthesis of phospholipids in liver. The complex of peptides and polysaccharides isolated from coelomic fluid was active in model of streptozotocin-nicotinamide-induced diabetic 2 types possess antidiabetic activity and significantly dose-dependently reduced DPP IV activity. It was found that the lipophilic extract of gonads has hypoglycemic, antihypertensive, anti-ischemic and vasodilatory properties in rats. It was established that oral administration of special extract from gonads of green sea urchin improved erectile function of rats and affected to the generative function of male rats, increased sperm motility. Complex of sulfated fucans and polypeptides from the digestive tract of sea urchins have anti-inflammatory and immunomodulating activity by inhibiting the activation of MAP-kinase p38.

Thus, the green urchin is reach source of biological active compound and must be processed and valorised to produce number of value-added natural medicines.

CONFORMATIONAL DYNAMICS AND DRUG DESIGN APPROACHES THROUGH NMR

Birkou M.1, Tsapardoni M.1, Marousis K.1, Chasapis C.T.1, Bentrop D.2, Episkopou V.3, Spyroulias G.A.1

1 Department of Pharmacy, University of Patras, GR-26504, Patras, Greece.

2 Institute of Physiology II, University of Freiburg, D-79104 Freiburg, Germany.

3 Imperial School of Medicine, Hammersmith Hospital, London W12 0NN, United Kingdom

E3 ubiquitin ligases play a key role in the proteolytic degradation of proteins through the Ubiquitin-Proteasome pathway [Hershko A & Ciechanover A, *Annu Rev Biochem* 1998, 67, 425]. ARKADIA is the first example of an E3 ligase that positively regulates TGF- β family signaling through its C-terminal RING finger domain [Episkopou V et al. *PLoS Biol* 2007, 5, e67].

The ARKADIA RING finger, was cloned and expressed in its zinc-loaded form and studied through multi-nuclear and multi-dimensional NMR Spectroscopy [Kandias NG et al. *BBRC* 2009, 378, 498]. The 3D NMR solution structure of ARKADIA RING finger was determined and deposited in PDB (2KIZ). Additionally, NMR-driven titration studies were also performed to probe the interaction interface of ARKADIA RING and the partner E2 (UbcH5B) enzyme and the RING-E2 complex was constructed through an NMR-driven docking protocol [Chasapis CT et al. *Proteins* 2012, 80, 1484].

Additionally, this study resulted to the identification of ARKADIA RING functionally important residues, such as the conserved, in many RING domains, Trp972. Trp972 is considered as one of the key residues for E2 recognition and binding [Huang A, et al. *J Mol Biol* 2009, 385, 507]. According to recent experimental evidence, the mutation of the Trp972 to Arg abolishes the ability of Arkadia to amplify TGF- β -Smad2/3 signaling responses in tissue culture transcription assays [Episkopou V, et al. *Cancer Res.* 2011, 71, 6438] suggesting that this residue is essential in the ubiquitin ligase enzymatic activity, consistent with the E2 recruitment. Various ARKADIA Trp mutants were prepared and are studied through NMR spectroscopy in order to obtain an atomic-level insight about the structural base of ARKADIA RING capability to select and bind the appropriate E2 in order to exhibit its ubiquitin ligase activity.

Acknowledgments: FP7-REGPOT-2011 "SEE-DRUG" (nr. 285950)

WHOLE ANIMAL IMAGING APPLICATIONS IN NANOTECHNOLOGY

Georgios T. Stathopoulos, MD PhD

Assistant Professor of Physiology, Faculty of Medicine, University of Patras

The various modes of intravital whole-body (macroscopic) imaging of small animals have yielded numerous contributions to current biomedical research, as they allow for rapid and repeated biologic observation of living organisms. The techniques employed range from plain X-ray to bioluminescent and biofluorescent imaging and differ in accessibility, speed, throughput, cost, repeatability, resolution, tissue penetrance and type of information conveyed (structural versus functional). In recent years, small animal imaging has become a powerful tool for the study of nanoparticles in vivo, and, in turn, nanomedicine has opened up new avenues of research for preclinical imaging. The present talk is aimed at highlighting examples of the synergies between nanotechnology and macroscopic preclinical imaging and at familiarizing basic and translational researchers with the possibilities for imaging applications in nanotechnology. Examples will include real-time studies of nanoparticle fate tracing in vivo and new imaging modes facilitated by nanoparticles.

DENDRIMERIC NANOMATERIALS AND THEIR BIOMEDICAL APPLICATIONS

Barry R. Steele

Institute of Biology, Medicinal Chemistry and Biotechnology

National Hellenic Research Foundation, 48 Vassileos Constantinou Avenue, 11635, Athens, Greece

E-mail: bsteele@eie.gr

In recent years, research in the field of dendrimers has experienced an exponential development both at an academic and at a technological level and this is a result of the wide range of applications that have been foreseen for them in areas ranging from biomedical to material science. Dendrimers are discrete molecules characterised by a core from which well-defined branching units extend. For biomedical applications in particular, the interest in the development of dendrimers as diagnostic and therapeutic tools can be related to their precise architecture which can offer an advantage over other generally polydisperse nanoparticles in that there is the possibility of stricter control of their pharmacodynamic profile. Dendrimers of a certain size have the capacity to encapsulate and deliver small molecules while a particularly attractive feature is the presence of a number of end-groups on the surface of the dendrimer which permit multivalent interactions with biological substrates. In addition, the surface may be decorated with various groups which have different functions such as those for promoting solubilisation, for targeting specific sites or for imaging purposes. More recently, the incorporation of dendrimeric units with liposomes and other types of nanoparticle has received increasing attention. These potentially offer even greater control over therapeutic or diagnostic efficacy. This presentation will provide an overview of the properties of selected types of dendrimers and dendrimer-modified nanoparticles with recent examples of their relevance to biomedical applications.

DISCOVERY OF BIOACTIVE LEAD COMPOUNDS FROM THE PLANT KINGDOM- IN SILICO APPROACHES COMBINED WITH CONVENTIONAL METHODS

H. Stuppner

University of Innsbruck, Institute of Pharmacy/Pharmacognosy, Center of Molecular Biosciences Innsbruck (CMBI), Innrain 52c, 6020 Innsbruck, Austria

Inflammation is part of numerous pathological conditions, including atherosclerosis, the metabolic syndrome, sepsis and cancer; all of them lacking satisfying treatment and/or effective concepts of prevention. Natural products (NPs) have always been an important source of new drug leads. Almost half of the drugs currently in clinical use are of natural product origin and even today, in the post genomic era, plants, fungi, marine organisms, and microorganisms are still an important source for the development of new drugs [1].

In the course of a national research network project involving scientists of six Austrian universities we aim to identify and characterise natural products capable to combat inflammatory processes specifically in the cardiovascular system. This is approached by a unique combination of strategies including i) pharmacophore modelling and virtual screening filtering experiments in order to identify compounds promising for pharmacological evaluation (molecular/computational approach) and ii) exploitation of traditional knowledge about plants to select promising candidates for phytochemical and subsequent pharmacological investigation (ethnopharmacology/bioguided approach). Candidates of both approaches are subjected to mechanistic studies as well as preclinical profiling. Results of this interdisciplinary project will be presented.

Acknowledgements: This work is financially supported by grant no S107 „Drugs from Nature Targeting Inflammation“ from the Austrian Science Fund (<http://www.uibk.ac.at/pharmazie/pharmakognosie/dnti/>).

References:

[1] Newman, D.J. and Cragg, G.M., 2012. Natural Products As Sources of New Drugs over the 30 Years from 1981 to 2010. *J Nat Prod*, 75, 311-335
email address of corresponding author: hermann.stuppner@uibk.ac.at

BIOWAIVER APPROACH FOR BCS: DISCUSSION OF BIOWAIVER MONOGRAPHS FOR IMMEDIATE-RELEASE SOLID ORAL DOSAGE FORMS

Zeynep Safak Teksin

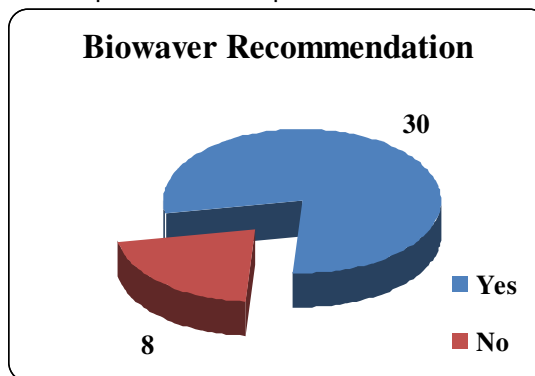
Gazi University Faculty of Pharmacy, Department of Pharmaceutical Technology, Ankara, Turkey

zsteksin@gazi.edu.tr

Literature data relevant to the decision to allow a waiver of in vivo bioequivalence (BE) testing for the approval of new immediate release (IR) solid oral dosage forms containing APIs are reviewed in biowaiver monograph series by FIP. This approach is supported by WHO and takes published guidances of the WHO, FDA and EMA into consideration as well as scientific developments in this field. Until now, BCS classification and recommendation for the biowaiver according to biowaiver monographs for more than 35 drug substances have been available at FIP website at www.fip.org/bcs. Although, the monographs have no formal regulatory status, they represent the best scientific opinion currently available.

In biowaiver monographs, drug substance's solubility and permeability characteristics and dosage forms' in vitro dissolution behavior according to the BCS, as well as its therapeutic indications, side effect, available dosage form strengths and dose, therapeutic index and toxicity, its physicochemical properties (salts, esters, or hydrates forms, stereochemistry, polymorphism, partition coefficient, pKa), its pharmacokinetic properties (absorption and bioavailability, permeability, distribution, metabolism and elimination), its dosage form performance (bioavailability (BA), bioequivalence of different formulations, excipients, food interactions, manufacturing variations, dissolution and in vitro-in vivo correlations) and reported BE/BA problems are taken into consideration. Additionally, the monographs are considered BCS parameters (solubility, absorption and permeability, dissolution), BCS classification and eligibility for the biowaiver, risks with respect to excipient and/or manufacturing variations, surrogate techniques for in vivo BE testing, patient's risks associated with bioinequivalence as well. On the basis of these considerations, a recommendation can be made as to whether a biowaiver is advisable or not. Until now, the recommendation for the biowaiver according to the FIP biowaiver monographs is shown in figure as follows.

The regulations on BCS based biowaivers differ between the FDA, EU and WHO. Therefore, the biowaiver monographs are important to optimize and harmonize



biowaiver guidances on a global basis.

ADVANCED THERAPY MEDICINAL PRODUCTS (ATMPs): DEVELOPMENT AND REGULATION IN EUROPE

Prof. Asterios S. Tsiftoglou

Laboratory of Pharmacology, Dept. of Pharmaceutical Sciences, Aristotle University of Thessaloniki, Greece and Core Member of the CAT Committee, European Medicine Agency(EMA), London (tsif@pharm.auth.gr)

The use of conventional human medicines and biopharmaceuticals/biologics since 1980's led to the successful therapy of many diseases. However, the use of these agents still can not cure a large number of degenerative disorders. These include certain types of cancer, metabolic and genetic diseases, neurodegeneration, viral diseases, hematological malignancies, cardiomyopathies and many other rare disorders. The rapid progress achieved over the years in gene cloning and expression systems, gene therapy, stem cell research, somatic cell cloning and nuclear reprogramming of adult cells into induced pluripotent stem cells (iPSCS) provided novel platforms and technologies for manufacturing ATMPs. This class of new medicinal products include (i) somatic cell therapy products, (ii) gene therapy products and (iii) tissue engineering products (TEPs) of simple and complicated nature. While the first two groups of products are intended for cell and gene therapy, respectively, the TEPs are expected to repair, replace and regenerate the damaged tissue. In most cases, the ATMPs are manufactured to deliver their therapeutic effects via metabolic, pharmacological and immunological function. These products, however, are considered complex products and differ from the conventional human medicines and biologics in many respects.(size, complexities, cellular heterogeneity, manufacturing formulation, stability, administration, risk), just to mention a few. Therefore, their manufacturing process, pharmacokinetics, pharmacodynamics and many other quality attributes can not be applied directly to these products. To provide guidance and prevent the use of unauthorized ATMPs, European Commission in 2007 issued a new regulatory framework (Regulation 1394/2007) (1) to set rules and procedures for manufacturing, evaluation and market authorization of ATMPs based on quality, preclinical and clinical assessment. This has been an important development (2) not only for new products, but also for cell and gene based therapy products developed earlier at national level and being circulated in the market. The regulatory framework aims to foster innovation in this field, help the stakeholders to manufacture high quality ATMPs and provide guidance for evaluation and market authorization via a central process in the EMA. Both scientific and regulatory aspects of ATMPs in Europe will be presented and discussed.

Regulation (EC) N01394/2007 of the European Commission and the Council on Advanced Therapy Medicinal Products and amending Directive 2001/EC and Reg. No 726/2004

Schneider CK, Salmikangas P, et al, Challenges with ATMPs and how to meet them. *Nat. Rev. Drug. Discov.* 9:195-201,2010

ARGININE AND LYSINE-BASED FUNCTIONALIZED PEPTIDES FOR THE STABILIZATION AND CONTROLLED RELEASE OF INSULIN

D. Tsiourvas

National Centre for Scientific Research "Demokritos", IAMPPNM, Dept. of Physical Chemistry, 15310 Aghia Paraskevi, Attiki, Greece.

The standard treatment of insulin-dependent diabetic patients is the periodical subcutaneous injection of insulin which is, however, associated with poor control of blood glucose level and poor patient compliance.¹ Insulin oral administration is certainly the most attractive route of insulin administration,² but this delivery mode is hindered by several obstacles such as the presence of proteolytic enzymes and the sharp pH gradients of the peptic system, as well as the low epithelial permeability. Therefore, protein oral delivery systems relying on complexation and assembly of proteins with polymers are currently under investigation.³ These polymers form nanoscale complexes with proteins mainly through electrostatic interactions, protecting them against loss of biological activity and increasing their transmucosal uptake. Previous studies have established that cell penetrating peptides, mainly arginine-rich peptides, are efficiently taken up by cells,⁴ and that their conjugation with proteins improves their permeability through cell membranes.⁵

In the present study, we have investigated the complexation of insulin with a biodegradable poly(L-lysine) dendrigraft (DL) or with arginine end-functionalized DL at physiological pH.⁶ The interaction, resulting in stable dendrigraft/insulin complexes, was studied by dynamic light scattering, ζ -potential, circular dichroism and isothermal titration calorimetry (ITC). Binding occurs in two steps: at low dendrigraft/insulin molar ratios (≤ 0.07) interaction is accompanied with the endothermic dissociation of insulin dimers, while at higher molar ratios, complexation of insulin monomers with dendrigraft derivatives occurs exothermically.

Additionally, PEGylated oligolysine and oligoarginine homopeptides also interact spontaneously and efficiently with insulin, at physiological pH, affording stable ionic complexes.⁷ FTIR spectra suggest that the positively charged oligopeptides interact with the B chain C-terminus of insulin. The ITC profiles are complex, displaying significant endothermic and exothermic contributions. Oligoarginine derivatives interact more strongly than oligolysine derivatives, while PEGylation with high molecular weight chains leads to larger enthalpy changes. This is attributed to PEG-induced formation of stable nanocomplexes due to the depletion attraction effect.

In all cases, high levels of insulin complexation efficiencies ($> 99\%$) were determined. Stabilization of complexed insulin against enzymatic degradation by trypsin and α -chymotrypsin is observed especially for the highly end-functionalized arginine dendrigrafts and for the high molecular weight PEGylated arginine-based derivative. Insulin release rates in simulated intestinal fluid can be controlled by the number of arginine end-groups and by the length of PEG chains. More importantly, released insulin retains its secondary structure as established by circular dichroism spectroscopy.

In conclusion, complexes of arginine-based peptides with insulin have significant potential to be further studied as novel insulin delivery systems, given the enzyme-degradable character of oligopeptides, the presence of arginine end-groups that are expected to enhance insulin intestinal absorption, the control of insulin release rate and the improved protection of insulin against enzymatic degradation.

References

1. V. Sabetsky, J. Ekblom, *Pharmacol. Res.* (2010) 61:1.
2. K. Wadher, R. Kalsait, M. Umekar, *J. Pharm. Sci. Res.* (2011) 3:1052.

3. M.R. Rekha, C.P. Sharma, J. Controlled Release (2009) 135:144.
4. I. Nakase, T. Takeuchi, G. Tanaka, S. Futaki, Adv. Drug Delivery Rev. (2008) 60:598.
5. R. Sawant, V.P. Torchilin, Mol. BioSyst. (2010) 6:628.
6. Z. Sideratou, N. Sterioti, D. Tsiourvas, L.-A. Tziveleka, A. Thanassoulas, G. Nounesis, C. M. Paleos, J. Colloid Interface Sci. (2010) 351:433-441.
7. D. Tsiourvas, Z. Sideratou, N. Sterioti, A. Papadopoulos, G. Nounesis, C. M. Paleos, J. Colloid Interface Sci. (2012) 384:61-72.

THE NEED FOR VALIDATED BIORELEVANT DRUG PRODUCT PERFORMANCE TESTS

Maria Vertzoni

Department of Pharmaceutical Technology, National and Kapodistrian University of Athens

Prediction of intraluminal performance of an orally administered dosage form and the active pharmaceutical ingredient (API) with in vitro tests, i.e. biorelevant in vitro performance testing, requires appropriate simulation of luminal conditions. Key luminal parameters to be simulated may vary with the process to be simulated, the structure of the active pharmaceutical ingredient (API) and the type of dosage form. During the last two decades our knowledge on luminal composition and hydrodynamics has been increased substantially and this has resulted into the development of reliable in vitro tests in various situations. However, in certain cases, the reliable evaluation of intraluminal dosage form and/or API performance, after oral administration remains problematic.

In this presentation, two such situations will be presented. Firstly, our limited ability to predict supersaturation of and precipitation in the contents of the upper small intestine after administration of a weak base will be discussed. Based on recent luminal data and despite to what is generally believed, precipitation of lipophilic weak bases after oral administration is limited. A proposal for closing this gap based on luminal data will be presented. Second, the problematic evaluation of API stability characteristics in the colonic region will be discussed. Despite the widespread use of fecal material (with varying composition), based on recent information, it may not be appropriate for reliable estimation of colonic stability, at least for certain type of degradation reactions.

PERSONALIZED NANOMEDICINE CROSSING THE BORDERLINES BETWEEN PHARMACOGENOMICS AND NANOTECHNOLOGY TO ADVANCE CANCER THERAPEUTICS DECISIONS

Ioannis S. Vizirianakis

Laboratory of Pharmacology, School of Pharmacy, Aristotle University of Thessaloniki, GR-54124 Thessaloniki, Greece

The existed cancer cell heterogeneity coincides with the variability of molecular mechanisms that contribute to tumorigenicity, the complexity in genomic profiles and clinical phenotypes, as well as with the crucial involvement of other cell-type interactions coming from the well-known "tumor microenvironment". Such diversity contributes also to anticancer drug response variability and affects the clinical outcome. To this regard, the advancements in cancer cell biology, cancer genomics and cancer stem cell theory coincide with the efforts for early detection and imaging of tumor cells, as well as innovative anticancer therapeutics development. As a matter of fact, clinical practice has been deeply affected by this notion during the past couple of decades switching into an interest at the molecular level where nanotechnology applications also seem to more suitably and properly fit these needs. The advent of personalized nanomedicine as a new discipline in medicine and pharmacy by merging the nanotechnology and genomics knowledge could create improved profiles for specific populations and individual patients for prognosis, diagnosis and drug treatment protocols as well as monitoring across

medical research and clinical care. Through the application in everyday clinical practice of specialized nanomedicines that carry validated biomarkers or imaging signals, the improvement of diagnosis and therapy outcomes can be achieved in a cost-affordable way, as well in real-time by permitting the stratification of patients suffering the same illness. Furthermore, the parallel implementation of genomics knowledge unequivocally empowers the practical clinical utility of personalized medicine decisions to enter routine healthcare. Moreover, the clinical translation and exploitation of genomics knowledge to drug delivery decisions lead toward establishing pharmacotyping as the new direction in drug prescription process, where targeted nanovehicles as drug delivery systems could also contribute a lot. And this can be accomplished to ensure maximum both safety and efficacy profiles for most, if not all, individuals.

IMATINIB INTRACELLULAR UPTAKE IN LEUKOCYTES: METHOD FOR DETERMINATION AND CORRELATION WITH TREATMENT SUCCESS

Simon Žakelj, Eva Kralj, Jurij Trontelj, Albin Kristl

Faculty of Pharmacy, University of Ljubljana, Aškerčeva cesta 7, 1000 Ljubljana, Slovenia

With the introduction of imatinib to the therapy of Chronic Myeloid Leukemia (CML), an enormous progress was made, but options for individualization and optimization of therapy remained. The sub-optimal response of some patients can probably be linked to pharmacokinetic causes in the majority of cases. The relevance of uptake and efflux transport proteins seems to be great in the process of imatinib intestinal absorption as well as in its uptake from the blood to the target cells but is still poorly understood. The imatinib plasma concentrations, which are known to correlate well with the therapeutic success, are highly variable and are often not measured also because of technical or logistical difficulties involved. We have therefore analyzed the intestinal permeability and active transport of imatinib as well as introduced a DBS (Dried blood spots) technique for determination of imatinib plasma concentration with good accuracy (% bias < 13.2) and precision (CV < 10.3%). Furthermore, the intracellular concentrations of imatinib in leukocytes could not be measured at all. This was resolved by a two stage concentration in the sample-prep procedure coupled with a sensitive ultra-high performance liquid chromatography tandem mass spectrometry. A validation of all necessary method parameters has shown an impressive lower limit of quantification of 0.5 ng imatinib per 10⁶ cells, still at the signal to noise ratio of 670. Samples of mononuclear cells and granulocytes obtained from patients are being analyzed and the results obtained from the first group of patients are already available. The intracellular concentrations of imatinib in granulocytes are 20-fold higher than the blood plasma concentrations due to the activity of organic cation transporter 1 (OCT1). It is interesting that the measured activity of this transporter could prove to correlate with the therapeutic success even better than its end result – the intracellular imatinib concentrations.

**ORAL & POSTERS
EXTENDED ABSTRACTS**

OP001

PRECLINICAL EVALUATION OF $^{111}\text{In}/^{99\text{m}}\text{Tc}$ -LABELED HUMAN GASTRIN I ANALOGS IN THE DETECTION OF CCK2R⁺-CANCER

A. Kaloudi¹, E. Lymperis¹, E. P. Krenning², M. de Jong², B. A. Nock¹, T. Maina¹

¹. NCSR "Demokritos", Athens, Greece, ². Erasmus MC, Rotterdam, The Netherlands

E-mail: katerinakaloudi@yahoo.gr

As a part of our ongoing search toward successful localization of cholecystokinin subtype 2 receptor (CCK2R)-expressing cancer with the aid of radiopeptides (Laverman et al. 2011, Nock et al. 2005) we present three new radioligands: [^{111}In]SG1 ([^{111}In -DOTA)Gln¹,Nle¹⁵]GI, GI: pGlu-Gly-Pro-Trp-Leu-(Glu)₅-Ala-Tyr-Gly-Trp-Met-Asp-Phe-NH₂), [^{111}In]SG2 ([^{111}In -DOTA)Gln¹,DGLu⁶⁻¹⁰,Nle¹⁵]GI) and [$^{99\text{m}}\text{Tc}$]SG6 ([$^{99\text{m}}\text{Tc}$ -N₄)Gln¹]GI) and compare their biological profiles in CCK2R-expressing cells and mouse models. SG2 exhibited the highest binding affinity against [^{125}I -Tyr¹²,Leu¹⁵]GI during competition assays in A431-CCK2R(+) cell membranes (22°C/1 h), followed by SG1 and SG6 (Table 1). Labeling of SG1/SG2 with ^{111}In and SG6 with $^{99\text{m}}\text{Tc}$ afforded the respective radioligands in high yield and high purity, as verified by RP-HPLC. All radioligands specifically internalized in A431-CCK2R(+) cells (37°C/ 1 h) (Table 1). HPLC analysis of blood collected 5 min postinjection (pi) in healthy Swiss albino mice ranked radioligands according to stability as follows: [^{111}In]SG2 > [$^{99\text{m}}\text{Tc}$]SG6 > [^{111}In]SG1 (Table 1). Biodistribution studies in SCID mice bearing AR4-2J xenografts at 4 h pi revealed superior tumor uptake for [^{111}In]SG1 (5.7%ID/g) followed by [$^{99\text{m}}\text{Tc}$]SG6 (3.3%ID/g) and the (DGLu)⁶⁻¹⁰-substituted [^{111}In]SG2 (2.6%ID/g) (Figure 1). This trend was preserved for the CCK2R-positive mouse stomach. On the other hand, renal uptake was unfavourably high for [^{111}In]SG1 (Figure 1). These results demonstrate that radiopeptides based on human gastrin I sequences can effectively target CCK2R-positive tumors *in vivo*. They further demonstrate that metal-chelate and Glu⁶⁻¹⁰ by DGLu⁶⁻¹⁰-substitution greatly affect key biological parameters of end-radioligands, such as metabolic stability, tumor uptake and renal clearance.

GI analogs	IC ₅₀ * (nM)	% I	% PP
[$^{99\text{m}}\text{Tc}$]SG6	9.3	19	34
[^{111}In]SG1	3	25	28
[^{111}In]SG2	0.6	20	43

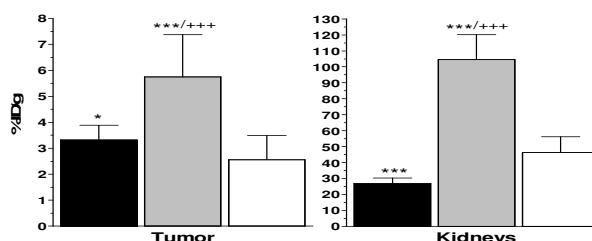


Table 1. Comparison of CCK2R affinities in A431-CCK2R(+) cell membranes, internalization in the cells and stability in mice. *non-metallated analogs, I= internalized, PP= Parent peptide.

Figure 1. Comparative uptake (%ID/g) for [$^{99\text{m}}\text{Tc}$]SG6, [^{111}In]SG1 and [^{111}In]SG2 in AR4-2J tumor-bearing SCID mice at 4 h pi. Statistically significant differences (*) between [^{111}In]SG1 and (†) between [$^{99\text{m}}\text{Tc}$]SG6 and the other radiopeptides: * $P < 0.05$, ***/ $****P < 0.001$ (Student's t-test).

References

- Laverman, P., Joosten, L., Eek, A., Roosenburg, S., Peitl, P.K., Maina, T., Mäcke, H., Aloj, L., von Guggenberg, E., Sosabowski, J.K., de Jong, M., Reubi, J.C., Oyen, W.J., Boerman, O.C., 2011. Comparative biodistribution of 12 ^{111}In -labelled gastrin/CCK2 receptor-targeting peptides. *J. Nucl. Med. Mol. Imaging* 38, 1410.
- Nock, B.A., Maina, T., Béhé, M., Nikolopoulou, A., Gotthardt, M., Schmitt, J.S., Behr, T.M., Mäcke, H.R., 2005. CCK-2/gastrin receptor-targeted tumor imaging with ($^{99\text{m}}\text{Tc}$)-labeled minigastrin analogs. *Eur. J. Nucl. Med. Mol. Imaging* 46, 1727.

OP002

STEROIDAL AROMATASE INHIBITORS IN BREAST CANCER RESEARCH. STRUCTURE AND SUBSTRATE-GUIDED DESIGN, SYNTHESIS AND STRUCTURE-ACTIVITY RELATIONSHIPS (SAR)

C. Varela^{a*}, F. Roleira^a, S. Costa^a, R. Carvalho^b, C. Amaral^{c,d}, G. Correia-da-Silva^{c,d}, N. Teixeira^{c,d}, E. Tavares da Silva^a

^a CEF, Center for Pharmaceutical Studies & Pharmaceutical Chemistry Group, Faculty of Pharmacy, University of Coimbra, Coimbra, Portugal

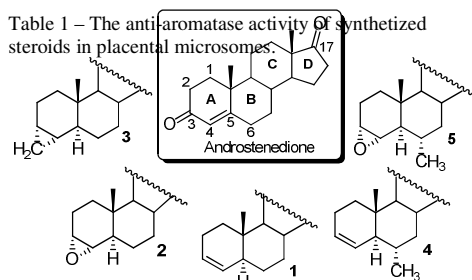
^b Faculty of Science and Technology & Center for Neuroscience and Cell Biology (CNC), University of Coimbra, Coimbra, Portugal

^c Faculty of Pharmacy, University of Porto, Porto, Portugal

^d Institute for Molecular and Cell Biology (IBMC), University of Porto, Porto, Portugal

Breast cancer is the most common malignancy in women worldwide. Many breast tumors are dependent on estrogens for their development and growth; hence controlling estrogen production has been one of the bases for treating this disease. This can be achieved by inhibiting aromatase, enzyme involved in the biosynthesis of estrogens. The recent elucidation of the active site of aromatase, which provided structural basis for the interactions with its ligands, was an important breakthrough (Ghosh et al., 2009). This has revealed and confirmed the establishment of hydrogen bonds between the C3- and C17-keto oxygen atoms of steroids and specific residues of the active site of the enzyme. Besides, in other studies was observed that C-6 alkyl substitution can be beneficial for aromatase inhibition, since the linear side chain can protrude into an access channel immobilizing catalytic residues.

In this work, we were interested in designing, synthesizing and evaluating the anti-aromatase activity of steroidal inhibitors obtained by introducing C-6 methyl substituents in strong aromatase inhibitors previously reported by our group (Fig. 1) (Varela et al., 2012). Further, we were interested in investigating how the planarity in the A-ring and the establishment of a C-3 hydrogen bond are important features for aromatase inhibition. For this, we synthesize and evaluate Δ^1 , Δ^2 , Δ^3 (**1**) and Δ^4 -olefins, the corresponding epoxides, and also a 3,4-cyclopropane derivative (**3**). Olefins were prepared by several strategies, and epoxides were synthesized by performic acid oxidation (Varela et al., 2012). Derivative **3** was prepared through an adaptation of the Simmon-Smith reaction. The two C-6 methyl derivatives **4** and **5** were prepared through a three- and four-step strategies.



Compounds	Aromatase Inhibition (%) \pm SEM ^{a)}	IC ₅₀ (μ M)
1	95.90 \pm 0.60	0.225
2	96.40 \pm 0.10	0.145
3	95.35 \pm 0.57	0.110
4	93.47 \pm 1.06	0.560
5	96.72 \pm 0.37	0.175
Formestane	99.65 \pm 0.06	0.042

Fig. 1. Structure of some synthesized androstenedione derivatives ^{a)}SEM: standard error of mean

The aromatase inhibitory activity of the modified steroids was evaluated in human placental microsomes by a radiometric assay (Varela et al., 2012). Considering the A-ring olefins and the respective epoxides, it was observed that olefins are generally more active than epoxides, except for **2** (Varela et al., 2012). Derivative **3** revealed to be more active than **2** (Table 1). Compounds **4** and **5** revealed to be very active, although slightly less potent than the corresponding derivatives without the alkyl substituent (compare **4** with **1**, and **5** with **2**) (Table 1).

In summary, some of the synthesized compounds are potent AIs, confirming that planarity in A,B-ring is important for aromatase inhibition. The 3,4-epoxide **2** is slightly more potent than the corresponding olefin **1** allowing hypothesizing that 3,4-epoxide oxygen resembles the carbonyl oxygen of androstenedione, the natural aromatase substrate (Varela et al., 2012). Nevertheless, the 3,4-cyclopropane derivative **3** revealed to be even more potent than **2** showing that, besides the C-3 hydrogen bond, other features contribute for an efficient aromatase inhibition.

REFERENCES

Ghosh, D., Griswold, J., Erman, M., Pangborn, W., 2009. Structural basis for androgen specificity and oestrogen synthesis in human aromatase. *Nature* 457, 219-224.

Varela, C., Tavares da Silva, E., Amaral, C., Correia da Silva, G., Baptista, T., Alcaro, S., Costa, G., Carvalho, R.A., Teixeira, N.A.A., Roleira, F.M.F., 2012. New structure-activity relationships of A- and D-ring modified steroidal aromatase inhibitors: design, synthesis, and biochemical evaluation. *J. Med. Chem.* 55, 3992-4002.

*Corresponding author e-mail address: carla.varela@portugalmail.com

OP004

Pharmacological profile of essential oils from *Aloysia citriodora* Palau & *Melissa officinalis* L. Relevance to neurodegenerative disease

Sawsan Abuhamdah^{1*}, Suleiman Olimat¹, Rushdie Abuhamdah² and Paul.Chazot²

1. Faculty of Pharmacy, University of Jordan, Amman, Jordan

2. School of Biological & Biomedical Sciences, Durham University, Durham, UK

*Corresponding author: s.abuhamdah@ju.edu.jo

In traditional medical practice, numerous plants have been used to treat symptoms common in neurodegenerative diseases.

A detailed pharmacological study of essential oils derived from *Aloysia citriodora* Palau (Lamiaceae) leaves, cultivated in Jordan and locally known as 'Melissa', was performed in comparison to the pharmacological properties of the essential oil from *Melissa officinalis* L. (Lamiaceae), known as 'Melissa' and cultivated in Europe.

Essential oils derived from dried and fresh leaves of *Aloysia citriodora* and *Melissa officinalis* were analysed by GC/MS and were investigated pharmacologically.

The major components detected in *Aloysia citriodora* oils from dried and fresh leaves included: limonene (20.1, 13.6%), geranial (6.3, 20.1%), neral (3.7, 15.1%), 1,8-cineole (9.4, 9.2%), curcumene (6.3, 3.5%), spathulenol (5.0, 3.1%) and caryophyllene oxide (8.4, 2.2%), respectively. A number of these components were shared with *Melissa officinalis*, but a number were distinct. Fresh *Aloysia citriodora* leaf essential oil inhibited [³H] nicotine binding to well washed rat forebrain membranes (apparent mean IC₅₀ = 0.0018 mg/ml), whereas *Melissa officinalis* elicited no significant effect. In contrast, the former elicited no effects on GABA_A receptors, while the latter elicited a dose-dependent inhibition of [³⁵S] TBPS binding to the GABA_A receptor (IC₅₀ 0.040± 0.001mg/mL). *Aloysia citriodora* displayed concentration-dependent anti-cholinesterase inhibitory properties, DPPH radical scavenging effect and moderate anti-oxidant activity in a ferrous chelating test (all at 0.01 mg/ml and above), while *Melissa officinalis* lacked these properties (up to 1 mg/ml).

we report for the first time that *Aloysia citriodora* essential oils have a diverse range of pharmacological properties, suggesting potential as a source for plant-based treatment of degenerative diseases.

Table 1: Comparative constituents of EOs derived from *Aloysia citriodora* Palau. & *Melissa officinalis* L.

References:

	<i>Aloysia citriodora</i> Palau.	<i>Melissa officinalis</i> L.
Major Constituents		
GC-MS Analysis		
Monoterpenoids	Limonene 13.6% 1,8-cineole 9.2% Neral 15.1% Geranial 20.1%	Geranial 31.3% Neral 21.7%
Sesquiterpenoids	Caryophyllene oxide 2.2% Curcumene 3.5% Spathulenol 3.1%	Caryophyllene 12.2% Caryophyllene oxide 3.7% ^[29]

• Huang L, Abuhamdah S, Howes MJ, Dixon CL, Elliot MS, Ballard C, Holmes C, Burns A, Perry EK, Francis PT, Lees G, Chazot PL., *J Pharm Pharmacol.* 11, 1515-22 (2008).

• Abuhamdah S., Abuhamdah R., Howes MJ, Olimat S. & Chazot.P. Pharmacological profile of an essential oil derived from leaves of lemon verbena (*Aloysia citriodora* Palau): cholinergic, anti-oxidant and iron chelation properties. *J Pharm Pharmacol.* (InPress).

OP005

***In vitro* antitumor activity of *Sarcopoterium spinosum* leaf extract with bioactive natural compounds**

Ceren Sunguc^a, Ipek Erdogan^a, Mehmet Emin Uslu^a, Oguz Bayraktar^{b*}

^a Izmir Institute of Technology, Department of Biotechnology and Bioengineering Department, Izmir, Turkey

^b Izmir Institute of Technology, Department of Chemical Engineering, Izmir, Turkey

* Corresponding author. Address: Izmir Institute of Technology, Department of Chemical Engineering, Izmir, Turkey. Tel: +90 2327506657 Fax: +90 2327506645.

E-mail address: oguzbayraktar@iyte.edu.tr

Cancer cell lines cause generation of reactive oxygen species and free radicals at high levels (Wang and Yi, 2008). Then generated free radicals lead to breakdown of the structure of DNA, lipid or protein (Gul et al., 2011). When plant extracts including antioxidant phytochemicals are exposed to the redox reactions, the harmful effects of free radicals are effectively prevented. The aim of present research was to evaluate the antitumor potential of the extract derived from *Sarcopoterium spinosum* leaves. The leaves of *S. spinosum* were collected in Izmir, Turkey. Total phenol content of ethanolic extract of *S. spinosum* leaves was determined using Folin-Ciocalteu method. Total antioxidant capacity of the extract was measured with ABTS⁺ assay. The cytotoxicity of the extract on different cell lines was performed using MTT viability assay. In order to explain the results at molecular level, Real time-PCR (RT-PCR) was used. *Caspase 3* expression level was used as an indicator of apoptosis. *S. spinosum* leaf extract had significant total antioxidant capacity, along with high total phenolic content. Our results revealed the *in vitro* cytotoxic activities of *S. spinosum* leaf extract against different cancer cell lines and normal cell line. The leaf extract of *S. spinosum* showed promising cytotoxic activities at low concentration range, between 50 µg/ml and 200 µg/ml, against breast cancer cell line (MCF7) and colon cancer line (Caco2). On the other hand, it was not cytotoxic to mouse fibroblast cell line (NIH-3T3). Among cancer cell lines, the MCF7 cell line was found to be the most sensitive against the extract treatment. Cytotoxic activity was also confirmed with increased *caspase 3* expression level retrieved from RT-PCR analysis. *Caspase 3* expression level was lowest for 3T3 fibroblast cells. MCF7 cells were more prone to apoptosis, in the presence of extract.

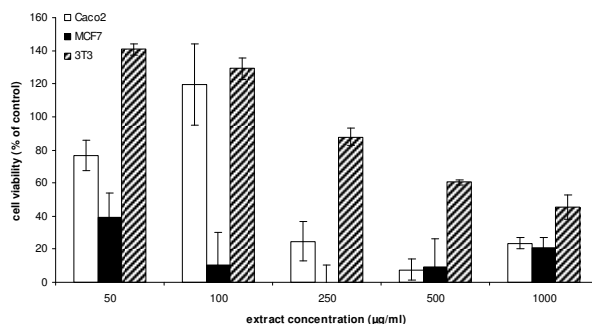


Figure 1. Cell viability of *S. spinosum* extract-treated cell lines. Caco2, MCF7 and 3T3 represent colon cancer, breast cancer and fibroblast cell lines, respectively.

The extracts obtained from the *S. spinosum* leaves may represent an important source of novel potential antitumor natural compounds due to their significant and selective cytotoxic actions towards different cancer cell lines.

References

- Wang, J., Yi, J., 2008. Cancer cell killing via ROS: To increase or decrease, that is the question. *Cancer Biology & Therapy*. 7, 1875-1884.
- Gul, M.Z., Bhakshu, L.M., Ahmad, F., Kondapi, A.K., Qureshi, I.A., Ghazi, IA. 2011. Evaluation of *Abelmoschus moschatus* extracts for antioxidant, free radical scavenging, antimicrobial and antiproliferative activities using *in vitro* assays. *BMC Complement Altern Med*. 11: 64.

OP008

ANTI-BACTERIAL ACTIVITY OF NOVEL BIOADHESIVE OFLOXACIN OCULAR INSERTS

N. Üstündağ Okur¹, E. Homan Gökçe¹, A. Yoltaş², G. Ertan¹, Ö. Özer¹

¹ Faculty of Pharmacy, University of Ege, Bornova, Izmir, Turkey

² Faculty of Science, University of Ege, Bornova, Izmir, Turkey

The aim of the present study was to develop novel insert formulations and compare their antibacterial activity for ocular application for treatment of bacterial keratitis. NLC formulation (F1) was prepared by means of high shear homogenization method employing oleic acid(1.456%) as oil, Compritol HD5 ATO(0.728%) as solid lipid, Tween 80(0.728%) as surfactant, and water(97.088%). Insert formulation was prepared by means of solvent casting. F1 was mixed with 0.75% chitosan oligosaccharide lactate (COL) or alginate and 5% of glycerin or PEG 400 was added as plasticizers. The mixture was poured onto the petri dishes and dried at 40°C for 36h to obtain inserts. Formulations were loaded with 0.3% ofloxacin(OFX). Bioadhesion was quantified using a Texture Profile Analyzer. Minimum Inhibitory Concentration(MIC) defined as the lowest concentration of material that inhibits the growth of an organism (1), was performed with gram negative *E. coli* ATCC 8739 and gram positive methicillin susceptible *S. aureus* ATCC 29213 the as recommended Clinical and Laboratory Standards Institute(CLSI). Microorganisms were incubated at Mueller-Hinton II Agar medium at 37°C for 17-18 hours. After the incubation, pure cultures of the microorganisms were prepared in sterile saline solution (0.85%) and were adjusted to give an inoculum with an equivalent cell density to 0.5 McFarland turbidity standard. 1 g/mL OFX concentration were studied. 100µL of sterile Mueller-Hinton II broth, 100 µL microorganism suspension and 100 µL prepared OFX concentrations transferred to each well and incubated for 24h at 37°C. After incubation, turbidity of microplate wells were observed. Disc diffusion method was used to evaluate antimicrobial activity of the inserts against *E. coli* ATCC 8739 and *S. aureus* ATCC 29213 according to the guidelines of CLSI. Pure cultures of the microorganisms were prepared in sterile saline solution and were adjusted to give an inoculum with an equivalent cell density to 0.5 McFarland turbidity standard. 100 µl of each suspension were spreaded evenly onto Mueller-Hinton II Agar and allowed to dry. Sterile discs were then placed onto agar plates and 10 µl of every formulation was applied to the discs. Plates were incubated at 37°C for 24 to 48h and the zone diameters of each formulation for each isolate were measured (2).

Inserts which on the basis of NLC formulations, were obtained successfully. Chitosan inserts contains glycerin as plasticizer was found more bioadhesive than alginate inserts (Table 1).

Table 1: Formulation components and results of bioadhesion

Formulations	Components	Force (N)	AUC
F2	COL (0.75%) + Glycerin	0,293±0,003	1,835±0,155
F3	COL (0.75%) + PEG 400	0,138±0,017	0,295±0,022
F4	Alginate (0.75%) + Glycerin	0,157±0,010	1,135±0,258
F5	Alginate (0.75%) + PEG 400	0,115±0,009	0,176±0,018

MIC value of test inserts and OFX solution against *E. coli* and *S.aureus* was observed 0,390µg/mL and 0,781µg/mL, respectively at 48h. The diameter of inhibition zone reflects magnitude of susceptibility of the microorganism. The chitosan acted as an anti-bacterial agent so growth inhibition ring of chitosan insert was found 36 and 49mm against *S. aureus*

and *E. coli*, respectively. The growth inhibition ring of *S. aureus* and *E. coli* treated by alginate inserts was 35 and 40mm, respectively. The chitosan inserts had higher anti-bacterial activity than the alginate inserts

This study revealed that inserts containing COL showed highest anti-bacterial activity and thus could be suggested as an alternative ocular drug carrier for OFX.

Reference

1. Qi L et al. 2004. *Carbohydr Res*;339:2693–700.

CLSI, 2008. CLSI Document M100-S18, *Clinical and Laboratory Standards Instit*

OP009

PACLITAXEL RELEASE FROM PH SENSITIVE LIPOSOMES: COMPARISON BETWEEN DIALYSIS AND ULTRAFILTRATION

METHODS

J. O.Eloy, J.M.Marchetti

College of Pharmaceutical Sciences of Ribeirão Preto – University of São Paulo

eloy@fcrp.usp.br

The aims of this study were to prepare and characterize a liposomal formulation composed by dioleoylphosphatidylethanolamine (DOPE) and oleic acid (OA) to encapsulate paclitaxel and evaluate its release, compared through the dialysis and ultrafiltration methods. Furthermore, the pH sensitivity of the formulation was investigated. Liposomes were prepared according to the thin-film hydration method.¹ Briefly, drug and lipids were solubilized in chloroform and submitted to rotaevaporation until formation of a lipid film, which was hydrated using 8.0 pH phosphate buffer. Suspension was then homogenized under pressure. Liposomes were characterized by dynamic light scattering and paclitaxel encapsulation efficiency. Liposomes were evaluated for paclitaxel release in 50 mL pH 5.0 and 7.4 phosphate buffers containing 1% sodium lauryl sulfate with agitation speed at 150 rpm. In this study, samples were placed inside PVC tubes wrapped with 50 KDa MWCO (molecular weight cut-off) cellulose dialysis membranes and connected to the dissolution shafts of the apparatus 1. In the experiments that evaluated the ultrafiltration method, samples were placed directly in the vessels, agitated with minipaddles, and the released drug was separated from encapsulated drug by ultrafiltration using Amicon 50 KDa MWCO ultra-2 centrifugal filter units (Millipore). Samples were collected until 72 h and were analyzed by high pressure liquid chromatography, using a 25 mm C-18 column with 5 µm particles, mobile phase with acetonitrile and water (50:50, v/v) at a flow rate of 1 mL/min and wavelength at 227 nm. Characterization studies demonstrated that the liposomal formulation exhibited nanometric size and high paclitaxel encapsulation efficiency (Table 01). Figure 01 showed that using the conventional dialysis method, paclitaxel was slowly released from the commercial solution, but was rapidly and completely released when the ultrafiltration method was employed. The liposomal formulation released only 5% and 30% after 72 h in pHs 7.4 and 5.0, respectively, with the dialysis method. Using the alternative ultrafiltration method, however, drug release was considerably higher, equivalent to 75% and 100% after 72 h in pH 7.4 and 5.0, respectively. Thus, the dialysis method provided slower release results, which could be a consequence of drug interaction with cellulose dialysis membrane, as already reported.² In conclusion, the ultrafiltration method seems to be more appropriate to evaluate paclitaxel release. Moreover, the enhanced paclitaxel release from DOPE and OA liposome in acid buffer was demonstrated.

Table 01. Liposomal characterization.

Analytical Characterization	Result
Particle Size (nm)	167,5
Encapsulation Efficiency (%)	68,2

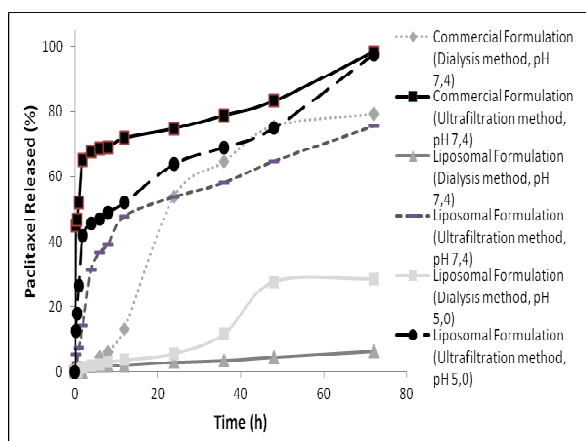


Figure 01. Paclitaxel *in vitro* release

References

- ¹ YANG, T. et al. Enhanced solubility and stability of PEGylated liposomal paclitaxel: In vivo and In vitro evaluation. **International Journal of Pharmaceutics**, v. 338, p. 317-326, 2007.
- ² ZAMBITO, Y., PEDRESCHI, E., DI GOLO, G. Is dialysis a reliable method for studying drug release from nanoparticulate systems? – A case study. **International Journal of Pharmaceutics**, v. 434, p. 28-34, 2012.

OP010**PREPARATION , CHARACTERIZATION AND RELEASE STUDY OF MICROSPHERES LOADED WITH MYCOPHENOLIC ACID USING DIFFERENT RATIOS OF TWO MOLECULAR WEIGHT PLGA.****Israa H. Al-Ani * , Alaa A. Abdulrasool** and Jabar A. Faraj*** Faculty of Pharmacy and Medical Sciences, Al-Ahliyya Amman University, Jordan, dr_issra@yahoo.com

** College of Pharmacy, Baghdad University.

Microspheres as controlled drug delivery technology has proved many advantages in controlling drug release for long period of time. Different types of polymers have been used in preparation of microspheres with different characteristics. Biodegradable polymers offer the advantage of being degraded in the body to biocompatible materials, thus no need to remove the residuals after drug release. The aim of this study was to investigate the effect of molecular weight of the carrying polymer (PLGA) on the pattern, mechanism and time of release of mycophenolic acid from prepared microspheres using different ratios of two different molecular weight PLGA (RH202 and RH203).

The microspheres were prepared by solvent evaporation method and characterized for their morphology, yield value, loading efficiency, size distribution, bulk density, degree of hydration and DSC analysis. Six batches with different ratios of both polymers were prepared as in table(1). Then the release of the drug was studied in 37 °C phosphate buffer saline pH 7.4 using suitable dialysis cell.

Results showed that ratio of 40:60 RH202:RH203 gave the most uniform zero-order drug release over 70 days in phosphate buffer saline pH 7.4 and 37°C with anomalous type of drug diffusion in addition to polymer erosion.

SEM photos taken in different stages of drug release showed the gradual loss of microspheres spherical shape which may be the cause behind the anomalous diffusion of the drug due to the non uniform hydrolysis of the polymer. However batch C which contains (40:60 RH202:RH203) could preserve zero –order release over about 70 days. Other used ratios gave less uniform drug release that could not meet the criteria of controlled drug delivery systems.(Figure1)

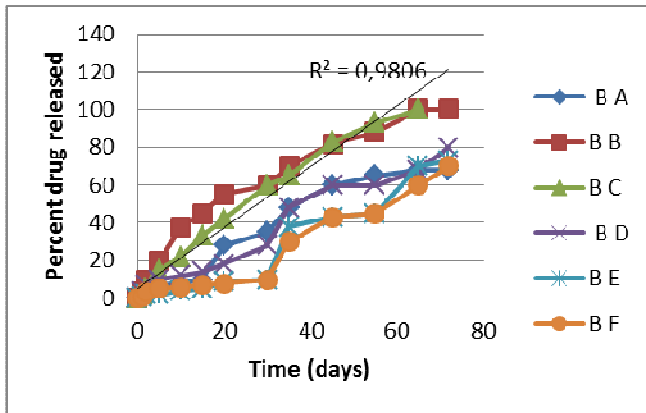
In addition mycophenolic acid showed high stability in the release media since nearly 100% of its mass was recovered suggesting good stability of the prepared microspheres.

It was concluded that mycophenolic acid can be loaded on two molecular weight PLGA blend successfully with good yield value and loading efficiency and ratio of 40:60 RH202:RH203 gives zero –order drug release in vitro for about 70 days in phosphate buffer saline pH 7.4

Table 1 : Composition of Mycophenolic Acid Microspheres of the Prepared Batches Using A Mixture of Different Ratios of R202H and R203H PLGA.

Batch code	A	B	C	D	E	F
% R202H	100	80	40	30	10	0
% R203H	0	20	60	70	90	100

Figure1. Release profile of mycophenolic acid from the prepared six batches of microspheres in 0.1M PBS pH 7.4 at 37°C.



Key words: microspheres, PLGA, RH202 and RH203, mycophenolic acid, zero-order release, controlled drug release.

OP012

COLD ATMOSPHERIC-PRESSURE PLASMA FOR LIPOSOMAL MEMBRANE DISRUPTION

S. H. Matrali¹, P. Svarnas², F. Clément³, S. G. Antimisiaris^{1,4}

¹ University of Patras, Department of Pharmacy, Laboratory of Pharmaceutical Technology, 26504 Rion, Greece

² University of Patras, Department of Electrical and Computer Engineering, High Voltage Laboratory, 26504 Rion, Greece

³ Université de Pau et des Pays de l'Adour, IPREM – LCABIE, Plasmas et Applications, 64000 Pau, France

⁴ FORTH/ICES, 26504 Rion, Greece (santimis@upatras.gr)

The possibility of using atmospheric-pressure cold plasma of electrical discharges instead of detergents for disrupting liposomal membranes is investigated. The plasma system, the chemically reactive species produced and the related physical mechanisms have been considered elsewhere [Svarnas et al. (2012); Gazeli et al. (2013)]. The used gas is helium (N50) flowing free in the atmospheric air.

In this work, large multilamellar vesicle liposomes (MLVs) consisting of phosphatidylcholine (PC), cholesterol (Chol) and phosphatidylglycerol (PG) are prepared by the thin film hydration technique and subjected to plasma treatment. Liposomes encapsulate calcein (100 mM), i.e. a small hydrophilic dye whose plasma-induced release from liposomes is used as a measure of liposome membrane integrity and consequently of the plasma action on the lipid bilayers. A parametric study takes place and the principal results are depicted in **Figure 1** or discussed below.

The effect of plasma treatment increases with the increase of lipid concentration. Samples with negative surface charge (PG) showed significant release of calcein (ca. 10% of the initial encapsulation) after only 2 min of treatment. More calcein (up to 11%) was released from all the samples as the treatment became longer (2 to 4 min). These effects that are manifested for samples with a volume of 100 μ L were not (or only marginally) observed when the specimen volume was doubled (200 μ L). On the other hand, post-treatment effect on the samples was observed for this double volume only; the reduction immediately after plasma treatment found to be practically 0%, but reached 7% after 48h and up to 17% after 96 hours. Both the direct and post-treatment influences of the flowing gas itself were always negligible as compared to those with the plasma switched-on, under the same experimental conditions.

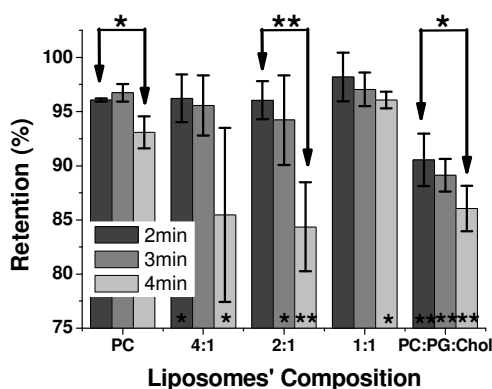


Figure 1: Calcein release from MLV liposomes (60 mg/mL, 100 μ L) following plasma treatment for 2, 3 and 4 min. MLVs consisting of PC/Chol are denoted by their PC:Chol ratio. PC:PG:Chol was 9:1:5 (mol). Significance is marked with * ($p < 0.05$) or ** ($p < 0.01$).

The above representative results, suggest a new way for liposomal membrane disruption, based on the dry chemistry of cold plasmas. Their importance is however wider. Cold plasma reactors are promising modern medical devices for many bio-applications [Svarnas et al. (2012); Gazeli et al. (2013)] and their design could be probably facilitated by testing them on specific liposomes used e.g. as cell models._

REFERENCES:

- Svarnas P., Matrali S. H., Gazeli K., Aleiferis Sp., Clément F., Antimisiaris S. G., 2012. Appl. Phys. Lett. 101, 264103
- Gazeli K., Svarnas, P., Vafeas, P., Papadopoulos, P. K., Gkelios, A., Clément, F., 2013, J. Appl. Phys., in press

OP013

FORMULATION OF NOVEL BRINZOLAMIDE NANOCRYSTAL SUSPENSIONS FOR OPHTHALMIC DELIVERY: REDUCTION OF ELEVATED INTRAOCULAR PRESSURE *IN VIVO*

A. Sarnes¹, P. Liu¹, J. Puranen², S. Rönkkö², T. Laaksonen¹, G. Kalesnykas^{2,3}, Johanna Laru⁴, Olli Oksala⁵, Jukka Ilkka⁶, K. Järvinen², J. Hirvonen¹, L. Peltonen¹

¹ University of Helsinki, Helsinki, Finland

² University of Eastern Finland, Kuopio, Finland

³ Kuopio University Hospital, Kuopio, Finland

⁴ Orion Pharma R&D, Formulation Research, Espoo, Finland

⁵ Santen Oy, Tampere, Finland

⁶ Oy Medfiles Ltd., Kuopio, Finland

Corresponding author: annika.sarnes@helsinki.fi

Ocular drug delivery is considered to be among the most challenging and fascinating research areas within pharmaceutical drug development, because of the complex, pharmacokinetically delicate and demanding environment of the eye. Nanocrystal-based drug delivery systems provide efficient tools for ocular formulation development, especially when considering poorly soluble drugs. The objective was to formulate ophthalmic, intraocular pressure reducing, nanocrystal suspensions from a poorly soluble drug, brinzolamide (BRA), using a rapid wet milling technique [1]. Different stabilizers (hydroxypropyl methylcellulose (HPMC), poloxamer F127 and F68, polysorbate 80) for the nanocrystals were screened. In order to investigate both the effect of an added absorption enhancer (polysorbate 80) and the impact of the amount of free drug in the nanocrystal suspension, formulations in phosphate buffered saline (PBS) at pH 7.4 and pH 4.5 were prepared. Particle size, polydispersity (PI), solid state (DSC), morphology (SEM, TEM) as well as dissolution behavior and the uniformity of the formulations were characterized. The effects of nanocrystal formulations on human corneal epithelial cell (HCE-T) viability were tested. Elevated intraocular pressure (IOP) lowering effect was investigated *in vivo* using a rat ocular hypertensive model. Marketed BRA product was used as control throughout the study.

BRA nanocrystal suspensions (450 – 530 nm / PI 0.1 - 0.2) were successfully prepared by wet milling in PBS pH 7.4 and pH 4.5, using HPMC as stabilizer. The final nanocrystal formulations I-III (BRA, 1 w/v%; HPMC, 0.25 w/v%; benzalkoniumchloride 0.01 w/v%; with and without polysorbate 80, 0.25 w/v%) were obtained by diluting the nanocrystal suspensions with PBS pH 7.4 or pH 4.5, respectively (Table 1). Both the uniformity of the formulations and the remained crystalline state of BRA after milling were confirmed. The rapid dissolution of BRA (in PBS pH 7.4) from all the nanocrystal formulations was demonstrated; after one minute 100 percent of the drug was fully dissolved. The slow dissolution of unmilled bulk BRA was proven as well; only 50 percent of the drug was dissolved after 30 min. Prior to the *in vivo* experiments the effects of the nanocrystal formulations and the marketed product on the cell viability were proven to be comparable. Experimentally elevated IOP reduction was evidenced *in vivo* with all the formulations. The effect was significantly pronounced at pH 4.5, where the amount of free drug was at its highest. Notably, the experimentally elevated IOP reduction was comparable to the marketed product. In conclusion, three ophthalmic BRA nanocrystal formulations in PBS (pH 4.5 and 7.4), which all showed advantageous dissolution and absorption behavior, were successfully developed using a straightforward rapid wet-milling technique. The results are applicable in general to the formulation development of poorly water-soluble compounds. Additionally, in contrast to the polymeric nanoparticles, nanocrystal suspensions confer a clear regulatory

advantage, since they contain no matrix material and only consist of the drug and a comparatively small amount of stabilizer. In conclusion, the results revealed that nanocrystal suspensions are extremely potential candidates for ophthalmic drug delivery and valid therapeutic approaches.

References

[1] P. Liu, X. Rong, J. Laru, B. van Veen, J. Kiesvaara, J. Hirvonen, T. Laaksonen, L. Peltonen, Nanosuspensions of poorly soluble drugs: Preparation and development by wet milling, *Int. J. Pharm.* 411 (2011) 215-222.

OP014

TARGETING HELA CELLS USING HEPATITIS B VIRUS-LIKE PARTICLE (HBVLP) DECORATED WITH NANOGLUE-CELL-INTERNALIZING PEPTIDES

K. W. Lee^{1,*}, B. T. Tey³, K. L. Ho², B. A. Tejo², W. S. Tan²

¹. Taylor's University Lakeside Campus, Subang Jaya, Selangor, Malaysia

². Universiti Putra Malaysia, UPM Serdang, Selangor, Malaysia

³. Monash University, Bandar Sunway, Selangor, Malaysia

*khaiwooi.lee@taylors.edu.my/khaiwooi_2@yahoo.com

Recombinant viruses have been employed as a delivery vector to deliver therapeutic DNA materials and drugs into cells. In viral vector development, retroviruses, adenoviruses, adeno-associated viruses and herpesviruses have been widely used as human gene therapy. These viruses have been genetically engineered to incorporate therapeutic nucleic acids of interest, and delivered into a specific host cells in their replicative cycle. This approach is complicated and labour-intensive. Furthermore, it may have the risk of mutagenesis and oncogenesis. Nanoparticles and recombinant virus-like particle (VLP) are highly organised structure with discrete size and shape. They can be easily manufactured in large quantity and moulded to fit specific needs via genetic or chemical modification. Numerous studies on the employment of nanoparticles and VLPs for targeted drug and gene delivery have been reported. The recombinant hepatitis B virus core antigen (HBcAg) produced in bacterial system self-assembles into hollow icosahedral VLP (HBVLP) which can be served as potential nanovehicle. HBVLP possesses repetitive amino acid residues which contain functional side chains for chemical modification (Fig. 1). The modification sites can either be the natural amino acid (aa) residues or the genetically inserted aa residues in the viral proteins. We have shown previously that the chimeric HBcAg system, displaying a liver specific ligand at its N-terminus was able to deliver fluorescein molecules into liver cells, *in vitro* (1). Therefore, it is important to investigate the common ligand display capability of the HBVLP in order to facilitate the development of HBVLP into a cell-targeting delivery system. In this study, the HBV capsid-binding peptide (CBP; nanoglue) was employed to present HeLa cell-internalizing peptides (CIPs) on the HBVLPs. The CIP was co-synthesized at the N-terminal end of the CBP and conjugated at the tips of the spikes of the HBVLPs by using chemical cross-linkers (CIP-HBVLPs). In order to assess the potential of the CIP-HBVLPs as a delivery vehicle, fluorescent molecules were employed and tested on HeLa cells *in vitro* (2). Fluorescence microscopy showed that HBVLPs carrying the fluorescent molecules were translocated into HeLa cells by using this method (2). This study demonstrated a proof of principle for cell-targeting delivery via CBP conjugation on HBVLPs.

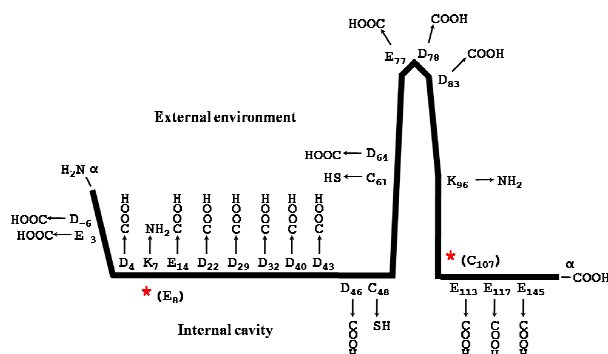


Fig. 1: The exposure of aa functional groups for HBcAg polypeptide (subtype *adyw*). E₈ and C₁₀₇ are not accessible.

REFERENCES

1. Lee, K. W., Tey, B. T., Ho, K. L., Tan, W. S., 2012. Delivery of chimeric hepatitis B core particles into liver cells. *J. Appl. Microbiol.* **112**. 119-131.
2. Lee, K.W., Tey, B.T., Ho, K.L., Tejo, B.A., 2012. Nano-glue: An alternative way to display cell-internalizing peptide (CIP) at the spikes of hepatitis B virus core nanoparticles for cell-targeting delivery. *Mol. Pharm.* **9**, 2415-2423.

OP015

PEO-b-PCL/DPPC chimeric nanocarriers: self-assembly aspects in aqueous and biological media and drug release studies

Natassa Pippa^{1,2}, Stergios Pispas², Aristides Dokoumetzides¹, Costas Demetzos^{1,*}

¹Department of Pharmaceutical Technology, Faculty of Pharmacy, National and Kapodistrian University of Athens, Athens, Greece

²Theoretical and Physical Chemistry Institute, National Hellenic Research Foundation, Athens, Greece

(*) Corresponding author: Prof. Costas Demetzos; e-mail: demetzos@pharm.uoa.gr

In this work, we report on the self assembly behavior and on stability studies of mixed amphiphilic nanosystems consisting of DPPC (dipalmitoylphosphatidylcholine) and poly(ethylene oxide)-b-poly(ϵ -caprolactone) (PEO-b-PCL) block copolymer in HPLC-grade water, phosphate buffer saline (PBS) and fetal bovine serum (FBS). These nanosystems are sterically stabilized nanovectors and can be utilized as chimeric advanced Drug Delivery nano Systems (aDDnSs) with stealth properties (Pispas 2011). A gamut of light scattering techniques (static, dynamic and electrophoretic) and fluorescence spectroscopy were used in order to extract information on the structure, morphology, size, effective charge and internal nanostructure of the nanoassemblies formed, as a function of block copolymer content, as well as temperature and concentration. The incorporation of PEO-b-PCL leads to nanoassemblies of smaller size. All the mixed formulations were found to retain their original physicochemical characteristics for the course of two weeks. The hydrodynamic radii (R_h) of mixed nanosystems decreased in the process of heating up to 50°C (Fig. 1). Gradual degradation of the polymeric chain in an acidic dispersion medium, which leads to gradual structural changes of the chimeric nanovectors, was observed (Pippa et al., 2013). The micropolarity of the hydrocarbon region of nanocarriers changed significantly in HPLC grade water and PBS with increasing block copolymer content. The incorporation of indomethacin (IND) led to a decreased size of chimeric nanocarriers (Table 1). The incorporation efficiency of mixed liposomal/block copolymer formulations for IND was increased in PBS in comparison to the HPLC-grade water, due to electrostatic interactions between drug molecule and choline headgroups. It is observed that the *in vitro* release of the drug from the prepared chimeric nanostructures is quite fast especially for the mixed nanovectors prepared with the lower ratio of gradient block copolymer (Pippa et al., 2013). The combination of block copolymers with liposomes for the development of a novel chimeric nanovector appears very promising, mostly due to the fact that the PEO-b-PCL acts as a modulator for the release rate of IND. PEO-b-PCL grafted DPPC liposomes are found to be effective nanocontainers for the encapsulation of IND, especially at the highest molar ratio of the block copolymer.

References

Pippa, N., Kaditi, E., Pispas, S., Demetzos, C., 2013. PEO-b-PCL/DPPC chimeric nanocarriers: self-assembly aspects in aqueous and biological media and drug incorporation. *Soft Matter* 9, 4073-4082.

Pispas, S., 2011. Vesicular structures in mixed block copolymer/surfactant solutions. *Soft Matter* 7, 8697-8701.

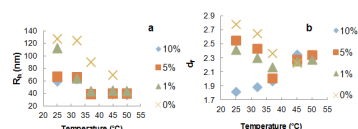


Fig. 1. (a) R_h and (b) d_f vs. temperature for DPPC:PEO-b-PCL mixed liposomes with 0, 1, 5 and 10mol% of incorporated block copolymer.

Composition DPPC:PEO- PCL :IND	R_h (nm)	d_f	% IE
9:0.1:1	32.5	2.6	10.6
9:0.5:1	34.1	2.4	11.5
9:1:1	38.4	1.9	13.5

Table 1. The physicochemical characteristics of mixed liposomes incorporating indomethacin (IND).

OP017

INVESTIGATION OF ELECTROSPUN NANOFIBERS AND THEIR INFLUENCE ON CELL GROWTH

J. Pelipenko¹, P. Kocbek¹, J. Zupan¹, J. Kristl^{1*}

¹ University of Ljubljana, Faculty of Pharmacy, Ljubljana, Slovenia

*julijana.kristl@ffa.uni-lj.si

Electrospun polymeric nanofibers are gaining increasing importance in the field of biomedicine, including tissue engineering, wound healing and drug delivery applications. In tissue regeneration nanofibers mimic the fibrillar elements of natural extracellular matrix, which provides biological and physical support for cell growth. The aim of our work was to prepare well-characterized poly(vinyl alcohol) (PVA) nanofibers, to evaluate their properties, and to investigate the influence of their thickness and alignment on cell growth in order to discover the crucial properties for clinical use.

Aqueous solution of PVA (Mowiol[®] 20–98, Mw 125,000 g/mol) was used for preparation of electrospun nanofibers, which were subsequently thermally stabilized. Morphological properties, mechanical characteristics and swelling behavior of produced nanofibers were investigated. Cells, either keratinocytes or fibroblasts, were seeded on nanofibrillar support (randomly oriented or aligned nanofibers) or glass coverslip used as a control. The rate of cell adhesion was determined by counting of unattached cells, while cell migration by agarose drop assay. Proliferation was tested by MTS assay and effect of nanofibrillar support on cell morphology was evaluated by confocal fluorescence microscopy. Additionally, the effect of PVA nanofibers on cell gene expression was determined by PCR after 3 and 6 days of incubation.

Optimization of polymer solution and electrospinning conditions enable preparation of beadless PVA nanofiber, which were resistant to rapid aqueous dissolution after thermal treatment. The keratinocyte attachment rate on PVA nanofibers was determined to be lower compared to their attachment to glass coverslip used as a control. Cell morphology was strongly influenced by nanotopography and alignment of nanofibers. The morphology was less spread when cells were grown on randomly oriented nanofibers (Fig. 1A) compared to cells growth on glass coverslip (Fig. 1C). On the other hand, it was shown that aligned nanofibers can successfully direct the migration and proliferation of cells (Fig. 1B). The influence of the thickness of nanofibrillar supports on cell metabolic activity and morphology was also confirmed. Mobility of cells grown on randomly oriented nanofibers was limited due to partial cell entrapment between nanofibers. Randomly oriented nanofibers increased proliferation of keratinocytes, while decreased proliferation of fibroblasts. Aligned nanofibers strongly increased proliferation of keratinocytes, while the proliferation of fibroblasts was comparable to the proliferation of fibroblast grown on glass coverslip. Nanofibers significantly affected gene expression in keratinocytes and fibroblasts, at both investigated time points. To sum up, the nanofibrillar support with nanosized interfibrillar pores enables efficient cell proliferation and could therefore accelerate wound healing *in vivo*, but it does not support 3D tissue regeneration.

Our research work represents a significant step forward towards the production and application of nanofibers in clinical practice as advanced dressings for chronic wound healing. Critical aspects of nanofiber–cell interactions have been highlighted.

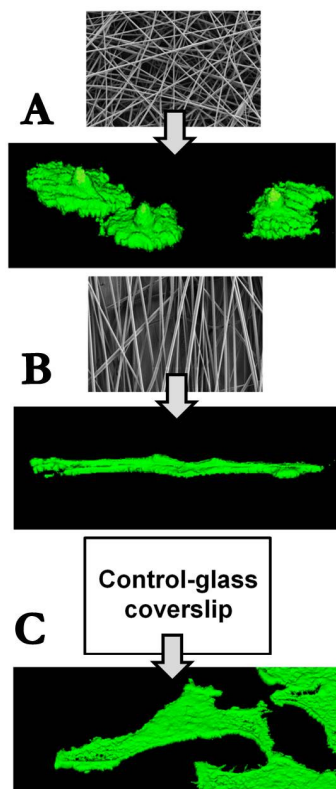


Fig. 1: Morphology of cells grown on different supports: (A) randomly oriented nanofibers, (B) aligned nanofibers, and (C) glass coverslip as a control.

REFERENCES

- Bhardway N., Kundu S.C. *Biotechnol. Adv.* 2010, 28: 325-347.
Pelipenko J. et al. *Eur. J. Pharm. Biopharm.* 2013, 84: 401–411.

OP018

Decoration of NPs with a new type of curcumin-derivative and its application on A β -aggregation.

S. Mourtas¹, E. Markoutsas,¹ S. G. Antimisiaris^{*1,2}

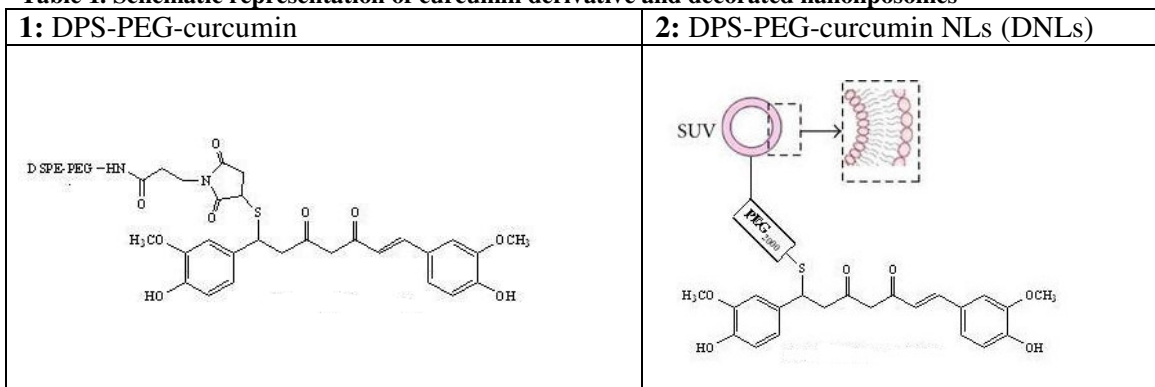
¹University of Patras, Patras, Greece;

²Institute of Chemical Engineering and High Temperatures, FORTH/ICE-HT, Patras, Greece

Among several approaches aimed at inhibiting progression of Alzheimer's disease (AD), targeting the production and clearance of the amyloid-beta (A β) peptide is the most advanced. In order to target amyloid-beta (A β) peptide our group synthesized new curcumin (curc)-derivatives and immobilized them on nanoliposomes (NLs) [Mourtas et al. (2010); Lazar et al. (2013)]. Such approaches increase the binding affinity of curcumin derivatives for A β peptides, due to multivalency. Herein we synthesized a novel non-planar DPS-PEG-curc derivative (**1**; Table 1) and the corresponding DPS-PEG-curc surface-decorated nanoliposomes (DNLs – **2**; Table 1). The effect of DNLs on A β_{1-42} aggregation was tested. For DPS-PEG₂₀₀₀-curc (**1**) synthesis, commercially available DSPE-PEG₂₀₀₀-maleimide was reacted with 4-methoxytrityl-thiol / DIPEA to give the corresponding DSPE-PEG₂₀₀₀-S-Mmt, which was purified by column chromatography and identified using ESI-MS and ¹H-NMR. Removal of Mmt-group in presence of 1% trifluoroacetic acid (TFA)/triethylsilane (TES) (95:5) gave the unprotected DSPE-PEG₂₀₀₀-SH, which was further reacted with curc in presence of DIPEA to the desired DPS-PEG₂₀₀₀-curc (**1**). This new lipidic-curc derivative was purified and identified as above.

NLs consisting of DPPC/Chol (2:1) and 10 mol% DPS-PEG₂₀₀₀-curc were prepared via thin film method to give DPS-PEG₂₀₀₀-curc DNLs (**2**; Table 1). Physicochemical characterization (particle size, polydispersity and zeta-potential) of vesicles was performed by DLS (Nano-ZS, Malvern, UK) at 25°C.

Table 1. Schematic representation of curcumin derivative and decorated nanoliposomes



The mean diameter of DNLs was 120 nm (PDI: 0.200) and ζ -potential was -2.03 mV. The effect of DPS-PEG₂₀₀₀-curc DNLs on A β aggregation was evaluated by the ThioflavinT (ThT) assay. A β_{1-42} was de-seeded before the experiment using an age reversal protocol. Finally, a mixture of A β_{1-42} in Tris-HCl, ThT in Tris-HCl and DPS-PEG₂₀₀₀-curc DNLs [or in absence of NLs (control-1) or in presence of plain NLs (control-2)] were incubated and FI measurements were taken at specific time points. Results (Figure 1) show that DPS-PEG₂₀₀₀-curc DNLs (**2**) are able to substantially inhibit aggregation of A β_{1-42} in vitro, in the same way as the previously studied DNLs without PEG spacer [Lazar et al. (2013)], while the control NLs had no effect. Such DNLs can be further decorated with additional ligands (for brain targeting) and explored as a novel treatment for Alzheimer's disease.

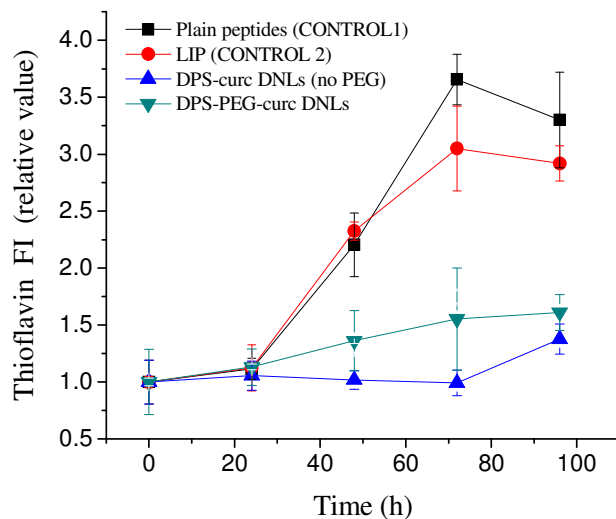


Figure 1. A β peptide aggregation in absence and presence of DNLs (or control NLs)

Acknowledgements

Project received funding from the European Community's Seventh Framework Programme (FP7/ 2007-2013) under grant agreement no. 212043.

References

Lazar, A., Mourtas, S., Youssef, I., Parizot, C., Dauphin, A., Delatour, B., Antimisiaris, S.G., Duyckaerts, C., 2013. Curcumin-conjugated nanoliposomes with high affinity for amyloid deposits: possible applications to Alzheimer disease. *Nanomedicine*. 9(5), 712-721.
Mourtas, S., Canovi, M., Zona, C., Aurilia, D., Niarakis, A., La Ferla, B., Salmons, M., Nicotra, F., Gobbi, M., Antimisiaris, S.G., 2011. Curcumin-decorated nanoliposomes with very high affinity for amyloid- β 1-42 peptide. *Biomaterials*. 32, 1635-1645.

OP021

IN VIVO BIODISTRIBUTION AND INFLAMMATION-IMAGING STUDIES WITH NEW, ^{99m}Tc-LABELLED, DERIVATIVES OF THE IMMUNOMODULATORY PEPTIDE PROTHYMOSIN α

C.-E. Karachaliou¹, C. Triantis¹, C. Liolios¹, L. Palamaris², C. Zikos¹, O. Tsitsilonis³, G. Loudos², M. Papadopoulos¹, I. Pirmettis¹, E. Livaniou¹

¹. National Center for Scientific Research "Demokritos", Athens 15310, Greece.

². Technological Educational Institute, Athens 12210, Greece.

³. Faculty of Biology, University of Athens, Athens 15784, Greece

e-mail: xrisak15@hotmail.com, livanlts@rp.demokritos.gr

Prothymosin alpha (ProT α) is an ubiquitously expressed polypeptide (109 amino acid long in human) exerting a dual role: an intracellular one, associated with cell proliferation and an extracellular one, associated with the enhancement of cell mediated immunity¹. According to some previous data, the dominant immunoreactive site of the molecule is located in its C-terminus, i.e. the amino acid region 100-109². In the present study, two specific derivatives of ProT α , both containing the C-terminal decapeptide ProT α (100-109) [TKKQKTDEDD], were synthesized, purified, characterized, labelled with the radioisotope ^{99m}Tc and used in *in vivo* biodistribution and imaging studies in an inflammation mouse model, along with suitable negative control - peptides (scrambled peptides), in order to follow the radioactivity accumulated in the inflammation locus at various time intervals. More specifically, the ProT α peptide-derivatives as well as the corresponding scrambled peptides were synthesized following the Fmoc strategy, purified with RP-HPLC and characterized with ESI-MS. Then, they were ^{99m}Tc-labelled and analyzed in terms of their radiochemical purity and stability with well-established methods. The overall yield of the peptide synthesis was > 20% and the derivatives' purity was >95%. The radiolabelling yield was also >95%, without colloid formation. The stability tests showed no significant transchelation of the radiometal, as well as satisfactory plasma stability. The radiolabelled peptides were administered in Swiss albino mice bearing experimentally induced inflammation and the mice were either sacrificed 2min, 30min or 2h post injection (p.i.) for biodistribution studies (organ excision and radioactivity measurement), or anesthetized for dynamic whole body imaging using a high resolution SPECT microcamera in planar mode. Regions of interest were defined to inflamed and control organs using the opensource ImageJ software. The biodistribution of the radiolabelled ProT α derivatives demonstrated fast clearance from the blood, heart, lungs and normal muscle. The high percentage of radioactivity in the urine from the first 30 min p.i., combined with low activity in the liver and intestines, indicates excretion predominantly via the urinary system. The most important data is the slow clearance of radioactivity from the inflammation locus, resulting in high contrast ratios of inflamed/control tissue for both derivatives. The biodistribution data clearly agreed with the results of the imaging studies. In parallel, *in vitro* cell-binding studies using human neutrophils are currently under way. Concluding, two new ProT α derivatives were designed, synthesized, successfully radiolabelled with ^{99m}Tc and seem promising inflammation targeting agents; moreover, the new derivatives may contribute to further elucidation of the multifaceted biological role of ProT α in living organisms. References: 1. A. Mosoian, Future Med Chem. 2011 Jul;3(9):1199-208, 2. M. Skopeliti et al., Cancer Immunol Immunother. 2006 Oct;55(10):1247-57

OP022

IMITATION OF PHASE I METABOLISM OF ANABOLIC STEROIDS BY TITANIUM DIOXIDE PHOTOCATALYSIS

Miina Ruokolainen^a, Minna Valkonen^a, Tiina Sikanen^a, Tapio Kotiaho^{a,b}, Risto Kostiainen^a

^aDivision of Pharmaceutical Chemistry, Faculty of Pharmacy, University of Helsinki, P.O. Box 56 (Viikinkaari 5E), FI-00014, Finland

^bLaboratory of Analytical Chemistry, Department of Chemistry, P.O. BOX 55 (A.I. Virtasen aukio 1) FI-00014, Finland

e-mail: risto.kostiainen@helsinki.fi

The most important pathways in phase I metabolism are enzyme-catalyzed oxidations. Therefore, various oxidation methods, such as metalloporphyrins, Fenton reaction and electrochemical reactions have been studied as alternatives for *in vitro* phase I metabolism studies (Lohmann and Karst 2008). Also oxidation products from titanium dioxide (TiO₂) photocatalysis have been recently shown to correlate with metabolism products (Calza et al. 2004). The aim of this study was to further investigate the feasibility of TiO₂ photocatalysis for imitation of phase I metabolism of anabolic steroids.

The photocatalytic reactions of testosterone, methyltestosterone, metandienone, nandrolone and stanozolol were carried out in liquid phase using TiO₂ Degussa P25 particles and ultra violet (UV) light. The duration of UV exposure (225 mW/cm²) was optimized to produce maximal amount of reaction products. The metabolism reactions were studied *in vitro* using human liver microsomes (HLM). The samples were analyzed with ultra high performance liquid chromatography electrospray quadrupole time-of-flight mass spectrometry in positive ion mode.

The reaction products formed fast in TiO₂ photocatalysis. The optimal length of UV exposure was 2 min for testosterone, methyltestosterone, metandienone and nandrolone, and 15 min for stanozolol, because there was more inhibiting acetonitrile in the reaction mixture due to poorer water solubility of stanozolol. For all the steroids studied, the main reactions observed both in TiO₂ photocatalysis and HLM incubations were dehydrogenation, hydroxylation or combination of these two. Several isomers of hydroxylation and hydroxylation+dehydrogenation products were formed in both systems. The similarity of the products having the same mass and retention time in HLM and TiO₂ photocatalytic reactions was evaluated based on the product ion spectra. Many of the products observed in HLM reactions were also formed in TiO₂ photocatalytic reactions. However, products characteristic to either of the systems were also formed.

In conclusion, TiO₂ photocatalysis is a fast and simple method for imitation of phase I metabolism reactions. Although the main reactions were same in TiO₂ photocatalysis and HLM reactions, the stereochemistry of the products might be different and the feasibility of photocatalytic reactions for simulation of drug metabolism needs to be further studied.

References

- Calza, P., Pazzi, M., Medana, C., Baiocchi, C., Pelizzetti, E., 2004. The photocatalytic process as a tool to identify metabolic products formed from dopant substances: the case of buspirone J. Pharm. Biomed. Anal. 35, 9–19
- Lohmann, W., Karst, U., 2008. Biomimetic modeling of oxidative drug metabolism. Anal. Bioanal. Chem. 391, 79–96

OP024

Simulations investigating Bayesian dose individualization of oral Busulfan

Efthymios Neroutsos, Georgia Valsami, Aris Dokoumetzidis

¹. National & Kapodistrian University of Athens, Greece

Correspondence: Aris Dokoumetzidis, adokoum@pharm.uoa.gr

Busulfan is widely used as an alternative to total body irradiation (TBI), in the preparative regimens before hematopoietic stem cell transplantation (HSCT) and presents a high variability, so its administration must be individualized based on AUC. The AUC after oral Busulfan administration needs to be estimated by a Bayesian method, using prior information from a popPK model. Although it is best to build an in house popPK model for Bayesian individualization, often prior information is obtained from literature.

The aim of the present study was to investigate the usage of a popPK model from literature for Bayesian individualization of oral Busulfan dosing in pediatric patients from a different hospital. This was performed by simulating patients using a popPK model from literature and adjusting the dose by applying a different popPK model also from literature. Furthermore, a scheme including an initial i.v dose followed by regular oral busulfan administration was studied.

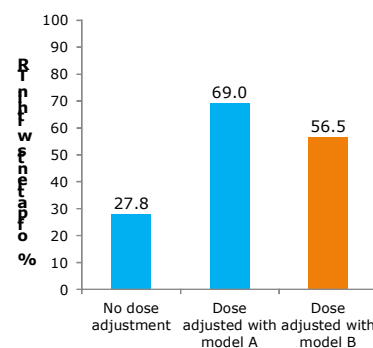
A total of 10000 children were simulated in NONMEM for three different blood sampling schemes, according to a PopPK model from literature (model A) [Trame et al., 2011]. Based on the posthoc estimates of clearance for these patients using the same model (model A), the AUC was calculated and the dose was individualized targeting AUC=1125 $\mu\text{M}\cdot\text{min}$ (therapeutic range of Busulfan 900-1350 $\mu\text{M}\cdot\text{min}$) while the AUC of the second day of administration was recorded by simulating again. Patients that fall outside the therapeutic range (TR) were counted before and after the dose adjustment (day 1 vs day 2 of treatment). The dose of the same simulated patients was also adjusted by applying a different model from literature (model B) [Schiltmeyer et al., 2003] using the same procedure.

Without dose individualization, for a blood sampling scheme at 2, 4, 6 hours, the percentage of patients whose AUC fell within the therapeutic range was 27.8%. After individualization with model A (the same one used for simulation) patients within therapeutic range increased to 69% while after individualization with model B (a different model to the one used to simulate the patients) increased to 56.5% (Figure 1). As expected better performance was achieved with an in-house model while the overall performance even of the in-house model is moderate. Richer sampling schemes, namely at 2, 3, 4, 5, 6 h and 1.5, 3.5, 5, 6, 8, 12 h, or initial i.v. administration followed by regular oral busulfan administration, performed similarly without offering significant improvement (Table 1).

Table 1. % of patients falling within TR before and after dose individualization for the different sampling schemes and type of administration.

Sampling scheme	% patients in TR		
	Before dose individualization	After dose individualization with model A	After dose individualization with model B
Oral			
A	27.8	69.0	56.5
B	28.4	70.4	56.4
C	28.6	76.8	57.3
IV & Oral			
A	26.7	81.5	57.4

Figure 1: Percent of patients within TR before and after dose individualization. The first column



corresponds to the % of patients within TR without dose individualization (dose 1 mg/Kg). The second and third columns correspond to the % of patients who come into the TR after dose adjustment using model A and B, respectively.

In conclusion, in the present study we observed that Bayesian individualization of oral Busulfan dosing offers significant improvement while the development of an in-house model rather than the use of a literature model is deemed necessary.

References

1. Trame MN, Bergstrand M, Karlsson MO, Boos J, Hempel G. Population pharmacokinetics of busulfan in children: increased evidence for body surface area and allometric body weight dosing of busulfan in children. Clin Cancer Res. 2011 Nov 1;17(21):6867-77.

2. Schiltmeyer B, Klingebiel T, Schwab M, Mürdter TE, Ritter CA, Jenke A, Ehninger G, Gruhn B, Würthwein G, Boos J, Hempel G. Population pharmacokinetics of oral busulfan in children. *Cancer Chemother Pharmacol.* 2003 Sep;52(3):209-16.

OP025

APPLICATION OF THE SIMCYP® SIMULATOR IN THE PHARMACOKINETIC DRUG-HERB INTERACTION STUDY OF LOSARTAN WITH *RHODIOLA ROSEA*

Marios Spanakis^{1,2}, Ioannis S. Vizirianakis², Ioannis Niopas^{2*}

¹ Institute of Computer Science, Foundation for Research and Technology Hellas (FORTH)-Heraklion, Greece.

² Department of Pharmacognosy and Pharmacology, School of Pharmacy, Aristotle University of Thessaloniki (AUTH), Thessaloniki, Greece

*Corresponding authors email: niopas@pharm.auth.gr, ivizir@pharm.auth.gr

In a recent work we have assessed the *in vivo* pharmacokinetic (PK) interaction between a herbal product of the “*adaptogen*” *Rhodiola rosea* (*R. rosea*, golden or arctic root) and losartan (1). In this work we have attempted to investigate through the application of a PB/PK model the potential extend of interaction between losartan and *R. rosea* extract in humans. PK experimental data were taken from published studies related to losartan and its metabolite, EXP3174, as well as from *R. rosea*, and were appropriately fitted in the Simcyp v.12 simulator (Simcyp Ltd, Sheffield, UK) to generate a PB/PK model. The inhibitory capacity of the herbal product in PK processes was estimated by carrying out *in vitro* experiments with recombinant *CYP2C9* and *CYP3A4*, as well as, by assessing P-glycoprotein function in Caco-2 cells. Simulations were run in population of healthy volunteers with simultaneous administration of single dose of losartan (50 mg) and *R. rosea* extract (10 mg of rosavin in which the herbal extract product was standardized). The *CYP2C9* polymorphisms were taken into account for the evaluation of the results. The extent of interaction was estimated through the AUC ratio as proposed from the FDA guidance for industry. The data taken from simulations have shown a 1.42 and 1.61 mean fold increase in AUC and C_{max} respectively for losartan plasma concentrations and 1.28 mean fold increase in AUC ratio of portal vein concentrations. In addition to these results, the C_{max} and AUC ratio in plasma and portal vein concentrations for the main losartan metabolite, EXP3174, have shown a mean reduction by 19% and 28%, respectively. Differences in the AUC ratio were observed between *CYP2C9* polymorphisms. The results obtained from the simulations tend to propose that *R. rosea* extract mainly modulates losartan’s absorption and metabolism during the first-pass effect without significant influence in the PK profile of EXP3174, which is in line with the conclusions regarding the previous *in vivo* interaction study (1). Losartan, as well as drugs with similar PK properties could be used in PB/PK models and moreover, in PK drug-herb interaction studies where *in vitro* results indicate both inhibition of transport and metabolism (2). Importantly, the data obtained in this study indicate the usefulness of the methodology presented toward the pharmacological evaluation of herbal medicinal products and the application of Simcyp® platform in assessing clinically relevant drug-herb interactions.

References

1. Spanakis M, Vizirianakis IS, Batzias G, Niopas I. (2013) Pharmacokinetic Interaction between Losartan and *Rhodiola rosea* in Rabbits. *Pharmacology*, 91(1-2):112-6.
2. Hellum BH, Tosse A, Hoybakk K, Thomsen M, Rohloff J, Georg Nilsen O. (2011) Potent *in vitro* inhibition of *CYP3A4* and P-glycoprotein by *Rhodiola rosea*. *Planta Med*,76(4):331-8.

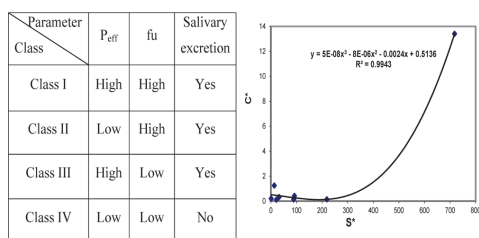
OP027

Saliva versus Plasma Pharmacokinetics: Theory and Application of a Salivary Excretion Classification System

Nasir Idkaidek* and Tawfiq Arafat

College of Pharmacy and Jordan Center for Pharmaceutical Research, University of Petra, Amman, Jordan

The aims of this work were to study pharmacokinetics of randomly selected drugs in plasma and saliva samples in healthy human volunteers, and to introduce a Salivary Excretion Classification System. Saliva and plasma samples were collected for 3–5 half-life values of sitagliptin, cinacalcet, metformin, montelukast, tolterodine, hydrochlorothiazide (HCT), lornoxicam, azithromycin, diacerhein, rosuvastatin, cloxacillin, losartan and tamsulosin after oral dosing. Saliva and plasma pharmacokinetic parameters were calculated by noncompartmental analysis using the Kinetica program. Effective intestinal permeability (Peff) values were estimated by the Nelder–Mead algorithm of the Parameter Estimation module using the SimCYP program. Peff values were optimized to predict the actual average plasma profile of each drug. All other physicochemical factors were kept constant during the minimization processes. Sitagliptin, cinacalcet, metformin, tolterodine, HCT, azithromycin, rosuvastatin and cloxacillin had salivary excretion with correlation coefficients of 0.59–0.99 between saliva and plasma concentrations. On the other hand, montelukast, lornoxicam, diacerhein, losartan and tamsulosin showed no salivary excretion. Estimated Peff ranged $0.16\text{--}44.16 \times 10^{-4}$ cm/s, while reported fraction unbound to plasma proteins (fu) ranged 0.01–0.99 for the drugs under investigation. Saliva/plasma concentrations ratios ranged 0.11–13.4, in agreement with drug protein binding and permeability. A Salivary Excretion Classification System (SECS) was suggested based on drug high (H)/low (L) permeability and high (H)/low (L) fraction unbound to plasma proteins, which classifies drugs into 4 classes. Drugs that fall into class I (H/H), II (L/H) or III (H/L) are subjected to salivary excretion, while those falling into class IV (L/L) are not. Additional data from literature was also analyzed, and all results were in agreement with the suggested SECS. Moreover, a polynomial relationship with correlation coefficient of 0.99 is obtained between S^* and C^* , where S^* and C^* are saliva and concentration dimensionless numbers respectively. The proposed Salivary Excretion Classification System (SECS) can be used as a guide for drug salivary excretion. Future work is planned to test these initial findings, and demonstrate SECS robustness across a range of carefully selected (based on physicochemical properties) drugs that fall into classes I, II or III.



- (1) Amidon, G. L.; Lennernäs, H.; Shah, V. P.; Crison, J. R. A theoretical basis for a biopharmaceutic drug classification: the correlation of in vitro drug product dissolution and in vivo bioavailability. *Pharm. Res.* 1995, 12 (3), 413–420.
- (2) Guidance for Industry: Bioavailability and Bioequivalence Studies for Orally Administered Drug Products General Considerations. March 2003. Division of Drug Information, Center for Drug Evaluation and Research, Food and Drug Administration

5600 Fishers Lane Rockville, MD 20857, USA.

OP028

DEVELOPMENT AND VALIDATION OF AN ELISA METHOD FOR CETUXIMAB QUANTIFICATION

R. Petrilli, C. S. Bitencourt, N. Najar, R. F. V. Lopez
University of Sao Paulo, Ribeirao Preto, Sao Paulo, Brazil
raquelp@fcrp.usp.br

Cetuximab is a chimeric monoclonal antibody direct against epidermal growth factor (EGFR), a known marker for squamous cell carcinoma¹ (SCC). The use of cetuximab is currently restricted to systemic therapy leading to various side effects. In this context, we purpose the topical application of cetuximab for skin SCC. Therefore, indirect ELISA quantifications were performed using carrier free EGFR as antigen (BD biosciences), Blocker Blotto in TBS: Blocker Casein in TBS (20:80 v/v) (Thermo Scientific, USA) as plate blocker and a mix between HRP conjugated and unconjugated antibody (1:5, v/v) as the secondary antibody. TMB solution (Invitrogen, USA) was added to detect complex between drug and secondary antibody and the reaction was stopped using hydrochloric acid 1M. The yellow color was read using a plate reader² (Multiskan FC, Thermo Scientific, USA) at 450 nm. The method optimization was proceeded by testing different concentrations of antigen EGFR (0.5, 1.0, 1.5 and 1.75 $\mu\text{g/mL}$) and of detection antibody (from 0.5 to 4.0 $\mu\text{g/mL}$). Cetuximab dilutions were tested in different media (water, PBS 100 mM pH 7.4, citrate buffer 30 mM pH 6.0 and assay buffer). The concentrations of coating and detection antibody chosen for method validation were those able to provide the greatest signal:noise ratio, without blank background. The method was validated using ICH Q2-R1 guideline. EGFR carrier free concentration and antibody detection concentrations were optimized for 1.75 $\mu\text{g/mL}$ and 4.0 $\mu\text{g/mL}$, respectively. Cetuximab dilutions in water showed a better profile than for the buffers tested and were chosen for method validation and for future liposomal preparations. Lower limit of quantification was determined as 0.125 $\mu\text{g/mL}$. Linearity was obtained in the range of 0.125 $\mu\text{g/mL}$ to 0.75 $\mu\text{g/mL}$ with $R > 0.99$. Intra-day and inter-day precision and accuracy were tested in all concentration levels ($n=6$) and revealed CV values under 15% for precision and recovery between 87.3% and 107.2% for accuracy. Based on the results, a method for cetuximab quantification by ELISA was developed using EGFR at 1.75 $\mu\text{g/mL}$ in PBS for plate coating and detection antibody at 4.0 $\mu\text{g/mL}$. The method was validated in the range of 0.125 to 0.75 $\mu\text{g/mL}$ with adequate linearity, accuracy and precision.

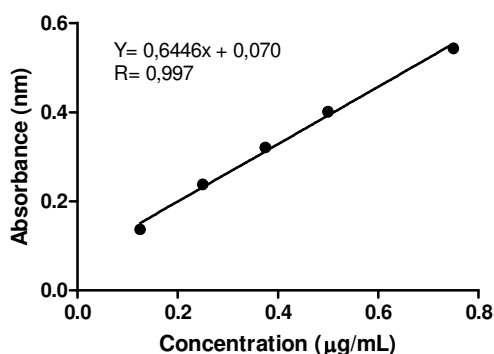


Figure 1. Standart curve for cetuximabe solutions from 0.125 to 0.75 $\mu\text{g/mL}$.

Table 1. Precision and accuracy of the method

Concentration	Intra-day	Intra-day	Inter-day	Inter-day
---------------	-----------	-----------	-----------	-----------

($\mu\text{g/mL}$)	Precision (%)	Accuracy (%)	Precision (%)	Accuracy (%)
0.125	14.6	96.5	14.4	99.0
0.25	13.8	101.8	13.6	101.4
0.375	7.6	103.3	7.9	107.2
0.5	16.2	104.6	13.9	93.6
0.75	10.3	87.3	8.3	94.0

References

¹ Ch'ng et al. (2008). Epidermal growth factor receptor: a novel biomarker for aggressive head and neck cutaneous squamous cell carcinoma. *Hum. Path.* 39, p. 344-349.

² Hantash, J. et al (2009). The development, optimization and validation of an ELISA bioanalytical method for determination of Cetuximab in human serum. *Anal. Methods* 1, p. 144-148.

PP005

SYNTHESIS, CHARACTERIZATION AND BIOLOGICAL ACTIVITY OF HYDROXAMIC ACIDS DERIVED FROM OLIVE OIL TRIACYLGLYCERIDES

M. Barbarić¹, Ž. Marinić², D. Vikić-Topić², M. Zovko Končić¹, K. Mišković³, M. Baus Lončar^{2,3}, M. Jadrijević-Mladar Takač^{1*}

¹ Faculty of Pharmacy and Biochemistry, Zagreb, Croatia; ² Institute Ruđer Bošković, NMR Center, Zagreb, Croatia; ³ School of Medicine, Osijek, Croatia

* Corresponding author: mjadrijevic@pharma.hr

Fatty hydroxamic acids (FHAs), obtained from olive oil triacylglycerides by hydroxylaminolysis (Hoidy et al., 2010) (Fig. 1) were evaluated for their biological activity, *i.e.* against radical scavenging activity (RSA), metal chelating activity (ChA), antioxidant activity (AOA) in β -carotene-linoleate assay, FHAs reducing power (RP), as well as for their cell toxicity on normal (fibroblast) cell line (BJ) and tumour cell line (HeLa). Elemental analysis, IR and ¹H and ¹³C 1D NMR spectroscopy data indicate that the obtained products are predominantly *N*-oleoyl hydroxamic acids (OHA) with some percentage of *N*-linoleoyl hydroxamic acid (LHA). This was additionally confirmed by HMQC and HMBC 2D NMR spectra and MALDI-TOF /TOF mass spectrometry.

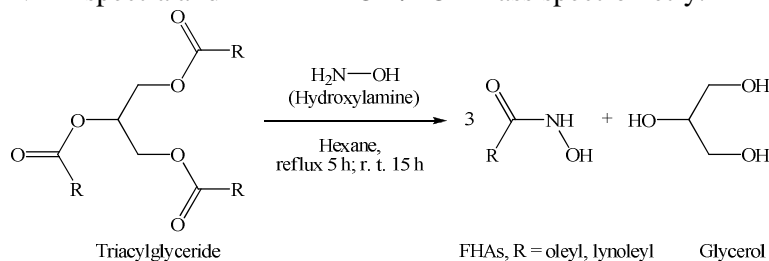


Fig. 1. The reaction equation of fatty hydroxamic acids (FHAs) from olive oil.

The results of *in vitro* assays of FHAs showed notable antioxidant, radical-scavenging and chelating properties (Table 1).

Table 1. The results of biological activity testing of FHAs

Sample	RSA EC ₅₀ ($\mu\text{g/ml}$)	ChA EC ₅₀ ($\mu\text{g/ml}$)	AOA EC ₅₀ ($\mu\text{g/ml}$)	RP EC _{0.5} ($\mu\text{g/ml}$)
FHAs	235.66 \pm 54.01 ^{a*}	1226.53 \pm 58.33 ^{b*}	55.71 \pm 1.29 ^{a*}	395.71 \pm 47.37 ^{c*}
Standard	24.46 \pm 2.54 ^a	12.64 \pm 2.81 ^b 1177.96 \pm 175.73 ^d	45.61 \pm 0.11 ^a	97.028 \pm 10.87 ^c

Values ($\mu\text{g/ml}$) are means \pm SD (n = 3); Standards: ^aButylated hydroxyanisol, ^bEDTA, ^cAscorbic acid, ^dQuercetin; *Statistical differences with the corresponding standards ($P < 0.05$)

The cell toxicity testing revealed that FHAs affected more normal cells (fibroblasts) by reducing their growth while the effect on fast growing tumor cell line was mild. *N*-oleoyl hydroxamic acid (OHA) and its corresponding carboxylic acid (oleic acid, OA) were analysed by using Molinspiration software engine v2011.06, with the aim of prediction of bioactivity scores for the most important drug targets. The following drug-likeness scores were computed: for OHA, the enzyme inhibitor (0.55) and protease inhibitor (0.58) and for OA the enzyme inhibitor (0.27) and the nuclear receptor ligand (0.23). ADMET PredictorTM 6.5 calculated properties predicted the OHA is CYP 2E1 substrate, and OA as non-substrate. The predicted ADMET risk and TOX MUT risk of OHA are 2.0 and its TOX risk 0.0, while predicted parameters for OA are 4.0, 0.0 and 1.0, respectively. The results of biological activity testing and computed data for FHAs spotlight OHA as a promising lead-compound for further research.

Reference: Hoidy W.H., Ahmad M.B., Jaffar Al-Mulla E.A., Zin Wan Yunus W.M., Bt Ibrahim N., 2010. Synthesis and Characterization of Fatty Hydroxamic Acids from Triacylglycerides. *J. Oleo. Sci.* 59, 15-19.

PP007

ESSENTIAL BIOMETALS (Fe, Zn, Mg, Mn, K) IN THE TEA MIXTURES FOR THE TREATMENT OF NUTRITIONAL ANEMIA IN THE BALKAN PENINSULA (SERBIA)

R. Nikolić¹, N. Krstić^{1*}, V. Dimitrijević¹, I. Arsić², J. Jovanović³, M. Nikolić¹

¹Faculty of Sciences and Mathematics, University of Nis, Serbia; ²Faculty of Medicine, University of Nis, Serbia; ³High medical school, Cuprija, Serbia; *Corresponding author:* nenad.krstic84@yahoo.com

Biometals are carriers of vital functions of the body and they are part of different enzymes and other bioactive complexes that are required for the performance of vital processes. Change of biometal concentration can lead to a variety disorders. The required daily amount of biometals enter the body mainly by food. One of disorders caused by the deficiency of biometals is nutritional anemia. (Hussain et al., 2006; Tokalioğlu, 2012) In this study was determined the content of some essential biometals in tea mixtures that are traditionally used for the treatment of nutritional anemia in the Balkan Peninsula (Serbia).

Plant species that are used for the preparation of tea mixtures are Stinging nettle (*Urtica dioica L.*), *Sideritis scardica* (*Sideritis scardica Griseb.J Lamiaceae*) and *Rosa canina* (*Rosa canina L.*). The plant material was dried, burned ($t = 110-150\text{ }^{\circ}\text{C}$) and then annealed at temperatures up to $500\text{ }^{\circ}\text{C}$. After that it was mineralized (conc. $\text{HNO}_3/\text{conc. HCl}$) and, finally, the dry residue dissolved in deionized water. Concentration of essential biometals (Fe, Zn, Mg, Mn, K) in the tea mixtures were determined by inductively coupled plasma-optical emission spectrometry (ICP-OES).

The results presented in Figure 1, showed that tea mixtures which were selected contain relatively high amount of Fe (0.9-1.9 mg/g). Stinging nettle also contains large amount of K and Mg (25.1 mg/g K i 3.3 mg/g Mg).

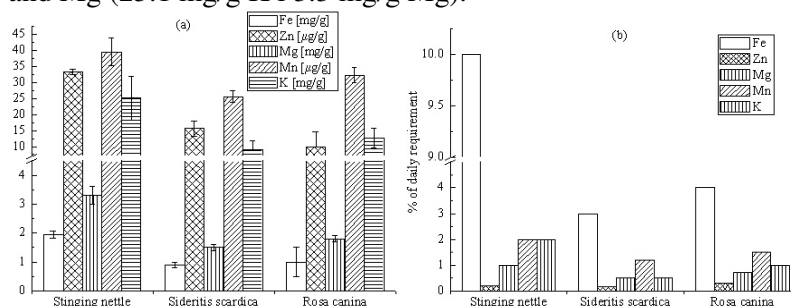


Figure 1: Concentration of biometals in the tested plant species (a) and % of the daily requirement (d.r.) of biometals in a cup of tea (n=5, n-number of samples) (b)

Based on the results of the study the selected tea mixtures can be used as supplements in the treatment of nutritional anemia due to the high concentration of Fe. By consuming a cup of tea we also intake other essential biometals. Using Stinging nettle as adjunct to vegetable in meals can increase the intake of biometals up to half of daily needs.

Acknowledgements: This work was supported by the Ministry of Education, Science and Technological Development of the Republic of Serbia under the Project No. III45017.

References: Hussain, I., Khan, F., Khan, I., Khan, L., Walli-Ulah, 2006. Determination of heavy metals in medicinal plants. *Jour. Chem. Soc. Pak.* 28(4), 347-351.

Tokalioğlu, S., 2012. Determination of trace elements in commonly consumed medicinal herbs by ICP-MS and multivariate analysis. *Food Chem.* 134, 2504-2508.

PP008

DESIGN, SYNTHESIS AND EVALUATION OF NEW STEROIDAL 17 β -CARBOXY DERIVATIVES AS 5 α -REDUCTASE INHIBITORS

C. Varela^a, E. Tavares da Silva^a, C. Amaral^{b,c}, G. Correia-da-Silva^{b,c}, R. Carvalho^d, S. Costa^a, S. Cunha^e, J. Fernandes^e, N. Teixeira^{b,c}, F. Roleira^{a*}

^a CEF, Center for Pharmaceutical Studies & Pharmaceutical Chemistry Group, Faculty of Pharmacy, University of Coimbra, Coimbra, Portugal

^b Faculty of Pharmacy, University of Porto, Porto, Portugal

^c Institute for Molecular and Cell Biology (IBMC), University of Porto, Porto, Portugal

^d Faculty of Science and Technology & Center for Neuroscience and Cell Biology (CNC), University of Coimbra, Coimbra, Portugal

^e REQUIMTE, Faculty of Pharmacy, University of Porto, Porto, Portugal

The androgens testosterone (T) and dihydrotestosterone (DHT), besides playing an important role in prostate development and growth, are also responsible for the development and progression of benign prostate hyperplasia (BPH) and prostate cancer. Therefore, the actions of these hormones can be antagonized by preventing the irreversible conversion of T into DHT, inhibiting 5 α -reductase. Steroidal 5 α -reductase inhibitors (RIs), finasteride and dutasteride, are used in clinic for BPH treatment and have been also proposed for chemoprevention of prostate cancer. Nevertheless, they still promote bone and muscle loss, impotency and occurrence of high-grade prostate tumors. Hence, it is important to search for other potent and specific molecules with lower side effects.

In this work, new steroidal RIs were designed and synthesized by structural changes at the C-17 β carboxy group of 4-androsten-3-one-17 β -carboxylic acid **1**, an analog of 5 α -reductase substrate (T), with carboxamide and carboxyester functions, through the reaction of the acid with the respective amine, in dichloromethane, using triethylamine, dimethylformamide and the coupling reagent BOP (Fig. 1). The carboxyester **5** was synthesized without the amine reagent. The inhibitory activity was evaluated in human prostate microsomes using a new methodology that was developed by our group, based on dispersive liquid-liquid microextraction followed by gas chromatography-mass spectrometry (Amaral et al., 2013a). The antiproliferative effects were studied in a human androgen-responsive prostate cancer cell line (LNCaP cells) (Amaral et al., 2013b). It was observed that the C-17 β carboxylic acid **1** is a weak inhibitor (Table 1). Among the amides synthesized and evaluated, the *N*-tert-butylcarboxamide (**2**) (molecule combining the A-ring of the substrate T and the C-17 β carboxamide of finasteride) showed the best activity. Regarding derivatives with *N*-propylcarboxamide (**3**) and *N*-hexylcarboxamide (**4**) groups, these revealed to be also strong inhibitors. However, they were less active than derivative **2** showing that a hindered *N*-alkyl group in the C-17 β carboxamide derivative favors the inhibitory activity. Concerning the carboxyester derivative (**5**), it revealed only moderate activity. It was also observed that carboxamide derivatives allowed a decrease in the viability of stimulated LNCaP cells in a 5 α -reductase dependent way, being even more effective than finasteride. (Amaral et al., 2013b)

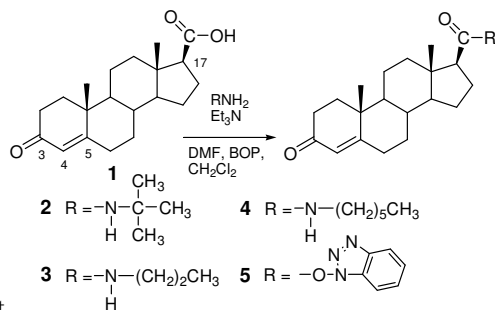
In summary, taking into account the studied compounds, it is possible to conclude that the C-17 β lipophilic carboxamide group along with the 3-keto- Δ^4 moiety in the A-ring seem to be favorable key features for achieving 5 α -reductase inhibitory activity, being the C-17 *N*-tert-butylcarboxamide derivative the best RI. Furthermore, the most potent steroids synthesized revealed to induce a decrease in the viability of stimulated LNCaP cells in a 5 α -R dependent-manner, being the synthesized steroids even more effective than finasteride. This study can help the future design of new steroidal RIs, with fewer side effects.

REFERENCES

Amaral, C., Cunha, S.C., Fernandes, J.O., Tavares-da-Silva, E., Roleira, F.M.F., Teixeira, N., Correia-da-Silva, G., 2013a. Development of a new gas chromatography-mass spectrometry (GC-MS) methodology for the 5 α -reductase activity. *Talanta* 107, 154-161.

Amaral, C., Varela, C., Correia-da-Silva, G., Tavares-da-Silva, E., Carvalho, R.A., Costa, S.C.P., Cunha, S.C., Fernandes, J.O., Teixeira, N., Roleira, F. M.F., 2013b. New steroidal 17 β -carboxy derivatives present anti-5 α -reductase activity and anti-proliferative effects in a human androgen-responsive prostate cancer cell line. *Biochimie*, *in press*.

Corresponding author e-mail address:



froleira@ff.uc.pt
studied compounds as RIs

Fig. 1. General reaction to prepare the

Table 1 – The anti-5 α -reductase activity of synthesized steroids in human prostate microsomes.

Compounds	Reductase Inhibition (%) \pm SEM ^{a)}	IC ₅₀ (μ M)
1	29.55 \pm 3.09	-
2	73.08 \pm 3.05	0.37
3	69.33 \pm 1.03	0.46
4	63.56 \pm 1.08	0.61
5	49.20 \pm 2.51	-
Finasteride	84.62 \pm 1.21	0.096

^{a)}SEM: standard error of mean

PP009

**SYNTHESIS, IMMUNOMODULATORY ACTIVITIES AND
MOLECULAR CALCULATIONS IN GROUP OF ISOXAZOLE
DERIVATIVES**

M. Maczyński¹, J. Artym², M. Kocięba², M. Zimecki², E. Drozd-Sczygieł¹, A. Sochacka-Ćwikła¹, A. Koll³, S. Ryng¹

¹. Wrocław Medical University, Borowska 211a, 50-556 Wrocław, Poland

². Institute of Immunology and Experimental Therapy, Polish Academy of Sciences, Weigla 12, 53-114 Wrocław, Poland

³. University of Wrocław, 14F Joliot-Curie str., 50-383 Wrocław, Poland

The aim of this report was to select a most biologically active compound and proceed molecular calculations among a series of substituted benzylamides of 5-amino-3-methyl-4-isoxazolecarboxylic acid.

The described derivatives were synthesized in reaction of substituted benzylamines with 5-amino-3-methyl-4-isoxazolecarboxylic acid azide. The immunological methods encompassed: determination of phytohemagglutinin A (PHA)-induced human peripheral blood mononuclear cell (PBMC) proliferation, cytokine production by human whole blood cell cultures, humoral immune response of mouse splenocytes *in vitro* to sheep erythrocytes (SRBC), cellular immune response in mice *in vivo* to ovalbumin (OVA), and inflammatory response to carrageenan in mice.

The compounds exhibited differential, but generally immunosuppressive properties in the applied tests. MO5 compound was selected in *in vivo* experiments as the most active in inhibition of: PHA-induced cell proliferation, humoral immune response and tumor necrosis factor α (TNF α) production. Interestingly, MO5 stimulated the inductive phase of the cellular immune response but strongly inhibited the effector phase of this response. The compound inhibited also the carrageenan reaction that confirmed its strong anti-inflammatory character. In summary, MO5 combines anti-proliferative and anti-inflammatory activities, and its effect on the humoral and cellular immune responses is differential. The molecular calculations revealed that the isoxazole ring plays an important role in the observed immunological activities. The differences in the observed immunosuppressive properties of the studied derivatives of isoxazole are a good reason for the theoretical investigations. The performed *ab initio* calculations provided useful information on the electron charge distribution in described molecules. The isoxazole ring is common part of all studied compound and can be considered as the reference molecular subunit. The charge distribution of the isoxazole ring should be related with the electronic structure of whole molecule.

Due to its interesting and beneficial properties, MO5 compound should be further investigated in more advanced models. The molecular calculations suggest that distribution of atomic charges at synthesized derivatives may condition its distinct immunoregulatory nature.

The study was supported by grant of Polish National Science Centre nr N N405 682840.

PP010

EXEMESTANE POTENTIAL METABOLITES – DESIGN, SYNTHESIS AND STUDIES IN BREAST CANCER CELLS

C. Varela^a, F. Roleira^a, A. Lopes^{b,c}, C. Amaral^{b,c}, G. Correia-da-Silva^{b,c}, N. Teixeira^{b,c}, E. Tavares da Silva^{a*}

^a CEF, Center for Pharmaceutical Studies & Pharmaceutical Chemistry Group, Faculty of Pharmacy, University of Coimbra, Coimbra, Portugal

^b Faculty of Pharmacy, University of Porto, Porto, Portugal

^c Institute for Molecular and Cell Biology (IBMC), University of Porto, Porto, Portugal

Exemestane (Aromasin[®]) is the only steroidal aromatase inhibitor (AI) that is orally active and highly potent leading to an irreversible inhibition of the enzyme aromatase. It is used in the treatment of hormone-responsive breast cancer in postmenopausal women. Exemestane is extensively metabolized in the body and, as observed for many drugs, the resulting metabolites can be active compounds. Therefore, we were interested in synthesizing potential metabolites, structurally related to exemestane, by substitution of double bonds by epoxide functions, since epoxidation reactions are proposed in the metabolic pathways for metabolizing exemestane.

Epoxide derivatives were synthesized from exemestane (Figure 1) by two kinds of oxidative reactions. For derivative **2**, it was used performic acid and for **3**, hydrogen peroxide in alkaline medium, as oxidants. Concerning the 17 β -hydroxy derivative **1**, it was obtained as a by-product from the reaction with the reductive mixture of trifluoroacetic acid, acetic acid, acetonitrile and sodium borohydride, in an attempt to reduce the C3-carbonyl group.

The prepared compounds were evaluated in placental microsomes by a radiometric assay (Varela et al., 2012). Their effects in cell proliferation and cell viability in breast cancer MCF-7aro cells were also studied, according to reported methods (Amaral et al., 2013).

Regarding the epoxides (**2** and **3**), substitution of the C-6 exocyclic and C-1/C-2 double bonds by the epoxide function led to very potent derivatives, being the compound resulting from the exocyclic substitution (**2**) slightly more potent than the resulting from substitution at C-1/C-2 (**3**). The C-17 β -hydroxy derivative (**1**), although being less active than exemestane, is also a strong AI. All the synthesized compounds revealed to induce a decline in cell viability and cell-proliferation in a time- and dose-dependent manner.

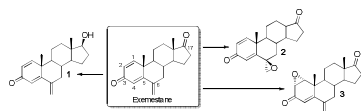


Figure 1. Structure of exemestane derivatives

In summary, results revealed that, according to that we have already observed for other steroidal AIs, the chemical substitution of a double bond by an epoxide function allows obtaining very strong AIs. Further, the substitution of the C-17 carbonyl group by the hydroxyl group leads to a slightly decrease in potency. In addition, the potential metabolites inhibit cell proliferation even more efficiently than exemestane, showing that other mechanisms of cell death, in addition to aromatase inhibition, may be involved.

REFERENCES

- Amaral, C., Varela, C., Azevedo, M., Tavares da Silva, E., Roleira, F.M.F., Chen, S., Correia-da-Silva, G., Teixeira, N., 2013. Effects of Steroidal Aromatase Inhibitors on Sensitive and Resistant Breast Cancer Cells: Aromatase Inhibition and Autophagy. *J. Steroid Biochem.* 135, 51-59.
- Varela, C., Tavares da Silva, E., Amaral, C., Correia da Silva, G., Baptista, T., Alcaro, S., Costa, G., Carvalho, R.A., Teixeira, N.A.A., Roleira, F.M.F., 2012. New Structure-Activity Relationships of A- and D-Ring Modified Steroidal Aromatase Inhibitors: Design, Synthesis, and Biochemical Evaluation. *J. Med. Chem.* 55, 3992-4002.

*Corresponding author e-mail address: etavares@ff.uc.pt

PP012**ASSESSMENT OF THE NITROGEN AND COMPOST DIFFERENT LEVELS EFFECTS ON QUALITATIVE AND QUANTITATIVE PERFORMANCE OF *Calendula officinalis* L.****Amin rezazadeh sarabi¹*, Parisa Farahpour¹, Morteza sam deliri¹**¹*Agriculture department, Islamic Azad University of Chalous, Chalous, Iran**E-mail: Aminrezazade.agc@gmail.com

Recently, the harmful side effects of chemical drugs on human health cause that researchers focus on Medical herbs more than last decades. Nitrogen has a basic effect on qualitative and quantitative performance of plants. *Calendula officinalis* L is a medicinal plant from Astraceae family. Several studies revealed that fertilizers specially nitrogen increases the yield amount of medical plants; however, it may reduce its healing effects. So, assessing the effect of fertilizers on qualitative and quantitative performance of medical plants are very important. In order to investigate the effects of nitrogen and compost different levels on qualitative and quantitative performance of *Calendula officinalis* L. herb, an experiment was carried out in the research field of Chalous Azad University in 2011-2012. The experiment was done in factorial form as a randomized complete block design, in three replicates. Treatments consisted of nitrogen and compost. Considered nitrogen levels consisted of $N_0=0$, $N_1=50$, $N_2=100$ kg/ha and compost levels were including $C_0=0$, $C_1=6$, $C_2=12$ ton/ha. Investigated characteristics consisted of flower dry weight, number of flowers in plant, flower diameter, flavanoid content. Data were analyzed by MSTATC software and Mean of characters was compared by one-way ANOVA test and 2-sided Duncan test for post hoc multiple comparison (in 8 harvest levels). The results were shown in table-1. Nitrogen and compost treatments had statistically significant influence ($p \leq 0.01$) on studied characteristics. Flower dry weight, flower diameter and number of flower in plant characteristics has been studied in eight harvest; as, the performance of these characteristics had increasing procedure from the first harvest up to the forth harvest; and, in the forth harvest, it has reached to its` maximum level and from fifth harvest, it had decreasing procedure. As, up to the forth harvest, the maximum flower dry weight, flower diameter and number of flower in plant obtained by $C_1 \times N_2$ ($C_1=6$ ton/ha compost and $N_2=100$ kg/ha nitrogen treatment) and from fifth up to the eighth harvest, it was obtained by $C_2 \times N_2$ ($C_2=12$ ton/ha compost and $N_2=100$ kg/ha nitrogen) treatment. Also, the maximum flavonoid content obtained by $C_2 \times N_1$ ($C_2=12$ ton/ha compost $N_1=50$ kg/ha nitrogen) treatment. In conclusion, application of compost as a biological fertilizer plays an effective role in enhancement of quantitative performance and increment of the flavonoid content of the plant (1, 2).

Table-1: Comparison the mean of different characteristics of *Calendula officinalis* L, treated by different levels of Compost and Nitrogen fertilizers in 8 harvests.

Characteristics	Treatment Type	1 st	2 nd	3 rd	4 th	5 th	6 th	7 th	8 th
		Harvest	Harvests	Harvest	Harvest	Harvest	Harvest	Harvest	Harvest
Number of Flowers in Plant	C0×N0	3.00	5.33	7.66	14.67	14.00	12.33	7.66	2.06
	C1×N1	13.00	15.67	25.33	30.67	28.67	22.00	11.33	6.67
	C2×N2	11.00	14.67	22.67	26.67	29.33	23.67	15.67	10.66
Flower Dry Weight	C0×N0	7.63	16.19	38.37	62.72	55.19	25.19	17.78	6.05
	C1×N1	50.27	86.55	137.4	163.56	108.40	90.40	64.87	23.90
	C2×N2	45.44	78.19	88.59	153.20	130.20	116.8	76.92	35.69
Flower Diameter	C0×N0	2.33	2.86	3.06	3.36	3.46	3.40	3.00	2.56
	C1×N1	3.8	4.13	4.43	4.80	4.60	4.33	3.86	3.73
	C2×N2	3.63	3.86	4.30	4.70	4.86	4.23	4.00	3.80
Flavanoid Content	C0×N0	0.42							
	C1×N2	0.65							

References

- 1) Biesiada A., kuśA.,. The effect of nitrogen fertilization and irrigation on yielding and nutritional status of sweet basil (*ocimum basilicum L.*). **2010**, Acta Sci. Pol., 9 (2):3-12.
- 2) Rahmani N., Daneshian J., Farahani H.A. Effects of nitrogen fertilizer and irrigation regimes on seed yield of calendula (*calendula officinalis L.*). **2009**, J. Agric. Biotech. Sustain. Dev,1(1), 24-28.

PP013

Investigation of anti-tumoral activity of *Cistus creticus* extract against PC-3 cell line

Ipek Erdogan^a, Ceren Sunguc^a, Mehmet Emin Uslu^a, Oguz Bayraktar^{b*}

^a Izmir Institute of Technology, Department of Biotechnology and Bioengineering Department, Izmir, Turkey

^b Izmir Institute of Technology, Department of Chemical Engineering, Izmir, Turkey

* Corresponding author. Address: Izmir Institute of Technology, Department of Chemical Engineering, Izmir, Turkey. Tel: +90 2327506657 Fax: +90 2327506645.

E-mail address: oguzbayraktar@iyte.edu.tr

Recent studies have revealed that plant extracts show cytotoxic activities against cancer cell lines by ceasing cell division in particular phases (Xu et al., 2012, Yıldırım et al., 2013). Expression of specific genes was found to be activated according to pathway in which cell death occurs. Objective of this study was to identify antitumoural effect of *Cistus creticus*, which is a perennial shrub, found in Mediterranean region, against prostate cancer cell line by measuring the cytotoxic activities and apoptotic gene expression levels.

Extraction of *Cistus creticus* (*C. creticus*) was performed overnight in 80% aqueous ethanol solution. After ethanol removal by rotary evaporator, aqueous extract was lyophilized. Human prostate cancer cell line (PC-3), cultured in DMEM, was exposed to extract of *C. creticus*, between a concentration range of 10 to 3000 µg/ml for 24, 48 and 72 hour time periods. Cytotoxic activity was determined by MTT assay. Cytotoxicity results were verified by Real Time PCR (RT-PCR). Expression levels of *bcl-2* as antiapoptotic, *bax* and *caspase-3* as apoptotic genes were analyzed. *β-actin* was used for normalization.

Initiation of cytotoxic activity on PC-3 cells exposed to extract of *C. creticus* was observed after 24 hours as seen in Figure 1. Cell viability was decreased up to 1500 µg/ml extract concentration, after which it showed an ascending trend line. Gene expression analysis was performed with *C. creticus* extract-treated PC-3 cells at 1500 and 3000 µg/ml extract concentration for 48 hours, which former was initial point of viability increase and latter was the highest point of viability in the experiment. According to RT-PCR results, antiapoptotic *bcl-2* expression level of cells treated with extract at a concentration of 3000 µg/ml was 2.3 times higher than those treated with extract at a concentration of 1500 µg/ml. *Caspase-3* and *bax* expression levels were 1.6 and 5.8 times higher in cells treated with extract at a concentration of 1500 µg/ml, respectively, complying with the decreases observed in viability.

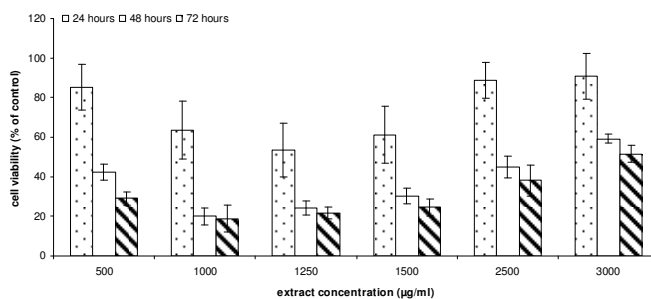


Figure 1. Cell viability of *C. creticus*-treated PC-3 cells. Cytotoxic activity showed tendency to decrease after 1250 µg/ml extract concentration.

C. creticus extract exhibited significant antitumoral activity against human prostate cancer cell line, PC-3. Cytotoxic activity profile showed tendency to increase up to 1500 µg/ml extract concentration, after which cell viability increased. Cell viability results also showed consistency with RT-PCR analysis. Expression levels of antiapoptotic *Bcl-2*, apoptotic *bax* and *caspase-3* changed in parallel with cell viability test results.

References

- Xu, R., Ye, H., Sun, Y., Tu, Y., Zeng, X., 2012. Preparation, preliminary characterization, antioxidant, hepatoprotective and antitumor activities of polysaccharides from the flower of tea plant (*Camellia sinensis*). Food and Chemical Toxicology. 50, 2473-2480.
- Yildirim, A., Karakas, F., Turker A., 2013. In vitro antibacterial and antitumor activities of some medicinal plant extracts, growing in Turkey. Asian Pacific Journal of Tropical Medicine. 6, 616-624.

PP015

PREPARATION AND CHARACTERIZATION OF CURCUMIN-IN-CYCLODEXTRIN-IN LIPOSOME FORMULATIONS

A. Matloob¹, P.Klepetsanis¹, S. G. Antimisiaris^{1,2}

¹University of Patras, Patras, Greece;

²Institute of Chemical Engineering, FORTH/ICES, Patras, Greece; santimis@upatras.gr

In order to investigate the interaction of curcumin-loaded liposomes with cancer cells liposomes in which curcumin (CURC) is loaded in the aqueous space, by preparing CURC-in-cyclodextrin (CD) –in-liposome hybrid formulations were developed, using the DRV technique, in order to achieve high CURC loading. For this, hydroxy-Propyl- β -CD (HP β CD) 400 mg/ml was prepared first and excess curcumin was added and incubated for 72 h; for HP γ CD, 59 mg CURC and 500 mg CD ($\frac{1}{2}$ mol/mol) were dissolved in methanol, which was evaporate until thin film formation; film was scraped and powder dissolved in 2 ml H₂O. Complexes were purified by centrifugation, and characterized by XRD. As seen (Figure 1) the co-precipitation mixture technique produced a good HP γ CD-CURC complex.

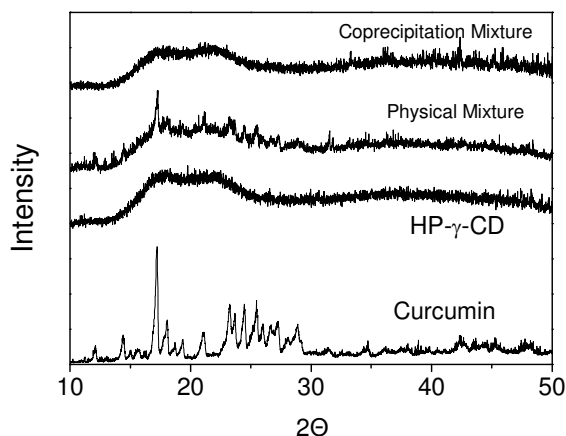


Figure 1. XRD analysis of HP γ CD/CURC complex

To prepare hybrid-liposomes, empty PC/Chol (2:1 mol/mol) liposomes were prepared by thin film hydration (hydrated with 10% PBS) and probe sonication. One volume of CD/CURC complex was mixed with one volume of empty liposomes (volume was increased to 10 ml with dd H₂O, in order to decrease the cryo-protecting effect of CDs) and the mixture was freeze-dried and rehydrated with a specific protocol [Antimisiaris (2010)]. Hybrid-formulations were characterized for CURC encapsulation, size distribution and polydispersity.

Table 1. Physicochemical properties of CURC encapsulating hybrid liposomes

Liposome Type	D/L (mol/mol)	Mean Diameter (nm)	PDI
PC/Chol + HP γ -CD/CURC	0.055	118 \pm 2.7	0.190
PC/Chol + HP β -CD/CURC	0.016	119 \pm 3 nm	0.166

The CURC content of the CD/CURC complex was 0.74 mg/ml, for the HP β CD, and 400 times higher for HP γ CD, explained by the larger size of the lipophilic interior space of the later CD molecule. When CURC was incorporated (as free molecule) in lipid-membrane of

SUVs (150-200nm mean diameter), CURC/lipid ratio was 0.019. Hybrid liposomes with HP β CD complex, had a CURC/lipid ratio of 0.018 and sizes between 900-1200 nm, and when extruded to 119 nm (PDI= 0.16) the CURC/lipid ratio decreased to 0.016 (Table 1). Loading of HP γ CD/CURC in DRV liposomes followed by extrusion (for size reduction) results in optimal CURC/LIPID ratio of 0.055 for 110 nm diameter, monodisperse (low PDI) vesicle (Table 1).

Thereby, it was proved that HP γ CD complex inclusion greatly increases the aqueous solubility of CURC which can be efficiently entrapped in the aqueous phase of DRV liposomes [Dhule et al. (2012)]. Such hybrid CURC encapsulating liposomes, with small size and high CURC encapsulation efficiency are currently used to investigate CURC- cell interactions.

References:

- Antimisiaris SG., 2010. Preparation of DRV liposomes. *Methods Mol Biol.*, 605:51-75.
Dhule SS, Penfornis P, Frazier T, Walker R, Feldman J, Tan G, He J, Alb A, John V, Pochampally R., 2012. Curcumin-loaded γ -cyclodextrin liposomal nanoparticles as delivery vehicles for osteosarcoma. *Nanomedicine*, 8(4):440-445.

OP016

Optimization of NSAID loaded liposomes

K. Pachis¹, A. Skouras¹, S. G. Antimisiaris^{*1,2}

¹. University of Patras, Patras, Greece

². FORTH/ICES, Platani, Patras, Greece

* To whom the correspondence should be addressed: santimis@upatras.gr

The purpose of this study is to prepare flurbiprofen sodium loaded liposomes, which provide high drug encapsulation efficiency and structural stability, aiming for prolongation of the drug's half life as well as a sustained release of the drug.

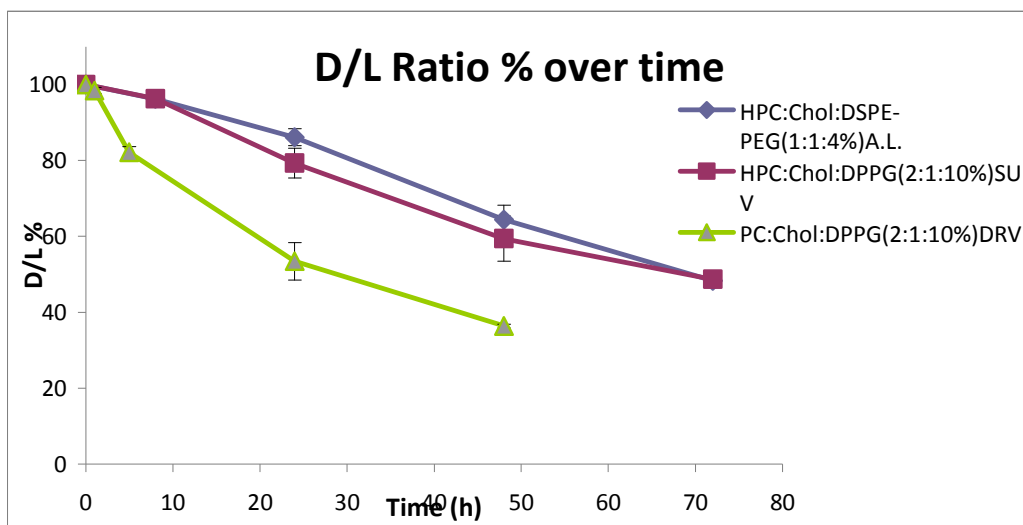
Flurbiprofen sodium liposomes of various lipid compositions (using phosphatidyl-choline (PC) or hydrogenated-PC (H-PC) and cholesterol) were prepared, using the thin film hydration (SUV), the dehydration - rehydration (DRV) and the calcium acetate gradient (remote loading) techniques [S.G.Antimisiaris(2010); D. Zucker et al.(2009)]. In brief, after preparing liposomes using the DRV technique [S.G.Antimisiaris(2010)], liposome size was reduced by probe sonication for 10-15 min, depending on the composition. For the remote loading techniques, the conditions (calcium acetate concentration, initial drug content used, incubation temperature and incubation time were optimized). The liposomal formulations were characterized for their particle size, surface potential and encapsulation efficiency, using dynamic light scattering (DLS), UV-VIS absorption (absorption at 291 nm) and HPLC (C18 column eluted with acetonitrile:distilled water:Trifluoroacetic acid (TFA) (50%:50%:0,08%) as a mobile phase at 1ml/min, using a Shimatzu LC – 20AB HPLC system). Experiments were carried out for evaluation of the drug release kinetics from different types of liposomal formulations, during incubation at 37°C for a prolonged time period (by measuring the drug/lipid ratio (D/L) of the liposomes at various time points).

SUV liposomes had encapsulation efficiencies ranging between 10% and 15% [% encapsulation (compared to initial D/L used)]; D/L ratio ranged between 0,06 and 0,09. Sonicated DRV liposomes had encapsulation efficiencies ranging between 1,5% and 4,5%; D/L ranged between 0,015 and 0,08. The liposomes prepared using the optimized remote-loading conditions, encapsulated up to 60% of the initial drug used for liposomes preparation and had D/L ratios ranging between 0,2 and 0,24 [Table 1]. Both types of liposomal formulations had particle sizes ranging from 80nm - 140nm. DRV liposomes entrapped up to 17,5% of initially used drug (with D/L between 0,17 and 0,31) and sizes above 1µm. Retention experiments showed that up to 86% of entrapped drug was retained after incubation for 24 hours at 37°C in the remote-loaded liposomes, while DRVs retained up to 79% of entrapped drug at the same conditions [Figure 1].

Table 1

Composition	D/L(SUV)	D/L(Active loading)
HPC:Chol (2:1)	0,086 ± 0,003	0,237 ± 0,007
HPC:Chol:DPPG (2:1:10%)	0,064 ± 0,004	0,237 ± 0,008
HPC:Chol:DPPG(1:1:10%)	0,08 ± 0,008	0,199 ± 0,019
HPC:Chol:DPPG:DSPE-PEG(1:1:10%:4%)	0,09 ± 0,006	0,233 ± 0,007
HPC:Chol:DSPE-PEG(1:1:4%)	0,074 ± 0,004	0,243 ± 0,004

Figure 1



The liposomal formulations prepared with the optimized remote loading method had high encapsulation efficiency, and good drug retention, depending on their lipid composition. Investigations are continuing for further optimization of encapsulation and sustained release.

References

S.G.Antimisiaris. Preparation of DRV liposomes. *Methods in Mol Biol.* 2010;605: 51-75

D. Zucker et al. Liposome drugs loading efficiency: A working model based on loading conditions and drug's physicochemical properties. *J Contr Release* 2009;139: 73-80

PP017

ENCAPSULATION OF SATUREJA MONTANA ESSENTIAL OIL IN B-CYCLODEXTRINE

E. Haloci^{1,2}, S. Manfredini², S. Vertuani², R. Shkreli³, E. Goci¹, V. Toska⁴

¹-Aldent Universtiy, Faculty of Medicine Department of Pharmacy, Tirane Albania

²- Ferrara University, Pharmacy Department, Ferrara, Italy

³- Kristal Universtiy, Faculty of Medicine, Department of Pharmacy, Tirana, Albania

⁴-Tirana University, Pharmacy Department, Tirane , Albania

***Corresponding author: Tel.: +355672022263**

E-mail address: entelahaloci@yahoo.com

Essential oils are lipid soluble well-known ingredient often applied to the skin for their important properties that ranges from antimicrobial, to antiinflammatory and skin whitening. Current applications of these volatile compounds turn out to be complicated because of chemical and physical properties. Therefore, microencapsulation could be a solution to problems of stability, evaporation and controlled release. For these reasons, direct contact with skin of high concentrations, should be avoided in favour of a slow release of lower concentrations. We investigated their inclusion in cyclodextrine complexes, in order to achieve better stability in emulsions and better compatibility with skin application.

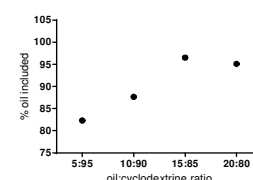
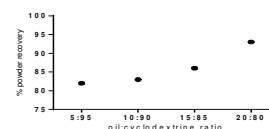
The aim of this study is to see the optimal ratio of mixture between Satureja Montana essential oils and β -cyclodextrin and to study if antibacterial and antimycotic properties are still alive after their complexion

Hydrodistilled essential oil was purchased from Filipi.Co (Albania). β -Cyclodextrin was purchased from Titolchimica (Italy). All others chemicals and thymol, borneol, carvacrol α -pinene standarts used in experiments were obtained from Aldrich Company. Complexes of β -cyclodextrine and essential oils were prepared by co-precipitation method with the four ratios oil: b-cyclodextrin as follows 10:90, 15:85, 20:80 and 25:75 (w/w) in order to determine the effect of the ratio on the inclusion efficiency of β -cyclodextrin for encapsulating oil. The characterization of the complex involved the analysis of the initial essential oil, surface and total extracted oils. The difference between total oil extracted and surface oil absorbed is the amount of essential oil complexed by the cavity of b-cyclodextrine. Total oil contents in the complex were determined by using extraction method with hexane and by its Gas/Fid results obtained. The method applied by Gas/Fid analyses is the one we have standardised in our previous research work.⁽²⁾ For the quantitative determination of essential oil components (present in the initial oil, total oil extracted from the powder and surface oil), a calibration curve with initial *S.Montana* oil was set up. Quantities of initial oil were weighed and dissolved in hexane, to obtain the concentration in the range of 1 - 20 mg/mL. Statistical analyses were performed by Graph Pad program. The retention of essential oil reached a maximum of 96.51% at the oil to b-cyclodextrin ratio of 15:85. The maximum inclusion efficiency of β -cyclodextrin was achieved at the ratio of 20:80. The qualitative and quantitative composition of the volatiles in the total oil extracts was similar to the starting ones.

The qualitative and quantitative composition of the volatiles in the total oil extracts was similar to the starting oil which means that essential may still have the antibacterial and antimycotic properties after encapsulation to β -cyclodextrine

5-Literature Reference

- 1- Entela Haloci, Stefano Manfredini, Vilma Toska, Silvia Vertuani, Paola Ziosi, Irma Topi, Henri Kolani - Antibacterial and Antifungal Activity Assesment of Nigella Sativa Essential Oils- World Academy of Science, Engineering and Technology 66 2012, pg.1198-1200
- 2- Entela Haloci, Stefano Manfredini, Vilma Toska, Silvia Vertuani, Paola Ziosi, - Characterization, antibacterial activity assesment and inclusion in CD of Satureja Montana L. essential oils, European Journal of Pharmaceutical sciences pg 168,ISSN 0928-0987



PP018

MODELING OF RELEASE KINETICS OF WATER- SOLUBLE MOLECULES FROM SUV LIPOSOMES

P.Tzanetopoulos¹, G.Kalosakas² S.G. Antimisiaris^{1,3*}

¹Department of Pharmacy, University of Patras, Greece

²Department of Material Science, University of Patras, Greece

³FORTH/ICEs, Patras, Greece, santimis@upatras.gr

The purpose is to mathematically model calcein (hydrophilic drug model) release from liposomes with varying membrane compositions [Zeng et al. (2011); Siepmann and Siepmann (2008)]. Small unilamellar (SUV) liposomes encapsulating calcein at a quenched concentration (100mM) were prepared, by the thin-lipid-film method and probe sonication. Physicochemical characterization (particle size, polydispersity and zeta-potential) of vesicles was performed by DLS (Nano-ZS, Malvern, UK) at 25°C. Calcein release during incubation at 37 °C for 48 h was monitored, from sample FI measurements (before and after disruption of the liposomes with Triton X-100). Phosphatidylcholine (PC), cholesterol (Chol) and polyethelene-glycol-2000 (PEG) were used in different compositions (PC, PC/Chol (4:1, 2:1 or 1:1 mole/mole), PC/Chol/PEG (2:1:0.04, 2:1:0.08 or 2:1:0/16 mole/mole/mole).

The physicochemical characteristics of some liposomes are presented in Table 1. Results are summarized in retention and release curves dependent on time in order to create a completed profile for every liposome structure. As expected, pegylated liposomes were more stable than vesicles without PEG coating and the permeability of calcein decreased significantly. This was also the case when Chol was included in the liposome membrane; vesicle integrity increased with increasing Chol concentration. The release curves were used for modeling (performed in Fortran environment), to describe the kinetics of calcein-release from liposomes, taking into account both their size and composition. A model three-parameter equation was used and modified in appropriate form, to describe the experimental results with accuracy. Parameters Kon, Koff (rate constants of association and disassociation, respectively) and Ks were used to describe the cumulative release. The Ks variables obtained from calcein release results; suggest that a high surface-to-volume ratio (A/V) of liposome results in enhanced drug release.

Table 2. Physicochemical characteristics of liposomes

Lipid Comp	Mean Diameter (nm) ±SD	Zeta-Potential (mV)	PDI
PC	72.4 (±1.2)	- 0.628	0.249
PC/Chol (4:1)	76.7 (±1.6)	- 0.473	0.166
PC/Chol (2:1) + PEG2000 (4 mol%)	112.0 (±2.3)	-2.53	0.166

The different types of equations used are the following:

$$\frac{M_t}{M_0} = \frac{1}{r+1} \times (1 - e^{-K_{on} \times t}) + \frac{r}{r+1} \times (1 - e^{-K_{off} \times t}) \quad (1)$$

$$\frac{M_t}{M_0} = 1 - e^{-Ks \times t} \quad (2)$$

To test the model we fitted it to the 11 sets of calcein-release data obtained from the 8 different liposome compositions. All the release data include the standard deviation of each mean (n=4). We used the initial drug release to estimate ΔG . Next the initial release rate (at t=0) is used to estimate Ks. Finally Koff that determines the kinetics of the sustained release is calculated; these estimated parameters ΔG , Ks, Koff were used as initial l input in fortran codes to give optimized results. Representative fitting appear in Figure 1.

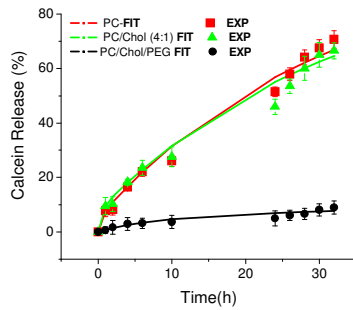


Figure 1. Examples of the fitting achieved with some of the liposomes compositions

References

- Zeng L., Lingling An, L., Wu, X. 2011. Modeling Drug-Carrier Interaction in the Drug Release from Nanocarriers, *J Drug Deliv.*, Art. 370308.
- Siepmann, J., Siepmann F. 2008. Mathematical modeling of drug delivery, *Int J Pharm.*, 364(2):328-43.

PP019

Development of targeted paramagnetic nanoparticles

D. Tzavara¹, K. Papadia¹, A. Bakandritsos², S.G. Antimisiaris^{*1,3}

¹. Department of Pharmacy, University of Patras, Greece

². Dept of Material Sciences, University of Patras, Greece

³. FORTH/ICES, Platani, Patras, Greece

* santimis@upatras.gr

Multifunctional and targeted small iron paramagnetic nanoparticles (SPIONs) as MRI-contrast agents / hyperthermia therapeutics, were prepared. SPIONs were synthesized from iron oxides precipitation and complexation with a polycarboxylic polymer. Nanocrystallites were covered with polyethylene glycol (PEG) for blood half-life prolongation-increased stability, and concurrent creation of binding sites for targeting-ligand attachment. 1-Ethyl-3-(3-dimethylaminopropyl) carbodiimide (EDC) and N-hydroxysulfosuccinimide (S-NHS) chemistry was applied, using NH₂-PEG[2000]-Methoxy or Maleimide [PEG-MAL] (for monoclonal antibody [MAb] attachment). After optimizing SPION decoration with PEG and PEG-MAL, a transferrin receptor specific MAb, OX-26 was immobilized on their surface at good yield (40-66%) (by Elisa). PEG-SPIONs (PEG-NPs) and targeted ones (TARGETED-NPs) were characterized by magnetophoresis, TGA, XRD, FT-IR, and morphologically (TEM, DLS). Furthermore, toxicity towards human endothelial cells (hCMEC/D3) was measured by MTT assay, in order to find non-toxic concentrations at which SPION (targeted and non-targeted) uptake by cells (which overexpress transferrin receptor [Markoutsas et al. (2011)]) is evaluated to verify targetability. Finally, magnetic field effect on SPION cytotoxicity was evaluated on B16 cancer cells.

Magnetophoresis results revealed a higher slope of absorption over time in presence of magnetic field for the constructed SPIONs, compared to a commercial formulation. Their magnetic-nucleous size ranged from 3.5-14 nm (depending on synthesis conditions) as estimated by XRD. Hydrodynamic diameters of PEG-NPs ranged between 80-100 nm; TARGETED-NPs were slightly larger due to MAb; while both types of coated SPIONs were stable for at least 15 d incubation in buffer (opposed to non-PEG SPIONs, which aggregated). ζ -potential was ~ -50 mV for non-coated NPs, and ~ -30 mV for PEG-NPs. PEG-NPs and TARGETED-NPs were not toxic towards hCMEC/D3 cells at concentrations between 0.1–1.0 mg Fe/10⁶ cells. The targetability of TARGETED-NPs was proven by uptake studies (Figure 1) where TARGETED-NP uptake was more than 2.5 times higher than PEG-NPs (control) ($p < 0.01$).

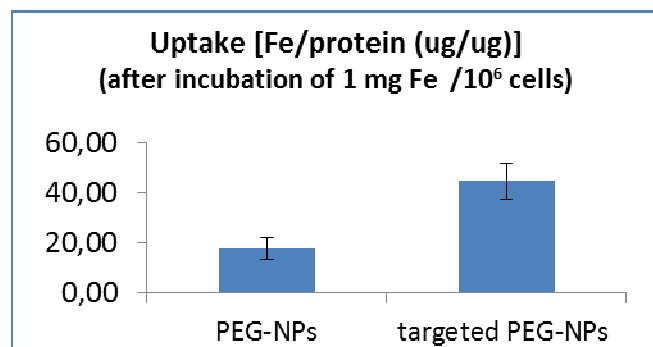


Figure 1. Uptake of OX-26-labelled SPIONs TARGETED and control (PEG-NPs) SPIONs by hCMEC/D3 cells.

The effect of magnetic field on cytotoxicity towards cancer cells of TARGETED and control SPIONs was evaluated on B16 cells, and results show that magnetization has an increased effect on TARGETED SPIONs compared to controls (Table 1).

Table 1. Viability of B16 cells after incubation for 48 h of $58\mu\text{g Fe}/10^6$ cells with TARGETED and control (PEG) SPIONS (magnet applied for 24h).

CONDITION→ SPION TYPE↓	-MAGNET	+ MAGNET
PEG	94.1 ± 6.1	88.1 ± 2.5
TARGETED	92.7 ± 1.7	65.9 ± 4.9

In conclusion, a stable multifunctional targeted-SPION was developed with proven targetability and good magnetic properties. Doxorubicin loaded SPIONS are currently studied, for potential synergistic activity.

References

Markoutsas, E., Pampalakis, G., Niarakis, A., Romero, I.A., Weksler, B., Couraud, P.-O., Antimisiaris, S.G., 2011. Uptake and permeability studies of BBB-targeting immunoliposomes using the hCMEC/D3 cell line, *EJPB*, 77: 2, 265-274.

PP020

DOXORUBICIN-LOADED TARGETED-MAGNETOLIPOSOMES

A.Skouras¹, K. Papadia¹, S.G. Antimisiaris^{1,2,*}

¹. University of Patras, Patras, Greece

². Institute of Chemical Engineering, FORTH-ICES, Patras, Greece

santimis@upatras.gr

In order to evaluate the effect of co-encapsulation of iron oxide nanoparticles (USPIOS) and doxorubicin (DOX) in liposomes (Lip) on their anticancer activity, USPIOS were encapsulated in liposomes to produce magnetoliposomes (MLs) (Skouras et al (2011)), while DOX was encapsulated in pre-formed MLs by the active loading method. Briefly empty liposomes (prepared by the thin film hydration method and sonication), were mixed with USPIOS and the sample was freeze dried. Following reconstitution and extrusion for size reduction, un-encapsulated USPIOS were removed by gel-filtration (Sephacrose4B). MLs were incubated with DOX for 1h at 60°C and then passed through Sepharose-4B to remove free drug. Targeted DOX-loaded MLs were also prepared by attaching the OX26 antibody (MAb) using the biotin-streptavidin method (Markoutas et al (2011)). Drug-loaded MLs were characterized for lipid, DOX and USPIO concentration as well as their hydrodynamic diameter and ζ -potential (Table 1). Activity of targeted and non-targeted DOX-loaded MLs (at various DOX concentrations between 0.5 – 20 μ M) was evaluated by the MTT assay, on B16 melanoma cells which over-express the transferrin receptor (targeted by OX26-MAb). Viability was also evaluated under magnetic field (in order to investigate whether magnetization of MLs could have any effect).

Table 1 Size distribution, USPIOS encapsulation efficiency (EE) and Dox encapsulation of MLs and corresponding control formulations (with or no ligand).

Sample	Lipid Conc. (mg/ml)	USPIO Encaps. (mMFe/(mg/ml lip))	Dox Conc. (mg/ml)	Z-Ave
DOX-Lip	1.05	-	72	123.5 \pm 4.5
DOX-ML	1.14	0.833	76	130.1 \pm 3.1
TARGETEDDOX-Lip	1.12	-	71	142.2 \pm 3.0
TARGETEDDOX-ML	1.08	0.89	74	154.1 \pm 6.1

Experimental results (Figure 1) show that co-encapsulation of DOX and USPIOS is feasible and does not affect DOX's anticancer activity. Importantly, USPIO entrapment is not affected during the DOX active loading process. Moreover, as expected, targeted-DOX-loaded MLs result in decreased B16 cell viability compared to non-targeted formulations, while the use of a magnetic field decreases the viability up to 20% more. The effect of the magnetic field is increased when targeted MLs are tested (compared to non-targeted MLs).

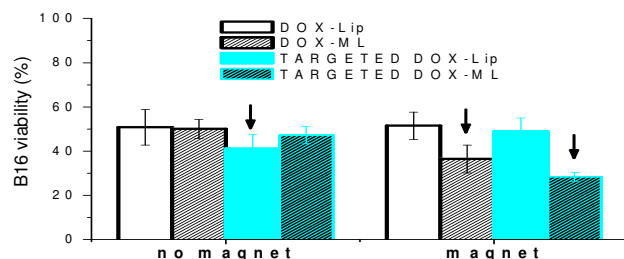


Figure 1 B16 viability (%) after 3h incubation with DOX-loaded MLs or control formulations, washing, and re-

incubation (45h); in presence or not of magnetic field.

REFERENCES

Markoutsas, E., Pampalakis, G., Niarakis, A., Romero, I.A., Weksler, B., Couraud, P.-O., Antimisiaris, S.G., 2011. Uptake and permeability studies of BBB-targeting immunoliposomes using the hCMEC/D3 cell line, *EJPB*, 77: 2, 265-274.

Skouras, A., Mourtas, S., Markoutsas, E., De Goltstein, M.-C., Wallon, C., Catoen, S., Antimisiaris, S.G., 2011. Magnetoliposomes with high USPIO entrapping efficiency, stability and magnetic properties, *Nanomedicine: Nanotechnology, Biology and Medicine*, 7 (5) 572-579.

PP021

Development of time-controlled pulsatile delivery system of montelukast sodium: in vitro and in vivo evaluation

Om Prakash Ranjan*, Usha Y Nayak, M Sreenivasa Reddy, Nayanabhirama Udupa

Department of Pharmaceutics, Manipal College of Pharmaceutical Sciences, Manipal University, Manipal-576104, Karnataka, India.

*E-mail: omprakasranjan@gmail.com

Delivery systems with a pulsatile-release pattern are receiving increasing interest for the diseased condition which follows circadian rhythm. Asthma and allergic rhinitis are two medical conditions which share a common core pathophysiology and have almost similar temporal pattern in the occurrence or exacerbation of their respective symptoms. Montelukast sodium has been considered as a useful common therapy to treat these diseased conditions. In the present study a novel time-controlled pulsatile delivery system (TPDS) of montelukast sodium has been developed, which can release the drug after a predetermined lag time of about 5 h.

The delivery system consists of a core tablet coated with a blend of ethylcellulose (EC) and hydroxypropyl methylcellulose (HPMC) in different ratio to get the desired lag time. The core tablets containing montelukast sodium, avicel 112, cross-carmellose sodium, magnesium stearate and purified talc were prepared by direct compression method. The core tablets were coated with a blend of EC10cps (water insoluble) and HPMC15LV (water soluble) in different ratio (60:40, 70:30 and 80:20). The effect of barrier layer comprising of the blend of EC/HPMC on the lag time of drug release was investigated. The release study was carried out for first 2 hr in FaSGF without enzyme (with 0.5% w/v tween 80) followed by in FaSSIF without enzyme (with 0.5% w/v tween 80). Pharmacokinetic studies of the optimized formulation were carried out in Newzealand white rabbits.

In dissolution studies, it was observed that lag time increases with decreasing concentration of hydroxypropylcellulose (HPMC 15LV) and increasing the coating level. A linear increase in lag time was observed with an increase in coat weight gain and decrease in HPMC content in coating membrane (Figure 1). The optimized formulation EC/HPMC (70:30; 9% w/w coated) has shown lag time of 5 h irrespective of environment. A lag time could therefore be controlled by manipulating both the coating level and the concentration of HPMC in the blend. The in vivo behaviour of TPDS appeared quite different as expected from that immediate release core tablet ($T_{max} = 2$ h) as it has shown drug release after a lag time with T_{max} at 7 h. The AUC and C_{max} of the TPDS were significantly higher than that of the core tablet indicating better extent and rate of absorption. The designed delivery system has shown in vivo lag time of 5 h. Thus, it can be used successfully in chronic therapy of asthma associated with allergic rhinitis which may reduce the mid night attacks and provide relief from early morning symptoms.

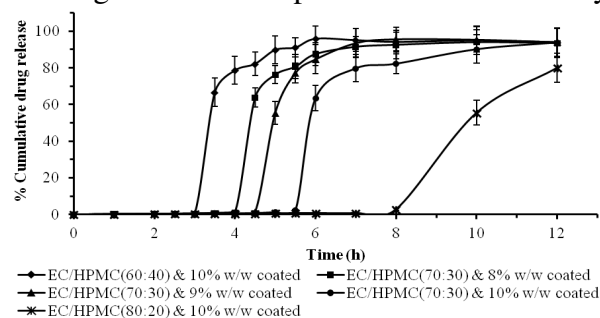


Figure 1. Cumulative drug release profile

References

Proceedings

5th BBBB International Conference – 26-28 September 2013

- Smolensky MH, Lemmer B, Reinberg AE. (2007). Chronobiology and chronotherapy of allergic rhinitis and bronchial asthma. **Adv Drug Del Rev**, 59, 852-82.
- Lecomte F, Siepmann J, Walther M, MacRae RJ, Bodmeier R. (2003). Blends of enteric and GIT-insoluble polymers used for film coating: physicochemical characterization and drug release patterns. *J Control Release*, 89, 457-71.

Acknowledgement

We are thankful to DST and ICMR for providing fund and Manipal University for providing infrastructure facility to carry out the research work.

PP023

INCORPORATING TERBINAFINE HYDROCHLORIDE.

1 2 2 1*

Ch. Koutsoulas , N. Pippa , C. Demetzos , M. Zabka

¹Department of Galenic Pharmacy, Faculty of Pharmacy, Comenius University, Bratislava, Slovakia

²Department of Pharmaceutical Technology, Faculty of Pharmacy, University of Athens, University Campus Zografou, 15784 Athens, Greece

(*) **Corresponding author:** Marian Zabka **e-mail:** zabka@fpharm.uniba.sk

The aim of this work is to design and develop a suitable liposomal gel incorporating terbinafine hydrochloride in order to overcome its water insolubility problem and enable further evaluation of its pharmacological

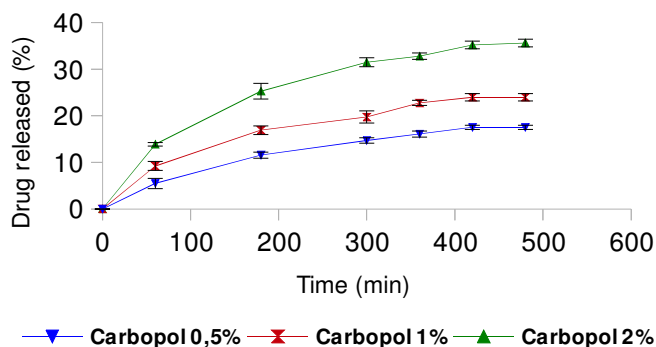
^{1,2} action .Terbinafine hydrochloride loaded EggPC-liposomes were prepared by thin film hydration method and hydrated at two different pH values in order to optimize the incorporation efficiency of the drug. Subsequently, three carbopol gels were prepared and used as carriers for the liposomes. Physicochemical characteristics were evaluated by measuring the size distribution (z -average mean), polydispersity index (PI) and ζ - potential of liposomes by Photon Correlation Spectroscopy. The mean hydrodynamic diameter (z -average mean), polydispersity index (P.I.) and ζ -potential of the particles were used for the characterization of the liposomal dispersion immediately after the preparation and for a period of three weeks. Gels were characterized to identify their rheological parameters using oscillatory rheometer. Finally, the release profile of all three liposomal gel was studied using franz diffusion cells at 37°C. The particle diameter was 200nm for the empty liposomes, while the incorporation of TBH leads to reduced sized of liposomal vectors. The ζ -potential values did not present any significant differenced after the incorporation of the antifungal agent into liposomes. All formulations were found to retain their original physicochemical at least for the time period that were measured. Effect of hydration media affected the incorporation efficiency of terbinafine hydrochloride in the liposomal membrane. Moreover, viscosity of the gel seemed to be of major importance in the release behavior of liposomal gels. In all cases, terbinafine hydrochloride was efficiently released, with the more viscous gel showing the highest release percentage. Finally, it was noticed that liposomes not only act as efficient solubilizers of TBH into hydrogels, but also as efficient carriers for the drug in the gel.

References:

1: Cevc G., Blume G., Schätzlein A., 1997. Transfersomes-mediated transepidermal delivery improves the regio-specificity and biological activity of corticosteroids in vivo. J. Control. Release. 45, 211

2: Dayan N, Touitou E., 2000. Carriers for skin delivery of trihexyphenidyl HCl: ethosomes vs. liposomes. Biomaterials. 21, 1879

Release profiles of terbinafine hydrochloride from liposomal gels (mean \pm SD, n=3).



PP025

HIGH-SPEED ROTARY SPINNING TECHNIQUE AS A POTENTIAL METHOD FOR THE FORMULATION OF NANOFIBER DRUG DELIVERY SYSTEMS

I. Sebe¹, B. Szabó², R. Zelkó^{1*}

¹University Pharmacy Department of Pharmacy Administration, Semmelweis University, Hőgyes Endre Str. 7-9, H-1092 Budapest, Hungary

²Gedeon Richter Plc., Formulation R&D, Gyömrői Str. 19-21, H-1103 Budapest, Hungary

*Corresponding author: Romána Zelkó Ph.D., D.Sc.

e-mail: zelko.romana@pharma.semmelweis-univ.hu

Fiber mats of different polymer ratios and of 0.4-20 μm average diameters were successfully prepared as potential drug delivery systems by high-speed rotary spinning technique and investigated the relationship between the microstructure, the physical properties and the prepared fibers intended for drug delivery purposes. Poly(vinylpyrrolidone) and poly(vinylpyrrolidone-vinylacetate) fibers mats (FI-V) of different polymer ratios (1:0, 2:1, 1:1, 1:2, 0:1) were prepared from aqueous solutions. The forming centrifugal force can be induced by a variable velocity of high speed rotary device. The obtained fiber mats were subjected to detailed physical-chemical analysis. Positron Annihilation Lifetime Spectroscopy (PALS) provided specific information about the free volume distribution and consequently the supramolecular structure of fibers by the lifetime of *o*-Positronium (*o*-Ps) particle (Szabó et al., 2012; Szabó et al, 2013). The thickness and the surface morphology of the fibers were characterized by Scanning Electron Microscopy (SEM) and Atomic Force Microscopy (AFM). Fourier Transform Infrared Spectroscopy (FT-IR) was applied to confirm the real composite ratios. Viscosity values of hydrogels (GI-V) were also determined in order to reproduce the technology. The tensile strength determination enabled the comparison of the mechanical properties of fiber mats as a function of their composition. The prepared micro- and nanofiber mats demonstrated their ability to use in practice. The *o*-Ps lifetime values and distributions revealed the changes of free volume (0.1nm-0.35nm) as a function of their composition. FT-IR spectra indicated that composite fibers formed in the predetermined ratios of polymers in the course of high-speed rotary spinning formation. Viscosity data were in accordance with the average fiber diameters. The highest gel viscosity resulted in the largest average diameter (Table 1). Figure 1 illustrates the physical characteristics of fibers of various compositions. The results indicate that the presence of vinylacetate increased the *o*-Ps lifetime values, consequently the free volume holes within the polymer; while it ordered the polymeric chains with intermolecular H-bonds thus forming more compact macrostructure of higher mechanical strength. The mechanical resistance of the monocomponent samples was higher compared to the composites containing two types of polymers in different ratios. The presence of the second component caused the inhomogeneity of the samples thus creating a looser and less homogeneous fiber structure of lower tensile strength. The application of high-speed rotary spinning technique enabled the preparation of fiber mats of required diameter and mechanical properties. The PALS technique was a useful mean for the tracking of the changes of the microstructure as a function of fiber composition. The proportion of the two types of polymers in the fibers influenced both their micro- and macrostructural characteristics.

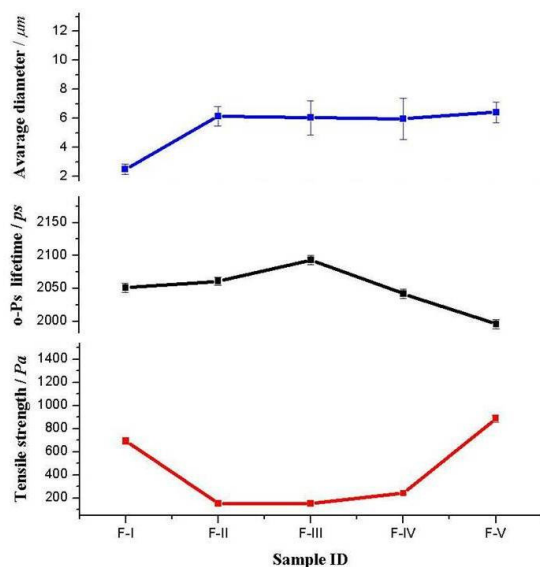


Fig.1: Physical characteristics of fibers

Table 1 – Viscosity values of various gels

ID	Ratio of PVP 25: PVP 64	Total concentration of PVP (% w/w)	Viscosity / Pas
G-I	0:1	57	3.4 ± 0.1
G-II	1:2	54	2.8 ± 0.3
G-III	1:1	56	3.3 ± 0.2
G-IV	2:1	57	3.6 ± 0.1
G-V	1:0	60	16.3 ± 0.2

References

1. Szabó, B., Süvegh, K., Zelkó, R., 2012. Real-time positron annihilation lifetime spectroscopy for the detection of the hydrocolloid gel-film transition of polymers. *Polym. Test.* 31, 546-549.
2. Szabó, B., Sebe, I., Kállai, N., Süvegh, K., Zelkó, R., 2013. Comparison of the micro- and macrostructural characteristics of biopolymer cast films. *Eur. Polym. J.* 49, 2422-2425.

PP025

APPLICATION OF THE SIMCYP® SIMULATOR IN THE PHARMACOKINETIC DRUG-HERB INTERACTION STUDY OF LOSARTAN WITH *RHODIOLA ROSEA*

Marios Spanakis^{1,2}, Ioannis S. Vizirianakis², Ioannis Niopas^{2*}

¹ Institute of Computer Science, Foundation for Research and Technology Hellas (FORTH)-Heraklion, Greece.

² Department of Pharmacognosy and Pharmacology, School of Pharmacy, Aristotle University of Thessaloniki (AUTH), Thessaloniki, Greece

*Corresponding authors email: niopas@pharm.auth.gr, ivizir@pharm.auth.gr

In a recent work we have assessed the *in vivo* pharmacokinetic (PK) interaction between a herbal product of the “*adaptogen*” *Rhodiola rosea* (*R. rosea*, golden or arctic root) and losartan (1). In this work we have attempted to investigate through the application of a PB/PK model the potential extend of interaction between losartan and *R. rosea* extract in humans.

PK experimental data were taken from published studies related to losartan and its metabolite, EXP3174, as well as from *R. rosea*, and were appropriately fitted in the Simcyp v.12 simulator (Simcyp Ltd, Sheffield, UK) to generate a PB/PK model. The inhibitory capacity of the herbal product in PK processes was estimated by carrying out *in vitro* experiments with recombinant *CYP2C9* and *CYP3A4*, as well as, by assessing P-glycoprotein function in Caco-2 cells. Simulations were run in population of healthy volunteers with simultaneous administration of single dose of losartan (50 mg) and *R. rosea* extract (10 mg of rosavin in which the herbal extract product was standardized). The *CYP2C9* polymorphisms were taken into account for the evaluation of the results. The extent of interaction was estimated through the AUC ratio as proposed from the FDA guidance for industry.

The data taken from simulations have shown a 1.42 and 1.61 mean fold increase in AUC and C_{max} respectively for losartan plasma concentrations and 1.28 mean fold increase in AUC ratio of portal vein concentrations. In addition to these results, the C_{max} and AUC ratio in plasma and portal vein concentrations for the main losartan metabolite, EXP3174, have shown a mean reduction by 19% and 28%, respectively. Differences in the AUC ratio were observed between *CYP2C9* polymorphisms.

The results obtained from the simulations tend to propose that *R. rosea* extract mainly modulates losartan’s absorption and metabolism during the first-pass effect without significant influence in the PK profile of EXP3174, which is in line with the conclusions regarding the previous *in vivo* interaction study (1). Losartan, as well as drugs with similar PK properties could be used in PB/PK models and moreover, in PK drug-herb interaction studies where *in vitro* results indicate both inhibition of transport and metabolism (2). Importantly, the data obtained in this study indicate the usefulness of the methodology presented toward the pharmacological evaluation of herbal medicinal products and the application of Simcyp® platform in assessing clinically relevant drug-herb interactions.

References

- 1.Spanakis M, Vizirianakis IS, Batzias G, Niopas I. (2013) Pharmacokinetic Interaction between Losartan and *Rhodiola rosea* in Rabbits. *Pharmacology*, 91(1-2):112-6.
- 2.Hellum BH, Tosse A, Hoybakk K, Thomsen M, Rohloff J, Georg Nilsen O. (2011) Potent *in vitro* inhibition of *CYP3A4* and P-glycoprotein by *Rhodiola rosea*. *Planta Med*,76(4):331-8.

PP026

A SIMPLIFIED METHOD TO ATTACH LIGANDS ON LIPOSOME SURFACES BY BIOTIN STREPTAVIDIN AFFINITY FOR RAPID SCREENING OF TARGETING

E. Markoutsas¹, K. Papadia¹, S.G.Antimisiaris^{1,2,*}

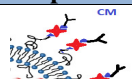
¹University of Patras, Patras, Greece;

²FORTH/ICES, Patras, Greece

*santimis@upatras.gr

The biotin-Streptavidin technique for attachment of monoclonal antibodies (mAbs) on liposome surface offers high attachment yield, however it is time consuming and expensive due to the number of steps used. Herein, a simplified fast and economic technique, by incubating pre-mixed biotin-mAb/STREP with biotin-liposomes (Table 1), at a 3:1:1 biotin-mAb/ STREP/ biotin-LIP mol ratio was evaluated.

Table 1. Scheme and steps of conventional and simple technique.

Preparation of BIOTIN-LIP	
 <p>Conventional Method</p>	 <p>Simple Method</p>
	
<p>(6 steps max)</p> <p>Incubate with STREP Purify from excess Concentrate? Incubate with BIOTIN-mAb Purify from non attached Concentrate?</p>	<p>(3 steps max)</p> <p>Mix STREP +BIOTIN-mAb - Incubate with BIOTIN-LIP Purify Concentrate?</p>

For LIP preparation, lipids were hydrated with PBS (or FITC dextran), and size was decreased by probe sonication. OX-26 mAb (specific for the transferrin receptor) was biotinylated and then attached on liposomes, by conventional method (CM) [1], or by the simplified method (SM) in one-step- incubation of STREP/biotin-TfR-mAb (1/3 mol/mol) complex (Table 1). LIPs were purified from non-attached complex and the yield of the MAb attachment was calculated by Elisa or Bradford technique [1]. The targeting potential of CM and SM LIPs was evaluated by measuring their uptake by hCMEC/D3 cells [1]. Mean diameters of all liposomes was between 125-150 nm, with PDIs below 0.25 [2]. MAb attachment yield ranged between 64.7 – 84.75 for CM and 66.4 – 85.3 for SM, having no significant difference (p>0.05). CM-LIP and SM-LIP uptake by cells was similar (ranged between 0.48-0.98 % and between 0.42 – 0.67 % for CM and SM-LIPs, respectively) (Figure 1), however when each uptake value was normalized with the specific attachment yield (NORM Fig 1) and the two different group values (mean value for CM-LIP was 9.47E-03±1.63E-03 and for SM-LIP 7.30E-03±6.68E-04) were compared, they were found to be statistically different (p<0.01). Thereby, it is concluded that the conformation of the MAb in triplets on the STREP molecule (Table 1), most probably slightly reduces the MAb binding

PP027

Preparation and characterization of matrix pellets via extrusion process

D. Hegyesi^{1,2}, M. Thommes³, P. Kleinebudde³, T. Sovány², P. Kása⁴, A. Kelemen², K. Pintye-Hódi², G. Regdon Jr.²

¹. Richter Gedeon Ltd., Budapest, Hungary

². University of Szeged, Szeged, Hungary

³. Heinrich-Heine-University, Düsseldorf, Germany

⁴. Evonik Industries AG, Darmstadt, Germany

The processes of extrusion-spheronization are applied within the pharmaceutical industry to produce different dosage forms, such as pellets.

There are many types of the extrusion process, such as wet extrusion, melt extrusion and solid-lipid extrusion. Pellets were produced by wet extrusion / spheronization method and process parameters were optimized with factorial design.

Enalapril maleate (Richter Gedeon Ltd., Hungary) was applied as active agent (API). Ethocel Standard 10 FP Premium (Colorcon Ltd., England) was used as matrix-former and MCC type 101 (Avicel 101, FMC Corporation, USA) as pharmaceutical excipients (filler and binder). A mixture form 1% TEC in an aqueous ethanol solution 96% (V/V) was used as granulation liquid. The powders were combined in a laboratory-scale blender (LM40, Bohle, Germany) for 10 min at 25 rpm and then transferred into the gravimetric powder feeder (KT 20, K-Tron Soder, Switzerland) of the extruder. The twin-screw extruder (Mikro 27GL-28D, Leistritz, Germany) was equipped with an axial screen with 1 mm diameter dies and 5 mm length. The wet extrudates were collected and spheronized in a spheronizer (Caleva 120, Sturminster, UK). The particles were dried in a fluid bed apparatus (GPCG 1.1, Glatt, Germany). The shape of the pellets was studied with Image Analyzer. (Leica MZ 75, UK). The surfaces and the structures were tested with a scanning electron microscope (SEM) (Hitachi S4700, Hitachi Scientific Instruments Ltd., Japan). The hardness of the particles were analysed by self developed texture analyser. The true density of the pellets was measured with Quantachrome Stereopycnometer, Multipicnometer (Quantachrome GmbH, Germany). The porosity was calculated with the help of the measured apparent and true density.

The study dealt with the effect of 3 process parameters - water content, friction speed plate and spheronization time – on the pellet properties (shape, tensile strength, breaking force and porosity). Mixed 2 and 3 level factorial design was applied to optimize the process parameters and the best composition for the experiments. These dependent variables influenced the properties of the pellets. The effect of the factors was evaluated with the use of Statistica for Windows 11 (AGA software).

The present work was focused on the optimization of the shape and mechanical properties of pellets prepared by extrusion-spheronization.

The shape of the pellets can be described with a maximum curve as the function of the factors. This non-linear change is caused by the liquid feed rate. All the three factors have a significant effect on the shape of the pellets. The use of the highest liquid feed rate resulted in the sample with the best properties regarding both the aspect ratio and breaking force. (Fig.1.)

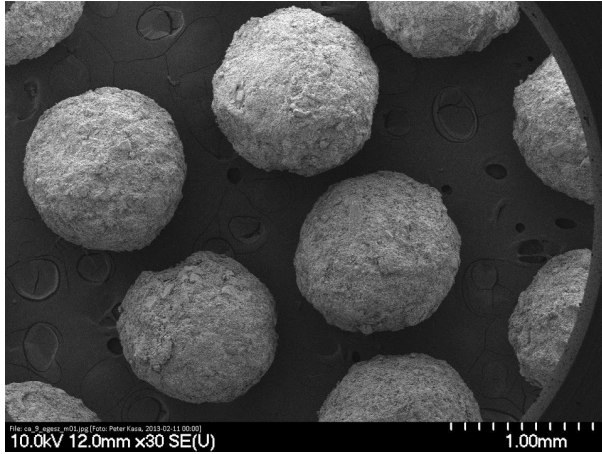


Fig. 1. : The pellets with the best AR

PP028

RAMAN SPECTROSCOPIC MEASUREMENT OF THE FILM THICKNESS OF COATED PELLETS

K. Nikowitz¹, F. Foltmann², M. Wirges², K. Knop², K. Pintye-Hódi¹, G. Regdon¹ jr.*, P. Kleinebudde²

¹. University of Szeged, Szeged, Hungary

². Heinrich-Heine-University, Düsseldorf, Germany

Corresponding author: geza.regdon@pharm.u-szeged.hu

The film thickness of tablets and its effect on the dissolution behavior have been thoroughly investigated. The topic is of similar importance for pharmaceutical pellets but determination of the film thickness is much more tedious in the case of pellets and no universally agreed guidelines exist regarding the methodology of such measurements. Dynamic image analysis is well suited for the fast measurement of a large number of particles, and as such is an ideal tool for the calibration of spectroscopic measurements that can be utilized in- or online during production (Müller et. al. 2012).

Pyridoxine hydrochloride-layered pellets were produced and coated in two different Strea-1 equipments. The API-layer comprised pyridoxine hydrochloride and Pharmacoat 606 in a 5:2 mass ratio. The fully formulated gastroresistant coating system Acryl-EZE® was used as coating. Film thickness was determined with the CamsizerXT image analysis system. Raman spectra were collected off-line with a RamanRXN2 analyzer and analysed to set up a calibration model based on the film thickness data calculated from Camsizer analysis results. Dissolution tests were done according to Ph. Eur. standards where the determination of drug concentration was done with a UV-VIS spectrophotometer.

Dynamic image analysis based on large sample sizes provided reproducible results for pellet size distribution. Film thickness could be calculated by taking the difference of coated and uncoated pellet size. While univariate analysis did not prove to be applicable to the whole sample pool (but gave good results for the two sample sets defined according to equipment used for production) evidenced by Fig. 1. multivariate analysis of the Raman spectra provided a good tool in the measurement of the film thickness of pellets (Nikowitz et. al. doi:10.3109/03639045.2013.795583).

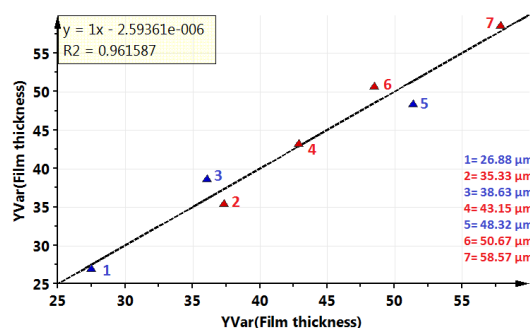


Figure 1. Calibration variance regression model for SNV Raman spectra (PLS)

A linear correlation between dissolution after 120 min in gastric acid and film thickness could be established above a certain film thickness threshold value. Pellets with a film thickness below the threshold value were not gastroresistant.

Raman spectroscopic measurement can provide accurate data of the film thickness even for small samples. Polymer weight gain showed a good correlation with film thickness but in turn did not predict dissolution results. Our investigation suggests that in the case of gastroresistant films a threshold value might exist for the film thickness above which it can be used to predict future dissolution results.

References

- Müller, J., Brock, D., Knop, K., Zeitler, J.A., Kleinebudde, P., 2012. Prediction of dissolution time and coating thickness of sustained release formulations using Raman spectroscopy and terahertz pulsed imaging. *Eur. J. Pharm. Biopharm.* 80, 690–697.
- Nikowitz, K., Foltmann, F., Wirges, M., Knop, K., Pintye-Hódi, K., Regdon, G. jr, Kleinebudde, P., Development of a Raman method to follow the evolution of coating thickness of pellets. *Drug Dev. Ind. Pharm.* (in Press, accepted manuscript DOI:10.3109/03639045.2013.795583)

PP029

KINETICS OF TRAMADOL HYDROCHLORIDE RELEASE FROM SOLID DRUG FORMS

K. Myslíková¹, D. Panochová¹, V. Lochař¹, A. Komersová¹

¹Department of Physical Chemistry, Faculty of Chemical Technology, University of Pardubice, Studentská 573, Pardubice 530 10, Czech Republic

Phone: +420 466 037 046, email: katerina.myslikova@student.upce.cz

The aim of this work is the study of active substance release from various controlled release drug forms (various matrix systems), evaluation of influence of physico-chemical properties of released active substance and effect of the drug matrix composition to the dissolution kinetics. Mathematical and kinetic models obviously assume full homogeneity of the system from which an active substance is released but the production of a fully homogenous drug form is impossible¹. Then actual order of the process (corresponding kinetic model) of active substance release from the drug form depends on such factors as the size and physico-chemical properties of the active substance molecules suspended or dissolved in the excipient or composition and structure of the drug matrix.

Release of active substance tramadol hydrochloride from original drug Tramal Retard and generic form Tralgit SR was measured at pH values corresponding to the pH in gastrointestinal tract (pH 1.6 - 7) in temperature range of 36 - 40°C. Dissolution procedures were carried out 24 hours for Tralgit SR and 18 hours for Tramal Retard. Determination of tramadol hydrochloride concentration was done by UV/VIS spectroscopy.

FTIR qualitative analysis of solid samples (active substance, Tramal Retard and generic form Tralgit SR) were performed through thin wafers with KBr.

Tab. 1 *The values of rate constant of tramadol hydrochloride release in dependence of pH:*

pH	Tramal Retard		Tralgit SR	
	Rate constant (min ⁻¹)	Correlation coefficient	Rate constant (min ⁻¹)	Correlation coefficient
1.6	5.296 * 10 ⁻³	0.9701	3.107 * 10 ⁻³	0.9736
4.5	5.221 * 10 ⁻³	0.9808	3.573 * 10 ⁻³	0.9940
6.9	5.138 * 10 ⁻³	0.9944	3.011 * 10 ⁻³	0.9924

The dissolution profiles of original drug form and generic forms were compared. FTIR spectroscopy was performed in order to identify the characteristic vibrations of the active substance in the original drug Tramal Retard and generic form Tralgit SR during dissolution test. The influence of temperature (36 - 40°C), pH and the other parameters to the active substance release rate were investigated. The dissolution profiles were fitted into different kinetic models such as zero order, first order, Higuchi and Weibull models. Corresponding parameters of the kinetic models were found and statistically evaluated. It was found that release of tramadol hydrochloride from original and generic form fulfills the first order kinetics. Rate constant values are shown in Tab. 1.

References:

1 [Maluf D. F., Farago P. V., Barreira S. M. W., Pontarolo R.: Lat. Am. J. Pharm. (2009), 28 (5), 723]

PP030

INCORPORATION OF DIMETHOXYCURCUMIN INTO CHARGED LIPOSOMES AND THE FORMATION KINETICS OF FRACTAL AGGREGATES OF UNCHARGED VECTORS.

Marilena Hadjidemetriou¹, Natassa Pippa^{1,2}, Stergios Pispas², Costas Demetzos^{1,*}

¹Department of Pharmaceutical Technology, Faculty of Pharmacy, Panepistimioupolis Zografou 15771, University of Athens, Athens, Greece

²Theoretical and Physical Chemistry Institute, National Hellenic Research Foundation, 48 Vassileos Constantinou Avenue, 11635, Athens, Greece

(*) Corresponding author: Prof. Costas Demetzos, Faculty of Pharmacy, Department of Pharmaceutical Technology, Panestimioupolis Zografou 15771, University of Athens, Athens, Greece; fax: 00302107274027; e-mail: demetzos@pharm.uoa.gr

Dimethoxycurcumin (DMC) is a lipophilic analog of curcumin found in *Curcuma longa* Linn., which is known to possess significant activity against various cancer cell lines. The purpose of this study was to develop suitable liposomal formulations in order to overcome DMC's poor water solubility and to study the aggregation kinetics profile using the fractal analysis. DMC was incorporated into liposomal formulations composed of DPPC (dipalmitoylphosphatidylcholine), DPPC:DPPG (Dipalmitoylphosphatidylglycerol):cholesterol (9:1:1 molar ratio) and DPPC:DODAP ((1,2- Dioleoyl-3-Dimethylammonium propane') :cholesterol (9:1:1 molar ratio) liposomes. Light scattering techniques were used to elucidate the physicochemical parameters of the liposomal formulations with and without DMC. The structural characteristics of DMC and especially its chemical tautomerism were found to be crucial for the physicochemical characteristics of liposomal formulations and promote the aggregation mechanism, depending also on the liposomes' composition. The incorporation of DMC into DPPC liposomes leads to rapid aggregation, whereas charged liposomes incorporating DMC retain their physicochemical characteristics at least for the time period that were measured (Pippa et al., 2012; Hadjidemetriou et al., 2013). The fractal approach to study the aggregation of DPPC liposomes incorporating DMC was applied in order to elucidate their morphological characteristics. An increase of fractal dimension was observed due to changes of the morphology and the shape of seed – particle. These changes are the result of the change of colloid parameters, like concentration (Fig.1.). The results of our study contribute to the overall scientific efforts to prepare efficient carriers for DMC and could be a useful tool in order to study more efficiently the kinetics of the aggregation process of liposomal carriers in general.

References

Pippa, N., Pispas, S., Demetzos, C., 2012. The fractal hologram and elucidation of the structure of liposomal carriers in aqueous and biological media. *Int. J. Pharm.* 430,65-73.

Hadjidemetriou, M., Pippa, N., Pispas, S., Demetzos C., 2013. Incorporation of dimethoxycurcumin into charged liposomes and the formation kinetics of fractal aggregates of uncharged vectors. *J. Liposome Res.* 23, 94-100.

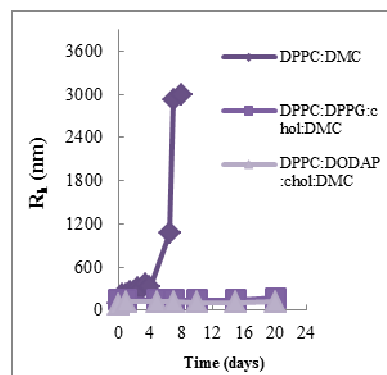


Fig. 1: Stability assessment of liposomal formulations incorporating DMC.

PP031

Complexation of cationic amphiphilic block polyelectrolyte aggregates with antitumor peptide

Natassa Pippa^{1,2}, Stergios Pispas¹, Costas Demetzos^{2,*}, Gregory Sivolapenko³

¹Theoretical and Physical Chemistry Institute, National Hellenic Research Foundation, Athens, Greece

²Department of Pharmaceutical Technology, Faculty of Pharmacy, National and Kapodistrian University of Athens, Athens, Greece

³Laboratory of Pharmacokinetics, Department of Pharmacy, University of Patras, Patra, Greece

(*) Corresponding author: Prof. Costas Demetzos, Faculty of Pharmacy, Department of Pharmaceutical Technology, Panestimiopolis Zografou 15771, University of Athens, Athens, Greece; fax: 00302107274027; e-mail:

demetzos@pharm.uoa.gr

The purpose of this study is to investigate the complexation of a cationic block polyelectrolyte aggregates with a synthetic anionic peptide. In the present work we employ dynamic (DLS), static (SLS) and electrophoretic (ELS) light scattering in order to examine the complexation process, as well the structure and solution behavior of the nanosized complexes in aqueous and biological media, formed between quaternized poly[3,5-bis(dimethylaminomethylene)hydroxystyrene]-b-poly(ethylene oxide) (QNPHOSEO), a cationic-neutral block copolymer, and PCK, which is a synthetic peptide with antitumor and anti-metastatic effects (Annabi et al., 2006). The concentration of QNPHOSEO copolymer is kept constant throughout the series of aqueous solutions of different ionic strength investigated. DLS results at low ionic strength (0.01M) show that all solutions exhibit a main peak at high R_h values (~40nm), which apparently corresponds to the formed mixed aggregates and a significantly smaller one at lower R_h values, which most probably denotes the presence of a small number of free unimer diblock copolymer chains in solution (Fig. 1(a)). The values of the scattering intensity, I_{90} , which is proportional to the mass of the species in solution, increase gradually as a function of C_{PCK} , providing proof of the occurring complexation (Fig. 1(c)). (Karayianni and Pispas, 2012). As peptide concentration increases each polyelectrolyte chain interacts with an increasing number of peptide molecules, the degree of charge neutralization becomes higher and the size distribution of the complexes decreases, especially in the lowest ionic strength. ζ -potential decreases in absolute value as the concentration of the peptide increases, or equivalently the effective positive charge of the complexes reduces as a function of the peptide concentration (Fig. 1(b)). The increase of the ionic strength in the solutions of the complexes induces charge screening and weakening of the electrostatic interactions. The physicochemical characteristics of the complexes, as a function of PCK concentration, remained unaffected at higher ionic strength (0.154M), while their morphology changed and more compact structures are observed. The size of complexes in biological medium (FBS) was not increased significantly. This observation indicates that QNPHOSEO copolymer imparts stealth properties and stability in the complexes. A shift of ζ -potential to negative values is observed presumably due to FBS proteins binding. In conclusion, this study provides interesting and useful new insights into the interaction mechanism between oppositely charged amphiphilic block polyelectrolyte aggregates with stealth properties and therapeutic peptides.

References

Annabi, B., Bouzeghrane, M., Currie, J.C., Dulude, H., Daigneault, L., Garde, S., Rabbani, S.A., Panchal, C., Wu, J.J., Béliveau, R., 2006. Inhibition of MMP-9 secretion by anti-metastatic PSP-94derived peptide PCK3145 requires cell surface laminin receptor signaling. *Anticancer Drugs*, 17,429-438.

Karayianni, M., Pispas, S., 2012. Complexation of stimuli-responsive star-like amphiphilic block polyelectrolyte micelles with lysozyme. *Soft Matter* 8,8758-8769.

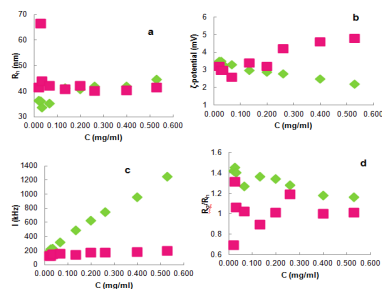


Fig. 1. (a) Hydrodynamic Radius, R_h , (b) ζ -potential, (c) light scattering intensity at 90° , I and (d) R_g/R_h of the complexes as a function of C_{PCK} , for the solutions of QNPHOSEO:PCK system at pH=7.0 and 0.01M NaCl (green) and at pH=7.4 and 0.154M NaCl (pink).

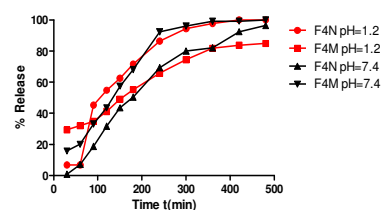
PP32

N-ACETYLSEROTONIN VS MELATONIN: CONTROLLED RELEASE IN AQUEOUS MEDIA FROM HYDROPHILIC MATRIX TABLETS

S. Flitouri, V. Ioannidou, G. Stavrou, S. Mavrokordopoulos, M. Vlachou*
National and Kapodistrian University of Athens, Athens, Greece

N-Acetylserotonin (NAS) is a naturally occurring chemical intermediate in the biosynthesis of melatonin (MT). During the last eight years we have conducted numerous studies on the controlled release of MT from solid pharmaceutical formulations. Our findings suggest that the nature and combination of excipients has a profound effect on both the onset and maintenance of sleep in patients suffering from insomnia sleeping (1, 2). The aim of this report is to extend our studies on melatonin to NAS containing tablets, in an attempt to probe its controlled release profile and ascertain whether NAS mimics the sleep-related antidepressant action of melatonin. A series of hydrophilic NAS and MT matrix tablets (F1_N-F14_N and F1_M-F14_M, respectively) was prepared and tested with respect to their ability to be released in a quick initial pace, aiming at achieving a satisfactory sleep-onset related anti-depressive profile. Moreover, it was intended to achieve completion of NAS and MT release within eight hours. Each matrix tablet was comprised of various excipients, as follows: HPMC K15M, low visc. sodium alginate, Avicel PH102, dextran, lactose monohydrate, PVP-MW:10000, PVP-MW:55000, MgStr. The dissolution experiments involved flat tablets (10 mm diameter, 200 mg weight and 8-10 kp hardness). The tablets were stirred at 50 rpm in a USP XXIII dissolution apparatus II containing 450 ml of either gastric (pH 1.2) or intestinal simulated fluids (pH 7.4) at 37±0.5 °C. Samples (5 ml) were withdrawn at predetermined time intervals, filtered and analyzed at $\lambda_{max}=278$ nm for MT and $\lambda_{max}=279$ nm for NAS using a Perkin–Elmer UV spectrophotometer. Comparative NAS vs. MT release data (pH 1.2 and 7.4) are presented in the following Figure for formulation (F4).

Ingredients	F1	F2	F3	F4	F5	F6	F7	F8	F9	F10	F11	F12	F13	F14
NAS or MT	2	2	2	2	2	2	2	2	2	2	2	2	2	2
Hpmc K15m	32	32	32	32	16	16	16		16					
Sod. alginate	60	104	124	144	76	104	144	144	144	144	144	144	144	144
Avicel PH 102	104	60	40	20	104	76	36	20	20					
Dextran								32	16					
Lactose m.												26	26	52
PVP 10000										52		26		
PVP 55000											52	26		
Mg str	2	2	2	2	2	2	2	2	2	2	2	2	2	2



In general, at pH 1.2 the release of NAS is higher than that of MT, whereas at pH 7.4 the release of MT is higher. This can probably be attributed to the fact that conversely to NAS, MT cannot form H-bonds at pH 1.2. At pH 1.2, substitution of HPMC with dextran in MT-containing tablets led to reduced MT release. On the other hand, the differences in the release of NAS at the two different pH's are less striking. NAS release from tablets containing lactose is very quick, irrespectively of the pH of the medium used. The reverse was observed in the case of lactose containing MT tablets at pH 7.4. At pH 1.2 the release of MT was much slower. Replacement of lactose with PVP in the tablets, showed once again a pH dependent release for the two drugs.

We have demonstrated how commonly used excipients affect the controlled release of NAS and MT from hydrophilic matrix tablets. Current studies involve various other formulants of different physicochemical characteristics and hence profile of interaction with NAS and MT.

vlachou@pharm.uoa.gr

References

1. Vlachou, M.; Eikosipentaki, A.; Xenogiorgis, V. *Curr. Drug Deliv.* **3**, 255-265 (2006)
2. Vlachou, M.; Tsiakoulia, A.; Eikosipentaki, A. *Curr. Drug Discov. Technol.* **4**, 31-38 (2007)

PP034

PREPARATION AND EVALUATION OF DICLOFENAC SODIUM GEL BY USING HYDROXYETHYLCELLULOSE POLYMER

Enkelejda GOCI^{a*}, Ledjan MALAJ^b

^aDepartment of Pharmacy, Faculty of Medical Science, Aldent University, Tirana, Albania

^bDepartment of Pharmacy, Faculty of Medicine, University of Tirana, Tirana, Albania

*Corresponding author: Tel.: +3550692777413

E-mail address: ledagoci2@yahoo.com

Diclofenac sodium (DS) is a nonsteroidal anti-inflammatory drug (NSAIDs) widely used clinically to reduce inflammation and pain in conditions such as rheumatoid arthritis, menstrual pain, dysmenorrhea, fever, osteoarthritis or acute injury¹.

It is well known that therapeutic efficacy of a topical formulation depends on both the physicochemical properties of the drug and the vehicle composition. The vehicle composition can affect drug release, and a number of vehicles, including simple creams, gels and emulsion based formulations (Emulgel) have been utilized in topical preparations. Gel based formulations are better percutaneously absorbed than creams and ointment bases. From the literature, the formulation with HEC gel base exhibited better properties for topical delivery of drugs when compared with the other formulations².

The present research has been undertaken with the aim to develop a topical gel of diclofenac sodium 1%, evaluation of its physicochemical characteristics and *in vitro* drug release through pig skin using vertical diffusion cell.

In the presented work were prepared three batch hydrophilic diclofenac sodium gels (DC) of hydroxyethylcellulose (HEC) as shown at table 1. Skin permeability of the preparation was evaluated *in vitro* using abdominal hairless pig skin, into water medium at 37°C and determined using spectrophotometer UV at 276 nm.

The HEC diclofenac sodium gels were transparent while commercial (Vurdon - Help) gel was white viscous, opalescent. All preparations were easily spreadable, with acceptable bioadhesion and fair mechanical properties. The pH values ranged from 7.33 to 8.35, which are considered acceptable to avoid the risk of irritation after skin application.

Considering the stability studies and physicochemical parameters, batch DC1 and DC3 were selected for *in vitro* permeability release studies as well as compared with the marketed gel. The results are shown at the figures 1.

Ingredients (%w/w)	Formulation		
	DC 1	DC2	DC3
Diclofenac sodium	1	1	1
HEC	2.5	2.5	2.5
Glycerol 85%	10	10	10
Nipagin	0.1	0.1	0.1
Nipazol	0.01	0.01	0.01
Water up to	100	100	100

Tab. 1 Preparation of gels formulations and commercial gel

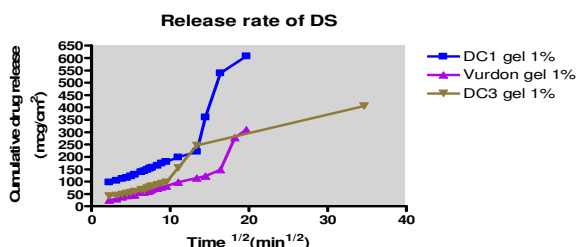


Fig.1 Release rate of DS from the two

From the study it was concluded that HEC gel containing diclofenac showed good homogeneity, spreadability, pH value and rheological properties within the limits allowed for dermatological preparations. HEC DS gel exhibited significantly better drug release when compared to commercial gel.

LITERATURE REFERENCE

¹Sanna V., Peana A.T., Moretti M.D.L., 2009. Effect of Vehicle on Diclofenac Sodium Permeation from New Topical Formulations: *In Vitro* and *In Vivo* Studies. *Current Drug Delivery*. 6, 93-100. ²Hasçicek C., Bediz-Ölçer A., Gönül N., 2009. Preparation and evaluation of different gel formulations for transdermal delivery of meloxicam. *Turk J. Pharm. Sci.* 6 (3), 177-186.

PP035**Fractal analysis of liposomal aggregation**Natassa Pippa^{1,2}, Stergios Pispas², Costas Demetzos^{1,*}¹Department of Pharmaceutical Technology, Faculty of Pharmacy, University of Athens, University Campus Zografou, 15784 Athens, Greece.²Theoretical and Physical Chemistry Institute, National Hellenic Research Foundation, 48 Vassileos Constantinou Avenue, 11635, Athens, Greece(*) Corresponding author: Prof. Costas Demetzos, Faculty of Pharmacy, Department of Pharmaceutical Technology, Panestimiopolis Zografou 15771, University of Athens, Athens, Greece; fax: 00302107274027; e-mail: demetzos@pharm.uoa.gr

The purpose of this study is to investigate the stability of uncharged and charged liposomal carriers, to determine their fractal dimension, specify the physicochemical characteristics in different media and quantify the aggregation kinetics of liposomal dispersions. Light scattering techniques were the primary tools used in order to elucidate the morphology, the internal structure and microenvironment and the physicochemical parameters of the uncharged and charged liposomal carriers in different media and their ageing characteristics, as well as their aggregation kinetics. Aggregation of uncharged dipalmitoylphosphatidylcholine (DPPC) liposomes in aqueous medium was observed, while d_f was 2.5 and remained unchanged during an ageing study (Pippa et al., 2012a). The existence of Lateral Cluster-Cluster Aggregation could be a possible explanation for the observed behavior. Physicochemical stability was observed for liposomes containing cholesterol [DPPC: cholesterol (9:1 molar ratio)] in aqueous and biological (Fetal Bovine Serum, FBS) medium. The structural properties of DPPC liposomes in aqueous medium are quite different from those in FBS, as demonstrated from fractal analysis, especially for liposomes without cholesterol. Anionic [DPPC:DPPG (Dipalmitoylphosphatidylglycerol) (9:1 molar)] and cationic [DPPC:DODAP (1,2- Dioleoyl-3-Dimethylammonium propane) (9:1 molar)] liposomes in aqueous medium were found to retain their original physicochemical characteristics at least for the time period that they were studied (Pippa et al., 2012b). The first order kinetics describes the protein induced aggregation of cationic liposomes due to the serum components (Pippa et al., 2012b). Additionally, DPPC:PAMAM G4 (9:1 molar ratio) liposomes displayed an unexpected behavior in Phosphate Buffer Saline (PBS) since the aggregation was limited and the fractal dimension decreased drastically ($d_f=1.91$). In conclusion, the fractal approach of the dimensionality of liposome aggregates and the extended DLVO theory would be the tools to explain the phenomenology and the functionality of lipidic aDDnSs. Moreover, these tools would be a state of the art methodology for the developing process of new drugs and open attractive horizons for the pharmaceutical industry and for regulatory considerations.

References

- Pippa, N., Pispas, S., Demetzos, C., 2012a. The fractal hologram and elucidation of the structure of liposomal carriers in aqueous and biological media. *Int. J. Pharm.* 430,65-73.
- Pippa, N., Pispas, S., Demetzos, C., 2012b. The delineation of the morphology of charged liposomal vectors via a fractal analysis in aqueous and biological media: physicochemical and self-assembly studies. *Int. J. Pharm.* 437,264-274.

PP037

SCLEROCARRYA BIRREA AND PSIDIUM GUAJAVA FRUIT EXTRACTS AS POTENTIAL PHARMACEUTICALLY-INACTIVE ORAL DRUG PERMEABILITY ENHANCING EXCIPIENTS

¹M.L.S. Mokhele, ¹G.M. Enslin, ^{1*}C. Tarirai.

¹Tshwane University of Technology, PRETORIA, South Africa. *Correspondence: tariraic@tut.ac.za

Different formulations containing *S. birrea* (marula) and/or *P. guajava* (guava) fruit extracts from Tarirai et al. (2012), alone and in combination, were granulated and/or compressed into mini-tablets using a 6 mm concave punch (Jambwa et al., 2011). Mini-tablets were physically characterized according to Pharmacopoeia tests and formulations without the fruit extracts were used as controls. *In vitro* drug permeability studies were performed across excised pig intestinal tissue in a Sweetana-Grass diffusion chamber (Tarirai et al., 2012). Data was analyzed (ANOVA single factor, p<0.05) using Ms Excel 2010. The melting point of cimetidine (Figure 1) did not deviate by >5% for all the excipients thus exhibiting no compatibility problems.

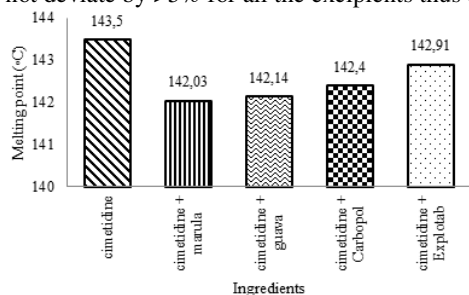


Figure 1: Differential scanning calorimetric data indicating excipients-drug compatibility

All granules exhibited passable powder flowability with angles of repose between 38.1°-41.5° while drug content was 0.27±0.01% w/w for granules and 0.25±0.02% w/w mini-tablets. Mini-tablets had average mass of 67.95±2.49 mg, dimensions (diameter 6.03±0.01 mm, thickness 3.57±0.06 mm), hardness 30.65±9.14 N, friability 0.34±0.10%, swelling indices 395.01±79.71%, and disintegration time >30 min while their mucoadhesive properties were acceptable. Average mean dissolution times of approximately 30 minutes were obtained at pH 7.4. Drug permeability data are summarized in Table 1.

Table 1: Cimetidine permeability data across excised intestinal tissue from granules and mini-tablets with different concentrations of extracts

FORMULATION*	GRANULES				MINI-TABLETS			
	P _{app} (A-B) (×10 ⁻⁷ cm/s)	P _{app} (B-A) (×10 ⁻⁷ cm/s)	P _{app} ratio	Net flux (µg/cm ² /min)	P _{app} (A-B) (×10 ⁻⁷ cm/s)	P _{app} (B-A) (×10 ⁻⁷ cm/s)	P _{app} ratio	Net flux (µg/cm ² /min)
CMD/CPL(77.2%)/EXP	3.79 ± 0.34	4.36 ± 0.27	4.13 ± 0.48	0.02 ± 0.25	6.36 ± 2.25	4.89 ± 1.76	0.79 ± 0.32	-0.04 ± 0.05
CMD/CPL/EXP/PGE (2.2%)	0.59 ± 0.18	1.81 ± 0.09	3.30 ± 0.30	0.08 ± 0.07	3.78 ± 0.71	0.27 ± 0.14	0.09 ± 0.07	-0.09 ± 0.15
CMD/CPL/EXP/SBE (2.2%)	11.18 ± 0.64	9.28 ± 0.57	0.83 ± 0.51	-0.7 ± 0.20	0.73 ± 0.53	3.64 ± 1.38	10.42 ± 0.65	0.10 ± 0.04
CMD/CPL/EXP/PGE/SBE (1.1%)	0.81 ± 0.22	3.75 ± 0.50	4.81 ± 0.05	0.13 ± 0.11	2.96 ± 0.83	1.33 ± 0.16	2.49 ± 0.89	-0.05 ± 0.12
CMD/CPL/EXP/PGE(0.6)/SBE(1.6)	4.28 ± 0.13	3.13 ± 1.74	2.26 ± 0.48	-0.03 ± 0.16	2.74 ± 1.42	7.78 ± 1.78	3.87 ± 0.55	0.15 ± 0.17
CMD/CPL/EXP/PGE(1.6)/SBE(0.6)	0.98 ± 0.70	1.69 ± 0.86	2.69 ± 0.52	0.04 ± 0.06	14.79 ± 1.10	2.42 ± 0.52	0.19 ± 0.15	-0.28 ± 0.20

*CMD = cimetidine 18.8%, CPL = carbopol 75%, EXP = explotab 4%, PGE = *Psidium guajava* fruit extract, SBE = *Sclerocarrya birrea* fruit extract
S. birrea and *P. guajava* fruit extracts did not affect the physical properties of granules and mini-tablets as was expected. The effects of the fruit extracts as oral drug absorption enhancing excipients in oral dosage forms were inconclusive and require further investigations using their pure phytochemical constituents.

References:

Jambwa, T., Viljoen, A.M., Hamman, J.H., 2011. Aloe gel and whole-leaf raw materials: Promising excipients for the production of matrix-type tablets. *SAPJ.*, 78(1):51-54.
 Tarirai, C., Viljoen, A.M., Hamman, J.H., 2012. Effects of dietary fruits, vegetables and a beverage on the *in vitro* transport of cimetidine: Comparing Caco-2 cells with pig jejunum tissue. *Pharm. Biol.*, 50(2):254-263.

PP038

IDENTIFICATION OF COUNTERFEIT MEDICINES FOR ERECTILE DYSFUNCTION BY VALIDATED RP-HPLC METHOD

Z. Poposka¹, Sh. Memeti¹, M. Shishovska¹, Z. Mustafa¹, K. Starkoska¹, Z. Arsova-Sarafinovska¹
¹. Institute of Public Health of Macedonia, 50 Divizija 6, 1000 Skopje, FYROM

The aim of the study was to develop a specific, sensitive, simple, and rapid RP-HPLC method with UV detection for identification of counterfeit medicines for erectile dysfunction: containing vardenafil, sildenafil, and tadalafil. HPLC analysis was performed using a Shimadzu LC-2010 chromatographic system (Shimadzu, Kyoto, Japan) consisting of a LC-20AT Prominence liquid chromatograph pump with DGU-20A5 Prominence degasser, a SPD-M20A Prominence Diode Array Detector, and a SIL-20 AC Prominence auto sampler. Data analyses were done using Class VP 7.3 Software. The elution was carried out on a column Chromolith® Performance RP-18e (50 x 4.6 mm i.d., monolithic rod), with a mobile phase consisted of acetonitrile and 0.02 mol L⁻¹ phosphate buffer (pH = 2.8) in a ratio of 29:71, (V/V), at flow rate of 0.6 mL min⁻¹, at controlled column temperature (40°C) and autosampler temperature at 4°C. Detection of vardenafil, sildenafil, and tadalafil was carried out with DAD detector at a wavelength of 285 nm. The injection volume was 20 µL. The samples included medicines for erectile dysfunction (sildenafil 50 mg tablets, tadalafil 20 mg tablets, vardenafil 10 mg tablets) and were submitted by the state regulatory authority, Bureau of the medicines. The method was fully validated according to the ICH (International Conference on Harmonization) guidelines by the determination of linearity, precision, accuracy, limit of detection (LOD) and limit of quantification (LOQ). Selectivity of the method was proved with the chromatographic peak resolution obtained between the peaks of vardenafil, sildenafil, and tadalafil and the characteristic UV spectra. Linearity of the method was tested in the range of 2.5 – 100 µg mL⁻¹ for all tested substances. Experimental data showed high level of linearity with the values of the correlation coefficients ($R^2 = 0.9991$, $R^2 = 0.9995$, $R^2 = 1.0$ for vardenafil, sildenafil, and tadalafil, respectively). The LOD and LOQ for vardenafil were 4.86 ng mL⁻¹ and 14.72 ng mL⁻¹, respectively; the LOD and LOQ for sildenafil were 3.75 ng mL⁻¹ and 11.37 ng mL⁻¹, respectively; while the LOD and LOQ for tadalafil were 0.56 ng mL⁻¹ and 1.69 ng mL⁻¹, respectively. The accuracy of the method was demonstrated by the values obtained from the recovery experiments (100.06%, 99.57%, and 99.53% for vardenafil, sildenafil, and tadalafil, respectively). The proposed HPLC method allows a simple, accurate, precise and rapid identification and determination of vardenafil, sildenafil, and tadalafil in potentially counterfeit products.

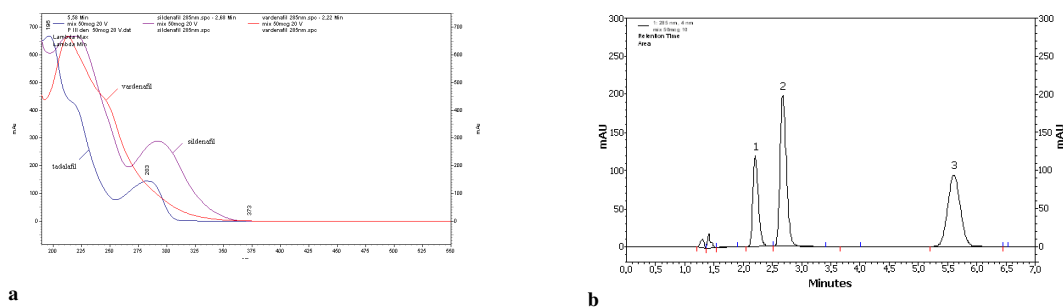


Figure 1. Spectra of standard solutions of: vardenafil, sildenafil and tadalafil (a) and a chromatogram of mix standard solution of: vardenafil, sildenafil and tadalafil (b)

References

1. ICH Q2R1: Validation of Analytical Procedures: Text and Methodology, Proceeding of the International Conference on Harmonization of technical Requirements for Registration of pharmaceuticals for Human Use, Geneva, Switzerland, 1996
2. Tomić S, Milčić N, Sokolić M, Martinac AI. Identification of counterfeit medicines for erectile dysfunction from an illegal supply chain. Arh Hig Rada Toksikol. 2010 Mar; 61(1):69-75. doi: 10.2478/10004-1254-61-2010-1953. PubMed PMID: 20338870.

PP039

INDIRECT SLOPE METHOD FOR IDENTIFICATION OF OOT RESULTS IN ON-GOING STABILITY STUDY

A.Torbovska¹, V. Petrusovski², R. Petkovska², S.T. Jolevska²

¹. ReplekPharm Ltd., 1000 Skopje, Macedonia, a.torbovska@gmail.com

². Faculty of Pharmacy, University of Ss Cyril and Methodius, 1000 Skopje, Macedonia

The lack of regulatory confirmed guideline for identification of OOT results within on-going stability data, aimed the authors to make statistical confirmation of the indirect slope method and prove its functionality in identification of OOT results in the on-going stability data. Also a comparison was made between the z-score method and the tolerance interval "TI" in terms of limits for OOT results identification.

A set of ten simulated batches were individually analyzed in comparison to the historical data composed of ten real batches placed on on-going study in accordance to the latest ICH guideline Q1A(R2). The reported data are results from the assay parameter, analyzed in accordance to the validated internal method of the manufacturer at the time points of 0, 3, 6, 9, 12, 18, 24 and 36 months. The z-score method and the TI were used to defined the limits for OOT results identification in the simulated data (2).

The indirect slope method provides analysis of each time point, of the on-going study, by analyzing the individual influence of each time point result on the regression line (1). The influence of each time point result is measured indirectly through the slope of the regression line comprised of all the data up to that time point. The first regression line consists the data of 0, 3 and 6 months, and the value of the slope is applicable for the time period of 0-6 months. The procedure is repeated until the last tested time point of the ongoing stability study. Any small change in the tested parameter from point to point, is precisely recorded in the slope value of each time interval, indirectly identifying the present OOT result.

The indirect slope method simulation resulted in identifying several OOT results in all of the simulated batches. The degree of deviation of the identified OOT results varied from 3 to 25 standard deviations (σ) from the average slope at the given time interval of the historical data. The z-score test provided constant limits of $\pm 2\sigma$, while the TI of $\pm 3.6\sigma$.

The indirect slope method detects any small change in the value of the tested parameter from point to point, indirectly through the slope value of the regression line. The z-score test produced limits that remain constant around all of the time points. TI's dependence of the number of samples included in the calculation, is a major drawback for its use. Finally, this paper highlights the necessity of issuing a regulatory confirmed guideline for identification of OOT results within on-going stability data.

References:

1. P.Rowe, 2007, Essential statistics for the pharmaceutical sciences, John Wiley & Sons Ltd., West Sussex, UK.
2. S. Bolton and C. Bon, 2004, Pharmaceutical Statistics- Practical and Clinical Applications, fourth ed. Vol. 135, Marcel Dekker Inc., Monticello, New York.

PP040

IBUPROFEN AND M(II) d-METALS: Cu, Co, Cd MICROQUANTITIES INTERACTION ANALYSIS

N. Krstić^{1*}, R. Nikolić¹, I. Kostić¹, N. Nikolić²

Ibuprofen is one of the most commonly used non-steroid antiinflammatory drugs with analgetic and antipiretic actions. Studying of M(II)-biometal and O-donor ligand (drug) interactions is interesting from multiple points of view, mainly because of improving drug dosage, drug biodistribution and tracking the pharmacokinetics of the drug. Also, because of decreasing unwanted effects of the drug, improving antimicrobial activity, synergistic actions with metals and improving antiulcerous and antitumorous activity and elimination (Dendrinou-Samara, 1998). There is an interaction of M(II)-ions of d-metals Cu, Co, Cd with ibuprofen (IB) when using molar and milimolar concentrations, which results in separation of solid products. Those products have been analyzed using FTIR technique and they have revealed that IB coordinates using carboxyl group. There is a limitation in application of this technique considering analysis of IB and M(II) metals interactions on their average content in organism, since they are only present in micromolar concentrations. In this paper, interaction between biometals Cu, Co and toxic Cd with IB as potential ligand has been analyzed using ESI-MS spectroscopy. Analyses have been performed using micromolar concentrations for analyzed metal and drug quantities characteristic for regular use.

M(II)-IB interaction has been analyzed in concentration range from 1 to 10 $\mu\text{mol}/\text{dm}^3$ IB and M(II), in molar ratio from 1:9 to 9:1, using solvent MeOH:H₂O, 80:20 (v/v). ESI-MS analyses have been performed on LCQ DECA Ion Trap Spectrometer (Thermo Finnigan, USA), with optimization of working conditions for ibuprofenate anion m/z 205 as a monitoring ion, using LOOP-chromatogram method. ESI-MS spectra and LOOP-chromatograms have been processed with Xcalibur LCQ Advantage 1.4 software. Based on the measured area under LOOP-chromatogram peaks for range m/z 204-206, calibration line ($y=a+bx$) has been derived after linear fitting. The line approximates observed dependency for IB itself as well as for binary systems of analyzed metals with IB. Integral under experimentally determined points has an area P_{IB} for pure IB, and $P_{\text{M(II)-IB}}$ for binary systems. Strength of M(II)-IB interaction has been measured using subintegral areas P_{IB} and $P_{\text{M(II)-IB}}$ and calculating their relative difference ΔP : $\Delta P = \frac{P_{\text{IB}} - P_{\text{M(II)-IB}}}{P_{\text{M(II)-IB}}} \times 100\%$, (Table 1).

Greater value of ΔP points to proportionally greater interaction in analyzed binary systems.

Table 1: Subintegral area values and their ΔP

	P	ΔP [%]
IB	254.45	/
Cu-IB	159.17	37.45
Co-IB	114.64	54.95
Cd-IB	160.89	36.77

Conclusions: Area under peaks on LOOP-chromatograms in presence of Cu(II), Co(II), Cd(II)-ions is smaller than the corresponding area for IB without metal ions which shows that there is a significant interaction M(II)-IB at micromolar level and that the interaction is the most expressed in Co(II)-IB system.

Acknowledgements: This work was supported by the Ministry of Education, Science and Technological Development of the Republic of Serbia, Project No. III45017.

Reference: Dendrinou-Samara, C., Tsotsou, G., et al., 1998. Anti-inflammatory drugs interacting with Zn(II), Cd(II) and Pt(II) metal ions. J. Inorg. Biochem. 71, 171-179.

PP043

ACCELERATED STABILITY TESTS AND EFFECTS OF EXCIPIENTS ON THE STRUCTURE OF HYDROXYPROPYLCELLULOSE FREE FILMS

M. Gottnek, G. Farkas, T. Sovány, O. Berkesi, K. Pintye-Hódi, G. Regdon Jr.*

University of Szeged, Szeged, Hungary

*geza.regdon@pharm.u-szeged.hu

The aim of the present study was to determine the physicochemical properties and the stability of Klucel[®] MF free polymer films in the presence of various concentrations of glycerol and xylitol as excipients.

Hydroxypropylcellulose was used as film-forming polymer. Xylitol was used as taste improver and glycerol was used as taste coverer. The film forming polymer was used in 2 w/w%. The excipients were all incorporated in the same concentration (5, 10 or 15 w/w % of the film-forming polymer).

All the films were made by the same pouring technology and stored at room temperature (25 °C/65%RH.) for a day and then placed into a climate chamber for a month (40 °C/75%RH.). The fresh and the one-, two- and four-week-old stored samples were measured by FT-IR spectroscopy, X-ray diffraction and TG-MS.

FT-IR spectroscopy: When glycerol was added at 5 or 10 w/w%, it entered the structure of the polymer, this fact was detected in ~2900 cm⁻¹ (CH₂ group) and ~1725 cm⁻¹ (CH₃CH₂CH-OH group) on FT-IR spectra. In case of 15 w/w% the excipient did not completely enter the film forming polymer (1597-1600 cm⁻¹). On the first week – under climate chamber storage – the samples absorbed water which had migration in the polymer matrix. This phenomenon had minimum-maximum ranges and finally the system was balanced. This state was local and the system was thermodynamically instable. After two weeks under storage, the 15 w/w% glycerol was entering the polymer. When xylitol was used alone, the same results were found. The two excipients used together entered the polymer matrix in all concentrations in fresh samples. Water migration was detected but the system was the most stable. In FT-IR studies the process of decomposition was not realized.

X-ray diffraction: Water migration was detected, but regularity was not found in this case. It was independent of compositions or concentrations. Probably during drying the glycerol and the xylitol had migration between the polymer chains and this caused inhomogeneous effect in the system, which was responsible for water absorption and migration. Amorphous xylitol was found in X-ray diffraction. Decomposition of the samples was not found.

TG-MS: These results confirmed that a stable film structure evolved in every case. First the absorbed water left the system and most water was absorbed in samples containing glycerol (Table 1.).

Table 1. Weight decrease of samples containing 15% glycerol.

Sample	Decrease of weight 1 st step (%)	Decrease of weight 2 nd step (%)
G 15% fresh	-3.65 ±0.07	-89.93 ±0.75
G 15% 1 st week	-3.28 ±0.14	-87.85 ±1.02
G 15% 2 nd week	-3.43 ±1.66	-87.86 ±1.14
G 15% 4 th week	-1.89 ±0.29	-87.83 ±2.05

Both excipients had marked effects on the tested polymers which were stable. Decomposition of the system was not realized. The most stable film structure was found if glycerol and xylitol were used together in samples. The used excipients enter the structure of the polymer in fresh samples or under the storage.

PP044

NEW AMIDE DERIVATIVES OF PYRROLIDINE-2,5-DIONE AS POTENTIAL WIDE RANGE ANTICONVULSANTS

K. Kamiński,^{1,*} J.J. Łuszczki,^{2,3} J. Obniska¹

¹. Jagiellonian University, Medical College, Krakow, Poland

². [Medical University of Lublin, Lublin, Poland](#)

³. [Institute of Agricultural Medicine, Lublin, Poland](#)

*Corresponding author: k.kaminski@uj.edu.pl

Even though significant advances have been made in epilepsy research, convulsions in almost one third of patients are inadequately controlled by standard drug therapy. Furthermore, compliance is often limited by adverse side effects most notably related to central nervous system exposure like diminished attention, executive function, intelligence, language skills, memory and processing speed. Taking into consideration the above continued search for safer, more effective and possibly antiepileptogenic drugs is urgently necessary.

In the current studies a library of twenty two differently substituted 1-[2-oxo-2-(4-phenylpiperazin-1-yl)ethyl]pyrrolidine-2,5-diones was synthesized. The structures of molecules were designed as further analogues of levetiracetam or brivaracetam, which are the newest and the most effective AEDs (especially in partial and therapy-resistant epilepsy). The synthetic procedures and structures of final compounds **9-30** are shown in **Fig. 1**.

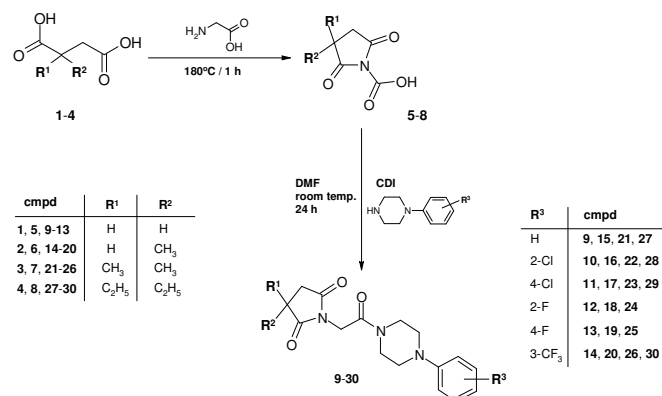


Fig.1.

The final compounds were obtained in coupling reaction of intermediate acids with appropriate amines in the presence of carbonyldiimidazole (CDI). The purities of all molecules were assessed by TLC and gradient HPLC chromatography. The structures were assigned on the basis of ¹H NMR, mass spectra (LC/MS) and elemental (C, H, N) analysis.

The initial anticonvulsant evaluation was performed within the Antiepileptic Drug Development (ADD) Program in the Epilepsy Branch, National Institutes of Health, National Institute of Neurological Disorders and Stroke (NIH/NINDS), Rockville, MD, USA. The anticonvulsant activity was determined in mice in the maximal electroshock (MES), subcutaneous pentylenetetrazole (*sc*PTZ), and psychomotor (6-Hz) seizure models after intraperitoneal administration.

Results: Except of inactive compound **27**, all other molecules were found to be effective in at least one seizure model (MES, *sc*PTZ, 6-Hz). The most active were 1-(2-oxo-2-{4-[3-(trifluoromethyl)phenyl]piperazin-1-yl}ethyl)pyrrolidine-2,5-dione (**14**), 1-{2-[4-(4-chlorophenyl)piperazin-1-yl]-2-oxoethyl}-3-methylpyrrolidine-2,5-dione (**17**), 1-{2-[4-(4-chlorophenyl)piperazin-1-yl]-2-oxoethyl}-3,3-dimethylpyrrolidine-2,5-dione (**23**) and 3,3-dimethyl-1-(2-oxo-2-{4-[3-(trifluoromethyl)phenyl]piperazin-1-yl}ethyl)pyrrolidine-2,5-dione (**26**). These compounds showed high activity in the 6-Hz psychomotor seizure test as well as were active in the maximal electroshock and subcutaneous pentylenetetrazole screens. It may suggest their potential effectiveness in different types of epilepsies including therapy-

resistant one. The SAR studies showed that the most potent are 3-unsubstituted, 3-methyl- and 3,3-dimethyl-pyrrolidine-2,5-diones. The introduction of longer ethyl groups decreases activity. Taking into consideration an amine function the presence of trifluoromethyl group or chloro and fluoro atoms (position-4) at phenylpiperazine moiety are preferential for anticonvulsant properties.

Acknowledgements:

The studies were supported by the Polish National Scientific Center grant 2012/05/D/NZ7/02328.

PP047

HPLC ANALYSIS OF NINE CORTICOSTEROIDS IN “NATURAL CREAMS” FOR ATOPIC ECZEMA

A. Ameti¹, Z. Poposka¹, Sh. Memeti¹, M. Shishovska¹, Z. Mustafa¹, K. Starkoska¹, Z. Arsova-Sarafinovska¹
¹ Institute of Public Health of Macedonia, 50 Divizija 6, 1000 Skopje, FYROM

The aim of the study was to determine whether “natural creams” sold for treatment of childhood atopic eczema illegally contain corticosteroids with a newly developed rapid and simple HPLC analysis with UV detection. HPLC analysis was performed using a Shimadzu LC-2010 chromatographic system (Shimadzu, Kyoto, Japan) consisting of a LC-20AT Prominence liquid chromatograph pump with DGU-20A5 Prominence degasser, a SPD-M20A Prominence Diode Array Detector, and a SIL-20 AC Prominence auto sampler. Data analyses were done using Class VP 7.3 Software. The elution was carried out on a column Purospher STAR[®] RP 18e (250 x 4.6 mm i.d., particle size 5µm), with a mobile phase consisted of acetonitrile and water in a gradient mode, at a flow rate of 1.0 mL min⁻¹, at controlled column temperature (25°C). Detection of nine different corticosteroids (dexamethasone, prednisolone, methylprednisolone, fluocortolone, hydrocortisone, mometasone, betamethasone, beclomethasone, and diflucortolone) was carried out with DAD detector at a wavelength of 240 nm. The injection volume was 10 µl. The samples were five different creams sold for the treatment of childhood atopic eczema (marketed as steroid free) and were submitted by the state regulatory authority, Bureau of the medicines. The method was fully validated according to the ICH (International Conference on Harmonization) guidelines by the determination of linearity, precision, accuracy, limit of detection (LOD) and limit of quantification (LOQ). Selectivity of the method was proved with the chromatographic peak resolution obtained between each of the nine different corticosteroids and the characteristic UV spectra. Linearity of the method was tested in the range of 0.4 – 8 µg mL⁻¹ for all substances analysed. Experimental data showed high level of linearity for all corticosteroids (ranging from R² = 0.9981 for diflucortolone to R² = 1.0 for dexamethasone, prednisolone, fluocortolone, hydrocortisone, mometasone, and beclomethasone). The accuracy of the method was demonstrated by the values obtained from the recovery experiments (ranging from 98.67%, for diflucortolone to 101.33% for beclomethasone). The method was successfully applied to the analysis of real samples of creams sold as steroid free. The analyses revealed that two of the samples contained corticosteroids. The proposed HPLC method allows a simple, accurate, and rapid identification of corticosteroids in creams used for the treatment of atopic eczema.

Table 1. LOD and LOQ of the method

Corticosteroid	RT (min) ¹	LOD (ng) ²	LOQ (ng) ³
Dexamethasone	5.20	0.18	0.56
Prednisolone	6.81	0.20	0.59
Methylprednisolone	7.44	0.20	0.60
Fluocortolone	9.91	0.42	1.29
Hydrocortisone	10.58	0.23	0.69
Mometasone	23.13	0.22	0.66
Betamethasone	23.56	0.36	1.09
Beclomethasone	25.64	0.46	1.40
Diflucortolone	26.56	0.78	2.36

¹ Retention Time

² Limit of Detection

³ Limit of Quantification

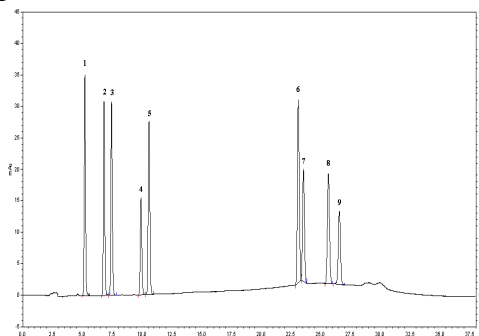


Figure 1. A typical chromatogram of the mixed standard solution containing: dexamethasone (1), prednisolone (2), methylprednisolone (3), fluocortolone (4), hydrocortisone (5), mometasone (6), betamethasone (7), beclomethasone (8), and diflucortolone (9).

Literature Reference

1. ICH Q2R1: Validation of Analytical Procedures: Text and Methodology, Proceeding of the International Conference on Harmonization of technical Requirements for Registration of pharmaceuticals for Human Use, Geneva, Switzerland, 1996.

2. Ramsay HM, Goddard W, Gill S, Moss C. Herbal creams used for atopic eczema in Birmingham, UK illegally contains potent corticosteroids. Arch Dis Child. 2003 Dec;88(12):1056-7. PubMed PMID: 14670768; PubMed Central PMCID: PMC1719403.

PP048

EVALUATION OF SUBSTITUTED UREAS POTENTIAL TOXICITY BY CORRELATION STUDIES USING TOPOLOGICAL INDICES, MOLECULAR DESCRIPTORS AND ADMET PARAMETERS

M. Jadrijevic-Mladar Takac¹, V. Takac², V. Crnek-Kunstelj³

¹ Faculty of Pharmacy and Biochemistry, University of Zagreb, Zagreb, Croatia

² Health Institution Stefanic Pharmacies, Zagreb, Croatia

³ Medical School, University of Zagreb, Zagreb, Croatia

The potential toxicity of several cyclic and acyclic urea derivatives were evaluated in correlation studies using topological indices, molecular descriptors and ADMET toxicological parameters. Urea derivatives (n=17) were synthesized in our labs and tested on cell viability on human acute monocytic leukemia THP-1 and human acute T cell leukemia Jurkat cell lines, as well as on the antibacterial activity against three E. coli strains (strains susceptible to antibiotics and resistant to macrolide and aminoglycoside antibiotics). (Kos et al., 2013)

Topological indices (TIs) were calculated by the *software* DRAGON 6.0, molecular descriptors (MDs) and ADMET parameters were predicted by MedChem StudioTM and ADMET PredictorTM 6.0 (Simulations Plus, Inc., USA). All analyses were performed using OriginPro 8.0 software (Origin Laboratories, USA).

Out of 16 indices used in these studies the best correlations were obtained with: Wiener number (W), Randić number (CID), Randić connectivity index (χ^1) and information index on molecular size (ISIZ) with molecular descriptors (Sv – sum of the van der Waals volume scaled on C, Mr - relative molecular mass and MLog P – lipophilicity). The following correlations were obtained: W vs M_r (R = 0.9464), ISIZ vs MLog P (0.7926), χ^1 vs MLog P (R = 0.7825), CID vs MLog P (R = 0.7797), M_r vs MLogP (R = 0.8761) and MLog P vs Sv (R = 0.8491). The best linear correlation was obtained between ISIZ and TOX hERG scores (R = 0.8170) while correlations of TIs and MDs with metabolic activity on THP 1 or Jurkat cell lines were of less significance. Parameters, predicted for these compounds by ADMET analyses are: ADMET risk between 1.0 - 7.0, CYP risk 0.0 - 2.0 and TOX risk 1.0 - 5.0.

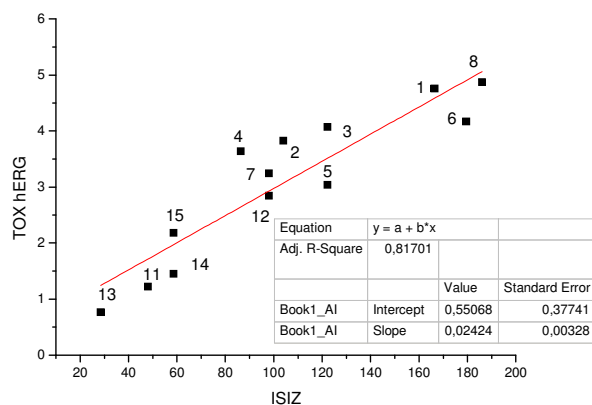


Fig. 1. The correlation between computed information index on molecular size (ISIZ) and predicted ADMET TOX hERG scores of investigated urea derivatives

Topological indices (W, CID, χ^1 and ISIZ) were successfully used in correlation studies with molecular descriptors (MDs) and ADMET parameters in a series of substituted urea derivatives. For compounds with the most significant metabolic activity either on THP 1 or Jurkat cell line (*N*-hydroxy- and *N,N'*-bisbenzyloxy-urea, *N*-hydroxy-, *N,N',N'*-tribenzyloxy-

and *N,N',N''*-trihydroxy-biuret) the highest scores for their toxicological parameters were revealed.

Reference. Kos[†] I., Jadrijevic-Mladar Takac M., Butula[†] I., Birus M., Maravic-Vlahovicek G., Dabelic S., 2013. Synthesis, antibacterial and cytotoxic activity evaluation of hydroxyurea derivatives. *Acta Pharm.* 63, 175-191; doi: 10.2478/acph-2013-0014.

PP052**EFFECT OF THE NATURE OF PLASTICIZER ON THE HOT MELT EXTRUSION AND RELEASE OF VENLAFAXINE HYDROCHLORIDE**

Melina Bounartzi, Athanasia Panagopoulou, Ioannis Nikolakakis
Department of Pharmaceutical Technology, School of Pharmacy, Faculty of Health Sciences,
Aristotle University of Thessaloniki, 54124, Thessaloniki, Greece

During hot melt extrusion (HME), phase changes and interactions due to thermo-mechanical stresses may affect the drug incorporation into polymeric matrices and the release rate. Two HME formulations of venlafaxine HCl (15%) with Eudragit[®] RSPO (70%) as the matrix polymer and either citric acid monohydrate (CA) or Lutrol[®] F127 as plasticizers (15%) were compared. Corresponding binary polymer/plasticizer mixtures of the same ratio as in the drug formulations were also prepared in order to examine the effect of drug on extrusion. Additionally, tablets with the same composition of the extruded formulations were prepared by direct compression of powder mixtures and their release profiles were compared with those of the extruded products. The temperatures in the different barrel zones and in the exit die that allowed extrusion were deduced, based on predictions from differential scanning calorimetry (DSC) measurements. Furthermore, the pressure exerted during extrusion in the barrel wall near the exit of the melt was recorded and the processability of the different compositions was estimated from the pressure ranges recorded at different extrusion rates (Table 1). Thermal changes in the extruded melts and powder X-ray Diffractograms (PXRD) were obtained to detect changes in crystallinity, manifested from the different appearance of the extrudates (Table 1). Dissolution of the drug from the extruded microcylinders as well as from direct compression tablets was tested on a USP II type dissolution apparatus and samples were analysed for drug content using fluorescence spectroscopy ($\lambda_{ex}=237$, $\lambda_{em}=301nm$).

It was found that both plasticizers in combination with Eudragit[®] RSPO enabled extrusion of venlafaxine hydrochloride, but Lutrol[®] at much lower wall pressure range, compared to CA (Table 1). This can be explained due to their different plasticizing mechanisms, indicating that interaction between Eudragit[®] and Lutrol through dispersion molecular forces is more efficient in reducing friction within the molten polymeric chains than H-bonding between Eudragit[®] and CA [1]. The PXRD results showed that in the extrudates with Lutrol[®], the drug remained mostly crystalline (data not shown) indicating dispersion of crystalline phase of drug, whereas, with CA a single phase amorphous transparent extrudate was obtained indicating solid solution (Table 1). The drug release from the extruded microcylinders clearly followed diffusion mechanism, whereas the release from the corresponding tablets was instant (Fig. 1). This is explained by the fact that in the extruded melt the drug particles are completely surrounded by the polymeric matrix material with dissolution occurring through diffusion of the drug in the channels created in the beginning of the test by the water soluble hydrophilic plasticizer.

Table 1. HME compositions, process conditions and melt appearance

Composition	Temp (°C)	Appearance pressure (psi)
Eudragit CA	T ₁ =100	Transparent 340-1600
	T ₂ =110	
	T ₃ =115	
	T ₄ =120	
Eudragit Lut	T ₁ =90	Transparent 80-1375
	T ₂ =100	
	T ₃ =110	
	T ₄ =115	
Eudragit CA Drug	T ₁ =100	Transparent 1100-1800
	T ₂ =110	
	T ₃ =115	
	T ₄ =120	
Eudragit Lut Drug	T ₁ =95	Opaque 325-1400
	T ₂ =110	
	T ₃ =115	
	T ₄ =120	

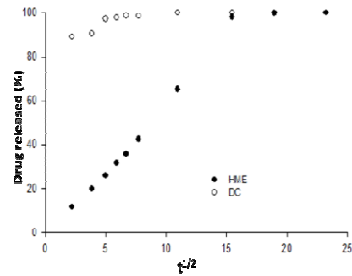


Fig. 1. Drug released (%) against square root of time for hot melt extruded microcapsules (solid symbols) and tablets (open circles) of venlafaxine hydrochloride with citric acid monohydrate

References

- [1] Bounartzi M. et al., 2013. J. Pharm. Pharmacol. doi: 10.1111/jphp.12117.

PP057

HEA-HEMA HYDROGELS AS DELIVERY SYSTEM FOR BIOPHARMACEUTICALS: INTERACTIONS WITH PROTEINS

E. Hackl¹, J.Falkenberg¹, V. Khutoryanskiy², I. Ermolina^{1*}

¹. De Montfort University, Leicester, UK

². University of Reading, Reading, UK

*e-mail: iermolina@dmu.ac.uk

Hydrogels, the three-dimensional polymeric networks which are capable of imbibing large amount of liquid, have attracted considerable attention over last years due to numerous applications, in particular as carriers for sustained drug delivery. Recently we described novel hydrogels consisted of 2-hydroxyethylmethacrylate (HEMA) and 2-hydroxyethylacrylate (HEA) [1]. We have shown that introduction of hydrophilic HEA significantly changes HEA-HEMA hydrogel morphology and physicochemical properties.

The aim of the present work was to characterise the interaction of HEA-HEMA hydrogels with proteins (chicken egg white lysozyme (14.3 kDa) and bovine serum albumin (66.5 kDa)) and to access the potential applications of these hydrogels as a drug delivery system for sustained release of large biopharmaceuticals.

Interaction of lysozyme and albumin with hydrogels having 11 different HEA-HEMA ratios has been studied. HEA-HEMA hydrogel morphology, mechanical properties, swelling kinetics, amount of free and bound water, protein *in vitro* loading and release profiles were examined using SEM, UV-Vis and fluorescence spectroscopy, FTIR, TGA, DSC, and texture analysis. The structure of proteins released from hydrogels was analyzed using UV-Vis spectroscopy, FTIR, fluorescence spectroscopy (intrinsic and ThT assay).

Protein uploading into HEA-HEMA hydrogels shows no significant effect on the hydrogel morphology (pore sizes) and swelling degree; however it leads to a minor redistribution of free and bound water in the samples. HEA-HEMA hydrogels can be relatively quickly loaded with lysozyme; the loading rate depends on the protein concentration, temperature and hydrogel composition. The rate of lysozyme release also depends strongly on the copolymer composition: an increase in the content of HEA leads to significant decrease in protein release time from about 10 hours for 70% of lysozyme release from HEA-HEMA (10:90 mol %) to about 40 min for HEA-HEMA (70:30 mol %). Lysozyme released from hydrogels produces UV, FTIR and fluorescence spectra typical for a native protein. However, when an additional stress (protein freeze-drying with no protectant) has been applied, lysozyme released from HEA-low (0-30%) hydrogels reveals some alterations in the protein secondary structure and increased tendency to aggregate. In contrast to lysozyme, albumin uptake by HEA-HEMA hydrogels was very low (especially for HEMA-rich samples) regardless of albumin concentration and time of hydrogel incubation in protein solution.

Our results show that HEA-HEMA hydrogels can be applied as a drug delivery system for biopharmaceuticals such as relatively small proteins. Varying the HEA-HEMA hydrogel composition a desirable protein release time can be achieved. Proteins released from hydrogels with intermediate and high HEA content preserve their native conformation.

Reference

[1] Khutoryanskaya O.V. et al. *Biomacromolecules*, 9 (2008) 3353.

PP058

HEA-HEMA HYDROGELS AS DRUG DELIVERY SYSTEMS: STUDY OF THE PHYSICO-CHEMICAL PROPERTIES

I. Ermolina^{1*}, E. Hackl¹, V. Khutoryanskiy²

¹ De Montfort University, Leicester, UK

² University of Reading, Reading, UK

* e-mail:iermolina@dmu.ac.uk

Hydrogels are three-dimensional hydrophilic polymeric networks, which can absorb large amounts of water. These materials have been used in many pharmaceutical and biomedical applications, i.e. drug delivery systems, contact lenses and wound dressings. The hydrogels prepared by copolymerisation of HEMA and HEA have shown potential for various biomedical applications.

The aim of this work was to study the physicochemical properties of 2-hydroxyethylacrylate-*co*-2-hydroxyethylmethacrylate (HEA-HEMA) hydrogels with different copolymer compositions to evaluate their potential applicability as drug delivery systems. The hydrogel samples were synthesised by three-dimensional free-radical copolymerisation of HEA and HEMA [1]. Eleven hydrogel samples with different HEA/HEMA ratios were prepared starting from pHEMA (HEA0:HEMA100) to pHEA (HEA100:HEMA0) with 10 mol % step. Hydrogel structures and physicochemical properties were studied using SEM, thermoanalytical methods (TGA, DSC), spectroscopic methods (broadband dielectric spectroscopy (BDS) and FTIR), mechanical analysis (Texture analysis (TA) and friability assay), and drug loading/release assays. SEM analysis was performed for the samples fully swollen in water. The structure and morphology of hydrogels significantly changes depending on the composition of copolymers: the pore size increases with increase in HEA content, but the main effect is the dramatic increase in porosity and as a result in the swelling capacity of hydrogels. TGA study confirms that the amount of water absorbed by polymeric network dramatically increases for hydrogels with HEA content >40%. Rate and profile of water evaporation from fully swollen samples was also analysed as a function of time. The combination of TGA and DSC results allowed estimating the amount of free and bound water in hydrogel samples. Dielectric spectroscopy, employed to assess the water-polymer molecular dynamics in hydrogels, confirmed the existence of two types of water. Two relaxation processes were observed in a wide range of frequencies and temperatures. The HEA-HEMA composition of hydrogels also affected the drug release properties. The time of drug release was found to be strongly dependent on the hydrogel composition with decreasing from 10-15 hours for pHEMA to < 1 hour for pHEA. Study of mechanical properties has shown that the hydrogels become fragile and difficult to handle as the HEA content is increased. Physicochemical properties of HEA-HEMA hydrogels are strongly dependent on the composition of the co-polymeric network and notably change at ~40% of HEA content. An increase in the content of the hydrophilic HEA in hydrogel enhances the swelling degree and the rate of drug release, but significantly weakens the mechanical properties. The thermodynamic and mechanical properties as well as drug release rate can be controlled and improved by adding HEA to HEMA monomer to prepare hydrogels. Variation in the copolymer composition allows obtaining the hydrogels with the desirable properties for drug delivery.

Reference:

[1] Khutoryanskaya O.V. et al.. *Biomacromolecules*, 9 (2008) 3353.

PP059

OVER TIME ADAPTIVE QSPR ON IAM CHROMATOGRAPHIC INDICES

T. Vallianatou, D. Vrakas, N. Malaki, A. Tsantili-Kakoulidou*
University of Athens, Panepistimiopolis, Zografou, Athens, Greece

In the present study, Multiple Linear Regression (MLR) and Partial Least Squares (PLS) were implemented for the establishment of QSPR models for the prediction and rapid screening of IAM chromatography retention. Over-time validation of the derived models with

test compounds was attempted in order to evaluate their robustness and predictive power and for further updating.

The initial MLR model [1], including 56 structurally diverse drugs as training set, was validated using a test set (I) of 37 drugs of comparable diversity and a test set (II) of 5 sartan derivatives, measured in our laboratory at different time periods. The model included experimental logD values and fraction of positive and negative species as the only variables. Next, PCA/PLS models based on computational descriptors (lipophilicity expressed as ClogP) were established for the same training set and validated with the test sets I and II. Deviation from 1:1 correlation between observed and predicted value was considered as criterion for model performance. The PCA scores plot and the Distance to Model were used to assess the applicability domain (AD) of the models. In all cases, the test sets were integrated to the last model. Table I summarizes the results of representative model validation and updating. The simple MLR model, although inferior in statistics proved more robust in prediction and integration of test set I, in comparison to the PLS model. Most sartans (test set II) with unsatisfactory predictions were found to lie outside the AD of the models. In conclusion, model validation and updating over time, based on additional metrics besides R^2 , is necessary to improve predictions, broaden the AD as well as to identify chemotypes outside the AD.

Table 1.

MLR models							
Model	R^2	slope	intercept	Model	R^2	slope	intercept
Training set	0.880	1.000	9.1×10^{-7}	Train.+test I	0.830	1.000	9.9×10^{-7}
Test set I	0.825	0.928	0.131				
Test set II*	0.958	1.118	1.080	Test set II	0.958	1.208	0.793
PLS Models							
Training set	0.923	0.995	0.030	Train.+test I	0.865	0.997	0.016
Test set I	0.738	0.999	0.183				
Test set II*	0.957	1.835	-2.746	Test set II	0.886	1.614	-2.793

*Unsatisfactory predictions despite the high R^2

Reference

[1] D.Vrakas, C. Giaginis, A. Tsantili-Kakoulidou., J. Chromatogr.A 1187 (2008) 67-78

*Corresponding author, e-mail address: tsantili@pharm.uoa.gr

PP060

COMPARISON OF THE PERFORMANCE OF NEURAL NETWORK AND PLS MODELS IN THE PREDICTION OF PPAR- α AND - γ AGONISM.

T.Vallianatou¹, B. Hedayati², N. Dimopoulos², A. Tsantili-Kakoulidou^{1*}

¹University of Athens, Panepistimiopolis, Zografou, Athens, Greece

²University of Victoria, Victoria, CANADA

Dual PPAR- α/γ agonists may improve both lipid and glycemic profiles leading to anti-diabetic agents with reduced side effects; thus considerable research efforts are directed towards this approach. In silico predictions of dual or multi-target activities permit rapid screening of compound libraries and contribute to the design of novel drug candidates faster. For this purpose different statistical techniques may be applied which need to be validated in respect to their trustworthiness.

In the present study we used a new method based on neural networks to generate models for PPAR- α and - γ agonism and compare their performance with that of linear models, previously established for the same data set [1]. The training set included 71 compounds with biological data taken from literature and further 23 compounds were used as a blind validation set. The proposed NN method creates a number of trained neural networks, and then selects a subset of them whose responses are averaged to produce the response of the model. The criteria of selection aim to reject trained NN that do not contribute to the local smoothness of the response. Additionally, the method selects trained NN that have responses, when they are presented with an arbitrary single exemplar, that are consistent with each other, and they are not “outliers”. Details of the method can be found in ref. [2]. The pool of descriptors comprised physicochemical /molecular properties; 3-D descriptors, connectivity and electrotopological state indices, which after Principal Component Analysis were reduced to 30 Principal Components according to the largest eigenvalues of the cross-correlation matrix, including 99.5% of the information.

For PPAR- α both methods produce roughly equivalent results. Based on the geometric mean of the relative errors, the NN-based model improves the average error of the response by 0.0043 or by 8.4% for the blind validation set. More importantly, the NN-based model was able to predict successfully the highly active ligands, mispredicted in the PLS model. Inferior models were obtained for PPAR- γ activity. Although the geometric mean in the NN-based model was equally low and the average error of the response was improved by 0.053 or 53% in respect to the PLS model, there were five mispredictions of the test compounds.

In conclusion, NN models outperform PLS models in terms of predictions and are suitable for library screening. However, they do not provide insight of the mechanism of action and the physicochemical property requirements. On the other hand, the easier to interpret PLS models may be more useful for guiding further synthesis.

References

- [1] Vallianatou T., Lambrinidis G, Giaginis C., Mikros E., Tsantili-Kakoulidou A. Mol. Inform. (2013) 32: 431-445
[2] Hedayati B.K., Parra-Hernandez R., Laxdal E.M., Dimopoulos N.J., Alexiou P., Demopoulos V.J. Proceedings, 2012 International Joint Conference on Neural Networks doi: 10.1109/IJCNN.2012.6252798

*Corresponding author, e-mail address: tsantili@pharm.uoa.gr

PP062

NNRTI HIV CHEMOTHERAPEUTICS: DOCKING AND 3DQSAR AS COMPLEMENTARY STRATEGIES IN VIRTUAL SCREENING OF A QUINOXALINE ANALOGUES LIBRARY

L. Fabian¹, N. Gomez¹, G. Jasinski¹, D. Estrin², [A. Mogliani](mailto:amoglio@ffyb.uba.ar)¹

¹. FFyB, University of Buenos Aires, Buenos Aires, Argentina

². FCEN, University of Buenos Aires, Buenos Aires, Argentina

amoglio@ffyb.uba.ar

Non-nucleoside reverse transcriptase inhibitors (NNRTIs) are promising drugs for the treatment of HIV when used in combination with other anti-HIV drugs such as nucleoside reverse transcriptase (RT) inhibitors and protease inhibitors. The aim of this study was to design new NNRTIs candidates based on the analysis of a quinoxaline virtual library using 3DQSAR and docking studies as a synergistic approach.

3DQSAR models were developed applying a genetic algorithm implemented in McQSAR¹ 1.2 based on *in-vitro* biological data previously published² together with 3D descriptors calculated using PaDEL 2.15 (<http://padel.nus.edu.sg/software/padeldescriptor/>). The atomic coordinates of a set of 30 NNRTIs were extracted from crystal structures of HIV-1 wild type RT (<http://www.rcsb.org/>) and the statistical refinement of the 3DQSAR models was carried out with Origin 7.0.

A quinoxaline analogue virtual library was created using an *in-house* developed program, set to build molecular models based on drug-likeness characteristics and combinatorial chemistry paths previously developed in our laboratory. Virtual screening (VS) of this library was performed with AutoDock Vina 1.0 (<http://vina.scripps.edu/>) on the binding site of wild type and mutant HIV-1 reverse transcriptase. An *in-house* developed program was used to select those ligands with the highest AutoDock Vina scores (cutoff: -9.0 Kcal/mol) in at least 6 of the RT variants studied. Final compound candidates were selected according to the 3DQSAR model described above (cutoff: $\text{plog(IC}_{50}) = 8.0$).

A QSAR model, Ec. 1 (Table 1) was obtained based on NNRTIs with diverse chemical structure and reported biological activity.

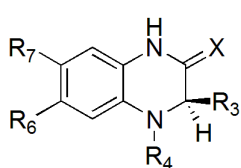
Table 1. 3DQSAR models obtained based on NNRTIs extracted from crystal structures of HIV-1 RT

Ec.	Log (1/CI ₅₀)	n ^a	r ^b	R ² ^c	R ² _{adj} ^d	SD ^e	F ^f
1	0.86(±0.11)XlogP + 3.85(±0.44)WD _{eneg}	30	0.95	0.91	0.90	0.58	92.95
2	0.53 + 1.02(±0.11)XlogP + 10.76(±1.28)Weta1 _{unity}	30	0.95	0.91	0.90	0.60	86.99
3	0.92(±0.11)XlogP + 5.40(±2.39)Weta1 _{unity} + 2.15(±0.85)WD _{eneg}	30	0.97	0.93	0.92	0.52	78.51

a: Number of observations. b: correlation coefficient. c: R square. d: adjusted R square. e: standard deviation. f: Fisher test.

In the aim of establishing SAR and developing new anti-HIV quinoxaline analogs a virtual library of 11686 compounds was generated using quinoxalin-2-ones and 3,4-dihydro-quinoxalin-2-ones as templates in combination with diverse substituents in positions 3, 3R, 3S, 4, 6 and 7 of this system. The compound selection was performed for this library by a VS experiment as the first selection stage, followed by application of the QSAR model criteria. Also, the 30 NNRTIs and 15 quinoxalin-2-one derivatives with reported biological activity were included for both SAR analysis and as validation samples for the QSAR model and VS. The validated selection process lead us to identify a series of quinoxalin-2-ones as candidates for synthesis and evaluation of RT enzymatic activity (Fig. 1).

Figure 1. Some of the substitution patterns selected for quinoxaline-2-one synthesis



R₃ = isoproyl, ethyl, ethylthio
R₄ = benzenesulfonyl, isopropylloxycarbonyl, isobutylloxycarbonyl, pyridyl-4-carbonil, 3-chloropropionyl, benzyloxycarbonyl.
R₆ = methyl, formylamino
R₇ = hydrogen, formylamino

A selection process based on the combination of 3DQSAR and docking was developed and applied in the design of new quinoxaline NNRTIs candidates. The SAR analysis performed

could likely be extended to other compound libraries by including more NNRTIs in the selection process. .

¹ M. J. Vainio and M. S. Johnson . J Chem Inf Model. 2005, 45, 1953-1961.

² J. Wang, et al. J Med Chem. 2005, 48, 2432-2444.

PP064

SWELLING AND RELEASE BEHAVIOR OF SODIUM ALGINATE MATRIX-TABLETS IN HYDRO-ETHANOLIC MEDIA

N. Al-Zoubi

Faculty of Pharmacy, Applied Science University, Amman, Jordan

Email: nizoubi@yahoo.com

In recent years, there has been a growing concern regarding the impact of concomitant intake of ethanol on the release from oral controlled-release dosage forms. The aim of this work is to investigate the effect of ethanol on the *in vitro* release behavior of sodium alginate (SA) matrix-tablets.

Two grades of SA (Protanal LF 200M and LF 120M) were obtained from FMC, USA. Metformin HCl (MH) was kindly donated by JPM (Jordan).

Five media comprising 0.1 N HCl with 0, 10, 20, 30 and 40% (v/v) ethanol were used in swelling and release studies to cover the concentrations found in alcoholic beverages.

SA was mixed with MH at 2:1 polymer:drug ratio for 15 min using a spatula. Thereafter, 1% magnesium stearate was added and additionally mixed for 5 min. Weighed samples (485 mg) of the mixture were then compressed in a KBr die set (d=13 mm) using a manual hydraulic press (370 MPa for 30 s)

The release study was performed in a USP paddle dissolution system at 100 rpm using 900 ml of the hydro-ethanolic medium at 37 °C. Samples were UV analyzed at 233 nm. The release data (<60%) were fitted to power law model.

Swelling experiments for SA matrix tablets were performed using 500 ml of the hydro-ethanolic media and the same apparatus and conditions used in drug release study. After 4 h of immersion, tablets were gently withdrawn from the media, weighed and dried to a constant weight. Swelling parameters were determined according to the following equations:

$$\text{Medium uptake} = (W_w - W_d) / W_d$$

$$\text{Mass loss (\%)} = (W_i - W_d) \times 100 / W_i$$

where W_i , W_w , W_d refer to the initial tablet weight, the weight of wet tablet and the weight of dried tablet, respectively. The swollen tablets were also imaged using a digital camera.

The release profiles of MH from SA matrix-tablets in hydro-ethanolic media (Fig. 1) show similar behaviour for both grades, where the release of MH was sustained for almost 8 h in acidic media with ethanol concentrations up to 20%. At higher ethanol concentrations (30 and 40%) very rapid drug release occurred (almost complete release within 15 min) associated with matrix disintegration (Figs.1 and 2).

The similarity between the two grades (with different SA molecular weight) might be partially attributed to the acidic conditions where matrix erosion is trivial and the main mechanism of release is drug diffusion through matrix pores, as indicated by low n values for 0 and 10% ethanol concentration (Table 1). At 20% ethanol concentration, tablets showed almost linear release (Fig. 1, Table 1) associated with remarkable medium uptake and softening, although no clear gel layer or increased erosion was noticed (Fig. 2, Table 1). Rapid matrix disintegration in media with higher ethanol concentrations (30 and 40%) did not allow accurate determination of swelling parameters or release modelling. However, greater medium uptake is expected, which might be responsible for disintegration by increasing internal pressure within the matrix-tablets.

CONCLUSION

The results of this study showed that the presence of ethanol in acidic dissolution media at concentrations relevant to strong alcoholic beverages caused dose dumping associated with disintegration of SA matrix tablets.

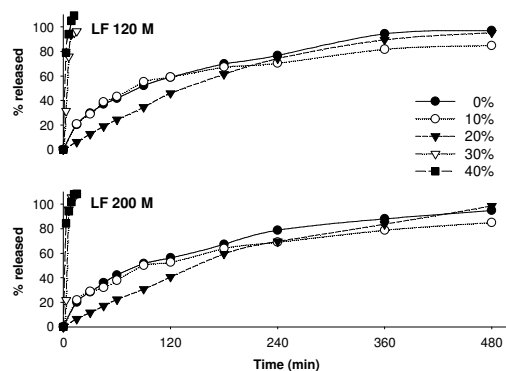


Fig. 1: Release profiles of MH from SA matrix-tablets in acidic hydro-ethanolic media.

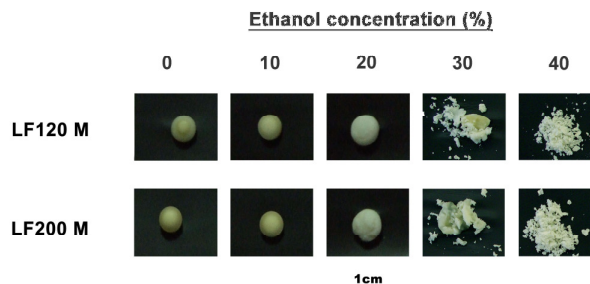


Fig. 2: Photographs of SA matrix-tablets after swelling test in hydro-ethanolic acidic media. The immersion time is 240 and 30 min for 0-20% and 30-40% ethanol concentration, respectively.

Table 1: Exponent (n) obtained by fitting of release data to power law model ($R>0.99$) and swelling parameters (Medium uptake, MU, and mass loss, ML, after 4 h of immersion) for SA matrices in hydro-ethanolic acidic media

Ethanol conc. (% v/v)	LF 120 M			LF 200 M		
	n	MU	ML (%)	n	MU	ML (%)
0	0.51	1.9	39.5	0.51	1.9	40.0
10	0.52	1.5	36.8	0.43	1.6	37.0
20	0.94	4.0	37.9	0.89	4.2	37.1

PP067

INVESTIGATION OF SUSTAINED RELEASE MATRIX-TABLETS PREPARED FROM COSPRAY-DRIED AND SIMPLE PHYSICAL MIXTURES WITH POLYVINYL ACETATE-POLYVINYL PYRROLIDONE EXCIPIENTS

N. Al-Zoubi*, G. Alobaidi

Excipients based on polyvinyl acetate (PVAc) and polyvinyl pyrrolidone (PVP) are showing increasing interest for use in sustained-release systems. This work aims to investigate PVAc-PVP matrix-tablets regarding the effect of increasing PVP percentage in the matrix former (MF) and to compare between matrix-tablets prepared from cospray-dried mixtures with Kollicoat SR 30D and those prepared from simple physical mixtures with Kollidon SR.

Kollicoat SR 30D, Kollidon SR and Kollidon K30 were kindly donated by BASF, Germany. Diltiazem HCl (DH) was kindly donated by UPM, Jordan.

Spray drying was performed in a Pulvis mini-spray GA32 (Yamato Scientific, Japan). Co-agglomerates with different drug:matrix former, D:MF, ratios (1:1, 1:2 and 1:3) and percentages of PVP in the MF (9, 14, 19, 29%) were obtained by changing the amounts of DH, Kollicoat SR 30D and Kollidon K30 in the feed dispersion. The operation conditions were set as follows: inlet air temperature 135 °C, outlet air temperature 58-62 °C, spray air pressure 1 kg/cm², spray nozzle 406 µm, spray feed rate 10 ml/min, feed solid concentration 20% w/v. DH matrix-tablets were prepared from spray-dried co-agglomerates (SD matrix-tablets) and equivalent simple physical mixtures of DH with Kollidon SR (PM matrix-tablets), Table 1. All tablets contained 180 mg of DH and were prepared in a KBr die set (d=13 mm) using a manual hydraulic press (14 kN force for 5 s).

The release study for matrix-tablets was performed in a USP paddle dissolution system at 100 rpm using 900 ml of distilled water at 37 °C. The concentration of dissolved drug was determined by UV spectroscopy. The release data (<60%) were fitted to power law model. The release profiles of DH from PVAc-PVP SD and PM matrix-tablets of different D:MF ratios are shown in Fig.1. It can be seen that the release is slower from SD matrix-tablets than the corresponding PM matrix-tablets. However, concomitantly, sharper decrease in release rate with time is seen and indicated also by smaller release exponent (*n*), Table 1.

The release profiles from PVAc-PVP matrix-tablets with different PVP percentages in the MF are shown in Fig. 2, where it can be seen that increasing PVP percentage from 9 to 29% causes a remarkable increase in release rate from SD matrix-tablets. The release exponent, *n*, is also increased (Table 1) indicating improvement in linearity of release profile, although not exceeding the value corresponding to Fickian diffusion (*n*=0.45). Furthermore, the release profiles for matrix-tablets prepared from spray-dried co-agglomerates and simple physical mixtures, at 19% PVP in MF, are very similar (*f*₂=70). Therefore, it can be concluded that the already existing difference in PVP content between Kollidon SR and Kollicoat SR 30D is a major reason for the difference in release rate and mechanism between PM and SD matrix-tablets seen in Fig. 1.

CONCLUSIONS

The results of this study indicate that PVP percentage in MF remarkably affects mechanism and rate of release from PVAc-PVP matrix-tablets. The results also indicate the possibility of optimizing release profile (i.e. changing rate and mechanism) for PVAc-PVP SD matrix-tablets by alteration of D:MF and PVP percentage in MF

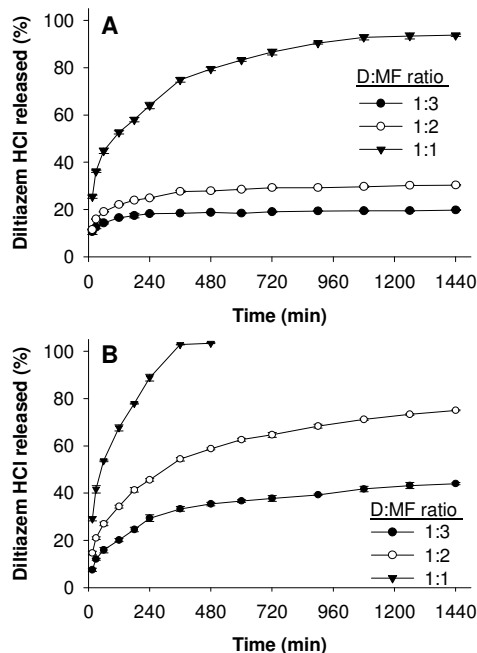


Fig.1: Release profiles of DH from PVAc-PVP matrix-tablets of different D:MF ratios prepared from co-agglomerates obtained by spray drying with Kollicoat SR 30D (A) and simple physical mixtures with Kollidon SR (B).

Fig.2: Release profiles of DH from PVAc-PVP matrix-tablets at 1:2 D:MF ratio and different PVP percentages in the MF (9, 14, 19 and 29%) prepared from co-agglomerates obtained by co-spray drying (SD) (solid line) and simple physical mixtures with Kollidon SR (dotted line).

Table 1: Formulation and release modelling parameters for the investigated matrix-tablets

Preparation method	D:MF ratio	PVP in MF (% w/w)	Power law model fitting parameters	
			<i>n</i>	R ²
SD	1:1	9	0.321	0.970
SD	1:2	9	0.193	0.930
SD	1:2	14	0.328	0.992
SD	1:2	19	0.419	0.996
SD	1:2	29	0.452	0.996
SD	1:3	9	0.126	0.909
PM	1:1	19	0.441	0.991
PM	1:2	19	0.396	0.997
PM	1:3	19	0.369	0.970

P. Estevez¹, V. Tripodi^{1,2}, O. Boscolo¹, D. Chiappetta^{1,2}, F. Buontempo^{1,3}, S. Lucangioli^{1,2}
¹. Faculty of Pharmacy and Biochemistry, University of Buenos Aires, Buenos Aires, Argentina
². National Scientific and Technical Research Council (CONICET), Argentina
³. Paediatric Hospital J.P. Garrahan, Argentina

Coenzyme Q10 (CoQ10) deficiency is involved in cardiomyopathies and degenerative muscle and neuronal diseases. Most patients with these deficiencies have shown clinical improvement with oral CoQ10 supplementation especially in pediatric patients (1). In the case of the active drugs with physicochemical characteristics of poor aqueous solubility, high hydrophobicity and consequently poor absorption like CoQ10, various formulation strategies can be used (2). The aim of this study was to develop two oil solutions, one of them with the addition of vitamin E and one oil-in-water emulsion of CoQ10 and study the chemical stability of CoQ10 by microHPLC in the proposed extemporaneous formulations stored at room temperature over 110 days.

Two CoQ10 oil solutions (50 mg/ml) were prepared by solubilising CoQ10 powder in soybean oil at 40°C. It was then added 0.05 % w/v of Vitamin E to one of the oil solutions. The vehicle of the O/W emulsion was prepared with xanthan gum 0.25% w/v, soybean oil 45%, syrup 30%, distilled water 23.85%, methylparaben 0.08%, propylparaben 0.02%, sodium saccharin 0.3% and orange essence 0.5%. The final CoQ10 concentration of the O/W emulsion was 20 mg/ml. All the trial formulations were stored in amber glass vials and kept at controlled room temperature (25°C). All samples were stored at 25°C. CoQ10 content of each formulation was analyzed in duplicate by MicroHPLC at 0, 3, 6, 15, 30, 60 and 110 days (Figure).

All formulations stayed stable at 25°C during the 110 days of the study. However, the oil solutions showed significant variations of CoQ10 concentrations (up to 26%), whereas the O/W emulsion stayed on a 10% range. At the end of the study (day 110), the amount of CoQ10 in all three formulations was between 97 and 103% (Table).

Significant content variations through all the study period for the oil solutions were founded, probably due to the vehicle chosen. This may potentially modify the amount of CoQ10 delivered to the patient, making them not suitable for pediatric practice in which more reliable dose adjustment is required. Moreover, no differences were found between the two oil solutions, with and without vitamin E. The O/W emulsion content instead was not significantly affected, making it the formulation of choice for pediatric administration of CoQ10. Stability data at controlled room temperature is very important since there is no need of using special storage conditions. In conclusion, the CoQ10 emulsion can be stored for at least 110 days at 25°C and it has proven to be safer when narrow dose adjustment is required.

REFERENCES

- Villalba, J., et. al. 2012. Therapeutic use of coenzyme Q10 and coenzyme Q10-related compounds and formulations. *Expert Opin. Investig. Drugs* 19 (4), 535-554.
- Hatanaka, J., et. al. 2008. Physicochemical and pharmacokinetic characterization of water soluble Coenzyme Q10 formulation. *Int J Pharm.* 363, 112-117.

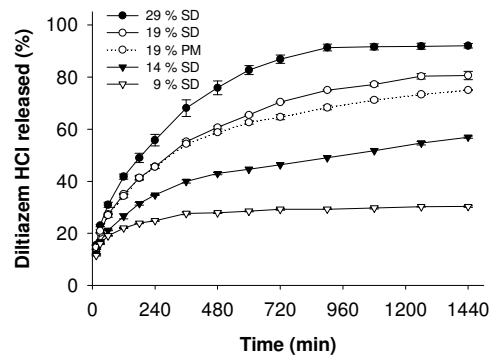


FIGURE: Chemical structure of CoQ10 and chromatograms of CoQ10 standard and formulations, placed on the same pair of axis. A: CoQ10 standard (2µg/ml), F1: CoQ10 (2µg/ml) oil solutions, F2: CoQ10 (2µg/ml) O/W emulsion.

PP070

NEW COMPOUNDS FROM HYDRAZINECARBOTHIOAMIDE AND TRIAZOLE CLASS WITH POTENTIAL ANTIOXIDANT ACTIVITY

Stefania-Felicia Barbuceanu, Diana Carolina Ilies, Ioana Sarameta, Valentina Uivarosib, Constantin Draghici, Valeria Radulescu

^a Organic Chemistry Department, Faculty of Pharmacy, University of Medicine and Pharmacy Carol Davila, 6 Traian Vuia Street, 020956, Bucharest, Romania

^b General and Inorganic Chemistry Department, Faculty of Pharmacy, University of Medicine and Pharmacy Carol Davila, 6 Traian Vuia Street, 020956, Bucharest, Romania

^c C.D. Nenitescu Institute of Organic Chemistry, Romanian Academy, 202B Splaiul Independentei, 060023, Bucharest, Romania

corresponding author: sbarbuceanu@gmail.com

1,2,4-Triazole and hydrazinecarbothioamide derivatives are reported to possess various biological properties including the antioxidant activity^{1,2}. Antioxidants are widely studied for their capacity to protect organism and cell from damage induced by the oxidative stress. For this reason, our aim was to synthesize new compounds from these classes which contain a diphenylsulfone moiety and to investigate the possible antioxidant activity.

The new heterocyclic compounds from triazole-3-thione class **4-6** were synthesized by cyclization, in basic media, of new acylhydrazinecarbothioamides **1-3** obtained by reaction of some 4-(4-X-phenylsulfonyl)benzoic acid hydrazides with 2,4-difluorophenyl isothiocyanate (Figure 1). The structure of the new compounds was confirmed by elemental analysis and spectral methods (IR, ¹H-NMR, ¹³C-NMR, MS).

The antioxidant activity against 1,1-diphenyl-2-picrylhydrazyl radical (DPPH) was measured for all new synthesized compounds according to the literature² with some modifications. The samples (ethanolic solution 500 μM for compounds and 400 μM for DPPH, 1:1 v/v) were incubated for 30 min at room temperature and then the absorbance was measured at 517 nm. The percentage of DPPH free radical inhibition for each compound was calculated. *Tert*-butyl-4-hydroxyanisole (BHA) and 2,6-bis(1,1-dimethylethyl)-4-methylphenol (BHT) were used as reference antioxidants. All analyses were performed in triplicate.

The results obtained by testing of antioxidant activity indicated that hydrazinecarbothioamides, the key intermediate of triazoles, have shown an inhibitory action of DPPH stable free radical (96.90-97.18%) better than BHA (89.30%) and much stronger than BHT (23.05%). 1,2,4-Triazole-3-thiones obtained by cyclization of hydrazinecarbothioamides have shown a lower antioxidant action (58.52-72.45%), but better than BHT (Table 1).

New compounds from hydrazinecarbothioamide and 1,2,4-triazole class were synthesized and characterized in order to evaluate their antioxidant activity. The results obtained indicate that hydrazinecarbothioamides have excellent antioxidant activity, better than reference antioxidants and triazoles.

Acknowledgements

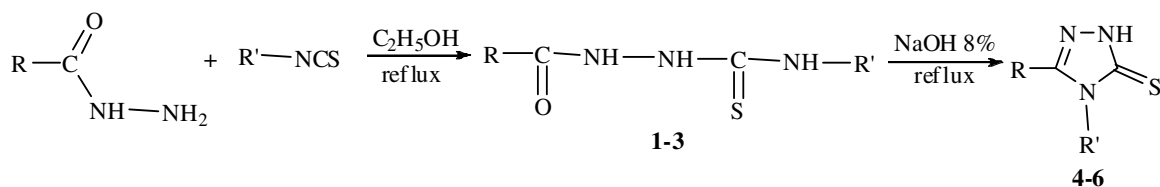
This work was supported by University of Medicine and Pharmacy "Carol Davila" Bucharest, a project number 28492/30.10.2012.

References

1. Kuş C., Ayhan-Kılıçgil G., Özbey S., Kaynak F.B., Kaya M., Çoban T., Can-Eke B., 2008, Synthesis and antioxidant properties of novel *N*-methyl-1,3,4-thiadiazol-2-amine and 4-

methyl-2*H*-1,2,4-triazole-3(4*H*)-thione derivatives of benzimidazole class, Bioorg. Med. Chem., 16, 4294–4303.

2. Khan I., Ali S., Hameed S., Rama N.H., Hussain M.T., Wadood A., Uddin R., Ul-Haq Z., Khan A., Ali S., Choudhary M.I., 2010, Synthesis, antioxidant activities and urease inhibition of some new 1,2,4-triazole and 1,3,4-thiadiazole derivatives, Eur. J. Med. Chem., 45, 5200–5207.



R: 4-X-C₆H₄-SO₂-C₆H₄-

R': 2,4-di-F-C₆H₃-

X= H, Cl, Br

Figure 1. The synthesis of designed compounds **1-6**

Table 1. Scavenging effects of tested compounds **1-6**

Compd.	X	Scavenging effect (%)
1	H	97.18±1.42
2	Cl	96.90±1.39
3	Br	97.11±1.12
4	H	67.70±1.68
5	Cl	72.45±1.42
6	Br	58.52±1.55
BHA	-	89.30±1.37
BHT	-	23.05±1.32

PP072

RHEOLOGICAL BEHAVIOUR OF IBUPROFEN SUSPENSIONS AND CONSEQUENCES ON THE IN-VITRO RELEASE PROFILES

Daniela E. Popa, George T.A. Burcea Dragomiroiu, Monica Bârcă, Dumitru Lupuleasa, Flavian □. Rădulescu, Dalia S. Miron

University of Medicine and Pharmacy „Carol Davila” Bucharest, Faculty of Pharmacy, 020956, Bucharest, Romania.

E-mail address of the corresponding author: flavian.radulescu@umf.ro.

The aim of the study was to evaluate the impact of structural characteristics of ibuprofen oral suspensions, corresponding to marked differences in qualitative and quantitative composition, on their in-vitro release profiles.

Six commercially available formulations of ibuprofen oral suspensions, in two dose strengths (100 and 200 mg / 5ml), were subject to in-vitro dissolution testing. Based on current recommendations, the tests were performed on a compendial paddle apparatus at 50rpm, using 900 ml of phosphate buffer pH=6.8. The formulations were re-suspended according to a standardized procedure and a volume of 5ml was slowly added in each vessel. For low-consistency products, samples of 5ml were collected for 60 minutes, whereas for high-viscosity suspensions, the tests were continued up to 240 minutes. The quantitative analysis of ibuprofen was performed using a validated spectrophotometric method, after appropriate dilution of the samples. The marked differences in consistency were assessed using a rotational viscosimeter, with SV-DIN coaxial cylinder. The shear rates interval was 0-25 sec⁻¹, on ramp up - ramp down routes, in 10 sec⁻¹ steps. The power law model was applied for the ascending interval of the shear rates.

The in-vitro release profiles of ibuprofen indicated a pronounced dependence on the structure of the formulations. The low viscosity of the semisolid vehicle generated a rapid dispersion of the matrix and a complete release in 60 minutes, but the kinetic profiles were highly different. In some instances, the dissolution pattern was adequately described by the first order kinetic model. An increased viscosity generated a switch to zero order kinetics, the rate-limiting step being the slow dispersion of the semisolid matrix. The fraction released exceeded 90% in 120 to 240 minutes (figure 1).

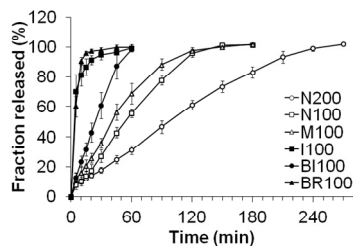


Figure 1. Mean dissolution profiles (n=6)

All suspensions presented a pseudoplastic behavior, the flow index value being lower than 1. The fraction released in 60 minutes was inversely related to the value of the flow consistency index, K (table 1). For two strengths of the same products, the quantitative difference in composition induced distinct flow behaviour and consequent non-similar dissolution profiles. Table 1. The parameters of the power law model

Product	K	n	R ²
N200	13,33	0,091	0,999
N100	6,97	0,098	0,996
M100	4,63	0,101	0,996
I100	1,01	0,399	0,999

BI100	2,86	0,247	0,998
BR100	1,81	0,650	0,998

Note: K - flow consistency index (Pa s), n - flow behavior index.

The release of ibuprofen from suspension formulations seems to be highly dependent on the structural parameters, generated by variations in qualitative and quantitative composition. The implemented in-vitro dissolution methodology was able to detect those differences, both consistency and flow behavior being rate-limiting factors release of active pharmaceutical ingredients from oral suspensions. For quality control purposes, increasing the stirring rate for high-viscosity suspensions to 75 rpm could allow the reduction of test duration, whereas for low-viscosity products, the hydrodynamic conditions at 25 rpm may display a more discriminatory power.

This work was supported by the Sectoral Operational Programme Human Resources Development (SOP HRD) 2007-2013, financed from the European Social Fund and by the Romanian Government under the contract number POSDRU/107/1.5/S/82839.

PP074

THE STRUCTURAL ANALYSIS IN THE DESIGN OF BIOADHESIVE SEMISOLID VEHICLES

Andreea A. Stănescu, Adrian A. Andrieș, Mirela A. Mitu, Oana Karampelas, Dalia S. Miron, Flavian □. Rădulescu

University of Medicine and Pharmacy „Carol Davila” Bucharest, Faculty of Pharmacy, 020956, Bucharest, Romania.

E-mail address of the corresponding author: flavian.radulescu@umf.ro.

The aim of the study was to analyze the impact of the qualitative and quantitative variations of composition on the rheological behavior of bioadhesive semisolid vehicles.

Four types of poly(methacrylic acid) agents (971P, 974P, 71G and 940) were used for preparation of bioadhesive semisolid vehicles. Several degrees of variation in qualitative and quantitative composition were generated, including the concentration of the macromolecular agent (1-4%), the pH of the system (2,5-7, adjusted by addition of triethanolamine), the nature of co-solvent polyols (glycerol, propylene glycol, polyethylene glycol) and of the absorption promoters (isopropyl myristate, alone or mixture with other lipophilic components, i.e. cetareth-20 and lanolin oil). The structural characteristics were assessed using a rotational viscosimeter Thermo Haake VT550 (ViscoTester VT550), Thermo Electron (Karlsruhe) GmbH, Germany, with a SV-DIN coaxial cylinder assembly (interval of shear rates: 0-100 s⁻¹; sample volume: 10 ml; six replicates per sample). The flow patterns at ambient temperature were characterized by three parameters: hysteresis area (difference in area under the share stress vs. share rate plot, for the ramp up/ramp down curves, Pa s⁻¹); flow index - n and consistency index - K, calculated according to Ostwald de Waele model

($\tau = K(\dot{\gamma})^n$, where τ is the share stress (Pa), $\dot{\gamma}$ is the share rate (s⁻¹)).

A linear dependence of viscosity on the pH value was observed in case of carbopol 71G, with a reduced consistency for the lower strength (1%; figure 1).

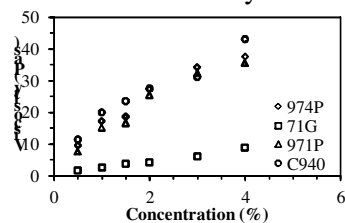


Figure 1. The dependence of the viscosity on the concentration of the gel forming agent. For carbopol 971P and 940, the critical pH interval of 4-4,5 for adhesion requests addition of neutralizing agents, therefore making difficult the inclusion of weak bases active pharmaceutical ingredients (table 1).

pH	Macromolecular agent			
	974P	71G	971P	C940
2,5	1574	7202	2443	1614
3	3752	8718	5496	2443
3,5	3923	9995	26760	26760
4	6452	10060	40250	52260
4,5	8386	12800	52260	53760
5	12570	13880	53760	54470
5,5	12960	15550	54470	54960
6	13940	15700	55620	55620
6,5	15570	17860	55800	55800

7	20230	18030	57890	57890
---	-------	-------	-------	-------

Table 1. The influence of the pH value on the area under curve (Pa s-1) for the ascending part of the deformation profile

The rheological data indicated that glycerol and propylene glycol induced an increase in viscosity, but the concentration of macromolecular agents remains the key factor in controlling the flow behavior. No area of hysteresis was recorded for carbopol 971P and 71G, a possible indicator of permanent structural deformations induced by the mechanical stress. The applicability of Ostwald de Waele model was confirmed by the values of the coefficient of correlation ($>0,999$). There was no direct dependence of the flow index value on the concentration level of carbopol, neither on pH. Nevertheless, the consistency index K seems to be a better indicator of the differences in composition and structure.

In conclusion, adequate bioadhesive semisolid vehicles were obtained based on poly(methacrylic acid) agents, with various combinations of co-solvents and absorption promoters. The formulations presented a pseudoplastic behavior and even thixotropic characteristics, manifest at pH values higher than 4.

This work was supported by the Romanian Partnership Programme PN II - supported by ANCS, CNDI – UEFISCDI, contract number 126/2012.

PP075

SUSTAINABILITY OF HEDERACOSIDE C BY HPTLC - SCANNER METHOD IN SEVERAL ALCOHOLIC EXTRACTS FROM HEDERA HELIX PLANT LEAVES COLLECTED IN ALBANIA

R. Shkreli^{1*}, E. Haloçi², L. Cama¹

¹Faculty of Medical Sciences, "Kristal" University, Tirana, Albania.

²PhD candidate at the University of Ferrara, Italy

*Corresponding author: Tel.: +3550692355145

E-mail address: rezishkreli@yahoo.com

Hedera Helix is a climber evergreen plant, widespread in Albania, found in rocks, walls and woods. Hedera leaves contain about 2.5-6% of bidesmosidic triterpenic saponins where the main ingredient is Hederacoside C¹. Saponins are used in medicine as expectorant, diuretic, antimicrobial and antimycotic agents.

The purpose of this study is to determine the sustainability of the principle Hederacoside C in extracts obtained with different methods and stored in different conditions.

Extracts prepared have as digestive alcohol 70% and are extracted in the ratio 1:1 with four methods: infusion, reflux-condensation, ultrasound and magnetic-mixing. Extracts were stored in different temperature, light and moisture conditions. Assessment of sustainability of hederacoside C in alcoholic extracts was carried out by the cromathographic method HPTLC-Scanner². Standard was obtained from Sigma Aldrich (Standard solution 0.502 ± 0.01 mg hederacoside C/ml).

Stationary phase: etilacetate:formic acid:acetic acid:water in ratio (50:5.5:5.5:13.5) V/V HPTLC Camag (Switzerland), semiautomatic applicator Camag Linomat IV, Camag CATS 4 software. Camera 20 x 10. Hamilton syringe 100 µl. Analytical scales Mettler H 20 T, Max. 160 mg, d = 0.01 mg

Relative changes in the content of the principle Hederacoside C in prepared extracts are shown at table 1 and figure 1.

Type of extract	Storage conditions		
	Colored packaging environment conditions	No-colored packaging environment conditions	Refrigerating conditions
Infusion	9.2	10.2	8.39
Reflux-cond.	7.7	19.8	13.1
Ultrasound	18.6	22	12.3
Magnetic mixing	13	16	8.1

Tab.1 Relative changes in % of the Hederacoside C in prepared extract

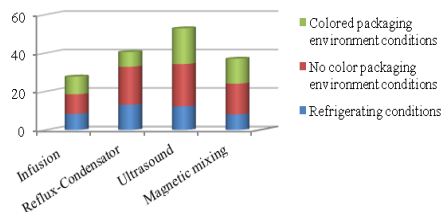


Fig. 1 Comparative changes in % of the principle in four different extracts

External environmental factors and the extraction method affect the stability of hederacoside C in all four extracts, the largest relative change in the content of the active principle was in extract obtained with ultrasound method and stored at no colored packaging environment conditions, the smaller relative one was in reflux-condensator extract stored at colored packaging environment conditions.

LITERATURE REFERENCE

¹European Medicines Agency/ London 14 January 2010/ Doc. Ref. EMA/ HMPC 289432/ 2009. Assessment Report on Hedera Helix L. Folium.

²Elke Hahn- Deinstrop. Applied- Thin _layer Chromatography. Best Practice and Avoidance of Mistakes, Second edition, 2007.

PP076

MAGNESIUM ALUMINOMETASILICATES AS API CARRIERS IN PELLETS

Krupa A.^{1*}, Jachowicz R.¹, Kwiecień M.², Figiel W.², Gruszkos J.¹

¹ Jagiellonian University, Medical College, Cracow, Poland

² Tadeusz Kosciuszko Cracow University of Technology, Cracow, Poland

*e-mail address of corresponding author: a.krupa@uj.edu.pl

Pellets properties depend on physicochemical characteristics of raw materials. Among excipients destined to form pellets by extrusion/spheronisation, plastic properties of microcrystalline cellulose (MCC) are widely used [1, 2]. In some cases, the preparation of highly porous pellets is necessary. Such pellets can serve as inert solid carriers for drugs in liquid form e.g. self-emulsifying drug delivery systems (SEDDS). The impregnation of inert cores with a liquid SEDDS, transforms them into solid self-emulsifying drug delivery systems.

The present study aims to examine the suitability of three kinds of magnesium aluminometasilicates (Neusilin[®] grades: US2, SG2, NS2N) to form porous pellets by extrusion/spheronisation. Properties of pellets were analysed taking into account: surface morphology, diameter, particle size distribution, circularity, porosity and adsorbent capacity. Finally pellets obtained were impregnated with ibuprofen solution in fluid-bed coating process. The influence of the coating process on pellets characteristics was studied.

The functionality of three kinds of magnesium aluminometasilicate such as Neusilin[®] grade: US2, SG2, NS2N (Fuji Chemical Industry, Japan) in extrusion/spheronisation process was studied. All pellets were composed of the silicate and MCC (Vivapur[®] PH101, JRS Pharma, Germany). Distilled water was used as a wetting agent to form a plastic mass. Nine formulations containing about 30%, 50%, or 70% of Neusilin[®] and MCC were prepared. Distilled water was used as a wetting agent. Twin cylinder extruder (Alexanderwerk GUN) and spheroniser (Caleva 120) were used to form pellets. They were dried in an oven at 40°C for 24 h.

Morphology and sphericity of pellets were examined using Morphologi G3 optical microscope (Malvern) and scanning electron microscope (SEM, Hitachi S-4700). Porosity was determined by measuring the apparent volume.

Impregnation of pellets was performed using laboratory fluid-bed coater Solidlab1 (BOSCH). Coating solution was composed of 10 g of ibuprofen (Shasun-Chemicals&Drugs, India) dissolved in 40 g of Labrasol (Gattefosse, France) and PEG 200 (POCH, Poland) in 1:1 ratio. It was shown that Neusilin[®] combined with MCC was suitable to prepare porous pellets, which could be used as solid carriers for liquid drug formulations. Amount of water necessary to form the plastic mass depended on the kind of the silicate and ranged from 46% to 72%. If the content of Neusilin[®] in the formulation was high, the amount of water necessary to prepare the plastic mass would also increase.

Sphericity, pore size distribution and adsorbent capacity depended on the kind and amount of Neusilin[®]. Pellets containing Neusilin[®] SG2 were three times less spherical than pellets with Neusilin[®] US2 or NS2N. The highest porosity over 46% was characteristic to pellets composed of 70% of Neusilin[®] US2 (Tab. 1). This silicate had the highest value of specific surface area. Thus the highest amount of ibuprofen solution was adsorbed on such pellets (Fig. 1).

Application of magnesium aluminometasilicates enable to prepare porous pellets in the extrusion/spheronisation process. Properties of pellets depended on physicochemical characteristics of Neusilin[®]. Such porous pellets could be used as solid carriers for APIs in liquid form. The highest amount of ibuprofen solution was adsorbed on pellets containing 50-70% of Neusilin[®] US2.

References:

1. Galland S., Ruiz T., Delalonde M., Krupa A., Bataille B., 2005. Texturing the spherical granular system influence of the spheronisation stage. *Powder Technol.* 157, 156-162.
2. Newton J.M., 1998. Extrusion-spheronisation, in: *Powder Technology and Pharmaceutical Processes*. Elsevier, vol. 9, pp. 391-401.

Table 1. Texture of pellets containing 70% of Neusilin[®] NS2N or Neusilin[®] US2.

Parameter	Uncoated pellets	Coated pellets	Uncoated pellets	Coated pellets
	NN3		NU3	
Diameter [μm]	1559,53	1448,91	1149,14	547,08
SD	154,14	207,07	411,04	243,81
Circularity	0,872	0,731	0,835	0,905
SD	0,048	0,065	0,087	0,053
Porosity [%]	42,47	12,00	46,45	5,30

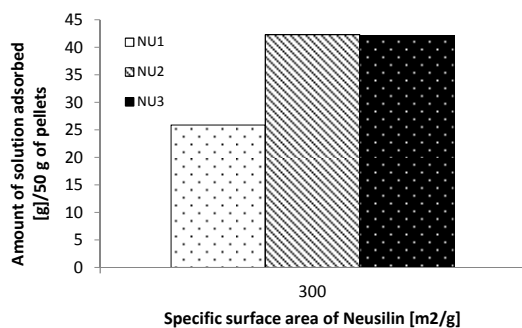


Fig. 1. Amount of ibuprofen solution adsorbed by pellets containing Neusilin[®] US2.

PP080

Investigation of the Therapeutic Effects of a Combinational Herbal Product Against Benign Prostate Hyperplasia

Yunes Panahi,^{a*} Amirhossein Sahebkar,^b

¹Chemical Injuries Research Center, Baqiyatallah University of Medical Sciences, Tehran, Iran

²Biotechnology Research Center, Mashhad University of Medical Sciences, Mashhad, Iran

Proceedings

5th BBBB International Conference – 26-28 September 2013

Yunes Panahi, Pharm.D, Ph.D, Professor of Clinical Pharmacy, Chemical Injuries Research Center, Baqiyatallah University of Medical Sciences, Mashhad, Iran. E-mail: yunespanahi@yahoo.com; amir_saheb2000@yahoo.com

Benign Prostate Hyperplasia (BPH) is a common condition in aging men that predisposes to lower urinary tract symptoms. The purpose of this randomized double-blind placebo-controlled trial to investigate the therapeutic effects of a herbal combination drop containing *Equisetum arvense*, *Zea mays*, *Viola odorata*, *Echium amoenum*, *Physalis alkekengi* and *Althaea officinalis* extracts for the treatment of BPH patients. Eighty-six patients with BPH were randomized to receive placebo (control group) or herbal drop (case group) for 2 weeks. Efficacy and safety of the product were evaluated by measuring BPH-related patient complaints, flowmetry, sonography, PSSS questionnaire and quality of life. In addition to urinalysis, the value of some biochemical tests such as Hb, WBC, PLT, lymphocyte, basophile, HCT, BUN, cratinin, enzyme activity (SGOT, SGPT and Alk-Ph) were checked before and after study. All episodes of any adverse effects throughout the study were also recorded. There was no statistically significant difference between the control and case groups regarding any of these findings. The effect of plants extract on reduction of urgency and nocturia was partially more effective than placebo group. Residual urine volume was same in two groups of study. In both case and placebo groups the PSSS score reduced and the quality of life was improved. No significant difference in the incidence of adverse effects attributable to the study drug was observed between the groups. Combination herbal treatment used in the present study was safe but its efficacy was not superior to placebo. **Keywords:** Benign Prostate Hyperplasia, Herbal medicine

PP086

RELATIVE BIOAVAILABILITY OF COENZYME Q10 FORMULATIONS FOR PEDIATRIC INDIVIDUALIZED THERAPY: PRELIMINARY STUDY

M. Martinefski¹, P. Samassa,¹ M. Contin,¹ S. Lucangioli^{1,2}, F. Buontempo¹ and V. Tripodi^{1,2}

¹Faculty of Pharmacy and Biochemistry, University of Buenos Aires, Buenos Aires, Argentina.

²Consejo Nacional de Investigaciones Científicas y Técnicas, Buenos Aires, Argentina

Corresponding author: e-mail vtripodi@ffyb.uba.ar

Coenzyme Q10 (CoQ10) deficiency is involved in degenerative muscle and neuronal diseases which have shown clinical improvement with oral CoQ10 supplementation specially if it is started during childhood. The administration of drugs in pediatrics is a unique challenge and

requires individualized therapy. Liquid formulations rather than solid dosage forms are preferred for oral administration to children specially in those with difficulty swallowing. In order to increase the bioavailability of CoQ10, facilitate its administration in pediatrics and therefore increase the therapeutic efficacy, we have previously developed an oil-in-water (O/W) liquid emulsion of CoQ10 with proved stability and safe when narrow dose adjustment is required (1). The objective of this work is to establish the relative bioavailability of this new developed liquid formulation in comparison to the solid CoQ10 form administered at low and high doses.

It was conducted a preliminary study. Six healthy male and female subjects participated in an open, consecutive, controlled, single-oral low dose (60 mg) and high dose (250 mg) bioavailability study. The same group was administered with both formulations and doses after a wash out of 15 days. Plasma concentration of CoQ10 was determined at baseline and at various intervals after administration over a 360-hour period. To compare bioavailability, maximum concentration (C_{max}), the time of its occurrence (T_{max}) and area under curve from 0 to last time analyzed (AUC_t) by linear trapezoidal rule were assessed. Plasma concentrations were determined using a microHPLC method previously developed (2). Analysis of variance (ANOVA) and *t*-tests were performed to evaluate significant differences between two formulations.

The kinetic profiles of CoQ10 revealed the same peak plasma concentration-time course at 6h independently of the formulation and dose administered. While there was no difference in the T_{max} between the two formulations, highest C_{max} values were seen after liquid CoQ10 formulation (table and figure). The relative bioavailability calculated using the AUC_t values, without correction by baseline levels of CoQ10, was 133.3% at low and 132.7% at high doses. Plasma concentration-time profiles were corrected for endogenous levels of CoQ10, and AUC_t^{corr} were calculated, obtaining a relative bioavailability of 641% at low and 672% at high doses.

The data presented suggests that O/W emulsion of CoQ10 improves the enteral absorption and the bioavailability of CoQ10 in humans with a linear pharmacokinetic profile justifying to continue the study in a higher number of healthy volunteers.

REFERENCES

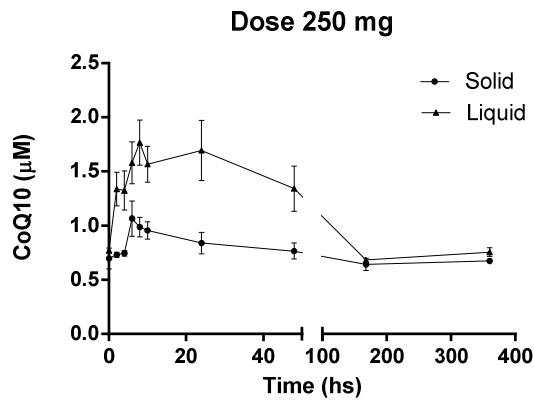
1. Estevez, P., et. al. 2012. Coenzyme Q10 stability in pediatric liquid oral dosage formulations. *Farm. Hosp.* 36 (6), 492-497.
2. Contin, M., et. al. 2011. Miniaturized HPLC-UV method for analysis of Coenzyme Q10 in human plasma. *J. of Liq. Chromatogr. and Rel. Tech.* 34(20), 2485-2494.

TABLE: Pharmacokinetic parameters of CoQ10 formulations.

Parameters	Formulation			
	Solid		Liquid	
Dose (mg)	60	250	60	250
C_{max} (μ M)	0.36 \pm 0.04	1.08 \pm 0.25	0.42 \pm 0.07*	1.77 \pm 0.36*
T_{max} (hs)	6	6	6	6
AUC_t (μ Mxh)	36.1 \pm 4.5	251.0 \pm 15.7	48.1 \pm 4.6*	333.0 \pm 25.2*
AUC_t^{corr} (μ Mxh)	6.6 \pm 5.8	19.8 \pm 9.8	42.5 \pm 34.4*	133.0 \pm 47.8*

Each value represents the mean \pm SEM, n=6. *p<0.05 compared with solid formulation at the same dose.

FIGURE: Plasma profiles of CoQ10 from solid and liquid formulations at high dose. Each value represents the mean \pm SEM, n=6



PP089

INCORPORATING VARIABILITY IN A PBPK MODEL OF CYCLOSPORINE AND EXTRAPOLATION TO A PEDIATRIC POPULATION

Kechagia Irene-Ariadne, Dokoumetzidis Aris
School of Pharmacy, University of Athens, Greece
Corresponding author e-mail: ikechag@pharm.uoa.gr

The aim of the present study was to implement a physiologically based pharmacokinetic (PBPK) model of cyclosporine for rats in SimBiology, a MATLAB-based tool, extrapolate the model to a pediatric population, carry out a sensitivity analysis, incorporate variability and perform Monte-Carlo simulations.

The PBPK model of cyclosporine for rats, published by Kawai et al. (1998), was re-implemented in SimBiology. To extrapolate the model to children the physiological and anatomical parameters, such as volume and blood flow of the organs, were given appropriate typical values, while values for drug specific parameters were either considered constant or scaled allometrically. A local sensitivity analysis was carried out in order to detect the parameters which mostly affect the response of the model and are therefore potential primary components of variability. In order to incorporate interindividual variability in the model, certain parameters found to be more sensitive were expressed, through MATLAB, according to age specific statistical distributions reported in literature. The model was used to perform simulations for a virtual pediatric population after oral and i.v. administration of cyclosporine.

The major parameters which the model is sensitive to were ranked in a descending order according to the magnitude of their influence on the cyclosporine concentration in the blood. The intrinsic clearance, the capacity and the dissociation constant of red blood cells binding site, the fraction unbound in plasma and the hematocrit contribute the most to the variability of cyclosporine pharmacokinetics. Monte-Carlo simulations show that the predictive capability of the model for the pediatric population is quite satisfactory, as it was evaluated by comparing the prediction interval to data from literature (Fanta et al. 2007).

The physiological framework of the PBPK model of cyclosporine along with sensitivity analysis allow obtaining an understanding of the factors which essentially affect the disposition of cyclosporine in the body and should they be taken into account, the observed variability can be explained.

References:

1. Kawai, R., Mathew, D., Tanaka, C., Rowland, M., 1998. Physiologically based pharmacokinetics of cyclosporine A: extension to tissue distribution kinetics in rats and scale-up to human. *J. Pharmacol. Exp. Ther.* 287, 457-468.
2. Fanta, S., Jönsson, S., Backman, J.T., Karlsson, M.O., Hoppu, K., 2007. Developmental pharmacokinetics of cyclosporin-a population pharmacokinetic study in paediatric renal transplant candidates. *Br. J. Clin. Pharmacol.* 64, 772-784.

PP090

MICROWAVE-ASSISTED SYNTHESIS OF CHITOSAN-OLIGO(CAPROLACTONE) GRAFT COPOLYMERS FOR DRUG DELIVERY APPLICATIONS

S. Quintana^{1,2}, R.J. Glisoni^{1,2}, A. Moglioni^{1,2}, A. Sosnik^{1,2}.

¹Faculty of Pharmacy and Biochemistry, University of Buenos Aires, Buenos Aires, Argentina.

²National Science Research Council (CONICET), Buenos Aires, Argentina.

Graft copolymerization of different biodegradable and biocompatible polymers using chitosan (CS) molecules as template is an attractive strategy to develop novel hybrid copolymers that capitalize on the advantages of each component, while blurring their drawbacks. In this work, we investigated the

grafting of ϵ -caprolactone (ϵ -CL) onto CS *via* microwave-assisted ring-opening polymerization reactions, in the presence of methanesulfonic acid (MeSO_3H) as solvent and catalyst. Due to the protective protonation of amine groups of CS in acidic medium, grafting of ϵ -CL took place mainly on hydroxyl groups of CS. Moreover, these amphiphilic graft copolymers have been evaluated as a platform for the development of mucoadhesive nanomaterials for biomedical applications. CS (low molecular weight and degree of deacetylation (DD) = 99.9%), ϵ -CL (99%, monomer) and MeSO_3H (>99.5%) were purchased from Sigma Aldrich and dried before used. The graft polymerization was carried out in a monowave 300 microwave reactor (Anton Paar). CS (0.5 g) was placed in a dried glass reactor and dissolved in MeSO_3H (7.5 mL), followed by the injection of a certain amount of ϵ -CL (4-12 mL). Then the reactor was irradiated at 45°C (5 min) and 70°C (5 additional min). Mixtures were thoroughly dialyzed against distilled water using Spectra/Pro membrane (MWCO = 3500 g/mol) for 72 h, frozen at -80°C (24 h) and freeze-dried (48 h). Lyophilized products were stored at 25°C and labeled as CS-*g*-PCL. CS-*g*-PCL copolymers with different molecular weight and hydrophilic-lipophilic balance were synthesized by adjusting the feed weight ratio of CS and ϵ -CL; CS: CL weight ratios of 1:8; 1:12; 1:16 and 1:24 were used. The native and modified polymers were fully characterized by ATR/FT-IR, ^1H - and ^{13}C -NMR, DSC, TGA, MALDI-TOF and WAXD, respectively. A series of CS-*g*-PCL copolymers were synthesized by a microwave-assisted technique under very mild temperature conditions. The reaction time was 10 min and the monomer conversion above 90%. The grafting of oligo(CL) blocks was confirmed by FT-IR and ^1H - and ^{13}C -NMR. Graft copolymers were readily soluble in DMSO and acetone, as opposed to pristine CS. DSC and TGA analysis showed different degradation behaviors, due to structural differences between the two polymers, while WAXD analysis revealed that the degree of crystallinity of CS in the copolymer was reduced upon graft copolymerization. Modification of CS by grafting PCL chains was successfully carried out by microwave irradiation. The obtained graft copolymers are expected to combine the advantageous properties of both polymers and they are promising platforms to prolong the residence time of drug-loaded nanocarriers in intestinal and respiratory mucosa owing to the mucoadhesive property of CS.

PP091**A NEW APPROACH IN THE RECOVERY OF MURINE MELANOMA LESIONS: ELECTROPORATION OF LYOTROPIC LIQUID CRYSTALS GENISTEIN BASED FORMULATION**

Danciu Corina¹, Ciurlea Sorina², Erzsébet Csányi³, Balazs Boglarka³, Codruta Șoica⁴ Avram Ștefana¹, Camelia Peev¹, Dehelean Cristina²

¹Department of Pharmacognosy, “Victor Babes” University of Medicine and Pharmacy, 2 Eftimie Murgu, 300041, Timisoara, Romania

²Department of Toxicology, “Victor Babes” University of Medicine and Pharmacy, 2 Eftimie Murgu, 300041, Timisoara, Romania

³Department of Pharmaceutical Technology University of Szeged, 6 Eotvos u., H-6720, Szeged, Hungary

⁴Department of Pharmaceutical Chemistry, “Victor Babes” University of Medicine and Pharmacy, 2 Eftimie Murgu, 300041, Timisoara, Romania

Corresponding author: corina_tiulea@yahoo.com

Genistein, a natural compound belonging to the class of isoflavonoids have been extensively studied for a wide range of pathologies including cancer. Its benefits regarding the recovery of skin lesions type malignant melanoma have been reported previously [1,2]. The aim of this study was to investigate the effect of local administration of a lyotropic liquid crystals (LLC) system containing 3% genistein (Gen) with and without electroporation employing the B16 model of mouse melanoma. On this purpose 1×10^6 B16A5 cells have been injected subcutaneous in the back of C57BL6J mice. Treatment was administered from the second day after inoculation, employing 2 ml of a 3% Gen LLC formulation using 6 min of high voltage electroporation (Mezoforte Duo Mez 120905-D) and classical application. Tumors arrived from day 8 after inoculation in case of un-treated and 3% Gen LLC classical treated mice. In case of electroporated 3% Gen LLC tumors arrived in day 10 after inoculation. Non invasive measurement of both melanin amount and erythema, performed every two days during the 3 weeks of experiment employing a Multiprobe Adapter System (MPA5) from Courage-Khazaka, Germany show a linear graph, with values increasing directly proportional with the number of the days. In case of the treated mice the values corresponding to these parameters were decreased compared to the un-treated group. Lower values were detected when electroporation was applied. Tumor growth was measured in millimeters, daily, using calipers, and tumor volume was estimated by the formula: $\text{length} \times \text{width}^2/2$ [1]. The average values at the end of the study were 1,38 mm³ for un-treated mice, 1,26 mm³ for 3% Gen LLC local treatment and 0,97 mm³ for 3% Gen LLC electroporated local treatment. In the last day of the experiment blood was collected from cava vein. Two melanoma specific marker concentration: S100 and NSE (neuron specific enolase) were investigated. The following average values were detected - in case of the un-treated mice 0,61 μg/l S100 and 9,2 ng/ml NSE. For the 3% Gen LLC local treatment 0,59 μg/l S100 and 9,05 ng/ml NSE. Better results were observed when the 3% Gen LLC formulation was electroporated, namely 0,24 μg/l S100 and 6,05 ng/ml NSE. Together with this, HE analysis and immunohistochemical detection of different markers (S100, PDGF, PDGFR beta) in the skin and tumors sustain the same findings. The simple LLC with or without electroporation had no effect for any of the parameters mentioned above. As a conclusion, electroporation of lyotropic liquid crystals genistein based formulation represent a promising strategy for the recovery of skin lesions type murine melanoma.

Acknowledgments: This work was supported by the UMFT grant 15250/19.12.2012

References:

1. Danciu C, Borcan F, Bojin F, Zupko I, Dehelean C. Effect of the isoflavone genistein on

- tumor size, metastasis potential and melanization in a B16 mouse model of murine melanoma. *Nat Prod Commun.* 2013 Mar;8(3):343–6.
2. Record IR, Broadbent JL, King RA, Dreosti IE, Head RJ, Tonkin AL. Genistein inhibits growth of B16 melanoma cells in vivo and in vitro and promotes differentiation in vitro. *Int. J. Cancer.* 1997 Sep 4;72(5):860–4.

PP093

Pharmacokinetics of silibinin in mice tissues and serum after *peros* and intravenous administration as a HP- β -CD lyophilized product

Ei. Christodoulou¹, S. Tzimas², N. Kostomitsopoulos³, E. Balafas³, E. Archontaki², A. Dokoumetzidis¹, G. Valsami¹

¹ Faculty of Pharmacy, National and Kapodistrian University of Athens

² Faculty of Chemistry, National and Kapodistrian University of Athens

³ Center for Experimental Surgery, Biomedical Research Foundation of the Academy of Athens

Correspondence: G. Valsami valsami@pharm.uoa.gr

The aim of this study is to determine tissue pharmacokinetics (PK) of the water insoluble hepatoprotective flavonoid silibinin (SLB), after *peros* and intravenous (i.v.) administration as a water soluble lyophilized product with hydroxypropyl-beta-cyclodextrin (HP- β -CD) to mice.

The recently developed lyophilized SLB-HP- β -CD product (unpublished data) was administered orally (50mg/kg body weight, 0.5mL solution, gavage technique) and i.v. (20mg/kg body weight, 0.2mL solution through the mouse tail artery) to 60 C57bl/6J male mice (age 12 weeks) after reconstitution with water for injection. Mice were divided into 12 groups of five mice per group and were sacrificed at selected time points (1, 5, 10, 15, 30, 60, 120, 360min after *peros* and 5, 15, 30, 60, 120, 360 min after i.v. administration) for blood and tissue (liver, brain, kidneys, heart, lungs and spleen) sampling. Serum and tissue samples were frozen at -70°C until quantitative analysis with a HPLC method developed for SLB assay in serum and homogenized tissues using naringenin as internal standard and calibration curves in human serum (equivalent to calibration curves in mouse serum) and blank mouse tissues. Free SLB (non-metabolized) and total SLB (metabolized plus non-metabolized, calculated after sample incubation with the enzyme β -glucuronidase for 1 h at 37°C) were determined.

The results of the present study showed that SLB is rapidly and extensively absorbed from GI tract after *peros* administration of the lyophilized SLB-HP- β -CD product and highly distributed in liver, kidneys, heart and lungs after both *peros* and i.v. administration having accomplished relatively high levels in tissue homogenates (Figure 1). The absolute oral bioavailability of free and total SLB after administration lyophilized SLB-HP- β -CD product was calculated equal to 10% and 45.5%, respectively. These values are 10 times higher than those calculated after oral administration of an ethanolic-PEG200 1:1 v/v SLB solution (Wu et al. 2007). Measured C_{max} values at each of the sampled tissues after i.v. and *peros* administration are used as measure of SLB tissue distribution and are given for both free and total SLB in Table 1. These values for liver and lungs are respectively 2 and 3 times higher than those reported by Zhao & Agarwal (1999) after oral administration of the same dose of SLB as solution containing 0.9% (w/v) sodium chloride, 3% (v/v) ethanol, 1% (v/v) Tween 80 and 6.6 mM sodium hydroxide.

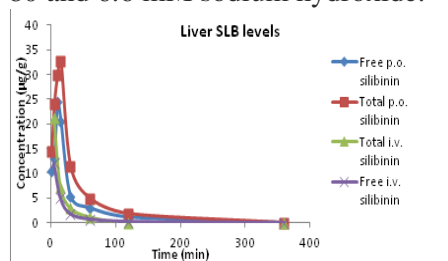


Figure 1. Measured SLB concentration (free and total) after *peros* and i.v. administration of the lyophilized SLB-HP- β -CD product

Table 1. SLB measured C_{max} values in sampled tissues

Tissue	Measured C_{max} ($\mu\text{g/g}$) \pm (SD)				Measured C_{max} ratio*	
	Free SLB p.o.	Total SLB p.o.	Free SLB i.v.	Total SLB i.v.	Free SLB	Total SLB
Liver	24.46 (8.97)	29.84 (2.21)	12.08 (2.50)	21.31 (3.10)	0.81	0.56
Lungs	7.43 (1.98)	13.57 (2.64)	5.74 (1.49)	9.22 (1.50)	0.52	0.59
Kidneys	9.67 (3.74)	12.65 (2.64)	26.80 (2.90)	8.21 (0.75)	0.14	0.62
Heart	2.23 (0.37)	6.98 (0.34)	1.41 (0.34)	10.68 (1.32)	0.63	0.26

* ($C_{max\ p.o.} \times \text{Dose}_{i.v.} / C_{max\ i.v.} \times \text{Dose}_{p.o.}$)

In conclusion, rapid and extensive absorption of SLB after *peros* administration of the lyophilized silibinin-HP- β -CD product and extensive distribution to liver, kidneys, heart and lungs is observed.

References

Jhy-Wen Wu, Lie-Chwen Lin, Shih-Chieh Hung, Chin-Wen Chi, Tung-Hu Tsai. Analysis of silibinin in rat plasma and bile for hepatobiliary excretion and oral bioavailability application Wu et al. J. Pharm. Biomed. Anal. 45:635-641, 2007.

J. Zhao and R. Agarwal. Tissue distribution of silibinin the major active constituent of sylimarin in mice and its association with enhancement of phase II enzymes: implication in cancer chemoprevention. Carcinogenesis, 20:2101-2108, 1999.

Effect of hyperhydration on urine levels of recombinant human erythropoietin and doping masking: A simulation approach

Ioanna Athanasiadou^{a,b}, Aristides Dokoumetzidis^a, Costas Georgakopoulos^c, Georgia Valsami^{a*}

^a School of Pharmacy, National & Kapodistrian University of Athens, Panepistimiopolis-Zographou 15771, Athens, Greece

^b Doping Control Laboratory of Athens, Olympic Athletic Center of Athens ‘Spiros Louis’, 37 Kifissias Ave., 15123 Maroussi, Greece Athens, Greece

^c Anti Doping Lab Qatar, P.O. Box 27775, Doha, Qatar

* Corresponding author: valsami@pharm.uoa.gr (G. Valsami)

The aim of the study was to design a clinical study that will investigate the influence of hyperhydration on the urine PK profile of recombinant human erythropoietin (rHuEPO) and its possible role as a doping masking procedure used by athletes, using a modelling and simulation approach. 1000 subjects administered subcutaneously single doses of 1500, 3000 and 6000 IU rHuEPO were simulated, by a two-compartment popPK model [1], using MatLab SimBiology toolbox. Urine production was modelled based on the renal regulation of urine volume and the conditions of water retention [2]. The model used is shown schematically in Fig. 1.

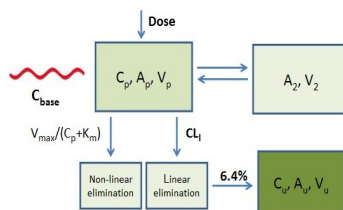


Fig. 1: Schematic representation of the PK model (Cp, Ap, Vp) used in conjunction to the urine compartment (Cu, Au, Vu).

The normal rHuEPO PK urine profile and additional PK profiles simulating hyperhydration effect were simulated for 3 hydration levels, expressed as 10, 20 and 30 ml of water consumption/kg of body weight. Different hyperhydration intake scenarios on rHuEPO PK urine profile were studied, i.e. application of hyperhydration twice per day or hyperhydration effect applied at the peak of rHuEPO concentration. Simulation of urine sampling collection schedule was used to evaluate the effect of hyperhydration on measured rHuEPO urine concentration during doping control analysis. Simulation analysis revealed that rHuEPO urine concentration follows the circadian rhythm of urine production regardless of hydration state, while at early time points after hyperhydration, a significant decrease on rHuEPO urine concentrations was observed compared to the normal profile as shown in Table 1 for the dose of 3000 IU. Similar results are obtained for the doses of 1500 and 6000 IU and the different hyperhydration scenarios.

Table 1: rHuEPO urine concentration decrease (%) at early time points after hyperhydration at all hydration levels compared to normal urine profile for the dose of 3000 IU (given as median values).

% rHuEPO Concentration Decrease						
Hydration level	Hyperhydration administered once daily			Hyperhydration administered twice daily*		
	Day					
	1 st	2 nd	3 rd	1 st	2 nd	3 rd
Low	-44.6	-43.4	-41.5	-51.8	-52.8	-52.2
Medium	-71.4	-71.2	-70.8	-76.0	-76.1	-75.7
High	-81.0	-80.4	-79.6	-83.9	-84.1	-84.5

* % rHuEPO urine concentration decrease after the second hyperhydration administration

Cases of undetectable rHuEPO have been reported in literature, attributed to inhibition of EPO production following EPO doping, highly diluted urine, and/or manipulation of urine samples with proteases. However, our simulation results showed that even in the normal PK profile, low concentrations compared to the sensitivity of the applied analytical methods may exist, due to the circadian rhythm of urine production. Clear effect of hyperhydration on rHuEPO urine profile was shown, supporting the reported cases of undetectable EPO urine levels. These findings may have practical implications regarding the timing of urine collection during anti-doping control sampling procedure and the subsequent detection of doping agents if hyperhydration could be used by athletes as a masking procedure. To verify this hypothesis, a single dose rHuEPO PK study in healthy male athletes with or without hyperhydration is designed, based on the present simulation analysis.

References:

- [1] Olsson-Gisleskog, P., Jacqmin, P., Perez-Ruixo, J.J., 2007. Population pharmacokinetics meta-analysis of recombinant human erythropoietin in healthy subjects. *Clin Pharmacokinet.* 46, 159-173.
- [2] Robertson, G.L., Norgaard, J.P., 2002. Renal regulation of urine volume: potential implications for nocturia. *BJU International* 90, 7-10.

PP096

Effects of Curcuminoids Supplementation on Circulating Concentrations of Interleukins

Amirhossein Sahebkar,^{a*} Majid Ghayour-Mobarhan,^a Shiva Ganjali,^a Elahe Mahdipour,^a Khadijeh Jamialahmadi,^a Sepideh Torabi,^a Saeed Akhlaghi,^a Gordon Ferns,^b Seyed Mohammad Reza Parizadeh^a

^a Cardiovascular Research Center, Mashhad University of Medical Sciences, Mashhad, Iran

^b Division of Medical Education, Mayfield House, University of Brighton, BN1 9PH, United Kingdom

*Correspondence to: Amirhossein Sahebkar, PharmD, PhD, Cardiovascular Research Center, Mashhad University of Medical Sciences, Mashhad, Iran. E-mail:

sahebkar@mums.ac.ir; amir_saheb2000@yahoo.com

Obesity is often associated with impairment of immune system functioning. The present study aimed to evaluate circulating levels of a panel of interleukins in obese dyslipidemic subjects. This study was a randomized cross-over trial among 30 obese dyslipidemic individuals. Subjects were assigned to curcuminoids (C3 complex[®]; Sami Labs Ltd., Bangalore, India; 1 g/day) or matched placebo for 4 weeks intermitted by a 2-week wash-out phase. Serum samples were collected and analyzed for IL-1 α , IL-1 β , IL-2, IL-4, IL-6, IL-8 and IL-10 levels using a multiplex biochip array technology based method. Curcuminoids were found to significantly reduce serum IL-1 β ($p = 0.042$) and IL-4 ($p = 0.008$) concentrations. However, serum levels of IL-2, IL-6, IL-8 and IL-10 remained statistically unaltered by the end of trial. Curcuminoids modulate circulating levels of IL-1 β and IL-4. Further investigations are required to clarify the clinical relevance of these alterations.

Keywords: Curcumin, Cytokine, Interleukins, Immunity, Inflammation

PP100

carrier of anticancer drugs

Katayoun Derakhshandeh, Majid Afshari, Leila Hosseinzadeh

Nano Drug Delivery Research Center, Faculty of Pharmacy, Kermanshah University of Medical Sciences, Kermanshah, IRAN. Kderakhshandeh@kums.ac.ir

Department of Pharmaceutics, Faculty of Pharmacy, Kermanshah University of Medical Sciences, Kermanshah, IRAN

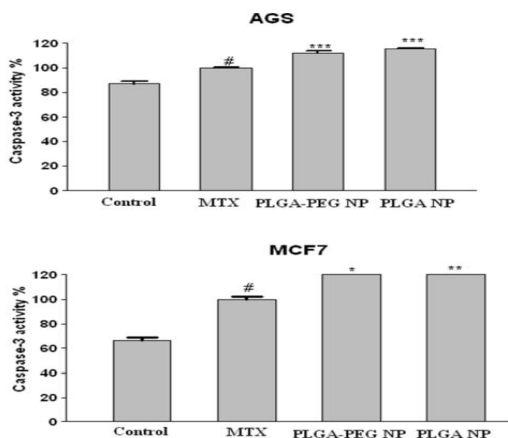
Toxicology and Pharmacology Department, Faculty of Pharmacy, Kermanshah University of Medical Sciences, Kermanshah, IRAN

Abstract: Methotrexate (MTX) widely used in the treatments of various types of malignancies, but high toxicity and short plasma half-life have limited its use.

The development of novel methods to overcome some of these obstacles to efficiently target delivery of anticancer is a major challenge. This study was aimed at developing a polymeric drug delivery system for improving the therapeutic index of this potent drug.

To achieve these goals, The MTX loaded PLGA and PLGA-PEG nanoparticles were prepared by the emulsification-solvent diffusion technique and were optimized for particle size and entrapment efficiency.

The optimum loaded nanoparticles were evaluated by cytotoxicity against cancerous cell lines and their ability to induce apoptosis compare to free drug by examination of caspase-3 activity. The results showed that optimized particles were 182 ± 14 nm in size for PLGA-PEG and 258 ± 10 nm for PLGA nanoparticles with narrow size distribution and an entrapment efficiency of more than 51%. The cytotoxicity experiment showed that the nanoparticles were more effective than pure MTX and increase activity of caspase-3 in MCF7 and AGS and A549 cell lines.



Caspase-3 activity in MCF7 and AGS cell lines. (Mean \pm SEM, n = 6). ## P< 0.05 vs. control, * P<0.01, **P< 0.001, ***P< 0.0001 vs. MTX treated cells

The results of cytotoxicity evaluation showed that nanoparticles have great effect on the cellular *in vitro* cytotoxicity and can significantly increase caspase-3 activation in MCF7 and AGS cell lines. These observations suggest that the present system offers an exciting mode of target delivery of potent anticancer drugs.

References:

1. Brigger I, Dubernet C, Couvreur P. Nanoparticles in cancer therapy and diagnosis. *Adv Drug Del Rev* 2002; 54:631–51.
2. Derakhshandeh K, Erfan M, Dadashzadeh S. Encapsulation of 9- nitrocamptothecin, a novel anticancer drug, in biodegradable nanoparticles: factorial design, characterization and release kinetics *Eur J Pharm Biopharm* 2007; 66: 34–41.

PP102

COX-2 inhibitors prevent proliferation of breast cancer cells by inducing apoptosis

Mona Salimi ^{a,*}, Mahnaz Norouzi ^b, Kayhan Azadmanesh ^c, Amir Amanzadeh ^d, Hassan Sanati ^d, Hirsra Mostafapour kandelous ^a, Saeed Irian ^b, Mohsen Amini ^e

^aDepartment of Physiology and Pharmacology, Pasteur Institute of Iran, Tehran, Iran

^bDepartment of Biological Sciences, Kharazmi University, Tehran, Iran

^cDepartment of Virology, Pasteur Institute of Iran, Tehran, Iran

^dNational Cell Bank of Iran, Pasteur Institute of Iran, Tehran, Iran

^eDepartment of Medicinal Chemistry, Faculty of pharmacy, Tehran University of Medical Sciences, Tehran, Iran

Introduction: Over the past few decades, the importance of chemotherapy has increased in the treatment of cancer. Major problems concerning established anticancer chemotherapy are the incidence of side effects induced by the non-specific targeting and the outgrowth of drug-resistant cancer cells. Recent studies have shown that celecoxib as a selective COX-2 inhibitor induces apoptosis in leukemia and breast cancer; however, its mechanism has not been well established (1, 2). The present study aimed to investigate the apoptosis induced by two synthetic COX-2 inhibitors, 3-(4-chlorophenyl)-5-(4-fluorophenyl)-4-phenyl-4,5-dihydro-1,2,4-oxadiazole (1) and 3,5-bis(4-chlorophenyl)-4-phenyl-4,5-dihydro-1,2,4-oxadiazole (2) using MCF-7 (human breast adenocarcinoma) and K562 (human myeloid leukemia) cell lines.

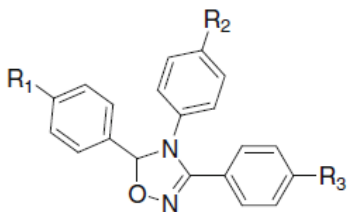
Materials and Methods: Cell cytotoxicity and morphological changes were measured by MTT assay and fluorescence microscope. PI-Annexin-V staining assay was analyzed by flow cytometry, and western blot was used to determine the Bax, Bcl2 and caspase-3 expressions.

Results: Our results indicated that these compounds inhibit proliferation of MCF-7 and K562 cells after 24 h treatment (IC_{50} value ranging from 6.5 to 22.23 μ M). Compound **1** remarkably induced MCF-7 cells to undergo apoptosis, demonstrated by cell morphology, annexin-V and propidium iodide staining. Proteolytic cleavage of caspase-3 after treatment of MCF-7 cells with compound **1** at 16 h, confirmed our evidence of cell apoptosis. Additionally, compound **1** significantly increased the expression of the Bax-to-Bcl-2 ratio in MCF-7 cells suggesting the mitochondrial apoptotic pathway. Our findings also demonstrated that compound **2** triggered apoptosis after 16 h treatment of K562 cells. However, no cleavage of caspase -3 showed the apoptotic mechanism through an independent caspase-3 pathway. Compound **2** significantly raised Bax-to-Bcl-2 ratio, which is relevant to the intrinsic apoptosis.

Conclusion: In conclusion, these results revealed that compound **1** may be a promising chemotherapeutic agent to treat breast cancer, whereas compound **2** needs further investigations to clarify its apoptotic mechanism.

References:

1. Gurung, R.L., Lim, S.N., Khaw, A.K., Soon, J.F.F., Shenoy, K. et al., 2010. Thymoquinone induces telomere shortening, DNA damage and apoptosis in human glioblastoma cells. PLoS ONE 5, e12124.
2. Head, J., Johnston, S.R.D., 2000. New targets for therapy in breast cancer-Farnesyltransferase inhibitors. Breast Cancer Res. 6, 262-268.



Compound **1**; $R_1=F$; $R_2=H$; $R_3=Cl$

Compound **2**; $R_1=Cl$; $R_2=H$; $R_3=Cl$

PP105

EFFECT OF INSAM-PAEDOK-SAN AND FERMENTED INSAM-PAEDOK-SAN ON PLATELET AGGREGATION IN EX VIVO WITH SD-RAT

B. Song¹, S. Hwang¹, B. Lee, H. Baek, J. Chae¹, K. Kwon¹.

¹Chungnam National University, Daejeon, Korea.

Email address of corresponding author: kwon@cnu.ac.kr

This study was conducted to elucidate the anti-aggregation effect of Insam-paedok-san (IPS) enhanced by fermentation.

IPS was composed of Glycyrrhizae radix, Platycodi radix, Ginseng radix alba, Hoelen, Bupleuri radix, Cnidii rhizome, Araliae Continentalis radix, Anthrisci radix, Poncirus trifoliata, Menthae herba, Zingiberis rhizoma. Before fermentation, autoclaving is performed. IPS was fermented by lactobacillus casei (IPS-693), lactobacillus amylophilus (IPS-161). IPS (control, IPS-693, IPS-161) was administered 1 g/kg every 12 hours, 6 times. Platelet aggregation was measured by Aggregometer (Model 570VS, Chrono-log, Haverston, PA, USA) with platelet rich plasma (PRP) of SD-rat. PRP was adjusted 3.5×10^8 platelet/mL. ADP and collagen was used as a stimulant of aggregation. T-test was applied to analyze measured data.

Compared with control, there was no anti-aggregation effect using ADP stimulant. However, Using collagen as an aggregation starter, aggregation was decreased 59%, 54.3 % in IPS-693, IPS-161, respectively (p <0.01).

IPS was found to inhibit collagen-induced platelet aggregation and had no effect on ADP-induced platelet aggregation. These results indicated that IPS inhibit activation of platelets and would be used to other herbal medicine studies.

References

1. Born G, Cross M., 1963, The aggregation of blood platelets, J Physiol. 168, 178-195
2. Lau A, et al., 2009, Antiplatelet and anticoagulant effects of Panax notoginseng: Comparison of raw and steamed Panax notoginseng with Panax ginseng and Panax quinquefolium. J Ethnopharmacol. 125,380-386

Table and Figure

Table 3. Ingredients of IPS and their weight

Ingredients	Weight (g)
Glycyrrhizae radix	200
Platycodi radix,	200
Ginseng radix alba,	200
Hoelen	200
Bupleuri radix	200
Cnidii rhizome	200
Araliae	200
Continentalis radix	
Anthrisci radix,	200
Poncirus trifoliata,	200
Menthae herba,	74.5
Zingiberis rhizoma	74.5

PP106

INDOMETHACIN EXTENDED-RELEASE CAPSULE DOSAGE FORM: FORMULATION DESIGN AND IN VITRO INVESTIGATION

Proceedings

5th BBBB International Conference – 26-28 September 2013

Neslihan Üstündag Okur¹, Aysu Yurdasiper¹, Buket Aksu², Mehmet Ali Ege¹, H. Yesim Karasulu¹

¹Ege University, Faculty of Pharmacy, 35100, Izmir, Turkey

² Santafarma Pharmaceuticals, Okmeydani, Boruçiçeği 20 Sisli, Istanbul, Turkey

The present study was designed to prepare of a new extended release capsules of indomethacin (IND) and to investigate the influence of pladone (PVP K-90) as a hydrophilic polymer, compritol-HD5 ATO (Comp) as a lipophilic polymer on the in vitro dissolution of IND from hard gelatin capsules and to explore the mechanism of drug release through mathematical modeling of dissolution data for all formulations.

A series of extended release capsules of IND were prepared fixed concentration of IND (75 mg) and varying concentrations of pladone (PVP K-90) and compritol-HD5 ATO (Comp). Each mixture were added 10% avicel pH 101 and 5% aerosil. Flow properties of the physical mixtures were evaluated by calculation of the Carr's index, angle of repose and Hausner ratio. DSC studies have been conducted to understand the role of the physical interaction among PVP, Comp and IND. The dissolution rates of the extended release capsules of IND were measured by using USP XXIII apparatus I (rotating basket). Dissolution efficiency (DE), relative dissolution rate (RDR) and mean dissolution time (MDT) parameters were used to also evaluate the dissolution profiles of extended release IND capsules. For dissolution stability evaluation, extended release capsules of IND were investigated over 3 months under different temperature and relative humidity (RH) conditions. Statistical analysis were conducted by one-way ANOVA using target significance levels of 0.05 ($P < 0.05$). Multiple regression analysis was undertaken using a computer program SPSS 10.0. The flowability of IND powder was poorer than the flowability of physical mixtures. Physical mixtures containing PVP possessed slightly higher flow rate than formulations including only Comp. Both the Carr's index and Hauser ratio indicated poor flow property in all formulations. The DSC thermogram of the physical mixtures showed that a slight change in melting peak of the IND suggesting the alteration in crystallinity of IND. Also, a peak intensity corresponding to the drug has decreased in all thermograms. It can be seen more conspicuous in those with higher proportions of PVP and Comp. The dissolution results have been compared with USP XXIII criteria (Table 1), it was observed that the release results of capsule formulations were similar to the USP criteria ($P < 0.05$) (Figure 1). An increase in the concentration of PVP may prevent drug aggregation or raise drug wettability resulting in a higher solubility (1). All formulations of RDR were more than 1 and the MDT values of all formulations at 1 hour were attested to be similar, which suggested a similar dissolution rate compared to IND powder. Certain mathematical models were used for evaluation of release profiles and the results supported by multiple regression analysis (2). It was observed that the best-fit model to determine the mechanism of the formulation which has shown the highest release was Higuchi square-root of time model ($r^2=0.969$). The stability study has indicated that all formulations were stable at $25 \pm 2^\circ\text{C}$, $65 \pm 5\%$ RH and $40 \pm 2^\circ\text{C}$, $75 \pm 5\%$ RH. IND capsule formulations can be an effective dosage form for modified release formulations and could be promising candidates for oral sustained drug delivery systems, especially for poorly soluble drugs.

Table 1. The percentages of indomethacin dissolved in a phosphate buffer of pH 6.2 and USP XXIII criteria of indomethacin extend release capsules according to time

Time (h)	Formulations					USP XXIII Criteria
	F1	F2	F3	F4	F5	Amount Dissolved

1	27.48±0.01	23.71±0.08	19.68±0.07	17.87±0.09	49.96±0.05	Between 12% - 32%
2	36.67±0.04	45.74±0.05	37.96±0.06	55.19±0.10	58.90±0.08	Between 27% - 52%
4	49.20±0.07	63.96±0.06	53.09±0.02	80.36±0.04	66.79±0.03	Between 50% - 80%
12	74.51±0.03	99.22±0.04	82.35±0.05	90.41±0.03	82.20±0.07	Not less than 80%

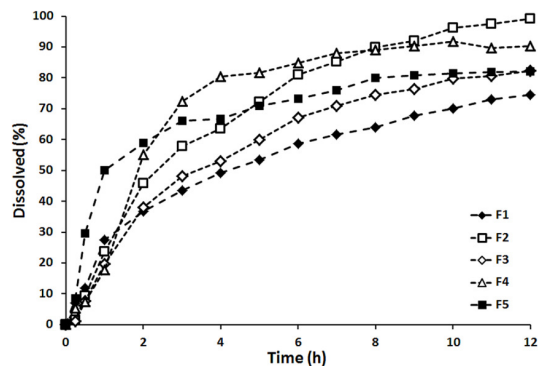


Figure 1. Comparison of release profiles using PVP and Comp by physical mixtures with pure drug (F1) (n=12). Error bars smaller than the symbols are not shown.

References:

1. Oliverira GGG, Ferraz HG, Severino P, Souto EB (2013). Compatibility studies of nevirapine in physical mixtures with excipients for oral HAART. *Mater Sci Eng C*. 33(2): 596-602.
2. Karasulu E, Karasulu HY, Ertan G, Kirilmaz L, Guneri T (2003). Extended release lipophilic indomethacin microspheres: formulation factors and mathematical equations fitted drug release rates. *Eur J Pharm Sci*. 19: 99-104.

PP107

SSAO activity and anti-inflammatory effect of an SSAO inhibitor in rat adjuvant arthritis model

A. Mérey

e-mail: anita.merey@gmail.com

address: Semmelweis University, Nagyvárad tér 4, 1089 Budapest, Hungary

T. Tábi

e-mail: tabi.tamas@pharma.semmelweis-univ.hu

address: Nagyvárad tér 4, 1089 Budapest, Hungary

É. Szökő

e-mail: szoko.eva@pharma.semmelweis-univ.hu

address: Semmelweis University, Nagyvárad tér 4, 1089 Budapest, Hungary

V. Tóth

address: Semmelweis University, Mária utca 41, 1085 Budapest, Hungary

P. Mátyus

address: Högyes Endre utca 7, 1092 Budapest, Hungary

K. Gyires

address: Semmelweis University, Nagyvárad tér 4, 1089 Budapest, Hungary

SSAO/VAP-1 enzyme activity. Inflammation. SzV-1287.

Semicarbazide-Sensitive Amine Oxidase (SSAO) enzyme was found to be identical to Vascular Adhesion Protein-1 (VAP-1) expressed on the luminal surface of endothelial cells and is involved in leukocyte trafficking, especially in the site of inflammation [1]. Its adhesion molecular function depends on its enzymatic activity [2].

Our aim was to determine the anti-inflammatory effect of a new SSAO-inhibitor, SzV-1287 (3-(4,5-diphenyl-1,3-oxazol-2-yl)propanaloxime), synthesized in the Department of Organic Chemistry, Semmelweis University in an animal model of chronic inflammation.

Adjuvant arthritis in rats was induced by the intraplantar injection of heat-killed *Mycobacterium tuberculosis* (0.1 mL; 10 mg/mL) into their right hind paws and then the inflammation was evaluated by measuring the diameter of the tibiodorsal joints and by scoring the secondary lesions. The SSAO activity in paw and serum samples was determined 6, 24, 48 hours and 6, 12 and 18 days after induction of arthritis by radiometric method using ¹⁴C-labeled benzylamine as substrate.

The novel SSAO inhibitor, SzV-1287 alleviated the symptoms of chronic inflammation. The increase in the diameter of the injected tibiodorsal joints was reduced by 30-40% in treated animals at the 6th, 12th, 18th days. In the contralateral paws significant inflammation developed after 18 days, which was reduced by 70 % in the SzV-1287 treated animals. The scores of the secondary lesions were decreased similarly (Table 1). The anti-inflammatory effect of SzV-1287 was not accompanied by macroscopic damage of the gastric mucosa. Unexpectedly, the SSAO enzyme activity in the inflamed paws was found lower than in the paws of the control animals. In the injected paws the activity decreased by 77% as early as 6 hours after injection and remained lower for 18 days. However, in the contralateral paws the only significant alteration was a transient elevation of the enzyme activity at 6th day. Enzyme activity in the serum of rats with arthritis showed a transient increase (170%) at the 6th hour than it dropped below the control level at the 24th hour and remained lower for 18 days (Figure 1).

The new SSAO inhibitor effectively decreased the symptoms of inflammation and it has no ulcerogenic activity. It was an unexpected finding that although the SSAO inhibitor showed significant anti-inflammatory effect, the enzyme activity was found lower in the tissue and serum samples of rats with adjuvant arthritis. The regulation of SSAO activity, as well as the precise mechanism of the anti-inflammatory effect of SSAO inhibitors need further clarification.

References

- [1] Salmi M, Tohka S, Berg EL, Butcher EC, Jalkanen S. *J. Exp. Med.* 1997; 186(4): 589-600.
- [2] Salmi M, Yegutkin GG, Lehtonen R, Koskinen K, Salminen T, Jalkanen S. *Immunity* 2001; 14(3): 265-76

Table 1

Inhibitory effect of SzV-1287 on signs of inflammation in adjuvant arthritis model

	Diameter of the tibiodorsal joint [% of control]				Secondary inflammatory lesion scores	
	Injected paw		Contralateral paw			
	Untreated	Treated	Untreated	Treated	Untreated	Treated
Days						
2	156±12	142±18	96±8	92±9	0	0
6	177±18	154±21*	98±6	92±9	0	0
12	160±13	135±27*	110±16	102±21	1.3±0.93	0.9±1.09
18	176±19	145±26*	161±21	118±23**	7.2±1.67	2.5±2.50**

n=5-8, *: p<0.05 vs. vehicle treated animals; **: p<0.01 vs. vehicle treated animals

Figure 1

SSAO activity in paw and serum samples of rats with adjuvant arthritis

PP108**MECHANISM OF VASORELAXATION INDUCED BY 16-O-ACETYLDIHYDROISOSTEVIOL IN RAT AORTA**C. Tocharus^{1*}, R. Pantan¹, A. Onsa-ard², S. Homvisasevongsa³, A. Suksamrarn⁴¹Department of Anatomy, Faculty of Medicine, Chiang Mai University, Chiang Mai, Thailand, ²Department of Biochemistry, Faculty of Medical Science, Naresuan University, Phitsanulok, Thailand, ³Department ofChemistry, Faculty of Science, Huachiew Chalermprakiet University, Bangkok, Thailand, ⁴ Department of Chemistry, Faculty of Science, Ramkhamhaeng University, Bangkok, Thailand

Hypertension is a chronic condition that blood pressure is elevated in systolic blood pressure (SBP) and/or diastolic blood pressure (DBP). The impairment of blood vessels leads to elevate of blood pressure. The wall of blood vessels consist of endothelial cell and smooth muscle cell which are importance in changing diameter of blood vessels via vascular tone regulation including vasoconstriction and vasodilation. 16-O-Acetyldihydroisosteviol (ADIS) is a chemically modified analog of isosteviol, a diterpene obtained from stevioside, which was extracted from the leaf of *Stevia rebaudina* Bertoni and have been reported to possess hypoglycemic and hypotensive effects. Preliminary work indicated that ADIS exerted potent vasorelaxant activity. The aim of the study was to investigate the mechanism of ADIS on vasorelaxant effect in rat aorta. Male Wistar rats (200-250 g) were obtained from the National Laboratory Animal Center, Thailand. The experiment protocol was approved by the Animal Ethics Committee in accordance with the guide for the care and use of laboratory animals prepared by Chiang Mai University.

Acid hydrolysis of stevioside yielded isosteviol, which upon reduction with sodium borohydride in THF furnished dihydroisosteviol. Acetylation of dihydroisosteviol gave 16-O-Acetyldihydroisosteviol (ADIS) (Fig.1). ADIS is a chemically modified analog of isosteviol, which was extracted from the leaf of *S. rebaudiana*. Rats were anesthetized by intraperitoneal injection using sodium pentobarbital. The aorta was immediately cut into rings have approximately 3 mm in length. The aortic rings were immersed in chamber bath at 37°C. After equilibration, resting tension was induced to contraction with PE for endothelium-intact and -denuded rings. Then, ADIS (10^{-7} - 10^{-3} M) was added cumulatively. The ability of ADIS to reduce KCl induced contraction was investigated.

To define the activity of ADIS on vasorelaxation, endothelium-intact and endothelium-denuded rings were used to assay with phenylephrine (PE) and KCl. The rings pre-contracted by PE and KCl were not significantly difference in relaxing the sustained contraction on a concentration-dependent manner (Table 1).

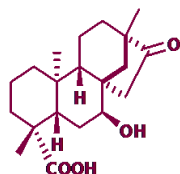


Figure 1 Structure of ADIS

Table 1. Vasorelaxant effect of ADIS against contraction induced by PE and KCl in endothelium-intact (+EC) and endothelium-denuded (-EC) rings.

ADIS against	-logEC ₅₀	
	+EC	-EC
PE	4.402 ± 0.063	4.351 ± 0.120
KCl	4.381 ± 0.137	4.177 ± 0.114

ADIS shows the vasorelaxant effect via endothelium-independent pathway.

This work was supported by a research grant from the Office of the Higher Education Commission and Faculty of Medicine, Chiang Mai University.

REFERENCES

1. Wonganan O, Tocharus C, Pudsing C, Homvisasevongsa S, Sukcharoen O, Suksamrarn A. (2013) Potent vasorelaxant analogs from chemical modification and biotransformation of isosteviol. *Eur J Med Chem* 62: 771-776.
2. Adaramoye OA, Anjos, RM, Almeida MM, Veras RC, Silvia DF, Oliveira FA, Cavalcante KV, Araujo IG, Oliveira AP, Medeiros IA. (2009) Hypotensive and endothelium-independent vasorelaxant effects of methanolic extract from *Curcuma longa* L. in rats. *J of Ethnopharmacol* 124: 457-462.

PP109

AMORPHOUS SOLID DISPERSIONS PREPARED BY A CRYOGENIC CO-GRINDING OF A POORLY WATER-SOLUBLE PIROXICAM AND CARRIER POLYMERS

A. Penkina¹, K. Semjonov¹, M. Hakola², S. Vuorinen², T. Repo², J. Yliruusi², K. Kirsimäe¹, K. Kogermann¹, P. Veski¹, J. Heinämäki¹

¹. University of Tartu, Tartu, Estonia

². University of Helsinki, Helsinki, Finland

In recent years, co-grinding and a number modifications of it have been increasingly used for formulation of poorly water-soluble drugs to improve their solubility, dissolution rate and bioavailability [1]. Piroxicam (PRX) is a poorly water-soluble, non-steroidal anti-inflammatory drug which belongs to Class II (high permeability, low solubility) in the Biopharmaceutical Classification System (BCS). For highly permeable and low soluble drugs, the limiting factor for oral absorption is a dissolution rate of drug and formulation. Amorphous state of PRX has been obtained by several methods including mechanical activation (ball milling), cryo-milling, electrospinning and melt spinning and quench cooling of a melt.

The aim of the present study was to investigate polyvinylpyrrolidone (PVP) and catalytic pretreated cellulose (CPSC) as carrier polymers in cryogenic co-grinding (amorphisation) of poorly water-soluble piroxicam (PRX). Isolation of cellulose (CPSC) from pine soft wood (*Pinus sylvestris*) was carried out according to the method described by Hakola et al. (2010) with some modification [2]. Polyvinyl pyrrolidone (PVP) was used as a reference polymer for cryogenic co-grinding. Cryogenic co-ground mixtures were prepared with a laboratory-scale ball mill and samples were taken within regular time periods at 30, 60, 120, 150 and 180 min. Co-ground mixtures were investigated immediately after preparation and during a short-term (at least 1-week) aging at an ambient controlled room temperature (25°C / 20% RH). Raman and FTIR spectroscopy, X-ray powder diffractometry (XPRD) and differential scanning calorimetry (DSC) were used for characterising the solid-state changes and drug-polymer interactions. The particle size and surface morphology of starting materials and co-ground mixtures were investigated with a high-resolution scanning electron microscope (SEM).

The results suggested that both CPSC and PVP improved the cryogenic co-grinding (amorphisation) of a poorly water-soluble PRX. After cryogrinding for 180 min, the amorphous form of PRXAH I was achieved with both carrier polymers (PVP, CPSC). However, in case of using CPSC as a carrier polymer the amorphisation of PRX was found to be only temporary (Fig.1). A phase transformation occurred and crystalline peaks were observed after 24 h of storage at an ambient controlled room temperature (25°C / 20% RH). PRX structure contains O-H and one N-H functional group, which probably forms hydrogen bonding with a carbonyl group of PVP. Controversially, CPSC acts as a physical matrix, where drug particles are located between cellulose microfibrils. Cryogenic co-ground mixtures of PRX and PVP (1:3) remained in an amorphous state over a one-week storage period.

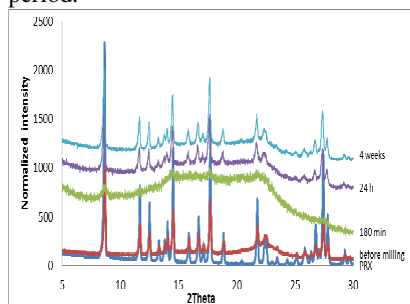


Figure 1. X-ray powder diffraction patterns of cryogenic co-ground mixture of PRX and CPSC (1:3) during a short-term aging for one week.

References:

- [1] Vogt, M., Kunath, K., Dressman J.B. Eur. J. Pharm. Biopharm. 68, 330-337, 2008.
- [2] Hakola M., Kallioinen A., Kemell M., et al. ChemSusChem 3 (10): 1142-1145, 2010.

corresponding author: anna.penkina@hotmail.com

PP111

NANOFIBER-BASED AMORPHOUS SOLID DISPERSIONS OF A POORLY WATER-SOLUBLE DRUG AND SYNTHETIC GRAFT COPOLYMER

U. Paaver, J. Heinämäki, I. Laidmäe, A. Lust, J. Kozlova, K. Kirsimäe, P. Veski, K. Kogermann
University of Tartu, Tartu, Estonia

Electrospinning is an effective and simple method to fabricate polymer nanofibers for a wide range of applications including various pharmaceutical and biomedical systems [1,2]. The aim of the present study was to investigate electrospinning as a novel technique for preparing amorphous solid dispersions (ASD) and polymeric nanofibers of a poorly water-soluble drug, piroxicam (PRX).

PRX was used as a model drug and Soluplus[®] (polyvinyl caprolactam - polyvinyl acetate - polyethylene glycol graft copolymer, PCL-PVAc-PEG) as a water-soluble and stabilizing carrier polymer. The ratio of PRX and PCL-PVAc-PEG used in the nanofibers was 1:13 (w/w). Acetone was used as a solvent system in electrospinning. Raman spectroscopy, X-ray powder diffraction (XPRD), differential scanning calorimetry (DSC), and scanning electron microscopy (SEM) were applied in the physical characterization of the ASD nanofibers. The *in vitro* dissolution tests of electrospun nanofibers were performed using an USP dissolution apparatus I (basket method).

The drug-loaded nanofibers were circular in cross-section with an average diameter ranging from 200 to 400 nm (SEM). The nanofibers were yellow in color suggesting that PRX existed in amorphous form, moreover Raman spectroscopy and XRPD confirmed the presence of amorphous PRX. The electrospun nanofibers dissolved rapidly and exhibited an absence of lag-time in the dissolution test *in vitro*. It is evident that the amorphous state of PRX decreased the lag-time for the drug release *in vitro*. However, when the drug-loaded nanofibers were filled into hard gelatine capsule shells, a gel-like barrier layer was observed in the dissolution test, and only 5% of PRX was released within several hours suggesting incompatibility between the ASD nanofibers and gelatine capsule shell.

Electrospinning can be used to prepare the ASD nanofibers of PRX and PCL-PVAc-PEG graft copolymer, and to stabilize the amorphous state of PRX. The loading of the present nanofibers into a hard gelatine capsule, however, can significantly impair the release and dissolution rate of a poorly water-soluble drug.

Acknowledgements: This work is part of the targeted financing project no SF0180042s09 and ETF grant project no ETF7980. This research was also supported by the European Social Fund's Doctoral Studies and Internationalization Program DoRa.

References:

1. Agarwal, S., Wendorff, J.H., Greiner, A., 2008. Use of electrospinning technique for biomedical applications. *Polymer* 49, 5603-5621.
2. Lu, X., Wang, C., Wei, Y., 2009. One-dimensional composite nanomaterials: Synthesis by electrospinning and their applications. *Small* 5 (21), 2349-2370.

urve.paaver@ut.ee

PP114

ELECTROSPUN NANOFIBERS AS A NOVEL DELIVERY SYSTEM FOR A POORLY WATER-SOLUBLE β -SITOSTEROL

U. Paaver¹, I. Laidmäe¹, H.A. Santos², J. Yliruusi², P. Veski¹, K. Kogermann¹, J. Heinämäki¹

¹. University of Tartu, Tartu, Estonia

Proceedings

5th BBBB International Conference – 26-28 September 2013

². University of Helsinki, Helsinki, Finland

Plant sterols such as β -sitosterol have a serum cholesterol lowering effect when administered orally [1,2]. Electrospinning was used as a novel technique for preparing solid dispersions (SD) and polymeric nanofibers of a poorly water-soluble crystalline β -sitosterol. The main hypothesis was that the SD nanofibers could improve solubility of β -sitosterol by affecting the physical solid state of the active substance.

Chitosan was used as a stabilizer and carrier polymer in nanofibers. The solvents applied in the electrospinning were trifluoroacetic acid (TFA) and 1,1,1,3,3,3-hexa-fluoro-2-propanol (HFIP). The geometric properties and surface topography of the nanofibers were characterized by means of a high-resolution scanning electron microscope (SEM). The physical solid-state analyses were made by Raman spectroscopy, X-ray powder diffraction (XPRD) and differential scanning calorimetry (DSC). Wetting and dissolution properties of the SD nanofibers were monitored *in situ* by using optical microscopy. Special attention was paid on the effects of a polymer and solvent system on the solid-state properties, wetting and dissolution of nanofibers.

Electrospinning of β -sitosterol-loaded nanofibers with chitosan using TFA and HFIP as solvent systems was found to be successful. The average diameter of the electrospun SD nanofibers ranged from 100 to 200 nm. β -sitosterol was homogeneously dispersed in the nanofibers after fabrication. The electrospun β -sitosterol-loaded nanofibers were freely water soluble and exhibited very short lag-time in releasing the active substance. Based on the *in situ* dissolution monitoring, however, β -sitosterol tended to recrystallise to crystalline form when released from the polymeric nanofibers. The tiny crystals of β -sitosterol were clearly visible immediately after addition of purified water or buffer solutions in a contact with nanofibers.

Electrospinning could be a future technology for formulation of poorly water-soluble crystalline plant sterols. A major challenge, however, is to stabilize the solid-state form of a plant sterol.

Acknowledgements: This work is part of the targeted financing project no SF0180042s09 and ETF grant project no ETF7980. This research was also supported by the European Social Fund's Doctoral Studies and Internationalization Program DoRa.

References:

1. Hallikainen, M., Sarkkinen, E., Uusitupa, M., 2000. Plant stanol esters affect serum cholesterol concentrations of hypercholesterolemic men and women in a dose dependent manner. *J. Nutr.* 130, 767-776.
2. Christiansen, L., Lähteenmäki, P., Mannelin M., Seppänen-Laakso, T., Hiltunen, R., Yliruusi, J., 2001. Cholesterol-lowering effect of spreads enriched with microcrystalline plant sterols in hypercholesterolemic subjects. *Eur. J. Nutr.* 40, 66-73.

urve.paaver@ut.ee

PP117

ANTI-DIABETIC AND RENOPROTECTIVE EFFECTS OF CLADOPHORA GLOMERATA KÜTZING EXTRACT IN HIGH FAT DIET WITH STREPTOZOTOCIN-INDUCED TYPE 2 DIABETIC RATS

Chutima Srimaroeng^{a*}, Atcharaporn Ontawong^b, Anchalee Pongchidecha^a, Varanuj Chatsudthipong^c

^a. Department of Physiology, Faculty of Medicine, Chiang Mai University, Chiang Mai, 50200 Thailand

^b. Division of Physiology, School of Medical Sciences, University of Phayao, Phayao, 56000 Thailand

^c. Department of Physiology, Faculty of Science, Mahidol University, Bangkok, 10400 Thailand

* Corresponding author email address: chutima.srimaroeng@cmu.ac.th

Cladophora glomerata (CG) is a freshwater macroalga that has been widely grown in Northern Thailand. Previous studies indicated that this species has high amount of nutritional compositions, including carbohydrate, fat, proteins, vitamins and minerals [1]. Recently, CG extract (CGE) exhibited anti-gastric ulcer, anti-inflammatory, analgesic, hypotensive, and antioxidant activities. However, the effect of CGE on a particular disease remains unknown. This study aimed to investigate anti-diabetic and renoprotective effects of CGE in type 2 diabetic mellitus (T2DM) rats. Diabetic rats were induced by a combination of high fat diet and low-single dose of streptozotocin. T2DM rats were fed daily with CGE (1 g/kg BW), high fat diet, or 30 mg/kg BW of the anti-diabetic drug, metformin, for 12 weeks. General characteristics of T2DM, renal malon-dialdehyde (MDA) levels, real time PCR and western blotting were analyzed. Renal cortical slices were used to determine renal transport function of organic anion, *para*-aminohippurate (PAH) and cation, 1-methyl-4-phenylpyridinium (MPP⁺) by organic anion and organic cationtransporters (Oats and Octs), respectively. Compared to T2DM, plasma glucose and triglyceride, insulin resistance, and high levels of renal MDA were significantly improved after CGE supplementation similar to that of metformin. The reduction of glutathione peroxidase (GPx), NFκB, and PKCα expressions were associated with antioxidant effect of CGE. The uptake of PAH in renal cortical slices was not different among experimental groups. This data correlated with Oats mRNA levels. In contrast, MPP⁺ transport was markedly reduced in T2DM rats, and this was restored in the slices from CGE administration. The present study demonstrated that CGE has anti-diabetic and renoprotective effects in long-term hyperglycemia induced reactive oxygen species in experimental T2DM rats. The mechanism by which antioxidant activity of CGE improved renal transport function was linked with antioxidant system and stress-sensitive signaling proteins. The beneficial information of our findings allows for further development of CGE into nutraceutical or pharmaceutical products for prevention of diabetic nephropathy.

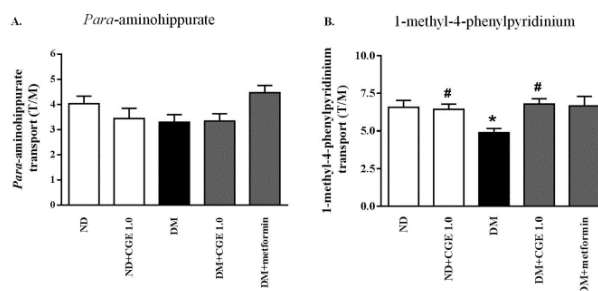


Figure 1. Effects of *Cladophora glomerata* on organic transport functions. Rat renal cortical slices were incubated in the buffer containing (A) 5 μ M [3H]PAH or (B) 1.25 nM [3H]MPP⁺. Data are expressed as tissue to medium ratio, and represented as mean \pm S.D (n=6).

Reference: [1] Peerapornpisal, Y., Amornledpison, D., Rujjanawate, C., Ruangrit, K., Kanjanapothi, D., 2006. Two Endemic Species of Macroalgae in Nan River, Northern Thailand, as Therapeutic Agents. *Sci Asia* 32 (Suppl 1), 71-76.

PP118

The effect of *Spirogyra neglecta* (Hassall) Kützing extract in experimental type 2 diabetic

Naruwan Saowakon^{a*}, Atcharporn Ontawong^b., Chutima. Srimaroeng^c.

^a. Institute of Science, Suranaree University of Technology, Nakhon Ratchasima, Thailand

^b. School of Medical Sciences, University of Phayao, Phayao, Thailand

^c. Faculty of Medicine, Chiang Mai University, Chiang Mai, Thailand

* Corresponding author email address: naruwan@sut.ac.th

The objective of this study was to investigate the effect of *Spirogyra neglecta* extract (SNE) in type 2 diabetes mellitus (T2DM) rats induced by high-fat diet with low-single dose streptozotocin (STZ) and observed by light microscopy. Male Wistar rats were divided into 7 groups: normal diet (ND), ND supplemented with SNE at the dose of 1.0 g/kg BW (ND+SNE 1.0), T2DM (DM), T2DM supplemented with SNE at the dose of 0.25, 0.5 and 1.0 g/kg BW, respectively (DM+SNE0.25, DM+SNE0.5 and DM+SNE1.0) and T2DM supplemented with vitamin C at the dose of 0.2 g/kg BW (DM+vit.C) was used as positive control. T2DM in rats was induced by a combination of high-fat diet and STZ at the dose 40 mg/kg BW. SNE or vitamin C was administered daily for 12 weeks. Finally, they were sacrificed; and collected kidneys in each group for histopathological assessment by hematoxylin and eosin (H&E) and periodic acid-Schiff base (PAS). The severity was graded to mild, moderate, and severe for focal changes with less than 25%, 25-50%, and greater than 50% of lesion, respectively. The kidneys of ND and ND+SNE1.0 group had normal renal structures including glomerulus capillaries and tubular compartments. In contrast, T2DM kidneys exhibited the glomerular and tubular hypertrophy, thickening of the mesangium and glomerular basement membrane (GBM). The mild lesion was occurred in the renal tubular compartment in DM+vit.C, implying that vitamin C did not improve the diabetic nephropathy. In DM+SNE0.25 and DM+SNE0.5 persistently increased in sizes. Interestingly, the kidney changes showed a significant decreased in both mesangial and tubular hypertrophy in DM+SNE1.0. We confirmed the results by PAS staining, the results showed similar to H&E observation. Similarly, previous study has shown that the hypertrophic appearance in both glomerular capillaries and tubular compartments were found in diabetic nephropathy rats, which resulted in impaired membrane permeability and function [1]. We have demonstrated the renal morphological changes in T2DM experimental rat model. SNE was able to improve the tubular and mesangial hypertrophy. Our findings will be guide for further development of SNE into a nutraceutical product for prevention of diabetic nephropathy in human.

References

[1] Fabris, B., Candido, R., Carraro M., et al.2001. Modulation of incipient glomerular lesions in experimental diabetic nephropathy by hypotensive and subhypotensive dosages of an ACE inhibitor. *Diabetes*. 50(11): 2619-2624.

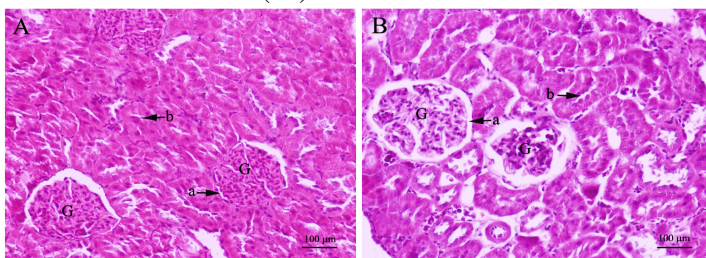


Fig.1 Micrograph of H&E staining of rat kidneys. (A) T2DM (B) DM+SNE1.0 group. Arrow “a” indicates the Bowman’s capsule space. Arrow labeled “b” indicated the proximal tubular lumen. Abbreviation: glomerulus (G)

PP119

FUNCTIONALIZED HYPERBRANCHED POLYMERS AS THERMOSENSITIVE NANOCARRIERS WITH PRECISELY CONTROLLED TRANSITION TEMPERATURES

M. Agathokleous, Z. Sideratou, T. A. Theodossiou, D. Tsiourvas

National Centre for Scientific Research "Demokritos", IAMPPNM, Dept. of Physical Chemistry, 15310 Aghia Paraskevi, Attiki, Greece.

Thermosensitive polymers respond at a certain, rather specific, temperature, usually referred to as lower critical solution temperature (LCST), by changing their conformation, their hydrophilic/hydrophobic balance and their solubility in water.^{1,2} LCST is, however, strongly dependent on polymer concentration, pH, ionic strength, as well as on the presence of specific molecules or ions in solution. Therefore, polymers with LCST values within 37-40 °C as needed in drug delivery applications, are not easily attainable.

In this study, we explored the possibility to accurately tailor the LCST of isobutyl functionalized hyperbranched poly(ethylene imine) (HPEI) by carefully selecting the degree of functionalization and demonstrated its ability to encapsulate and deliver a widely used anticancer drug, doxorubicin (DOX). A series of HPEI derivatives were obtained by complete functionalization of the primary amino end groups and the partial functionalization of the secondary amino groups of HPEI with isobutyl amide groups. It was found that increasing the degree of substitution of the secondary amines led to hyperbranched polymers with lower LCST values. Thus, it was possible to obtain thermoresponsive polymers with transition temperatures ranging from ~20 °C up to ~90 °C. The derivatives were spectroscopically characterized by FTIR, ¹H NMR and inverse gated ¹³C NMR in order to determine the degree of substitution of primary and secondary amines of HPEI. For the determination of LCST the turbidity method was employed. The effect of the degree of substitution of secondary amines on LCST was studied in aqueous media as a function of polymer concentration, phosphate salt concentration, sodium chloride concentration and pH.

A derivative with transition temperature in the range of 37-40 °C was further studied as potential drug delivery and controlled release system. Cytotoxicity studies on MCF7 cells showed no notable toxicity of this compound at temperatures either below or above the LCST, i.e. at 37 and 40 °C, respectively, and at concentrations up to 100 µM. The encapsulation of DOX, and its release profiles were registered at 37 and 40 °C. DOX loaded carriers were administered to MCF7 cells and cell uptake was studied by confocal microscopy at both temperatures. Increase of DOX uptake was observed for incubation at 40 °C (Fig. 1). The cytotoxicity of DOX loaded carriers was found to be significantly enhanced at 40 °C compared to media controls at the same temperature and to cells incubated with DOX loaded carriers at 37 °C.

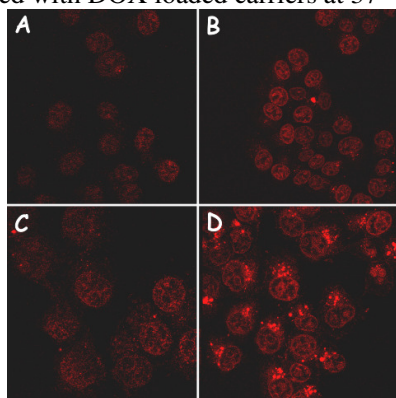


Fig. 1: Representative confocal microscopy images of MCF7 cells incubated at 37 (top) and 40 °C (bottom) with free DOX (left, 110 nM) and DOX-loaded thermoresponsive HPEI (right, 110 nM DOX, 10 µM thermoresponsive HPEI, 6 h incubation time).

In conclusion, by controlled functionalization of HPEI it is possible to obtain thermoresponsive polymeric carriers with a transition temperature between 37 - 40 °C, minimal cytotoxicity, and able to encapsulate and effectively release anticancer agents in a temperature controlled fashion.

References

Proceedings

1. C. Kojima, Expert Opin. Drug Deliv. (2010) 7(3):307-319.
2. Calderón M., Quadir M.A., Strumia M., Haag R., Biochimie (2010) [92](#)(9):1242-1251.

Corresponding author.

E-mail address: maria_chem@chem.demokritos.gr

PP120

PEGYLATED NANOLIPOSOME INTERACTIONS WITH IN VITRO BBB MODEL: EFFECT OF VESICLE PHYSICO-CHEMICAL CHARACTERISTICS

K. Papadia¹, E. Markoutsas¹, S.G. Antimisiaris^{1,2,*}

¹University of Patras, Patras, Greece;

²FORTH/ICES, Patras, Greece

santimis@upatras.gr

In order to evaluate the effect of liposome size and surface charge on their interaction with hCMEC/D3 cells (in vitro model of the BBB), pegylated liposomes (encapsulating FITC-dextran and Rhodamine-DSPE), and consisting of DSPC/Chol (2:1 mol/mol) and 8mol% PEG₂₀₀₀-DPPE, were prepared by the thin film hydration technique followed by extrusion through appropriate pore size polycarbonate filters (50, 100, 200 and 400 nm) to give vesicle diameters between 100 – 400 nm. LIP were characterized for size distribution and surface charge by DLS and their FITC and lipid content was estimated by FI and Stewart assay. The uptake of LIP by hCMEC/D3 cells was measured [1] and transport through cell monolayers was evaluated (at 20, 40 and 60 min) by measuring FITC and Rhodamine transport in the receiving compartment [2]. The effect of vesicle charge on interaction with cells was evaluated by replacing 5, 10 or 15 mol% of DSPC with DSPG in the LIP, in order to increase vesicle zeta-potential but keep the vesicle size constant.

Final liposome sizes measured were different from the pores of the extrusion membranes and where 104-108, 127-134, 209-231 and 326-389, for the 50, 100, 200 and 400 nm pore-size membranes, respectively. This is most possibly due to the specific composition used (2:1 lipid/cholesterol ratio) and the fact that a rhodamine lipid conjugate was additionally incorporated in the lipid membranes.

Table 1. Liposome size distribution and Polydispersity Index

Pore-size(nm)	Mean diameter range (nm)	PI
50	104-108	0.156
100	127-134	0.129
200	209-231	0.167
400	326-389	0.188

The uptake experiment results (not shown) indicate that liposomes can be categorized in two classes, those with mean-diameters < 150 nm, for which uptake by the cells was increased by 40-48%, compared to the second size-category liposomes with mean diameters > 200 nm. When liposome size was within the first category (< 150 nm) a very slight effect of surface charge on cell uptake (around 10% increase) was noticed, only when the vesicle zeta potential was > 15 mV (vesicle containing 15 mol% DSPG). From the transport experiments (Figure 1) it was seen that only when liposome diameter was > 209 nm, the %transported FITC and Rhodamine labels was decreased significantly.

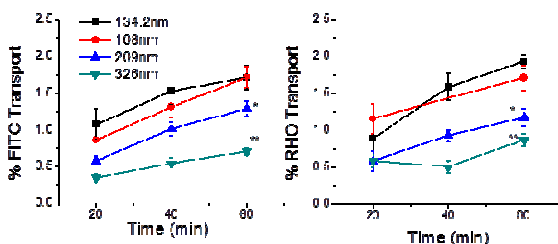


Figure 1. FITC and RHO transport across hCMEC/D3 monolayers

Concluding, the results obtained when testing liposomes on the hCMEC/D3 cellular BBB model are not affected by liposome characteristics when mean diameter is <150nm and z-potential <-15 mV (for uptake) & when diameter is <209 nm (for transport).

Acknowledgements

Funded from EU- FP7/ 2008-2013, under grant agreement 212043.

References

- [1] Markoutsas, E., Pampalakis, G., Niarakis, A., Romero, I.A., Weksler, B., Couraud, P.-O., Antimisiaris, S.G., 2011. Uptake and permeability studies of BBB-targeting immunoliposomes using the hCMEC/D3 cell line, *EJPB*, 77: 2, 265-274.
- [2] Markoutsas, E., Papadia, K., Clemente, C., Flores, O., Antimisiaris, S.G., 2012. Anti-A β -MAB and dually decorated nanoliposomes: Effect of A β 1-42 peptides on interaction with hCMEC/D3 cells. *EJPB*, 81(1): 49-56.

COMPARATIVE STUDY OF URSOLIC ACID POLYMERIC NANOPARTICLES PREPARED WITH POLOXAMER 407 AND 188 AS SURFACTANTS.

J. P. A. Barcellos, J. O. Eloy, E. C. O. Vargas, M. G. Trevisani, J. M. Marchetti

University of Sao Paulo, School of Pharmaceutical Sciences of Ribeirao Preto (FCFRP-USP), Ribeirao Preto, Brazil.

E-mail: julianapab@fcrp.usp.br

The purpose of this study was to develop and compare polymeric nanoparticles (NPs) prepared with different surfactants (poloxamers 407 and 188) and analyse the effect on particle size, polydispersity, zeta potential and encapsulation efficiency. The nanoparticles were prepared by the nanoprecipitation technique¹. This method is simple, fast, economic and employs non toxic solvents, and the mean particle size usually ranges from 100 to 500 nm. Briefly, the organic phase, containing ursolic acid (AU), poly-ε-caprolactone (PCL) (drug:polymer ratio 1:10), and acetone (12.5 mL) was dripped slowly into the aqueous phase (25 mL) containing 0.5% surfactant (poloxamer 407 or poloxamer 188), under gentle magnetic stirring (300 rpm) until complete evaporation of the solvent. The resultant NPs suspension was filtered (0.45 μm) followed by ultracentrifugation in order to eliminate the non-encapsulated drug and obtain nanoparticles with a regular size distribution and non-aggregated. The systems were evaluated regarding particle size distribution (dynamic light scattering), zeta potential value, polydispersity indexes and encapsulation efficiency (HPLC). The formulations with poloxamer 407 and 188 presented, respectively, a mean particle size equivalent to 173.17±4.20 and 198.67±33.09 nm. Both formulations exhibited a negative charge with zeta potential values ranging from -36 to -40mV. The polydispersity indexes were, respectively: 0.09±24.77 and 0.26±37.77, for poloxamer 407 and poloxamer 188. The two formulations presented the following values of encapsulation efficiency: 94.1±1.31 and 63.65±7.67%, respectively for NPs prepared with poloxamer 407 and 188. After these studies, scanning electron microscopy (SEM) was conducted with the nanoparticles containing poloxamer 407 and all the photomicrographs (Figure 1) showed slightly spherical and aggregated particles. This aggregation can occur due the drying process and due the coating of the poloxamer 407. In conclusion, both formulations exhibited diameters below 200 nm, low polydispersity indexes, indicating a homogeneous size distribution, and negative surface charge. About the encapsulation efficiency, the formulation with poloxamer 407 exhibited higher drug incorporation and will be selected for further studies, because the release rate tends to be higher in the case of formulations containing higher amount of drugs incorporated. Moreover, we argue for the selection of the surfactant poloxamer 407 because it has been demonstrated to better sustain drug release, compared to poloxamer 188, which is relevant for the intravenous administration².

Table 1: Particle size (nm), polydispersity indexes, zeta potential zeta and encapsulation efficiency (%) associated with different surfactants in the preparation of nanoparticles of PCL containing AU.

Formulation (Ratio AU:PCL/FO:FA/Surfactant)	Particle size (nm) ± CV (%)	Polydispersity indexes ± CV (%)	Zeta potential (mV) ± CV (%)	Encapsulation efficiency (%) ± CV (%)
1:10 / 1:2 / P 188	198.67±33.09	0.26±37.77	-40±11.47	63.65±7.67
1:10 / 1:2 / P 407	173.17±4.20	0.09±24.77	-36±9.43	94.1±1.31

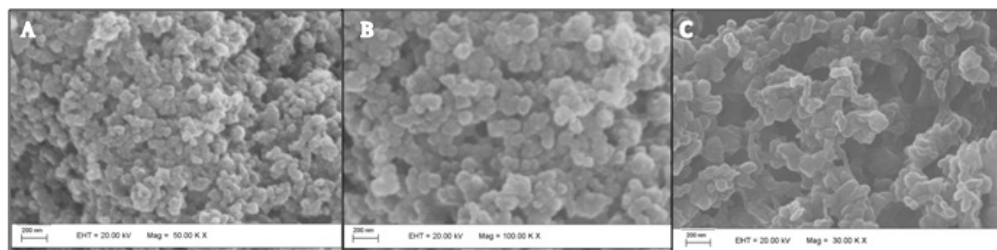


Figure 1: Photomicrographs of nanoparticles of polycaprolactone containing ursolic acid, ratio organic phase:aqueous phase 1:2 and ursolic acid:polycaprolactone 1:10, without remotion of poloxamer 407 (A and B) and with remotion of poloxamer 407 (C).

1. FESSI, H., PUISIEUX, F., DEVISSAGUET, J.P., AMMOURY, N., BENITA, S. Nanocapsule formation by interfacial polymer deposition following solvent displacement. **International Journal of Pharmaceutics**. vol 55. pag R1 – R4, 1989.

2. DUNN, S. E.; COOMBERS, A. G. A.; GARNETT, M. C.; DAVIS, S. S.; DAVIES, M. C.; LISBETH, I. In vitro cell interaction and in vivo biodistribution of poly(lactide-co-glycolide) nanospheres surface modified by poloxamer and poloxamine copolymers. **Jornal of Controlled Release**. vol 44. pag 65-76. 1997.

PP127

META-ANALYSIS OF THE EFFICACY AND SAFETY OF LORCASERIN IN REDUCING BODY WEIGHT IN OVERWEIGHT AND OBESE ADULTS

K. Tewthanom, N. Poolsup*, J. Jenvutipanish, J. Keawmanee, C. Chuenchit, P. Ubollert

Faculty of Pharmacy, Silpakorn University, Nakhon-Pathom, Thailand

*Corresponding author: npoolsup@hotmail.com

Lorcaserin is a novel selective serotonin 2C (5-HT_{2C}) receptor agonist designed to promote weight loss. It offers advantages over previously available drugs, fenfluramine and dexfenfluramine, which are nonselective serotonergic agonists. With its selectivity, the risk of serotonin-associated valvulopathy resulting from 5-HT_{2B} receptor activation is reduced. Lorcaserin is approved as a weight-loss pill at a dose of 10 mg twice daily in adults with a body mass index ≥ 30 kg/m² or ≥ 27 kg/m² with at least one weight-related comorbidity, such as hypertension, type 2 diabetes mellitus, or dyslipidemia, in addition to a reduced calorie diet and increased physical activity. We conducted systematic review and meta-analysis to evaluate the efficacy and safety of lorcaserin in overweight and obese adults.

A systematic literature search for randomized controlled trials was undertaken of Pubmed, the Cochrane Library, CINAHL, Web of Science[®], Scopus, and clinicaltrials.gov from their respective inception until February 2013. The bibliography of the retrieved articles was also examined. To be included in the meta-analysis, a study had to be (1) randomized, placebo-controlled trial of lorcaserin in overweight or obese adults, (2) reporting change in body weight (kg), or the proportion of patients achieving at least 5% or 10% reduction in body weight, and (3) published in English. Continuous outcome was estimated with mean difference and dichotomous outcome was estimated with relative risk (RR). Data were pooled using the inverse variance-weighted method. A random effects model was used when heterogeneity was significant at the level of 0.1, otherwise the fixed effects model was performed. The degree of heterogeneity was quantified using I-squared statistic. The statistical analysis was undertaken with RevMan version 5.2.6 (Cochrane collaboration). The significant level was set at $p < 0.05$.

Three randomised controlled trials involving altogether 6619 overweight or obese adults (3313 in lorcaserin group and 3306 in placebo group) were included. Details of these trials are presented in Table 1. Lorcaserin reduced mean body weight by 3.16 Kg (95% CI: 2.66-3.65 Kg, $p < 0.00001$). Overweight or obese adults who received lorcaserin were more likely to achieve at least 5% and 10% reduction in body weight compared with those given placebo (RR 2.16, 95%CI 1.69-2.75, $p < 0.00001$ and RR 2.65, 95%CI 2.08-3.36, $p < 0.00001$, respectively) (Figure 1). The risk of any adverse events was significantly greater with lorcaserin (RR: 1.10, 95% CI: 1.06-1.14, $p < 0.00001$). The common adverse events found more frequently in lorcaserin group were headache, upper respiratory infection, nausea, dizziness, and fatigue.

In summary, lorcaserin is effective in reducing body weight in overweight and obese adults. However, it may be associated with more adverse events. Further studies are needed to evaluate long-term safety of lorcaserin.

Table 1. Characteristics of three trials included in the meta-analysis.

Study (year)	N Lor:PB	Intervention	Duration	Subjects
Smith et al. (2009) ¹	116:118	lorcaserin 10 mg bid or placebo	12 weeks	Men and women between aged 18 and 65 and with BMI 30-45 kg/m ²
Smith et al.	1595:1587	lorcaserin 10 mg	2 years	Men and women aged 18 to 65

(2010) ²		bid or placebo		years and a BMI of 30 to 45 or of 27 to 45 with at least 1 coexisting condition (hypertension, dyslipidemia, cardiovascular disease, impaired glucose tolerance, or sleep apnea)
Fidler et al. (2011) ³	1602:1601	lorcaserin 10 mg bid or placebo	52 weeks	Men and women aged 18–65 yr with a body mass index between 30 and 45 kg/m ² or between 27 and 29.9 kg/m ² with an obesity-related comorbid condition

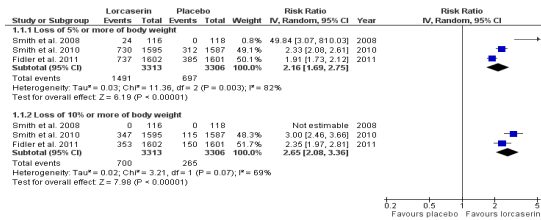


Figure 1. Meta-analysis of efficacy of lorcaserin versus placebo

References

1. Smith SR, et al. Lorcaserin (APD356), a selective 5-HT(2C) agonist, reduces body weight in obese men and women. *Obesity* 2009; 17: 494-503.
2. Smith SR, et al. Behavioral Modification and Lorcaserin for Overweight and Obesity Management (BLOOM) Study Group. Multicenter, placebo-controlled trial of lorcaserin for weight management. *N Engl J Med.* 2010; 363: 245-56.
3. Fidler MC, et al. A One-Year Randomized Trial of Lorcaserin for Weight Loss in Obese and Overweight Adults: The BLOSSOM Trial. *J Clin Endocrinol Metab* 2011; 96: 3067–77.

PP128

MELATONIN PROTECTS GLIOMA CELL AGAINST METHAMPHETAMINE -INDUCED APOPTOSIS THROUGH MITOCHONDRIAL DEATH PATHWAY

J. Tocharus^{1*}, P. Jumnonprakhon², P. Govitrapong³

¹ Department of Physiology, Faculty of Medicine, Chiang Mai University, Chiang Mai, Thailand, ² Department of Anatomy, Faculty of Medicine, Chiang Mai University, Chiang Mai, Thailand, ³ Research Center for Neuroscience, Institute of Molecular Biosciences, Mahidol University, Bangkok, Thailand

Methamphetamine (METH) is a highly addictive drug as a psychostimulant of the central nervous system (CNS). The direct interaction of METH with the CNS leads to the dopaminergic and serotonergic neuron dysfunction. Recently, have reported that the effects of METH to glial cells which are the supporting cells for the neuron, also play a role in the process of METH-induced cell injury. Previous studies demonstrated that METH could induce neuron and glial cell death, especially inducing glial cell- mediated neurotoxicity that plays a critical role in stress-induced CNS damage (1). Melatonin, a neurohormone synthesized by the pineal gland, has shown both antioxidative and anti-inflammatory effects via several mechanisms. Previous study demonstrated that melatonin attenuated METH toxicity and inhibited the expression of cytotoxic factor genes associated with ROS and RNS production in glial cells (2) Therefore, the aim of the present study is to investigate the molecular mechanisms underlying the effect of METH induced cell death in the glial cell and elucidated the role of melatonin in reducing this response. The antibodies; anti-Bax, anti-Bcl-X_L were from Millipore, Bedford, MA, USA). Melatonin was obtained from Sigma-Aldrich (St. Louis, MO).

Rat glioma (C6) cell lines were purchased from the American Type Culture Collection (ATCC, Mannassas, VA, USA)

Cell death was measured using FITC annexin V apoptosis detection kit (BD Bioscience, Canada). The percentage of apoptotic cells was calculated using DiVA software (FAC BIVA).

The expression of Bcl-X_L and Bax were determined by western blot analysis. The densitometry of each band was analyzed by using Image-J® software.

METH induced glial cells death in a concentration-dependent manner. METH also activates the up-regulation of the proteins relevant to apoptosis such as Bax and down-regulation of Bcl-X_L protein in cascade. Pre-treatment with melatonin effectively reduced glial cell death. Moreover, melatonin increased the Bcl-X_L/Bax ratio Therefore, these results demonstrated that melatonin could reduce the cytotoxic effect of METH by decreasing the mitochondrial death pathway activation in glial cells.

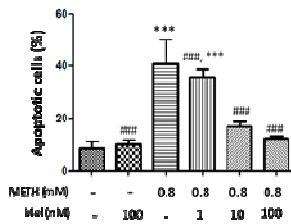


Fig1. The comparative results of the number of apoptotic cells by Flow cytometry.

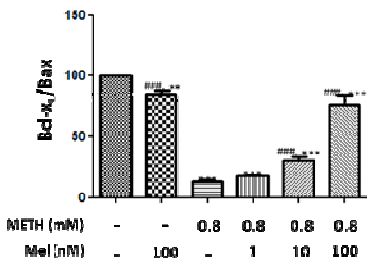


Fig.2 The expression of Bcl-X_L/Bax

Melatonin has a neuroprotective effect to glial cells.

This work was supported by a research grant from the Thailand Research Fund (TRF) and Faculty of Medicine, Chiang Mai University.

REFERENCES

3. Tocharus J, Khonthun C, Chongthammakun S, Govitrapong P (2010) Melatonin attenuates methamphetamine-induced overexpression of pro-inflammatory cytokines in microglial cell lines. *J Pineal Res* 48:347-352
4. Feng Z, Zhang JT (2004) Protective effect of melatonin on beta-amyloid-induced apoptosis in rat astrogloma C6 cells and its mechanism. *Free RadicBiolMed* 37:1790-1801

PP129

META-ANALYSIS OF THE EFFICACY AND SAFETY OF RIVAROXABAN FOR TREATMENT OF ACUTE SYMPTOMATIC DEEP VEIN THROMBOSIS

N. Poolsup^{1*}, N. Suksomboon², K. Wattanasopon¹, B. Kosumwisaisakul¹, P. Chaopantanon¹

¹. Faculty of Pharmacy, Silpakorn University, Nakhon-Pathom, Thailand

². Faculty of Pharmacy, Mahidol University, Bangkok, Thailand

* corresponding author: npoolsup@hotmail.com

Rivaroxaban is an orally active, direct factor Xa inhibitor. It is indicated for the prophylaxis of deep vein thrombosis (DVT) in patients undergoing knee or hip replacement surgery and has been used successfully in the treatment and prophylaxis of DVT and pulmonary embolism (PE). We performed systematic review and meta-analysis to assess the efficacy and safety of rivaroxaban 20 mg versus low molecular weight heparin (LMWH)/vitamin K antagonists (VKA) in the treatment of acute symptomatic DVT.

Clinical trials were identified through electronic search of MEDLINE, the Cochrane Library, CINAHL, Scopus, Web of Science, and clinicaltrial.gov up to February 2013. The reference lists of retrieved articles were also searched for relevant clinical trials. MeSH terms rivaroxaban and venous thrombosis were used. No language restriction was imposed. Studies were included in the meta-analysis if they were 1) randomized, controlled trials of rivaroxaban 20 mg daily compared with LMWH/vitamin K antagonists for acute symptomatic DVT, 2) reporting the efficacy in terms of symptomatic recurrent DVT, nonfatal PE, or venous thromboembolism (VTE) –related death. Treatment effects and adverse effects were expressed as odds ratio (OR). The inverse variance-weighted method was used for the pooling of OR and the estimation of 95% confidence interval. A random effects model was used when heterogeneity was significant at the level of 0.1, otherwise the fixed effects model was performed. The degree of heterogeneity was quantified using I-squared statistic. The statistical analysis was undertaken with RevMan version 5.2.6 (Cochrane collaboration). The significant level was set at $p < 0.05$.

Three trials met the inclusion criteria and contributed to the meta-analysis, involving 3883 patients evaluated for efficacy and 3946 for safety. Characteristics of these trials are shown in Table 1. The risk of symptomatic recurrent DVT was reduced by 54% with rivaroxaban (OR 0.46, 95%CI 0.26-0.83, $p = 0.01$). There were no significant differences between rivaroxaban and LMWH/VKA regarding nonfatal PE (OR 1.09, 95%CI 0.58-2.04) and VTE-related death (OR 0.82, 95%CI 0.25-2.66). (Figure 1) For safety profiles, no differences were detected in the risk of major bleeding (OR 0.74, 95%CI 0.39-1.42), clinically relevant nonmajor bleeding (OR 1.00, 95%CI 0.78-1.28) and death of any cause (OR 0.77, 95%CI 0.51-1.16).

In conclusion, rivaroxaban 20 mg daily may be more effective than conventional treatment in reducing recurrence of symptomatic DVT, while it was equally effective in reducing nonfatal PE and VTE-related death. It was comparably safe compared with conventional treatment.

Table 1. Characteristics of studies included in the meta-analysis.

Study	Duration	Study patients	Intervention (N)
-------	----------	----------------	------------------

ODIXa-DVT ¹	12 weeks	Patients with symptomatic acute thrombosis of the popliteal or more proximal veins	RX 10 mg bid (119) RX 20 mg bid (117) RX 30 mg bid (121) RX 40 mg OD (121) Enoxaparin/VKA (126)
EINSTEIN-DVT ²	84 days	Adult patients with acute symptomatic DVT	RX 20 mg OD (135) RX 30 mg OD (134) RX 40 mg OD (136) LMWH/VKA (137)
Acute DVT ³	12 months	Acute, symptomatic, objectively confirmed proximal DVT, without symptomatic pulmonary embolism	RX 20 mg OD (1731) Enoxaparin/VKA (1718)

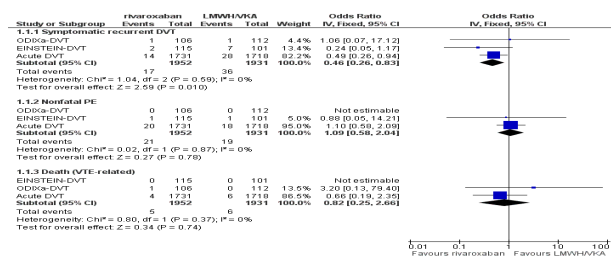


Figure 1. Meta-analysis of efficacy of rivaroxaban versus LMWH/VKA

References

1. ODIXa-DVT Study Investigators. Treatment of proximal deep-vein thrombosis with the oral direct factor Xa inhibitor rivaroxaban (BAY 59-7939): the ODIXa-DVT (Oral Direct Factor Xa Inhibitor BAY 59-7939 in patients with acute symptomatic deep-vein thrombosis) study. *Circulation* 2007;116:180-7.
2. EINSTEIN Investigators. Oral rivaroxaban for symptomatic venous thromboembolism. *N Engl J Med* 2010;363:2499-510.
3. Einstein-DVT Dose-Ranging Study investigators. A dose-ranging study evaluating once-daily oral administration of the factor Xa inhibitor rivaroxaban in the treatment of patients with acute symptomatic deep vein thrombosis: the Einstein-DVT Dose-Ranging Study. *Blood* 2008;112:2242-47.

PP130

DPPC:MPOx chimeric nanocontainers: the fractal sculpture of novel advanced drug delivery nano systems and drug release studies.

Maria Merkouraki,¹ Natassa Pippa^{1,2}, Stergios Pispas², Costas Demetzos^{1,*}

¹Department of Pharmaceutical Technology, Faculty of Pharmacy, National and Kapodistrian University of Athens, Athens, Greece

²Theoretical and Physical Chemistry Institute, National Hellenic Research Foundation, Athens, Greece

(*) Corresponding author: Prof. Costas Demetzos, Faculty of Pharmacy, Department of Pharmaceutical Technology, Panestimiopolis Zografou 15771, University of Athens, Athens, Greece; fax: 00302107274027; e-mail: demetzos@pharm.uoa.gr

In this work, we report on the self assembly behavior and on stability studies of chimeric systems consisting of DPPC (dipalmitoylphosphatidylcholine) and poly(2-methyl-2-oxazoline)-grad-poly(2-phenyl-2-oxazoline) (MPOx) gradient copolymer in Phosphate Buffer Saline (PBS). A gamut of light scattering techniques were used in order to extract information on the size and morphological characteristics of the nanoassemblies formed, as a function of gradient block copolymer content, as well as temperature. The colloidal stability of chimeric nanovectors and their thermoresponsive behavior indicates that these nanosystems are sterically stabilized nanocontainers (Kaditi et al., 2012; Pippa et al., 2013). DPPC:MPOx chimeric nanovectors were found to be effective nanocontainers for the incorporation of indomethacin (IND). The membrane micropolarity remains unaltered by the increase of MPOx content and decreased at 50°C. Incorporation of IND was achieved in these chimeric nanocarriers to an extent depending on lipid/gradient copolymer ratio and dispersion medium (Fig. 1.). The present studies show that there are a significant number of parameters that can be used in order to alter the morphology of chi-aDDnSs and this is advantageous to the design and the development of “smart” nanocarriers for drug delivery. The results presented highlight the existing potential for controlling the colloidal behaviour and the morphology of chimeric nanosystems in different media and conditions. In conclusion, the combination of gradient block copolymers with phospholipids for the development of novel chimeric nanovectors appears very promising, mostly due to the fact that the MPOx acts as a modulator for the release rate of IND.

References:

Kaditi, E., Mountrichas, G., Pispas, S., Demetzos, C., 2012. Block copolymers for drug delivery nano systems (DDnSs). *Curr. Med. Chem.* 19,5088-5100.

Pippa, N., Merkouraki, M., Pispas, S., Demetzos, C., 2013. DPPC:MPOx chimeric advanced Drug Delivery nanosystems (chi-aDDnSs): physicochemical and structural characterization, stability and drug release studies. *Int. J. Pharm.* 450,1-10.

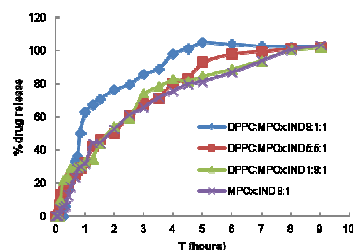


Fig. 1. Cumulative drug release from DPPC:MPOx: IND 9:1:1, 5:5:1, 1:9:1 and MPOx:IND 9:1 molar ratio. Mean of three independent experiments run in triplicate, SD<10%.

PP131

The interplay between the rate of release from advanced Drug Delivery nano Systems and their fractal morphology

Natassa Pippa^{1,2}, Aristides Dokoumetzidis¹, Stergios Pispas², Costas Demetzos^{1,*}

¹Department of Pharmaceutical Technology, Faculty of Pharmacy, National and Kapodistrian University of Athens, Athens, Greece

²Theoretical and Physical Chemistry Institute, National Hellenic Research Foundation

(*) Corresponding author: Prof. Costas Demetzos, Faculty of Pharmacy, Department of Pharmaceutical Technology, Panestimiopolis Zografou 15771, University of Athens, Athens, Greece; fax: 00302107274027; e-mail: demetzos@pharm.uoa.gr

The purposes of this study were to investigate the indomethacin (IND) release profile from Dipalmitoylphosphatidylcholine (DPPC) Poly(2-methyl-2-oxazoline)-grad-poly(2-phenyl-2-oxazoline) (MPOx) (9:0.1, 9:0.5, 9:1, 9:2 and 9:3 molar ratio) chimeric nanovectors, to examine the relevance of power law using these experimental release data, and to detect the relationship of the fractal dimension (d_f) of nanovectors with the fraction of the IND released. The fractal dimension of the chimeric nanovectors was determined by Static Light Scattering (SLS) during the release of IND from the nanocontainers and an increase of d_f values during the release of IND was observed. It is observed that the *in vitro* release of the drug from the prepared formulation from the chimeric nanostructures is quite fast especially for the mixed nanovectors prepared with the lower ratio of gradient block copolymer (Pippa et al., 2013). The fractal dimensions fell in the range from 2.18 to 2.47, depending on the molar ratio of MPOx component. It seems likely that the spatiotemporal variation in membrane permeability of the dynamically swelling MPOx polymer is close enough to the percolation threshold for non-classical diffusion effects to impinge on release kinetics. Additionally, we observed that there is a strong interplay between the morphology of the liposomes, as expressed by d_f values and the rate of release of IND from the chimeric nanovectors (Fig.1.). Namely, higher d_f values correspond to lower rates of release, while as the release progresses the morphology of the liposome is self-reassembled and d_f increases. A time delay is observed between each release snapshot and the corresponding change of d_f which reflects the time of reorganization of the morphology of the liposome (Fig.1). The release kinetics were studied by regression analysis of drug concentrations in fractal matrices with respect to time. A piece-wise power law function was fitted to the release data and the model parameters were estimated. Good fits were observed in all datasets analyzed, while distinct regions of different release rates corresponding to different d_f values were described. Each chimeric system of different fractal dimension exhibited a different release pattern of IND in which a trend of a decreased drug release rate with increasing fractal dimension was observed. In conclusion, the authors proposed that the fractal morphology of the chimeric nanocontainers affects the drug release and must be taken into account to develop liposomal drug with complete knowledge of their structural properties.

References

Pippa, N., Kaditi, E., Pispas, S., Demetzos, C., 2013. DPPC/poly(2-methyl-2-oxazoline)-grad-poly(2-phenyl-2-oxazoline) chimeric nanostructures as potential drug nanocarriers. J. Nanopart. Res. 15,1685.

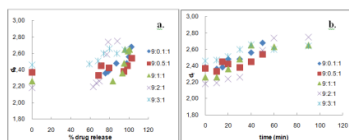


Figure 1. a. Fractal Dimension vs. % drug release and b. Fractal Dimension vs. time for DPPC:MPOx:IND nanosystems.

PP133

Comparison of ropivacaine concentrations during epidural infusion at fixed time intervals and continuous subcutaneous infiltration for postoperative pain relief

S.L.Markantonis¹, Melemeni A², M.Markidou¹, A.Fassoulaki²

¹Faculty of Pharmacy, University of Athens, Athens, Greece; ² Medical School, University of Athens, Athens, Greece

The aim of this study was to compare total plasma ropivacaine concentrations during epidural administration of the drug at fixed 6 hour time intervals and continuous subcutaneous infiltration of the wound for postoperative analgesia in patients undergoing enucleation of myomas or abdominal hysterectomy.

A total of 18 adult patients (ASA 1-2) were enrolled and randomly selected to receive either epidural (EP) (Group 1, n=8, median age 41(31-48) yr) or subcutaneous (SC) (Group 2, n=10, median age 44(32-54) yr) postoperative analgesia. After a 10ml 0.75% bolus dose, Group 1 patients were administered 10 ml of ropivacaine 0.2% every 6h via epidural catheter inserted at O3 - O4 and Group 2 ropivacaine 0.375% via a elastometric pump at 2 ml/h, both for 48 hours. Ropivacaine blood samples were collected before the bolus and at 2, 4, 8, 24, 48, 50, 60 and 72 hours; total plasma concentrations were measured using HPLC-UV.

In each group of patients significant interindividual variability in plasma ropivacaine levels was noted, as previously reported (1) (Figure 1). After administration of the bolus dose, the rate of entry of ropivacaine into the general circulation was found to be much slower after SC administration and a gradual increase in drug concentrations was observed only after 8 hours of continuous infusion reaching maximum concentrations (306 - 874 ng/mL) at the end of infusion, indicating that steady state was never achieved (Figure 1). In contrast, during EP administration the highest blood concentrations of ropivacaine were measured at 2 hours (240 - 377 ng/mL) and did not differ significantly from concentrations at 8 hours ($p = 0.927$) and 24 hours ($p = 0.977$), suggesting that concentrations had almost reached a plateau (Figure 1). Peak levels were in both cases below levels reported to be safe in adults (1.0-3.0 $\mu\text{g/mL}$). Although the rate of SC ropivacaine administration was more than double the average rate of EP administration, the SC/EP drug concentration ratios at 24 and 48 hours were 1.86 and 1.78 respectively, suggesting that the drug was possibly retained in adipose tissue around the wound.

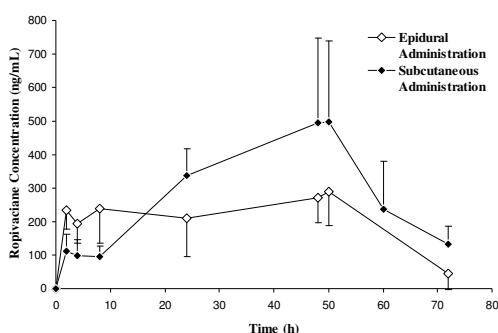


Figure 1: Ropivacaine concentrations (ng/mL) (mean \pm SD) following epidural and subcutaneous administration

In conclusion, plasma concentrations achieved after administration of ropivacaine via epidural catheter at fixed intervals and constant subcutaneous infiltration of the wound were found to be below levels reported to be safe. Further studies are needed to determine whether these modes of administration provide satisfactory pain relief compared with the conventional epidural administration by constant infusion.

Reference:

1. [Cusato M](#), [Allegrì M](#), [Niebel T](#), [Ingelmo P](#), [Broglia M](#), [Braschi A](#), [Regazzi M](#). Flip-flop kinetics of ropivacaine during continuous epidural infusion influences its accumulation rate. [European Journal of Clinical Pharmacology](#) 2010; 67(4):399-406.

PP134

POPULATION PHARMACOKINETICS OF MOSAPRIDE IN BEAGLE DOGS: SINGLE ORAL DOSE AND EFFECT OF FOOD INTAKE

Jung-Woo Chae ^a, In-Hwan. Beak ^b, Kwang-Il Kwon ^{a*}

^a. Chungnam National University, Daejeon, South Korea

^b. Kyungsoong University, Busan, South Korea

*E-mail address of corresponding author : kwon@cnu.ac.kr

The objectives of this study were to describe the population pharmacokinetics (PK) of mosapride in fasting and fed states. A single 5 mg oral dose of mosapride was administered to fasted (n=15) and fed (n=12) beagle dogs (Table. 1) and the plasma concentrations of mosapride were measured by LC-MS/MS. The resultant data were analyzed by modeling approaches using NONMEM (Nonlinear mixed effect models) 7.2. The plasma concentration time course of mosapride was described using one compartment model with first-order absorption and elimination. The model was evaluated by visual predictive check and bootstrap named internal validation to test the robustness and adequacy. The model building indicated that 1-compartment open PK model with first-order absorption with MTIME and first-order elimination was preferred over the other tested PK models based on Bayesian information criterion (Wen et al, 2013). The absorption rate constants of mosapride were significantly decreased under fed condition compared to that under the fasting condition (absorption rate constants in fasting and fed conditions; $1.276 \pm 0.174/\text{hr}$ and $0.131 \pm 0.000/\text{hr}$, $p < 0.001$). The observed bootstrap means were generally consistent with the population mean estimates. And, with the exception of some mosapride concentrations, most of observed data fell into the range between 5th to 95th percentiles of the simulated values (Post et al, 2008). Overall, the final model was able to describe the observed mosapride concentrations reasonably well (Fig. 1). These findings suggest that food intake affects both the rate and extent of absorption of mosapride, and that the pharmacological effect of mosapride can differ significantly according to food intake.

References

1. Post, T.M., Freijer, J.I., Ploeger, B.A., Danhof, M., 2008. Extensions to the visual predictive check to facilitate model performance evaluation. *J Pharmacokinet Pharmacodyn* 35, 185-202.
2. Wen, Y.G., Shang, D.W., Xie, H.Z., Wang, X.P., Ni, X.J., Zhang, M., Lu, W., Qiu, C., Liu, X., Li, F.F., Li, X., Luo, F.T., 2013. Population pharmacokinetics of blonanserin in Chinese healthy volunteers and the effect of the food intake. *Hum Psychopharmacol* 28, 134-141.

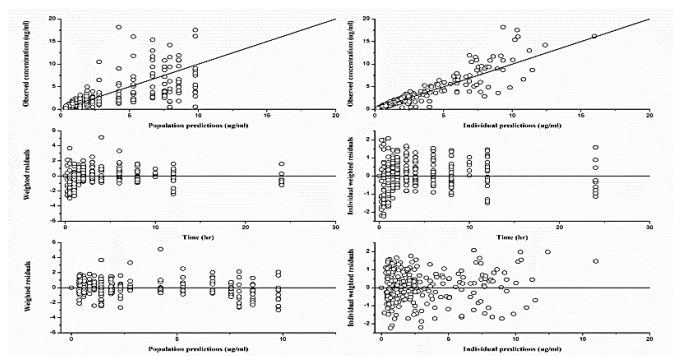


Figure 1.

Table 1

Demographic data	Age	Weight
Beagle dogs (n=27)	15 month	8.81-12.19 kg

PP135

PREDICTION OF PATIENT-SPECIFIC THERAPEUTIC ACTIVITY OF RADIOIODINE IN PATIENTS WITH GRAVES' DISEASE BASED ON POPULATION MODELLING OF TURNOVER FOLLOWING ADMINISTRATION OF DIAGNOSTIC ACTIVITY

D. Milosheska¹, I. Grabnar¹, E. Pirnat², P. Tomše², T. Gmeiner Stopar², S. Hojker²

¹Faculty of Pharmacy, University of Ljubljana, Ljubljana, Slovenia

²Department for Nuclear Medicine, University Medical Centre Ljubljana, Ljubljana, Slovenia

Correspondence to: iztok.grabnar@ffa.uni-lj.si

Radioactive I-131 is still considered the most cost-effective treatment of Graves' disease. Several clinical protocols for selection of therapeutic activity have been developed ranging from fixed activity to dosimetric approach based on I-131 uptake measurements and thyroid size. The alternative to complete thyroid destruction with high activity, which gives rapid control of hyperthyroidism but results in hypothyroidism demanding life-long thyroxine replacement, is patient specific selection of I-131 activity. The latter is preferable also from the radiation protection point of view. The aim of this study was to build a population model of I-131 turnover in the thyroid following administration of diagnostic and therapeutic activity and to evaluate, if therapeutic dose can be predicted from sparse measurements following diagnostic activity.

31 patients participated in this study. Uptake of diagnostic (6.5-8 MBq) and therapeutic (555, 740 or 925 MBq) activity in the thyroid was measured with scintillation and Geiger-Müller counter, respectively. Data were analysed with NONMEM using a one-compartment model. First-order absorption (K_a) and elimination (K_e) rate constants and fraction of the activity accumulated in thyroid (F) were estimated. Covariates tested were thyroid volume, patient's sex, weight and age, smoking status, endocrine ophtalmopathy, and levels of TSH, fT3 and fT4. Radioiodine turnover following administration of diagnostic and therapeutic activity was modelled simultaneously to assess the influence of administered activity on parameter values. The final model was used for Bayesian estimation of turnover parameters in individual patient based on diagnostic activity measurements at 2 and 24 h.

Mean (interindividual variability) parameter estimates of the base model for the therapeutic activity were 0.482 h^{-1} (CV=57.4%) for K_a , 0.00469 h^{-1} (CV=21.4%) for K_e and 0.841 (SD=0.232) for F . Residual variability was modelled using a combination error model ($\sigma_{\text{additive}}=10.7 \text{ MBq}$, $\sigma_{\text{proportional}}=3.02\%$). F was found to increase with the thyroid volume and was included in the final model using the following expression: $F=\theta_3 \cdot (1-\exp(\theta_4 \cdot \text{VOL}))$, where θ_3 and θ_4 are model parameters and VOL is thyroid volume. Parameters of the final model are summarised in Table 1. Visual predictive check of the final model is presented in Figure 1.

(Insert Table 1)

(Insert Figure 1)

Compared to diagnostic activity, K_a was 54.0% higher (CV=45.1%), K_e was 17.2% lower (CV=11.9%) and F was 6.3% lower (CV=56.7%) following administration of therapeutic activity. Mean error of the Bayesian predicted absorbed dose following administration of therapeutic activity was 7.2% with a root mean square error of 26.3%.

Absorbed dose ranged from 142 to 991 Gy. In the majority (71%) of patients the absorbed dose was higher than the targeted dose of 300 Gy. The study indicates that therapeutic dose can be reliably predicted from sparse measurements of diagnostic activity.

References

1. Areberg, J., Jönsson, H., Mattsson, S., 2005. Population biokinetic modeling of thyroid uptake and retention of radioiodine. *Cancer Biother. Radiopharm.* 20, 1-10.
2. Willegaignon, J., Sapienza, M.T., Buchpiguel, C.A., 2013. Radioiodine therapy for graves disease: thyroid absorbed dose of 300 Gy-tuning the target for therapy planning. *Clin. Nucl. Med.* 38, 231-236.

Table 1. Parameter estimates of the final radioiodine turnover model for therapeutic activity.

Parameter	Estimate	RSE (%)
θ_1, K (h^{-1})	0.468×10^{-2}	4.0
θ_2, K_a (h^{-1})	0.487	9.8
θ_3, F	0.916	3.9
$\theta_4, \text{VOL on } F$ (mL^{-1})	-0.0937	26.5
Interindividual variability		
K (CV%)	21.3	42.1
Ka (CV%)	57.5	27.9
F (SD)	0.114	29.8
Ka-F correlation	0.795	28.1
Residual variability		
Additive (MBq)	10.7	22.6
Proportional (%)	3.04	16.1

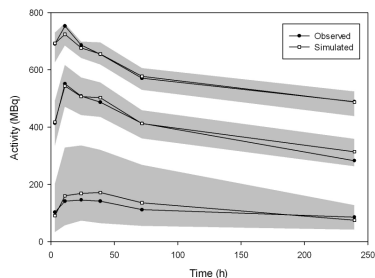


Figure 1. Visual predictive check of the final model for therapeutic activity. Median, 5th and 95th percentile of the observed and simulated data with 95% CI of the predictions (shaded).

PP136

ANTIVIRULENCE ACTIVITY OF FLAVONOIDS

L Mebarki*, M Kaid Harche

University of Sciences and Technology, Mohamed Boudiaf, Oran, Algeria

*Corresponding author. E-mail address: mebarki76@yahoo.fr

Medicinal plants represent a rich source of antimicrobial agents. Plants are used medicinally in different countries and are a source of many potent and powerful drugs. Using extracts from plants containing natural antifungal compounds for plant disease control is considered to be one of the desirable methods for plant protection in agriculture. The aim of this study was therefore to evaluate the effect of flavonoid extracts derived from some medicinal plants on the virulence of *Fusarium oxysporum* f. sp. *albedinis* (Foa) (The causal agent of vascular wilt of date palm).

In this study flavonoid extracts (from leaves of *Anvillea radiata*, *Bubonium graveolens* and *Cotula cinerea*, harvested from the area of Bechar, southwest of Algeria) were prepared as described by Lee et al. (1995), and the virulence assay was carried out as described by Herrmann et al. (1996) (with slight modification) using potato tuber tissue technique with different quantities of flavonoid extracts (0.25, 0.5, 0.75 and 1 mg). After 7 days of incubation in the dark, the necrotic tissues were weighted and the results were compared to the virulence of Foa (potatoes slice without plant extracts) as relative virulence (RV).

The results indicated that necrotic lesions were visible compared with the slices without Foa culture. The relative virulence of Foa on potato tuber tissue without plants extracts was 100% (518 mg of necrotic tissue weight). 83.33% of tests showed a decrease in the RV of Foa on potato tuber tissue compared to Foa virulence with no additions, and only 16.66% of tests revealed RV superior to Foa. The maximum value of relative virulence was exhibited by *Anvillea radiata* extracts at 0.25 mg (RV= 114.6% with 0.59 g of necrotic tissue weight), but the minimum relative virulence presented by *Cotula cinerea* extracts at 1 mg (RV= 72.3% with 0.37 g of necrotic tissue weight).

Table 1

Effect of flavonoids extracts on relative virulence of Foa.

Plant Species	Flavonoid extract quantity on potato slices (mg)							
	0.25		0.5		0.75		1	
	NTW	RV	NTW	RV	NTW	RV	NTW	RV
<i>C. cinerea</i>	0.45	86.8	0.41	79.15	0.377	72.7	0.37	72.3
<i>B. graveolens</i>	0.54	105.4	0.49	94.5	0.44	86.29	0.39	77
<i>A. radiata</i>	0.59	114.6	0.47	91.5	0.39	76.44	0.40	78.76

NTW: Necrotic tissue weight (g). RV: Relative virulence (%).

from these results it can be concluded that the use of flavonoid extracts could be considered as an antifungal available to develop novel types of natural fungicides and to control several plant pathogenic fungi.

References:

- Herrmann, M., Zoicher, R., Haese, A., 1996. Enniatin production by *Fusarium* strains and its effect on potato tuber tissue. *App. Environ. Microbiol.* 62 (2), 393-398.
- Lee, Y., Howard, L.R., Villalon, B., 1995. Flavonoids and antioxidant activity of fresh pepper (*Capsicum annuum*) cultivars. *J. Food. Sci.* 60 (3), 473-476.

PP137

PHARMACOKINETIC/PHARMACODYNAMIC MODELING OF TRIFLUSAL IN IMMEDIATE-RELEASE AND ENTERIC-COATED CAPSULE FORMULATIONS

Byung-yo Lee ^a, Jooyoung Chae ^b, Hwi-yeol Yoon^a, Jung-woo Chae ^a, Kwang-il Kwon ^a

^aChungnam National University, Daejeon, Korea

^bMinistry of Food and Drug Safety, Chungcheongbuk-do, Korea

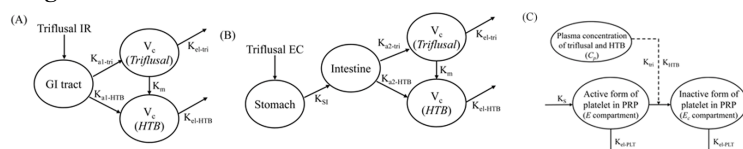
The objectives of this study were to compare the pharmacokinetics / pharmacodynamics of triflusal enteric-coated capsule with triflusal immediate release capsule after 9 days of dosing in healthy Korean male subjects using a compartmental modeling approach. 32 healthy Korean male volunteers were recruited for the PK/PD modeling of triflusal and its active metabolite HTB. All subjects received a single 900 mg oral loading dose on day 1, followed by seven 600mg/day maintenance doses (two 300 mg capsules once daily) on days 2-8. In day 9, triflusal 900mg was administered to the subject group as a last maintenance dose. The time courses of the plasma concentrations of active agents and the platelet aggregation effects were analysed using ADAPT V. The plasma concentration versus time profiles of triflusal and HTB were fitted simultaneously to a parent-metabolite compartmental model with first-order absorption and elimination. The absorption phase of EC formulation was described by first-order gastric emptying rate of enteric-coated pellets in the intestine, and first-order absorption of the drug after being released from the pellets. The PD effects of the triflusal were fitted to platelet aggregation effect model.

These PK/PD model describe the change of PK/PD and relationship between plasma concentrations and anti-platelet effect for triflusal IR capsule and ER capsule successfully. The estimated PK parameters were well explained characteristics of absorption, distribution, metabolism and elimination of the agents and have good correlations on platelet characteristics, such as platelet half life and platelet aggregation effect.

Table 1. Non-compartmental pharmacokinetic parameters of triflusal and HTB following administration of two formulations of triflusal

Parameter (unit)	Immediate release capsule	Enteric-coated capsule
Triflusal		
C _{max} (µg/mL)	17.20 ± 7.19	5.78 ± 2.81
T _{max} (h)	0.86 ± 0.50	2.84 ± 1.22
AUC _{last} (µg·h/mL)	29.51 ± 10.90	16.77 ± 6.76
Cl _r /F (L/h)	27.73 ± 10.10	53.60 ± 21.09
λ _z (h ⁻¹)	0.776 ± 0.475	0.327 ± 0.188
t _{1/2} (h)	1.82 ± 2.71	3.13 ± 2.37
Metabolite (HTB)		
C _{max} (µg/mL)	254.00 ± 63.69	272.07 ± 67.61
T _{max} (h)	4.13 ± 4.27	6.75 ± 4.12
AUC _{tau} (µg·h/mL)	4358.49 ± 905.93	5301.41 ± 1117.77
Cl _r /F (L/h)	0.215 ± 0.045	0.178 ± 0.043
λ _z (h ⁻¹)	0.021 ± 0.015	0.022 ± 0.012
t _{1/2} (h)	77.43 ± 108.27	56.11 ± 61.85

Figure 1. Model schemes for PK/PD characterization of the triflusal



References

1. McNeely W, Goa KL (1998). Triflusal. *Drugs* 55(6):823-833; discussion 834-825.
2. Bertrand J, Laffont CM, Mentre F, Chenel M, Comets E (2011). Development of a complex parent-metabolite joint population pharmacokinetic model. *The AAPS journal* 13(3):390-404.

PP138**THE COMPARISON OF ANTI-PLATELET EFFECTS OF KOREAN HERBAL MEDICINE AND THOSE OF BIOTRANSFORMED ONE ON HUMAN PLATELET.**B. Song¹, S. Hwang¹, B. Lee¹, H. Baek¹, J. Chae¹, K. Kwon¹.¹Chungnam National University, Daejeon, Korea.

This study was performed to elucidate which microorganism enhanced anti-platelet effect of Korean herbal medicine, Pyeong-wi-san (PW) and O-lyeong-san (OL).

Two Herbal medicines, PW and OL, were composed of 6, 5 herb, respectively. To transform these herbal medicines to fermented one, 16 species of *Lactobacillus* were used. Human washed platelet were prepared to measure platelet aggregation using Aggregometer (570VS, Chrono-log, Haverston, PA, USA) by optical method. Collagen (4 µg/mL) was added as a stimulant. WinNonlin (Pharsight Corporation Inc., CA, USA) and Excel (Microsoft, Redmond, WA, USA) was used to assess measured data.

OL was not enhanced by fermentation. However, anti-platelet effect of PW, which was fermented by *Lactobacillus acidophilus* (PW-341), *Lactobacillus bulgaricus* (PW-673) was increased 15.28% (p<0.05), 35.39% (p<0.01), respectively. E_{max} and EC₅₀ value of PW-341 and PW-673 was 66.45 % and 90.26 µg/mL and 84.68 % and 150.61 µg/mL, respectively. Biotransforming technique by lactobacillus species could enhance anti-platelet effect of Korean herbal medicine. A further study could be performed to develop PW as an adjuvant and these results could be used other herbal medicine study.

References

1. Born G, Cross M., 1963, The aggregation of blood platelets, J Physiol. 168, 178-195
2. Son C, et al., 2011, Anti-platelet aggregation study of fermented galgeun tang and fermented ssanghwa tang. Yakhak Hoeji. 55(5), 374-378

Figure and Tables

Table 4. Ingredients and weight of PW and OL

Ingredients	Weight (g)
PW	
Glycyrrhizae radix	2.4
Zingiberis rhizome	1.49
Zizyphi fructus	2
Aurantii nobilis pericarpium	5.6
Atractylodis rhizome	8
Magnoliae cortis	4
OL	
Atractylodis rhizome alba	6
Hoelen	6
Alismatis rhizome	10
Cinnamomum cassia	2
Polyporus	6

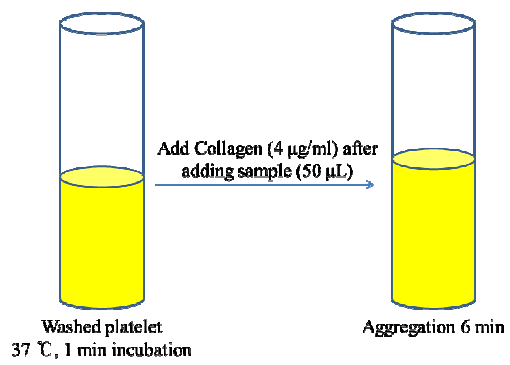


Figure 2. Procedure of optical method using washed platelets.

PP139

Pharmacokinetic interaction study of Olanzapine and its major Metabolites with a Propolis.

Hyun-moon Back^a, Jung-woo Chae^a, Byung-jung Song^a, Kwang-il Kwon^{a*}

^a. Chungnam National University, Dajeon, Korea,

This study conducted to investigate the potential of a pharmacokinetic interaction between olanzapine and propolis (Prior and Baker 2003).

For the in vivo PK interaction study, SD rats were selected and divided to control and test (low, high) group (n=4, each group). Test group received propolis (low, high) for 3 days (tab. 1), while control group received water for 3 days. In third day, all groups received olanzapine (30mg/kg) and plasma samples were obtained up to 24 hr after dosing. Concentration of OLZ and N-DMO in rat plasma was measured by LC-MS/MS (fig. 1) and pharmacokinetic parameters were analyzed by WinNonlin software (Jan et al, 2005).

Table 5. Test groups of study

	Control	Low	High
Olanzapine (mg/kg)	30	30	30
Propolis (mg/kg)	-	100	300

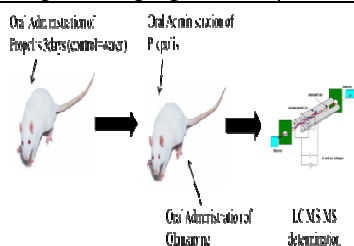


Figure 3. Experimental protocols of study

Following concomitant administration with propolis, pharmacokinetic aspect of OLZ and N-DMO were changed. As results of noncompartmental analysis, C_{max} and $AUC_{0 \rightarrow \infty}$ of olanzapine were increased while C_{max} and $AUC_{0 \rightarrow \infty}$ of N-DMO were decreased.

The effects of propolis on OLZ and N-DMO metabolism were confirmed by significant changing of pharmacokinetic parameters. These results showed that co-administration of OLZ and propolis could be changing the pharmacokinetic parameters of OLZ and N-DMO. And this interaction between OLZ and propolis should be considered and investigated in clinical situations. In addition, co-administration of propolis with another CYP1A2 substrate should be more concerned.

References

Prior, I, Trevor., Baker, B, Glen., 2003. Interactions between the cytochrome P450 system and the second-generation antipsychotics. *J Psychiatry Neurosci.* 28, 99-112.

Jan, W.C., Lin, L.C., Chieh-Fu-Chen., Tsai, T.H., 2005. Herb-drug interaction of *Evodia rutaecarpa* extract on the pharmacokinetics of theophylline in rats. *J Ethnopharmacol.* 102, 440-445

Corresponding author. Email: kwon@cnu.ac.kr

Keyword: Olanzapine, Propolis, Drug interactions, pharmacokinetics

PP140

STUDY FOR DRUG-DRUG INTERACTION IN THE TREATMENT OF CHRONIC DISEASE

Jung-Woo Chae ^a, Hyun-Moon Beak ^a, Byung-Jeong Song ^a, Byung-Yo Lee ^a, Ho-II Kang ^b, Kwang-II Kwon ^{a*}

^a. Chungnam National University, Daejeon, South Korea

^b. Ministry of Food and Drug Safety, Osong, South Korea

*E-mail address of corresponding author : kwon@cnu.ac.kr

The objectives of this project were to study interaction of chronic disease drugs with health-supplements for safe use of drug in chronic disease patient. Among the many candidate of health-supplements that had a possibility of drug interaction with chronic disease drug, propolis was selected. Cocktail assay confirmed that propolis inhibited the CYP1A2 isozyme. And, we selected duloxetine as a substrate of CYP1A2, for interaction study with propolis. Membrane permeability, transporter and CYP inhibition test were conducted for in vitro mechanism study of both material's interaction. For the in vivo PK interaction study, change of PK parameters in control group (only duloxetine administration) and test group (duloxetine and propolis concomitant administration) were compared and for the PK study, change of static, dynamic parameters in control group and test group were compared by forced-swimming test (Midorikawa et al, 2001). In study of membrane permeability, concomitant treatments of propolis (1, 10, 50 µg/ml) with duloxetine (50 µM) reduce apparent permeability coefficient (P_{app}) compared with only treatment of duloxetine (Fig. 1, Table. 1). And, in study of transporter, concomitant treatments of propolis (1, 10, 50 µg/ml) with duloxetine (1, 5 µM) inhibit the p-glycoprotein (p-gp). The clearance of duloxetine was significantly decreased and area under concentration-time curve, C_{max} , half-life was increased in propolis pretreatment when duloxetine was given (Chae et al, 2012). In Pharmacodynamic study, there is no significant difference between control and test group. Based on these results, chronic use of propolis could increase the concentration of duloxetine in vivo.

References

1. Midorikawa, K., Banskota, A.H., Tezuka, Y., Nagaoka, T., Matsushige, K., Message, D., Huertas, A.A., Kadota, S., 2001. Liquid chromatography-mass spectrometry analysis of propolis. *Phytochem Anal* 12, 366-373.
2. Chae, J.W., Baek, I.H., Kwon, K.I., 2012. Effect of decursin on the pharmacokinetics of theophylline and its metabolites in rats. *J Ethnopharmacol* 21, 248-254.

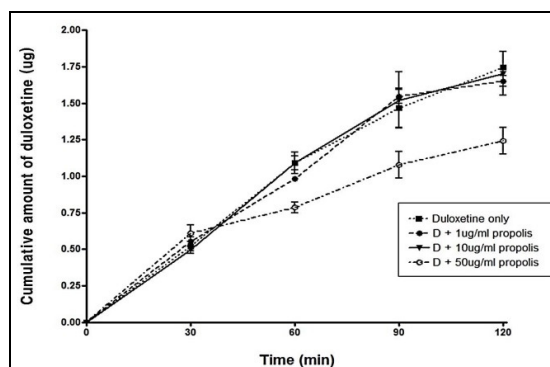


Figure. 1

Table 1

Compound	P_{app} ($\times 10^{-6}$ cm/s)
Duloxetine 50uM	15.0 ± 0.00
Duloxetine 50uM + propolis 1ug/ml	$14.0 \pm 0.52^*$
Duloxetine 50uM + propolis 10ug/ml	$14.3 \pm 0.29^*$
Duloxetine 50uM + propolis 50ug/ml	$11.0 \pm 1.04^{**}$

PP142

Sensitive HPLC Method for the Determination of Usnic Acid in Tablets

V. Tadic¹, S. Djordjevic¹, A. Zugic¹, I. Arsic², A. Bogdanovic³, I. Homsek⁴

¹Institute for Medicinal Plant Research "Dr Josif Pančić", Belgrade, Serbia

²University of Niš, Faculty of Medicine, Niš, Serbia

³University of Belgrade, Faculty of Technology and Metallurgy, Belgrade, Serbia

⁴Galenika ad, Belgrade, Serbia

Quality control of the product containing herbal extracts is a tedious and difficult job, because sometimes, singularly or in combinations, they contain a myriad of compounds in complex matrices in which the single active constituent, responsible for the overall efficacy, should be recognized. The aim of this study was to develop a sensitive HPLC method for determination of usnic acid in tablets containing the following extracts: *usneae barbatae extractum siccum*, *origani extractum siccum*, *satureae extractum siccum* and *siderites extractum siccum*.

Usnic acid assay in the tablets was analyzed by reversed-phase HPLC with a photodiode array detector at 325 nm. An Agilent Technologies XDB-C18 (100 x 4.6 mm; 1.8µm) column was the stationary phase; mobile phase was aqueous 0.1% acetic acid and acetonitrile gradient at flow rate of 0.10 ml/min. The temperature was held constant at 25°C. The retention time of usnic acid was approximately 42.3 min. The injection volume was 4µl. Validation experiments were performed to demonstrate system suitability, selectivity, linearity, accuracy and precision. System suitability test was performed by injecting five consecutive 4-µl portions of the standard solution into the instrument, recording the chromatograms and reading usnic acid peak areas. Chromatograms of the tested and placebo solutions were recorded in order to test the method selectivity. A series of usnic standard solutions in the concentrations ranging from 0.0005 to 0.0112 mg/ml level were prepared to define its linearity. Accuracy for the usnic acid assay is determined by applying the method in triplicate samples of mixture of placebo to which a known amount of usnic acid standard is added at different concentrations (80%, 100% and 120%). The analytical method precision was studied by analysis of multiple sampling of homogeneous sample.

The method system suitability of RSD=0.58% confirmed its repeatability. The interferences between the tested and placebo solutions were not detected at usnic acid retention time which confirmed the selectivity of the method. The linearity over the concentration range of 3.7-11.2 µg/ml was verified since the correlation coefficient was greater than 0.995. Accuracy was confirmed and recoveries were within 99-101%. The precision of the method was verified (RSD and recovery were 1.33 and 100.1%, respectively). Intraday and interday precision were in the requested range (99.44 and 100.04%, respectively).

The developed HPLC method can be used for determination of usnic acid in the tested tablet formulation due to its sensitivity and precision of performance.

References

1. Xiuhong J; Ikhlas KA. Quantitative determination of usnic acid in usnea lichen and its products by reversed-phase liquid chromatography with photodiode array detector, J. AOAC Int, 2005, vol 88, 1265-1268.
2. <http://www.pharmainfo.net/reviews/chromatographic-fingerprint-analysis-herbal-medicines-quality-control-tool>

DETERMINATION OF TIROFIBAN IN SERUM USING LIQUID CHROMATOGRAPHY WITH UV DETECTION

M. Darkovska-Serafimovska^{1,5}, Z. Arsova-Sarafinovska², T. Balkanov³, I. Gjorgoski⁴, N. Ugresic⁵, E. Janevik-Ivanovska¹

^{1,5} University Goce Delcev, Faculty of Medical Sciences, Krste Misirkov bb, 2000 Stip, Macedonia

² Institute for Public Health of the Republic of Macedonia, 50 Divizija 6, 1000 Skopje, Macedonia

³ University Ss. Cyril and Methodius, Faculty of Medicine, 50 Divizija 6, 1000 Skopje, Macedonia

⁴ University Ss. Cyril and Methodius, Faculty of Natural Sciences and Mathematics, Gazi Baba bb, 1000 Skopje, Macedonia

⁵ University of Belgrade, Faculty of Pharmacy, Vojvode Stepe 450, 11221 Belgrade, Serbia

The aim of this study is to develop a specific, sensitive, rapid, and simple HPLC method with UV detection to study pharmacokinetics of tirofiban in serum of rats alone or in the presence of heparin as simultaneous therapy. Thirty six Wistar rats were used randomly assigned in two groups: control group ($n = 18$), and group with venous thrombosis experimentally induced by ligation of the femoral vein ($n = 18$). Tirofiban hydrochloride was dissolved in sterile saline. The *i.v.* bolus doses (0.6 mg kg^{-1} ; 0.8 mg kg^{-1} ; 1 mg kg^{-1}) were injected using tail vein. Blood samples were taken in the presence of heparin during one hour: starting 15 minutes after injection in the intervals of 15 minutes. Tirofiban concentration was analysed immediately. Blood samples were centrifuged 5 min at $3500 \text{ rpm min}^{-1}$. The serum was treated carefully, then methanol was added for precipitation of proteins (in ratio serum: methanol = 1:3). The tubes were again centrifuged 5 min at $3500 \text{ rpm min}^{-1}$ and supernatant was injected into the HPLC column. HPLC separation was carried out at ambient temperature, using reversed-phase LiChrospher[®] 100 RP-18 column ($4.0 \text{ mm} \times 250 \text{ mm}$, $5 \mu\text{m}$ particle size). The chromatographic separation was performed by isocratic mode with of $0.1 \text{ M KH}_2\text{PO}_4$ ($\text{pH} = 5.0$, adjusted with 1.0 N sodium hydroxide) and acetonitrile in the ratio of $80:20 \%$ *v/v* as mobile phase with a flow rate of 1.0 ml min^{-1} . UV detection was performed at 274 nm . The injection volume was $50 \mu\text{l}$. Tirofiban concentration was also determined in spiked human and rat serum samples. System suitability was checked by evaluating different parameters (retention time, tailing factor, capacity factor, resolution, and selectivity). Tailing and capacity factors were obtained as 1.17 and 2.41 for tirofiban. Resolution factor for the system for tirofiban and heparin was 3.90. The retention times of tirofiban in methanol, human and rat serum samples were 9.1, 9.2, and 9.16 min, respectively (Figure 1.). The variation in retention time of tirofiban among five replicate injections of standard solution in methanol, human and rat serum samples was very little, giving relative standard deviations (RSD%) of 0.61%, 0.93%, and 0.82%, respectively. The response was linear over the range of $0.03 - 0.18 \text{ mg mL}^{-1}$ in mobile phase and serum samples. The limit of detection (LOD) for tirofiban was 1.84, 13.8 and $14.6 \mu\text{g mL}^{-1}$ in methanol, spiked rat serum and spiked human serum, respectively (Table 1.). Plasma concentration-time profile obtained from the experimental group was significantly different from plasma concentration-time profile obtained from the control group. The proposed RP-HPLC method is simple, accurate, precise, and rapid for the determination of tirofiban in serum and for monitoring its concentration in serum. The described method can be readily applied, without any interference from endogenous substances, to study pharmacokinetics of tirofiban in serum given alone or in the presence of heparin as simultaneous therapy and for therapeutic monitoring of levels of tirofiban in serum samples.

Table 1. Characteristics of the linear regression analysis of tirofiban

	Methanol	Human Serum	Rat serum
Linearity range (mg mL^{-1})	0.03–0.18	0.03–0.18	0.03–0.18
Slope	9200223	7942560	8795042
Intercept	2720.6	90750	23999
Determination coefficient (R^2)	0.9999	0.9943	0.9949
SE ^a of the intercept	5124.18	35082.2	36834.2
SE of the slope	43838.91	300276.9	315271.9
Detection limit (mg mL^{-1})	0.00184	0.0146	0.0138
Quantification limit (mg mL^{-1})	0.0056	0.0442	0.0419

^aSE – Standard error

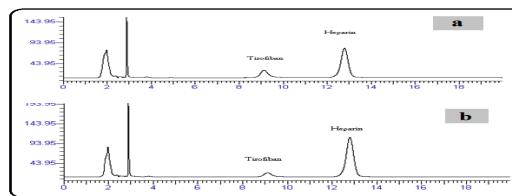


Figure 1. Chromatogram of standard solution of tirofiban and heparin in methanol (a) and chromatogram of serum spiked with tirofiban and heparin (b)

References

Oertel R, Köhler A, Koster A, Kirch W., Determination of Tirofiban in human serum by liquid chromatography-tandem mass spectrometry, *J Chromatogr B Analyt Technol Biomed Life Sci.* 2004 Jun 5;805(1):181-5.

PP145

A comparative in silico and in vitro study of drug – cytochrome P450 interactions: classic, atypical and novel antipsychotics

Jacek Wójcikowski*, Agnieszka Basińska, Anna Haduch, Maria Paluchowska, Władysława Anna Daniel

Institute of Pharmacology, Polish Academy of Science, 31-343 Kraków, Poland

The research was aimed at evaluating the usefulness of an in silico study for the estimation of drug-cytochrome P450 interactions of novel antipsychotics, 5HT-6 receptor antagonists with procognitive properties.

The following metabolic studies were carried out: (1) an in silico prediction of drug interactions (substrates and/or inhibitors) between main cytochrome P450 drug-metabolizing isoenzymes using the ADMET Predictor program (Simulations Plus, Inc, Lancaster, CA, USA); (2) an in vitro study into drug metabolism and enzyme inhibition in human liver microsomes; (3) an in vitro study into drug metabolism using human cDNA-expressed cytochrome P450 isoenzymes (CYP1A2, CYP2C9, CYP2C19, CYP2D6 and CYP3A4). The following antipsychotics were tested: classic phenothiazines (chlorpromazine, levomepromazine, perazine, thioridazine), atypical neuroleptics (clozapine, olanzapine, risperidone, ziprasidone) and novel antipsychotics (developed at our Institute).

The in silico study indicated that CYP1A2 (except perazine), CYP2D6 and CYP3A4 are the main enzymes involved in the oxidative metabolism of phenothiazines. Inhibition of both CYP2D6 and CYP2C9/19 and CYP3A4 was also suggested for most phenothiazines. The in vitro results were consistent with the majority of those predictions, but they did not confirm CYP2C or CYP3A4 inhibition and additionally showed perazine metabolism by CYP1A2 and CYP1A2 inhibition by this neuroleptic (Wójcikowski et al., 2010). As to atypical neuroleptics, a fairly good agreement between the in silico-predicted and the in vitro-found contribution (or inhibition) of cytochrome P450 isoenzymes (CYP1A2, CYP2D6, CYP3A4) to their metabolism was observed (Shin et al., 1999). In particular, a fair agreement was reported for CYP2D6 regarding both contribution and inhibition. The only exception was ziprasidon, for which the in silico test predicted contribution of many cytochrome P450 isoenzymes to its metabolism in addition to CYP3A4 found in vitro. Moreover, the in vitro study did not confirm the in silico results, which suggest CYP1A2 inhibition by clozapine, olanzapine and ziprasidon, or CYP2C9 and CYP2C19 inhibition by olanzapine. In the case of novel antipsychotics, their CYP1A2 inhibition found in vitro was not predicted in silico. On the other hand, some instances of in silico-suggested inhibition of other isoenzymes were not observed in vitro.

A comparison of the in silico with the in vitro study indicates the usefulness of the in silico test for predicting cytochrome P450 isoenzyme metabolism and inhibition by novel antipsychotics. However, the method of predicting drug interactions (substrates or inhibitors) with CYP1A2 or CYP2C isoenzymes still needs to be improved.

This study was supported by the project “Prokog”, UDA-POIG.01.03.01-12-063/09-00, co-financed by the European Union from the European Fund of Regional Development (EFRD).

References:

1. Shin, J.G., Soukhova, N., Flockhart, D.A., 1999. Effect of antipsychotic drugs on human liver cytochrome P-450 (CYP) isoforms in vitro: preferential inhibition of CYP2D6. *Drug Metab. Dispos.* 27, 1078-1084.
2. Wójcikowski, J., Boksa, J., Daniel, W.A., 2010. Main contribution of the cytochrome P450 isoenzyme 1A2 (CYP1A2) to N-demethylation and 5-sulfoxidation of the phenothiazine neuroleptic chlorpromazine in human liver – A comparison with other phenothiazines. *Biochem. Pharmacol.* 80, 1252-1259.

*Corresponding author. Email address: wojcikow@if-pan.krakow.pl

PP146

Analysis of the relationship between plasma inorganic mercury concentration and 4-indoxyl sulfate: A Pharmacokinetic/Pharmacodynamic modeling approach

K. Noh¹, J. Park¹, E. Kim², H. Kim³, O. Bae⁴, T. Jeong¹, W. Kang^{1*}

¹.Yeungnam University, Kyungbook, South Korea

².Chung-Ang University, Seoul, South Korea

³.SungKyunKwan University, Kyungkido, South Korea

⁴.Hanyang University, Kyungkido, South Korea

*Corresponding author

E-mail address : wonkuk@yu.ac.kr

Although a couple of physiologically based pharmacokinetic models for mercury have been reported, little is known about the quantitative relationship between systemic exposure of mercury and toxicodynamic biomarkers representing renal injury. This study therefore investigated the time course of plasma mercury concentrations and the change of 3-indoxyl sulfate (3-IS), a uremic toxin, in adolescent rats by using a pharmacokinetic/ pharmacodynamic modeling approach.

The first dose of mercuric chloride (HgCl₂) were orally given at the doses of 0.406 and 4.06 mg/kg, and then it was administrated at the doses of 0.203 and 2.03 mg/kg once every other day for 3-week in 4-week old rats. Blood samples were taken via jugular vein immediately before and 0.5, 3, 8, 12, 24, 48, 144, 240, 288, and 336 h after the first administration of mercuric chloride. Plasma mercury concentrations and 3-IS were measured using automatic mercury analyzer and HPLC-UV, respectively. The mean concentrations of these were fitted using ADAP5 software package (D'Argenio and Schumitzky, 2009). The model parameters were estimated by simultaneous regression, and maximum likelihood estimation was performed assuming that the measurement error has a standard deviation which is a linear function of the measured quantity.

Plasma concentrations of mercury were best described using a 1-compartment model with first-order absorption and elimination (Fig. 1). Estimated pharmacokinetic and pharmacodynamic parameters were shown in Table 1. Estimated k_a , k_{el} and V/F were 4.12 h^{-1} , 0.03 h^{-1} and 1.41 L , respectively. It means orally given HgCl₂ was rapidly absorbed while absorbed mercury was eliminated very slowly in rats (Morcillo and Santamaria, 1995). Pharmacokinetic parameters were estimated precisely within 8.1 % except k_a . The change of 3-IS was well explained using indirect response model with stimulation of 3-IS production by mercury. Estimated k_{in} , EC_{50} and E_{max} were $2 \text{ ng} \cdot \text{ml}^{-1} \cdot \text{h}^{-1}$, $2 \text{ ng} \cdot \text{ml}^{-1}$ and 8.2, respectively.

This work is for the first time to reveal the quantitative relationship between plasma mercury concentrations and the increase of 3-IS, a kidney injury marker, and may provide a better prediction of renal toxicity corresponding to the mercury exposure.

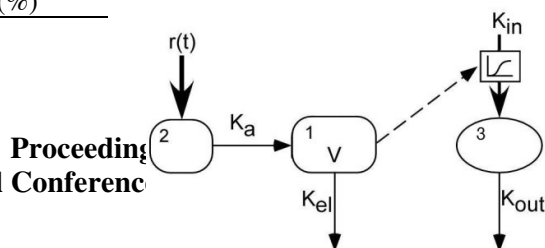
Reference

D'Argenio, D.Z., Schumitzky, A., 2009. ADAPT 5 User's Guide: Pharmacokinetic/Pharmacodynamic Systems Analysis Software. Biomedical Simulations Resource, Los Angeles.

Morcillo, M.A., Santamaria, J., 1995. Whole-body retention, and urinary and fecal excretion of mercury after subchronic oral exposure to mercuric chloride in rats. *Biometals*. 8, 301-308.

Table. Pharmacokinetic and pharmacodynamic parameters after repeated oral administration of HgCl₂ in rats

Parameter	Estimates	CV (%)
$k_a \text{ (h}^{-1}\text{)}$	4.12	67.1
$V/F \text{ (L)}$	1.41	8.1



k_{el} (h^{-1})	0.03	7.3
k_{in} ($ng \cdot ml^{-1} \cdot h^{-1}$)	2	31.1
EC_{50} ($ng \cdot ml^{-1}$)	268	40.2
E_{max}	8.2	41.3

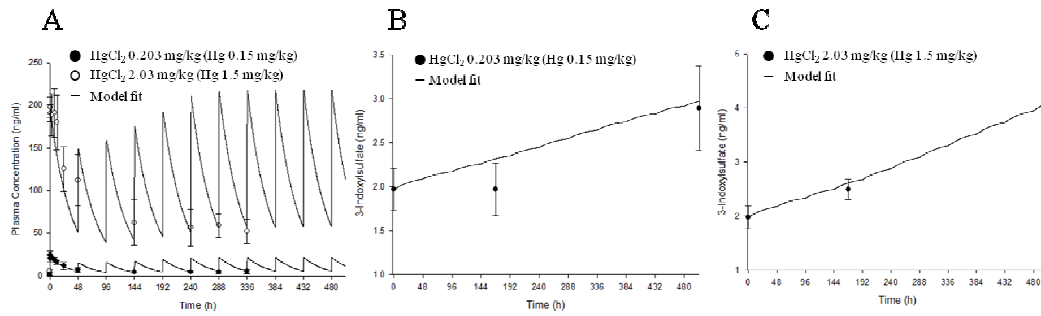


Figure. Measured (open and closed circles) and predicted (solid line) mercury (A), and 3-IP (B, C) concentration following repeated oral administrations of 0.203 and 2.03 mg/kg HgCl₂ in rats.

PP148

Pharmacokinetic study for the estimation of bioequivalence of two different inhalation treatments containing budesonide 400µg plus formoterol 12µg

K. Athanassiou¹, K. Papataxiarchou¹, N. Grekas^{1*}, S. Rizea Savu², L. Silvestro²

¹ ELPEN Pharmaceutical Co Inc., Pikermi, Greece

² 3S-Pharmacological Consultation and Research, Harpstedt, Germany

The use of dry powder inhalers (DPIs) to administer respiratory medicines is increasing. At the same time, innovating DPIs such as Elpenhaler[®] are launched in the market. The aim of this study was to assess bioequivalence of two budesonide plus formoterol (400+12)µg/dose formulations being delivered via Elpenhaler[®] (ELPEN Pharmaceutical Co Inc) and Turbuhaler[®] (AstraZeneca). The combination treatments were assigned as test (T) and reference (R), respectively. 100 adult controlled and partly controlled asthma patients were enrolled in a two-period, cross over, randomized, single dose study, which was designed to be carried out under fasting conditions. The bioavailability comparison was based on plasma levels of budesonide and formoterol measured after inhalation of the medication along with oral administration of activated charcoal for blocking absorption through the gastrointestinal tract¹. The charcoal was administered 2 min before drug administration and also 2, 60, 120 and 180 min after dosing. Biological samples were collected pre dose and 1, 3, 5, 10, 15, 30, 45 minutes and 1.0, 1.33, 1.67, 2.0, 2.33, 2.67, 3.0, 4.0, 5.0, 6.0, 8.0, 12.0, 16.0, and 24.0 h after drug administration. Bioanalysis was carried out using validated LC-MS-MS techniques. Blood glucose and potassium levels were also measured at pre dose and at 4 and 12 h post dose. Calculations were performed using SAS version 9.1 software. Equivalence in lung deposition is concluded if the 90% confidence interval (CI) for the T/R ratio of primary pharmacokinetic (PK) parameters falls within the regulatory limits (0.80 – 1.25). Data from 97 volunteers who completed the study were analyzed. Several PK parameters were estimated (Table 1), the area under the drug concentration in plasma vs time curve (AUC_{0-t}) and the maximum drug concentration in plasma (C_{max}) being the primary response variables. The T/R ratio for AUC_{0-t} was equal to 88.04 (90% CI: 81.25 - 95.41) for budesonide and 96.07 (90% CI: 92.63 - 99.64) for formoterol. T/R ratios for C_{max} were equal to 88.32 (90% CI: 81.09 - 96.21) and 97.68 (90% CI: 90.66 – 105.24), respectively. AUC_{0-inf} , elimination half-life ($t_{1/2}$) and mean residence time (MRT) were not significantly different between treatments for both active ingredients. 43 adverse events out of which 11 of mild and 32 of moderate intensity occurred in 32 participants. Serious adverse events were not recorded. The comparison which was made by the ANOVA test showed that there were no statistically significant differences in blood glucose and potassium levels between groups. The statistical analysis of PK data obtained in this study proves that the formulations are bioequivalent with regard to both rate and extent of absorption. The treatments were well tolerated.

References

1. O'Connor, D., 2011. Role of pharmacokinetics in establishing bioequivalence for orally inhaled drug products. *J Aerosol Med Pulm Drug Deliv.* 24(3), 119-135.

*Corresponding author. E-mail: n.grekas@elpen.gr

Table 1. Certain PK parameters for each of the active ingredients after a single inhalation of the combination treatments with concomitant oral administration of charcoal (results given as mean \pm SD).

PK parameter	Budesonide		Formoterol	
	Test	Reference	Test	Reference
AUC _(0-t) (pgml ⁻¹ h)	1,501.8 \pm 624.3	1,725.0 \pm 749.7	63.44 \pm 24.86	65.16 \pm 24.49
AUC _(0-∞) (pgml ⁻¹ h)	1,572.6 \pm 657.6	1,803.5 \pm 779.2	76.21 \pm 28.50	77.08 \pm 27.41
C _{max} (pgml ⁻¹)	695.8 \pm 278.5	815.8 \pm 398.3	10.18 \pm 4.85	9.97 \pm 4.64
t _{1/2} (h)	4.93 \pm 2.0	5.25 \pm 3.0	17.3 \pm 7.5	16.2 \pm 5.8
MRT (h)	4.91 \pm 1.8	5.00 \pm 2.0	24.5 \pm 10.2	23.0 \pm 8.1

PP151

A CONTRIBUTION TO BIOPHARMACEUTICAL CHARACTERIZATION OF DRUG SUBSTANCES: CEFACLOR CASE

I. Homsek¹, M. Dacević¹, S. Eric²

¹ Galenika ad, Belgrade, Serbia

² University of Belgrade-Faculty of Pharmacy, Belgrade, Serbia

The assessment of the drug physico-chemical parameters during the preformulation phase is important for the development of a safe, efficient and stable dosage form. For that purpose, in this work physico-chemical parameters were calculated and used for the prediction of distribution of the ionized and nonionized cefaclor forms in the pH gradient of 1 to 12, as well as construction of pH-dependent solubility and lipophilicity. Cefaclor intrinsic dissolution rates (IDRs) and its release *kinetics* from capsules were used to investigate the effect of medium pH values applied on the model substance behaviour and prediction of its *in vivo* performance.

For the prediction of pK_a, log P and log S_o, ADMET Predictor 6.00 software was used (1). On the basis of the calculated physicochemical parameters, the distribution of the ionized and nonionized drug species in the pH gradient of 1 to 8, pH-dependent solubility and lipophilicity curves of cefaclor have been constructed. The drug IDRs were tested in the following media: water, buffer solution pH 1.2, 4.5 or 6.8 by using the Wood apparatus. The same dissolution media (except water) were further applied in order to evaluate the dissolution rate of cefaclor from capsules. The similarity factor (f₂) was used to analyse the obtained data (2).

Cefaclor possesses three ionization centres, therefore three pK_a values were predicted (2.64, 6.54, 10.95). On the basis of predicted parameters, pH-dependent lipophilicity and solubility were constructed. The drug IDR in buffer pH 1.2 was more than 2 and 3 times faster compared to the results obtained in buffer pH 6.8 i.e. water and buffer pH 4.5, respectively. The cefaclor dissolution profiles for capsules in pH 1.2 were markedly different, but similar when pH 4.5 and pH 6.8 were applied (f₂>50). The drug release from the tested product in pH 4.5 and pH 6.8 was slow and incomplete, leading to less than 75% and 65% of cefaclor dissolved after 60 minutes, respectively. However, decrease in the pH value of the medium used resulted in the considerably higher drug release rate with more than 90% of cefaclor dissolved after 60 minutes of investigation in pH 1.2.

The results obtained from predicting the physico-chemical properties and from experimental evaluation of the model substance IDR and cefaclor dissolution rate from capsules, indicate the importance of physico-chemical characterization of the active substance during the preformulation study for predicting the drug behaviour in the body.

References

1. ADMET Predictor, version 6.0, SimulationsPlus Inc., Lancaster, CA, US.
2. Moore JW, Flanner HH. Mathematical comparison of curves with an emphasis on in vitro dissolution profiles. Pharm Tech 1996; 20: 64-74.

PP152

VIRTUAL TRIAL SIMULATIONS OF LEVOTHYROXINE ABSORPTION

I. Kocic^{1,*}, I. Homsek¹, S. Grbic², J. Parojcic², M. Prostran³, B. Miljkovic²

¹ Galenika ad, Belgrade, Serbia

² University of Belgrade - Faculty of Pharmacy, Belgrade, Serbia

³ University of Belgrade - Faculty of Medicine, Belgrade, Serbia

* corresponding author: ivana_kocic@yahoo.com

The aim of this study was to use the gastrointestinal simulation technology in order to develop a drug-specific absorption model for levothyroxine. Gastrointestinal simulation based on the advanced compartmental absorption and transit model (GastroPlus™ software) was used [1]. The required input parameters were experimentally determined, *in silico* predicted and/or taken from the literature. The validation of the absorption model was performed using the single simulation mode [2]. The derived drug-specific model was used to conduct virtual trial studies on 100 subjects in order to assess the combined effects of variations in gastrointestinal physiology and drug pharmacokinetics within population, as well as formulation variables on drug absorption profile. Dose, molecular weight, log P, pK_a value, particle density and diffusion coefficient were fixed, while other parameters, like human effective permeability, subject weight and clearance were defined as variables with log-normal distribution (Table 1). In order to evaluate the influence of *in vitro* drug dissolution kinetics on *in vivo* performance, different virtual *in vitro* inputs were used for simulations. Mean levothyroxine pharmacokinetic parameters predicted in virtual trial simulations were in accordance with the data observed *in vivo* (Figure 1). The predicted values were also similar to the parameters obtained in the single simulation mode conducted to validate the drug absorption model. Variations in drug dissolution kinetics were well reflected on the simulated profiles. However, it was evident that the differences observed *in vitro* were less pronounced in the predicted pharmacokinetic profiles because some of the simulated profiles overlapped. There were no significant differences observed between the absorption profiles that correspond to 85% of drug dissolved in 15 min and in 60 min. Therefore, the obtained results indicate that the predicted levothyroxine plasma concentration-time profiles are rather insensitive to the differences in drug input kinetics. The presented data indicate the potential of gastrointestinal simulation technology to predict levothyroxine absorption. The results also indicate that levothyroxine *in vitro* dissolution is not expected to be the limiting factor for its oral absorption.

Table 1. Virtual trial variable summary and distribution table

Parameter	lower limit	mean value	upper limit
permeability (cm/s x 10 ⁻⁴)	0.73	1.34	2.44
body weight (kg)	41	70	120
volume of distribution (L)	0.08	0.22	0.63
clearance (L/h)	0.8	3.6	16.1

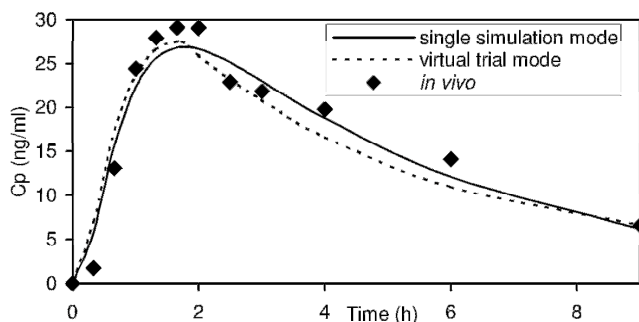


Figure 1. Simulated concentration-time profiles, along with the *in vivo* data

References

1. Agoram et al. *Adv Drug Deliv Rev.* 2001; 50 Suppl 1: S41-67.
2. Kocic et al. *Biopharm Drug Dispos.* 2012; 33(3): 146-159.

PP153

STABILITY OF PIROXICAM AND SOLUPLUS® SOLID DISPERSION AND ITS IMPLICATION TO THE DISSOLUTION OF ACTIVE PHARMACEUTICAL INGREDIENT

Andres Lust^{1,2}, Peep Veski¹, Jyrki Heinämäki¹, Jaakko Aaltonen², Clare Stachan², Jouko Yliruusi², Karin Kogermann¹

¹. University of Tartu, Tartu, Estonia

². University of Helsinki, Helsinki, Finland

andres.lust@ut.ee

The solid dispersion approach is a promising formulation strategy to improve the oral bioavailability of poorly water-soluble drugs. Nevertheless the physical instability of amorphous solid dispersions has to be taken into account during formulation of these materials. The purpose of this study was to investigate the stability of amorphous solid dispersion (SD) of piroxicam (PRX) and Soluplus® in different storage conditions by using Fourier transform infrared spectroscopy with ATR (FTIR-ATR) and Raman spectroscopy. In addition, dissolution tests were carried out in order to determine the importance of solid state change during storage to the release of PRX from SD.

PRX was obtained from Letco Medical, Inc. (USA). Soluplus® was kindly gifted by BASF SE (Germany). SD was prepared at a 1:4 weight ratio (PRX:Soluplus®) using a solvent method. All samples were passed through a 160- μ m sieve. Four different conditions were used for stability study: 0% RH/6°C, 0% RH/25°C, 40% RH/25°C and 75% RH/25°C. Sampling was performed for 6 months. Powder dissolution tests were performed using a paddle method. 900 ml of artificial gastric fluid (pH 1.2) was used as the dissolution medium at a temperature of 37 \pm 0.5°C.

At 0% RH / 6°C and at 0% RH / 25°C, the PRX in SD remained in an amorphous form as no crystallization was observed in samples by FTIR-ATR or Raman spectroscopy at any sampling point. At 40% RH, the FTIR-ATR detected recrystallization as PRX form I after four days of aging whereas the Raman spectroscopy detected this recrystallization after six months of storage. At 75% RH, PRX form I was detected after only one day of aging with FTIR-ATR. Raman spectroscopy enabled to detect PRX form I after one week and PRX monohydrate after one month. The dissolution tests revealed that the dissolution rate of PRX depends on the extent of recrystallization.

Dissolution rate decreased in samples where recrystallization had occurred (Fig. 1).

This work is part of the targeted financing project no SF0180042s09 and ETF grant project no ETF7980. This research was also supported by the Academy of Finland and European Social Fund's Doctoral Studies and Internationalization Program DoRa.

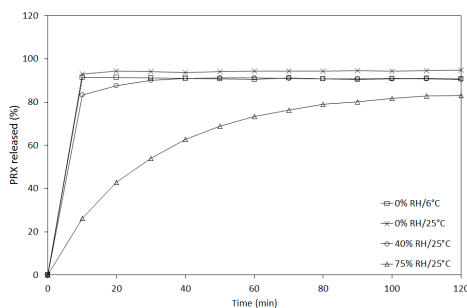


Fig. 1. Dissolution profiles of SD powder samples stored at different conditions for six months. Key: SD stored at 0% RH/6°C for 6 months (0% RH/6°C), SD stored at 0% RH/25°C for 6 months (0% RH/25°C), SD stored at 40% RH/25°C for 6 months (40% RH/25°C) and SD stored at 75% RH/25°C for 6 months (75% RH/25°C).

PP154

MARKET SURVEILLANCE OF FOUR BRANDS OF GLIMEPIRIDE TABLETS 3 mg COLLECTED FROM BOSNIA AND HERZEGOVINA MARKETS

S. Pilipović¹, A. Uzunović^{1*}, A. Elezović¹

¹ Agency for Medicinal Products and Medical Devices, Titova 9, 71000, Sarajevo, Bosnia and Herzegovina,

Corresponding author e-mail address: alijauzunovic@gmail.com

INTRODUCTION: The aim of the present study is to investigate the physicochemical equivalence of four brands of Glimepiride tablets (antihyperglycemic) sourced from retail pharmacies in Bosnia and Herzegovina capital Sarajevo and also to obtaining baseline data towards the establishment of bioequivalence of the tablets dosage forms from market.

MATERIALS AND METHODS: The quality and physicochemical equivalence of four different Glimepiride tablets 3 mg were assessed with pharmacopeia methods (European Pharmacopoeia EP and United States Pharmacopoeia USP) (1, 2). The assessment included the evaluation of uniformity of weight (EP, 2.9.5), friability (EP 2.9.7.), crushing strength (EP 2.9.8.) and dissolution tests (according to USP Glimepiride tablets). Twenty tablets were selected randomly, weighed individually and their average weight was calculated to determine the weight uniformity. Same we do for friability (perform on Pharma Test PTF-DR) and crushing strength (perform on Pharma Test PTB 311E). As L1 column we used Chromasil Performance C-18e 100x 4.6 mm, all other parameters of dissolution was according to USP monograph. Chromatographic test was done on Shimadzu Prominence UFLC, dissolution tests were done on Erweka dissolution tester DT 800. Working standard we purchased from EDQM (European directorate for quality of medicines) and all used chemicals was HPLC grade. All used equipment were validated and calibrated. Data for weight uniformity test, friability, crushing strength, and dissolution profile and drug contents of the tablets of each brands were analyzed by determining the mean \pm standard deviation.

RESULTS AND DISCUSSION: All the four brands of the tablets satisfied the European Pharmacopoeia (EP) requirement for uniformity of weight, friability and the hardness test. Results are presented in Table 1.

Table 1: Obtained results of quality checking samples collected in Sarajevo market

Brand	Dissolution 15 minutes (%)	Dissolution 30 minutes (%)	Hardness (Newton)	Average weight (mg)	Friability
Sample 1	88,70 \pm 1.14	101.35 \pm 1.75	151.91 \pm 5,32	169,73 \pm 0.77	0.04 \pm 0.00
Sample 2	96.29 \pm 1.98	105.77 \pm 1.31	193.56 \pm 6,12	179,63 \pm 2.02	0.09 \pm 0.01
Sample 3	87.52 \pm 2.73	99.59 \pm 4.47	207.76 \pm 7,16	178,94 \pm 1.92	0.01 \pm 0.01
Sample 4	88.53 \pm 2.33	96.88 \pm 0.93	182.43 \pm 4,35	178,80 \pm 1.10	0.11 \pm 0.01

There weren't significant differences in the dissolution profiles of the tablets. All the brands released >85% of Glimepiride within 15 min (USP Glimepiride tablet dissolution test 1). Friability percentage found was lower than 1 % w/w, for all tablets tested and these values are acceptable values according to pharmacopoeia requirements. The hardness of the eighteen brands of Glimepiride tablets show that the hardness value in the range between 153 N to 207 N. All tested samples showed acceptable uniformity of weight as none had percent deviation in weight greater than 7.5%.

CONCLUSIONS: Four brands of Glimepiride tablets that were analyzed passed all the EP or USP quality specifications and were physically and chemically equivalent. This study

highlights the need for constant market monitoring of new products, as well as existing products on market, to ascertain their equivalency to the innovator product.

REFERENCES:

1. Council of Europe. (2010). European pharmacopoeia 7th edition. Strasbourg: Council of Europe.
2. United States Pharmacopeia and National Formulary Revision Bulletin Official December 1, Rockville, MD: United States Pharmacopeia Convention; 2010 (Web site http://www.usp.org/sites/default/files/usp_pdf/EN/USPNF/glimepirideTabletsM35024.pdf)

PP156

IN-VITRO STUDY OF THE INFLUENCE OF CARBAMAZEPINE POLYMORPHIC FORM IN THE DISSOLUTION PROFILE OF GENERIC PRODUCT

L.Cama^{1,2,*}, **R.Klosi**², **A.Hasimi**³, **R.Shkreli**², **L.Deda**¹, **G.Boçari**¹

¹. Medical University of Tirana, Albania ; ² Kristal University, Tirana, Albania; ³ IGEWE, Polytechnic University of Tirana, Albania; * Corresponding author e-mail address: ledicama@yahoo.it

It is known that the polymorphisms of Carbamazepine (CBZ) do influence the dissolution profile of their solid dosage forms [1]. The present study has included several batches of final products currently found in the Albanian market. Measurements were performed on commercial samples of 200 mg Tegretol® tablets (patented product) and 200 mg Profarma Karbamazepine tablets (generic product). The crystalline structure of each of the active pharmaceutical ingredient (API) of the pharmaceutical products has been identified and compared to their respective primary substances used for tablets production.

A TMDSC (MDSC 2920 of TA Instruments) and a IR spectrometer (BJ270-30A) have been used to identify the polymorphic structures. The dissolution profiles were determined using a Dissolution Tester (Varian VK 7000) and UV-VIS Spectrometer (Specord 40 of Analytik Jena Instruments). For each sample, the polymorphic structure has been compared with the respective primary substances from the same pharmaceutical brand.

In addition, the dissolution profiles of commercial samples have been studied and compared to that of patented products, using the similarity factor (f_2) and the variability factor (f_1).

Our study showed that the API of patented product did preserve the morphic structure with its primary substances, thus meeting the release standards of the API, complying with the requirements of British and the United States Pharmacopoeias.

Release time (min)	Released API from patented product (%)	Released API from generic product (%)
0'	0 %	0 %
5'	38.6%	8.1%
15'	62.1%	56.8%
25'	70.4%	70.8%
35'	77.1%	77.6%
45'	83.3%	75.5%
60'	82.6%	77.1%

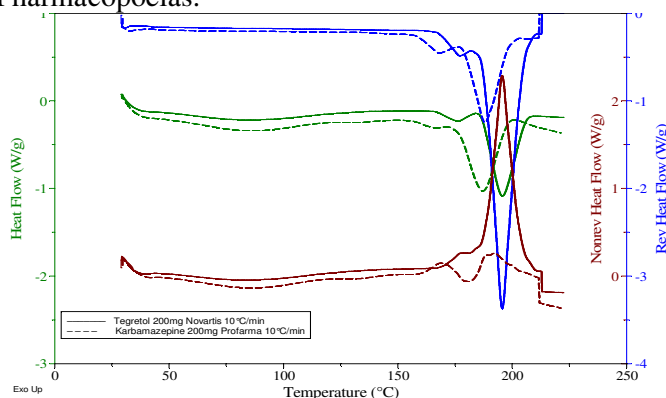


Fig.1 MT- DSC graph comparing generic and patented products

Tab.1 Release rates (%) of CBZ from generic and patented CBZ products

A change in the morpnic form of the active principle compared to its primary substance has been noticed in the generic product. Based on the results obtained from investigating the similarities and/or equivalencies of dissolution profiles, a clear discrepancy has been noticed, regarding the similarity factor of the generic product when compared to that of patented product because f_2 appears to be lower than 50 %. The change in morpnic form of the generic product could be due to the manufacturing process, most likely compression [2]. This change in morpnic form regarding the API of formulation has also impacted the solubility and the release kinetics. As a result the dissolution profile of the generic product is not equivalent to the respective one of the Tegretol® tablets.

Reference:

1. Solid-state study of polymorphic drugs: carbamazepine, [Volume 23, Issue 1](#), 41–54, Rustichelli et al., 2000.
2. Performance comparison of a co-crystal of carbamazepine with marketed product. [European Journal of Pharmaceutics and Biopharmaceutics](#), [Volume 67, Issue 1](#), 112–119, [Magali B. Hickey](#) et al., 2007.

PP162

Novel SPD304-like inhibitors targeting trimerization of human RANKL

Vagelis Rinotas^{1,2}, Fotini Violitzi^{1,2}, Polyxeni Alexiou¹, Fotini Liepouri⁴, Anna Maranti⁴, Katerina Tsiliouka⁴, Alexandros Strongilos⁴, Thanos Papakyriakou¹, Christos Papaneophytou³, George Kontopidis³, Elias Couladourous¹, Elias Eliopoulos¹, and Eleni Douni^{1,2,*}

¹Agricultural University of Athens, Greece; ²Biomedical Sciences Research Center "Alexander Fleming", Vari, Greece; ³Centre for Research and Technology-Thessaly, Karditsa, Greece; ⁴pro-ACTINA SA, Koropi, Greece

Receptor activator of nuclear factor- κ B ligand (RANKL), a trimeric tumor necrosis factor (TNF) superfamily member, is the central mediator of osteoclast formation and bone resorption. Functional mutations in RANKL lead to human autosomal recessive osteopetrosis (ARO), whereas RANKL overexpression has been implicated in the pathogenesis of bone degenerative diseases such as osteoporosis and its specific inhibition has been recently approved as a treatment for women with postmenopausal osteoporosis. Following a forward genetics approach using chemical random mutagenesis, we have recently shown that a novel loss-of-function allele of *Rankl* with a glycine-to-arginine mutation at codon 278 (G278R) at the extracellular inner hydrophobic F beta-strand of RANKL, causes severe recessive osteopetrosis in mice. RANKL^{G278R} monomers fail to assemble into homotrimers, are unable to bind and activate the RANK receptor but interact with wild-type RANKL exerting a dominant-negative effect on its trimerization and function in vitro [1]. Furthermore, as G278 is highly conserved within the TNF superfamily, we identified that similar substitutions in TNF and B-cell activating factor (BAFF) also impaired trimerization and binding to cognate receptors, resulting in loss of biological activity. Notably, SPD304, a small molecule inhibitor of TNF trimerization, also binds and inhibits RANKL, suggesting similar inhibitory mechanisms.

Small molecule inhibitors have emerged as an attractive alternative to biologics, profiting from easy and cost-effective drug development, as well as oral bioavailability. However, the high toxicity displayed by SPD304 in cell cultures prohibits its application in preclinical studies. Based on the trimeric structure of RANKL and its interaction with SPD304, novel small molecules were designed to abrogate trimer formation and biological function displaying higher specificity and less toxicity compared to SPD304. Of the 72 SPD304-like derivatives synthesized and tested, 13 displayed complete inhibition of human RANKL function in osteoclastogenesis assays with less cytotoxicity compared to SPD304 using MTT assays. Furthermore, the effect of selected SPD304-like derivatives on osteoclast activity as showed by tartrate-resistant acid phosphatase (TRAP) activity quantitation, was significantly reduced in a dose depended manner. Data about the effect of such compounds on human RANKL trimerization and on its binding in RANK receptor will also be presented. Conclusively, our studies identified potent small molecule inhibitors of human RANKL designed to target and block its trimerization. The more effective inhibitors will be further evaluated in vivo using our unique human RANKL-expressing transgenic mouse models of osteoporosis.

References

1. Douni E, Rinotas V, Makrinou E, Zwerina J, Penninger JM, Eliopoulos E, Schett G, Kollias G. A RANKL G278R mutation causing osteopetrosis identifies a functional amino acid essential for trimer assembly in RANKL and TNF. *Hum Mol Genet.* 2012;21(4):784-98.

*corresponding author: douni@aau.gr

PP163

ASSESSMENT OF PERMEATION OF PYRAZINAMIDE TABLETS BY *IN VITRO* PASSIVE ABSORPTION MODEL

A. Uzunovic ^{1*}, S. Pilipovic ¹, A. Sapcanin ², A. Elezovic ¹

¹ Agency for Medicinal Products and Medical Devices, Titova 9, 71000, Sarajevo, Bosnia and Herzegovina, Corresponding author e-mail address: alijauzunovic@gmail.com

² Faculty of Pharmacy, University of Sarajevo, Zmaja od Bosne 8, 71000 Sarajevo, Bosnia and Herzegovina

Pyrazinamide (PZA), an analog of nicotinamide, is a drug that has to be converted to the active form pyrazinoic acid (POA) in order to show bactericidal activity against *Mycobacterium tuberculosis*. Inside *M. tuberculosis*, acidic pH enhanced the intracellular accumulation of POA. In contrast, at neutral or alkaline pH, POA was mainly found outside *M. tuberculosis* cells (1). The aim of the present study is to investigate the influence of pH of the medium on lipophilicity (log D) and degree of ionisation of PZA. Investigation of permeability extent through the *in house* prepared *in vitro* passive absorption model, and the influence of pH on it, will be performed.

Log D and pKa of PZA were calculated using ACD/LogD v.9.0 software. PZA, phosphatidylcholine and cholesterol were provided by Sigma-Aldrich (Buchs, Switzerland). Assessment of permeation of PZA was performed using appropriate *in house* prepared *in vitro* passive absorption model. In this model, four HPLC vials (acceptor compartment) were adjusted on paddle of dissolution tester and positioned vertically with our artificial membrane downside oriented into dissolution vessel (donor compartment). Polytetrafluoroethylene filters, pore size 0.45µm (Sartorius, Goettingen, Germany), were impregnated with mixture of phosphatidylcholine and cholesterol. *In vitro* tests on PZA (500 mg) tablets were performed on dissolution tester ERWEKA DT800; USP apparatus 2, rotating speed 50 rpm at 37 °C; volume of dissolution medium 900 ml. Three different media were used in both compartments: simulated gastric fluid pH 1.2, phosphate buffer pH 4.5 and simulated intestinal fluid pH 7.4. Four HPLC vials were adjusted on each paddle of dissolution tester. Three of the four vials were impregnated with phospholipids; the fourth was blank and was used as a control to confirm that there is no significant permeation through non-impregnated membrane. Samples were withdrawn from the vials at the following intervals: 60, 120 and 240 minutes. Quantification of PZA was performed by UV/VIS spectrophotometric method at the absorption maximum at 267 nm.

RESULTS AND DISCUSSION: *In vitro* permeation of PZA was calculated as apparent permeability coefficient (2) measured in cm min^{-1} (P) and results were provided in Figure 1.

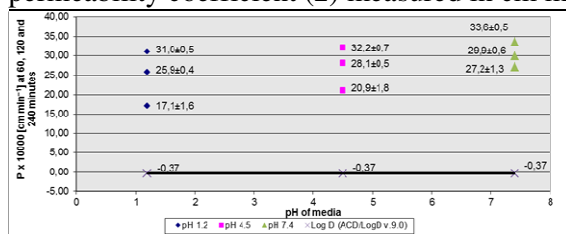


Figure 1: Permeation profile of PZA at different pH values of media and test duration

Apparent permeability coefficient achieved the highest value after the first hour of testing. This was caused by concentration gradient between donor and acceptor compartments which value was decreased during further testing. PZA is an extremely weak base ($\text{pKa} = 0.9 \pm 0.3$) and partially ionized in artificial gastric fluid at pH 1.2.

On the basis of our results, it can be concluded that degree of ionization of PZA is dependent on pH, which varies with location along gastrointestinal tract could influence *in vitro* permeation of PZA from pyrazinamide tablets.

REFERENCES:

1. Zhang Y, Wade MM, et al. Mode of action of pyrazinamide: disruption of *Mycobacterium tuberculosis* membrane transport and energetics by pyrazinoic acid. J. Antimicrob. Chemother. 2003; 52(5):790-795.
2. Corti G, Maestrelli F, et al. Development and evaluation of an *in vitro* method for prediction of human drug absorption II. Demonstration of the method suitability. Eur. J. Pharm. Sci. 2006; 27(4):354-362.

PP164

IMPLEMENTATION OF BCS BASED BIOWAIVER IN TURKEY

Serdar Tort¹, Halil Tunc Koksal², Zeynep Safak Teksin^{1*}

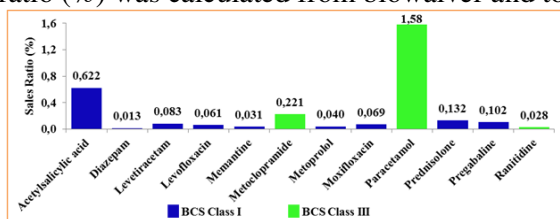
¹. Gazi University Faculty of Pharmacy, Department of Pharmaceutical Technology, Ankara, Turkey

². Pharmaceutical Manufacturers Association of Turkey, Ankara, Turkey

* Coresponding author: zsteksin@gazi.edu.tr

The biowaiver was originally proposed by Amidon and co-workers in 1995 and subsequently adopted by the FDA, WHO and EMA for implementation in the approval of some generic drug products. Until now, BCS classification and recommendation for the biowaiver according to biowaiver monographs for more than 30 drug substances have been available at FIP website at www.fip.org/bcs. Our aim is evaluation of BCS based biowaiver in Turkey. The FDA, EMA and WHO regulations and the FIP biowaiver monographs (2004-2012) have been implemented for BCS based biowaiver drug in Turkey. The pharmaceutical market sales and quantities of these drugs in Turkey were also examined from the data of IMS Health Turkey.

The BCS based biowaiver decisions in Turkey combine certain aspect taken from all three, the FDA (e.g. BCS Class I only) guideline, the EMA (e.g. BCS Class I and BCS Class III), and WHO guideline (e.g. providing list of drug substances eligible for the BCS based waiver). 21 of FIP-listed drugs are also available in Turkey. However, 4 of FIP-listed drugs proposed for BCS based biowaiver (cimetidine, stavudine, prednisone, and primaquine) are not available in Turkey. The BCS based biowaiver is accepted for BCS Class I and BCS Class III drug substances in Turkey. Fig.1 is shown BCS Class I and BCS Class III drug substances and sales ratios (%) between June 2012 and July 2013 in Turkish pharmaceutical market. The sales ratio (%) was calculated from biowaiver and total drug sales (boxes) for



each IR oral drug.

Fig 1. Biowaiver drugs and sales ratios (%) in Turkish pharmaceutical market.

Turkey implements on the BCS guidance to decide when a biowaiver based approval is appropriate for a generic drug product than having them subjected to in vivo bioequivalence studies. The BCS based biowaiver decisions in Turkey combine certain aspect taken from the FDA, EMA, and WHO guidelines as well as the FIP biowaiver monographs. Memantine has been accepted as a biowaiver drug substance in Turkey, so biowaiver decision could be depended on the country/region. The regulations on BCS based biowaivers also differ between the FDA, EU and WHO. Therefore, it is necessary to global harmonization for biowaiver regulations.

Reference: Zheng, N., Lionberger R.A., Mehta M.U., Yu. L.X., 2012. The Biowaiver Monographs: BCS based biowaivers. A regulatory overview. *Biowaiver Monographs* 2004 -2012, 52-67.

PP166

INVESTIGATION OF THE CELLULAR UPTAKE OF FLUORESCENT BETA-CYCLODEXTRINS

Ferenc Fenyvesi ^a, Katalin Réti-Nagy ^a, Zsolt Bacsó ^b, Milo Malanga ^c, Éva Fenyvesi ^c, Lajos Szente ^c, Judit Váradi ^a, Ildikó Bácskay ^a, Zoltán Ujhelyi ^a, Pálma Fehér ^a, Miklós Vecsernyés ^a

^a Department of Pharmaceutical Technology, University of Debrecen PO Box 78, H-4010 Debrecen, Hungary

^b Department of Biophysics and Cell Biology, University of Debrecen PO Box 39, H-4012 Debrecen, Hungary

^c Cyclolab Cyclodextrin R&D Laboratory Ltd., PO Box 435, H-1525 Budapest, Hungary

Cyclodextrins are widely used excipients for increasing water solubility, delivery and bioavailability of lipophilic drugs by forming host-guest complexes. They are considered hydrophilic, non-cell membrane permeating agents, which delivers the active drug molecules to the cell membrane and increase their penetration. Nevertheless their cellular uptake cannot be excluded. The aim of this project was to investigate the cellular uptake and internalization of fluorescent beta-cyclodextrin derivatives on Caco-2 colon cells.

FITC and Rhodamin labeled randomly-methylated β -cyclodextrin (RAMEB) was the product of Cyclolab Ltd., while all other reagents were purchased from Sigma. Caco-2 cells were seeded onto glass cover slips, treated with fluorescent cyclodextrin solutions in different concentrations for 30 minutes at 37 °C and washed several times. Cells were fixed with 3% formaldehyde solution, cell nuclei were stained with DAPI and the cellular fluorescence was analyzed in Zeiss Axio Scope.A1 fluorescent microscope. The mechanism of internalization was also examined by flow cytometry.

Fluorescent microscopic images clearly showed that both FITC-RAMEB and Rhodamin-RAMEB located in the cytoplasm of Caco-2 cells after the treatment. The fluorescent derivatives showed similar intracellular distribution and they were localized in small, bright granules in the cytoplasm. Flow cytometry measurements confirmed these results, cellular fluorescence increased in the function of fluorescent cyclodextrin concentration.

Our results clearly shows that cyclodextrins are able to enter the intestinal cells and thus the cellular uptake of cyclodextrins highlights new aspects of cyclodextrin drug delivery in the intestine.

„This research was realized in the frames of TÁMOP 4.2.4. A/1-11-1-2012-0001 „National Excellence Program – Elaborating and operating an inland student and researcher personal support system” The project was subsidized by the European Union and co-financed by the European Social Fund.”

Corresponding author: Ferenc Fenyvesi, fenyvesi.ferenc@pharm.unideb.hu

PP167

EFFECT OF CHITOSAN CONTENT ON THE QUALITY OF PELLETS PREPARED BY EXTRUSION/SPHERONIZATION AND ON THE RELEASE RATE OF PIROXICAM

Paraskevi Gkogkou, Ioannis Nikolakakis

Department of Pharmaceutical Technology, School of Pharmacy, Faculty of Health Sciences, Aristotle University of Thessaloniki, 54124, Thessaloniki, Greece

Drug release of pharmaceutical dosage forms is very important in the development of new formulations. A disadvantage of microcrystalline cellulose (MCC) pellets is the slow and incomplete release of poorly soluble drugs. As a solution to this problem, part of the MCC is replaced with hydrophilic polymers that facilitate penetration of the dissolution medium [1]. The aim of this study was to optimize formulations of the poorly soluble drug piroxicam (PXM), with the hydrophilic natural polymer chitosan (CH) and MCC, by application of mixture design, followed by numerical and graphical optimization for pellet quality and dissolution characteristics.

A medium viscosity, high de-acetylation CH grade (121-171cp, 90-95% deacetylation) was used and 10 batches (9 plus repetition) of PXM/CH/MCC pellets were prepared by extrusion/spheronization using PVP solution in water (7.5% w/w). The compositions of the batches were selected so as to follow a D-optimal experimental design (Table 1). Constraints were set for the proportions of ingredients as: 10%-80% for CH and MCC and 5%-70% for PXM. Size distribution of the pellets and shape (expressed as shape factor e_R with theoretical value one for perfect spheres) were determined using analytical test sieves and image analysis system. The release of the drug from the pellets was tested on a standard USP-basket apparatus with two dissolution medium of pH 1.2 and 5.6 and the dissolution parameters dissolution efficiency (DE%) and mean dissolution time (MDT), which describe the entire dissolution process, were calculated and compared for the different batches. The desirability function (with values from 0 to 1) was applied to the derived prediction models for optimization of the formulations [2].

It was found that the pellet size is affected mainly by the CH content while the shape by the combination of the CH and drug content, indicating interaction. The values of the shape factor (e_R) varied from 0.16 to 0.60 with greater values obtained for formulations E, F, I and J which had low to medium drug content (Table 1). A better dissolution profile, with higher DE% and lower MDT, was obtained from pellets of composition D with higher drug and low CH, MCC and composition I with medium drug, CH and low MCC content. The above observations are graphically demonstrated in the contour plot in Fig. 1 where the change in the value of desirability function with composition is shown. It can be seen that compositions giving higher desirability values, or maximum sphericity and DE% for dissolution in deionized water, can be obtained with low MCC, medium to high drug and medium CH content. For the dissolution in medium with pH 1.2, where the solubility of PXM in presence of CH is much higher, DE% were generally higher and MDT lower (data not shown).

TABLE 1. Pellet composition (%)

Batch	CH	MCC	PXM	e _R	DE%	MDT(h)
A	19.4	54.4	21.2	0.39	19.7	4.82
B	80	10	5	0.35	17.8	4.94
C	10	47.5	37.5	0.23	9.4	5.44
D	15	10	70	0.16	43.2	3.41
E	33.3	35	26.7	0.60	19.7	4.82
F	45	45	5	0.51	13.5	5.19
G	10	80	5	0.46	10.8	5.35
H	54.4	19.4	21.2	0.49	25.3	4.48
I	47.5	10	37.5	0.52	31.5	4.11
J	10	80	5	0.51	28.1	4.31

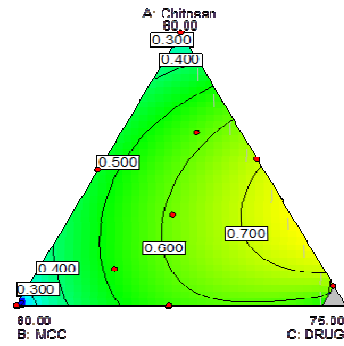


Fig. 1. Contour plots of desirability function for different PXM/CH/MCC compositions

References

- [1] Paavera U. et al. (2012) Int. J. Pharm. 431, 111- 119
- [2] Paterakis et al. (2002) Int. J. Phar. Sci. 28, 51-60

PP168

SYNTHESIS OF ARTEMISININ DIMERS AND THEIR BIOLOGICAL EVALUATION AGAINST MCF7 BREAST CANCER CELLS

P. Tsoukala¹, G.E. Magoulas¹, A. Antoniou¹, C.M. Athanassopoulos^{1*}, D. Papaioannou¹, E. Papadimitriou², T. Tsigkou² and M. Lamprou²

Departments of Chemistry¹ and Pharmacy², University of Patras, Patras GR-26504, Greece.

email: kath@chemistry.upatras.gr

The natural product Artemisinin (ART, **1**) and its derivatives are currently considered as the drugs of choice for the treatment of malaria. At the same time, a significant number of these drugs have also shown interesting anticancer activity. In the context of the present research work, ART itself was structurally modified and anchored to polyamines (putrescine, spermidine, spermine) to afford new ART dimer conjugates in order to evaluate their potential biological activity against MCF7 breast cancer cells.

Structural consistency and purity of all new compounds were evidenced with the use of conventional chromatographic and spectrometric methods (ESI-MS, ¹H-NMR, ¹³C-NMR, IR, RP-HPLC). The effect of the tested compounds (**5-13**) on the proliferation of MCF7 cells was evaluated using the MTT assay.

To achieve our goal **1** was modified at position 10 in order to bear a suitable linker through a C-O or C-C bond¹ and at position 11² by replacing oxygen by a nitrogen atom. This way, new analogues were synthesized bearing hydroxyl group containing linker, which upon activation with p-nitrophenyl chloroformate gave the intermediates **2-4**. Reaction of the latter with suitably protected polyamines afforded the ART symmetric conjugates **5-13** in good yields. Preliminary biological evaluation of compounds **5-13** against MCF7 cells showed increased anti-proliferative activity in comparison with the parent molecule (ART).

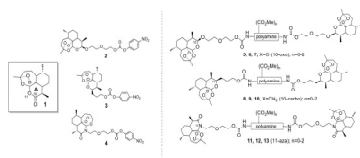


Figure 1. Structures of intermediates and final products encountered in the present work.

A series of 10-oxo (**5-7**), 10-carbo (**8-10**) and 11-aza (**11-13**) ART-Polyamine conjugates were synthesized through chemical modification of ART, followed by coupling with polyamines, in satisfactory overall yields. All ART-polyamine conjugates tested were more effective than ART in reducing the number of MCF7 breast cancer cells.

References

1. Hindley, S., Ward, S. A., Storr, R. C., Searle, N. L., Bray, P. G., Park, B. K., Davies, J., O'Neill, P. M., 2002. Mechanism-Based Design of Parasite-Targeted Artemisinin Derivatives: Synthesis and Antimalarial Activity of New Diamine Containing Analogues. *J. Med.Chem.* 45, 1052–1063.
2. Singh, A. S., Verma, V.P., Hassam, M., Krishna, N.N., Puri, S. K., Singh. C., 2008. Amino- and Hydroxy-Functionalized 11-Azaartemisinins and Their Derivatives. *Org. Lett.* 10, 5461-5464.

PP169

SYNTHESIS AND ANTIMICROBIAL ACTIVITY OF SOME NEW HYDRAZINECARBOTHIOAMIDES AND 1,2,4-TRIAZOLES

Laura Ileana-Socea^a, Manuela Anda Radu-Popescu^b, Stefania-Felicia Barbuceanu^a, Theodora Venera Apostol^a, Florin Mihalcea^a, Bogdan Socea^c

^a Organic Chemistry Department, Faculty of Pharmacy, Carol Davila University of Medicine and Pharmacy, 6 Traian Vuia Street, 020956, Bucharest, Romania

^b General and Pharmaceutical Microbiology Department, Faculty of Pharmacy, Carol Davila University of Medicine and Pharmacy, 6 Traian Vuia Street, 020956, Bucharest, Romania

^c Faculty of General Medicine, Carol Davila University of Medicine and Pharmacy, St. Pantelimon Emergency Hospital, 340-342, Soseaua Pantelimon Street, 021623, Bucharest, Romania
corresponding author: laurasocea@gmail.com

Motivated by numerous pharmacological actions of hydrazinecarbothioamide and 1,2,4-triazoles we report in the present investigation the synthesis, characterization and the antimicrobial activity of the new hydrazinecarbothioamides and their cyclization products, 1,2,4-triazole derivatives, containing 5H-dibenzo[a,d][7]annulene moiety.

New hydrazinecarbothioamides (**2a,b**) bearing 5H-dibenzo[a,d][7]annulene moiety were synthesized using classical procedures^{1,2} (Scheme 1). Cyclization of new hydrazinecarbothioamides in NaOH solution afforded the corresponding 1,2,4-triazoles-3(4H)-thiol (**3a,b**). Treatment of 1,2,4-triazoles-3(4H)-thiol with methyl iodine gives the corresponding S-methyl-1,2,4-triazole derivatives (**4a,b**). All the new compounds were extensively characterized by IR-, UV-, ¹H-NMR and ¹³C-NMR spectroscopy. The antimicrobial activity of all products was investigated *in-vitro* against *Escherichia coli* (ATCC 25922), *Pseudomonas aeruginosa* (ATCC 27853), *Bacillus subtilis* (ATCC 6663) and one yeast: *Candida scotti* by disk diffusion method. The MIC values were determined using dilution method.

¹H-NMR analysis of new hydrazinecarbothioamides indicated the existence of two conformational isomers, a major axial (about 75%) and a minor equatorial one (25%) which are interconvertible by middle ring inversion. Cyclization of hydrazinecarbothioamides in NaOH solution afforded the corresponding 1,2,4-triazoles-3(4H)-thiole which were separated as pure axial isomers. Thiole-thione tautomeric equilibrium of (**3a,b**) compounds is evidenced by IR spectra and obtaining S-methyl-1,2,4-triazole derivatives. The preliminary results of antimicrobial activities indicated that the tested compounds exhibited a low activity against *Escherichia coli* (ATCC 25922), *Pseudomonas aeruginosa* (ATCC 27853), *Bacillus subtilis* (ATCC 6663) and *Candida scotti* (table 1).

In conclusion, in this paper we describe the synthesis and spectral characterization of some new hydrazinecarbothioamides and new 1,2,4-triazoles possessing the 5H-dibenzo[a,d][7]annulene moiety. The occurrence of hydrazinecarbothioamides in two conformational isomeric forms was proved and a thiole-thione tautomeric equilibrium dependent on the physical state was observed for 1,2,4-triazoles-3(4H)-thiole. All new compounds were tested for antimicrobial activity. Generally 1,2,4-triazoles had better antimicrobial activity than hydrazinecarboxamides. This findings leads us to say that cyclization of hydrazinecarbothioamides to 1,2,4-triazoles-3(4H)-thiole and S-methylation of 1,2,4-triazoles-3(4H)-thiole is beneficial for antimicrobial activity.

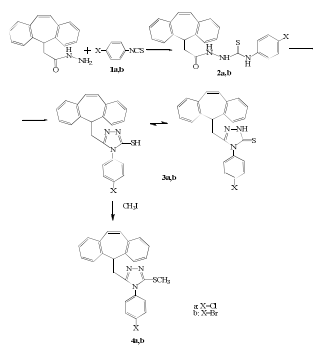
Reference

1. Socea L.I., Apostol T.V., Şaramet G., Bărbuceanu Ş.F., Drăghici C., Dinu M., 2012, Synthesis and root growth activity of some new acetylhydrazinecarbothioamides and 1,2,4-triazoles substituted with the 5H-dibenzo[a,d][7]annulene moiety, J. Serb. Chem. Soc., 77(11), 1541-154 ;
2. Şaramet I., Banciu A., Socea L., Drăghici C., Banciu M.D., 2003, Synthesis of new substituted 3-mercapto-1,2,4-triazoles possessing 5-H-dibenzo[a,d]cycloheptene moieties, Heterocyclic Communications, 9(6), 653-658.

Table 1. Antimicrobial activity of tested compounds MIC ($\mu\text{g/mL}$)

Compound	<i>E. coli</i>	<i>P. aeruginosa</i>	<i>B. subtilis</i>	<i>C. scotti</i>
2a	> 4096	2048	> 4096	> 4096
2b	> 4096	2048	> 4096	> 4096
3a	512	1024	128	> 4096
3b	512	1024	128	> 4096
4a	512	2048	128	128
4b	256	2048	128	128

Scheme 1. Synthesis of new compounds 2-4.



PP170

Human female sexual steroids into compounded semisolid formulations: evaluation of percutaneous absorption performance

Hudson C. Polonini^a, Marcos Antônio F. Brandão^a, Anderson O. Ferreira^b, Cristiano Ramos^a, Maria das Graças A. M. Chaves^a, Nádia R. B. Raposo^a

^a Universidade Federal de Juiz de Fora, Núcleo de Pesquisa e Inovação em Ciências da Saúde (NUPICS), Campus Universitário, 36036-900, Juiz de Fora, MG, Brazil.

^b Ortofarma Laboratório de Controle de Qualidade, 36120-000, Matias Barbosa, MG, Brazil.
E-mail address: nadiafox@gmail.com.

This study aimed to evaluate the percutaneous absorption performance of a widespread liposomal transdermal vehicle used by compounding pharmacies worldwide, as there is a lack of studies regarding it. The transdermal vehicle was evaluated regarding the compounding process (different combinations of techniques, and determination of their respective content uniformity) and its permeation performance for progesterone (P), oestradiol (E2) and oestriol (E3) in formulations containing each drug separately (P_{emuls} and E_{emuls}), as well as an association of E2 + E3 (Biest). For that, an *ex vivo* model (abdominal female human skin) was conducted using vertical diffusion cells ($t = 48h$). The experiments were conducted using full-thickness skin, finite doses, non-occlusion, and receptor medium consisted of 0.01 M phosphate buffer + 0.5% (w/v) of hydroxypropyl- β -cyclodextrin, pH 7.4. The drug retention was determined by horizontally cutting the skin (100 μm) using a cryostat microtome. All hormone quantifications were performed by HPLC. The best content uniformity results were found using a roll mill to homogenise the emulsions and reduce their particles size. Regarding percutaneous absorption (Figure 1), P showed the highest cumulative permeation (37.02 $\mu g cm^{-2}$). E2 and E3 in Biest had permeations approximately 4-fold lower (9.44 $\mu g cm^{-2}$ for E2 in Biest and 14.02 $\mu g cm^{-2}$ for E3 in Biest), and the profiles of E2 in E_{emuls} and in Biest were almost the same (9.46 $\mu g cm^{-2}$ for E_{emuls}). All formulations presented pseudo-first-order kinetics. The hormones steady-state flux (J_s , $\mu g cm^{-2} h^{-1}$) were: 4.55 (P), 1.15 (E2 alone), 1.13 (E2 in Biest) and 0.27 (E3 in Biest). A relatively high amount of the hormones was retained within the SC and the other epidermal layers. Despite this retention, the drugs had good permeation, as an expressive amount was encountered in deeper areas of the skin, where the connective tissue was present (i.e., permeated *in vivo*). As the drug delivered is high, one question to be pointed out is the possibility of decreasing the quantity of the product applied, which is directly related to increase in patient compliance. Therefore, the vehicle was able to provide percutaneous absorption rates compatible with and higher than existing clinical treatment needs. However, one must take into account that a high quantity of drug was delivered. Thus, care has to be taken regarding the quantity of emulsion used to avoid patient overdose.

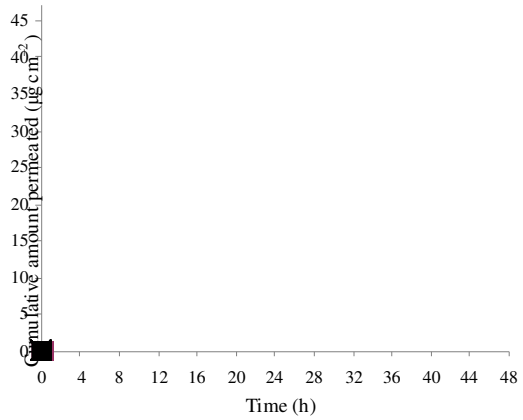


Figure 1. *Ex vivo* permeation profiles of human sexual hormones through excised human skin: (■) progesterone; (◆) oestradiol; (×) oestradiol in Biest; (•) oestriol in Biest. Results presented as the mean \pm S.D.

PP171

Improving bioavailability of resveratrol: *in vitro* studies on drug release and percutaneous absorption from transdermals

Priscila A. de Almeida^a, Michele C. Alves^a, Hudson C. Polonini^a, Anderson O. Ferreira^b, Maria das Graças A. M. Chaves^a, Marcos Antônio F. Brandão^a, Nádia R. B. Raposo^a

^a Universidade Federal de Juiz de Fora, Núcleo de Pesquisa e Inovação em Ciências da Saúde (NUPICS), Campus Universitário, 36036-900, Juiz de Fora, MG, Brazil.

^b Ortofarma Laboratório de Controle de Qualidade, 36120-000, Matias Barbosa, MG, Brazil.

E-mail address: nadiafox@gmail.com.

Resveratrol has physicochemical properties that are adequate for diffusion through the human skin such as low molecular weight and adequate lipophilicity. Thus, the aims of this study were: to develop and validate a method by reversed-phase high-performance liquid chromatography for quantification of *trans*-resveratrol in transdermal emulsion, and to determine its *in vitro* drug release and *ex vivo* human skin permeation. The method was optimized using a complete experimental design with eight experiments (2^3) and triplicate in the central point (ultrasound time for sample dissolution: X_1 , mobile phase flow rate: X_2 , and ACN percentage in mobile phase: X_3) and was validated for the parameters of International Conference of Harmonization guideline: specificity, linearity, limits of detection and quantification, precision, accuracy and robustness. The permeation experiments were conducted using polysulfone (*in vitro* release) or full-thickness abdominal female human skin (percutaneous absorption) and volumetric 7-mL static vertical diffusion cells with automatic sampling ($n = 6$, $t = 24$ h). The receptor medium consisted of artificial human sweat containing 20% of ethanol as solubiliser. Drug retention was carried out using the tape stripping technique. Using an octadecylsilyl column (250 x 4.6 mm, 5 μ m), a mobile phase composed by ACN and water (55:45 v/v), a flow of 1.4 mL min⁻¹, column temperature of 25 °C and detection at 307 nm, the compound was analyzed in 4 min. The best condition to prepare the sample was: 15 min of ultrasound and diluent system composed by mobile phase. This method is in accordance with the validation parameters realized. The model most appropriate for describe the release profile was Higuchi's model. The flux (JS, μ g cm⁻² h⁻¹) and lag time (LT, h) were respectively: 138.5 and 0.49. Regarding the percutaneous absorption (Figure 1), there was no effective permeated amount of *trans*-resveratrol, since no molecule within the receptor media was detected. However, the analysis of viable skin layers (epidermis + dermis) showed higher retention of *trans*-resveratrol when compared to the amount retained in the stratum corneum. This demonstrates a high potential for permeation *in vivo*, once that dermis is vascularized, being the drug able to reach the bloodstream. For this purpose, the percentage likely to permeate obtained was 64.96%. This study indicates that the *in vitro* *trans*-resveratrol release rate from vanishing cream is satisfactory. Furthermore, the *ex vivo* human skin permeation study suggests permeation potential *in vivo* for *trans*-resveratrol. Thus, the transdermal route has an effective therapeutic potential for systemic delivery of *trans*-resveratrol *in vivo*.

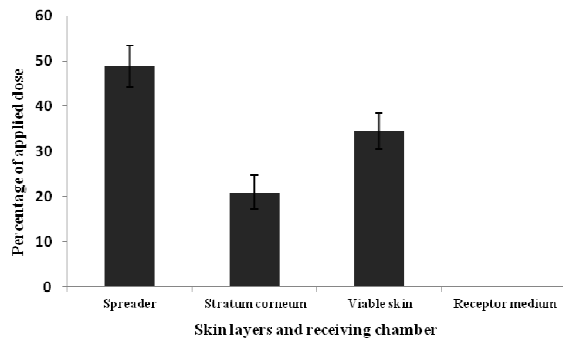


Figure 1. Mass balance of transdermal permeation of *trans*-resveratrol (percentage of applied dose \pm standard deviation).

PP175

EFFECTS OF PEG CONJUGATION ON THE STABILITY AND THE PHARMACODYNAMIC PROFILE OF THE ANTICANCER PEPTIDE TIGAPOTIDE

I. Bampouri^{1*}, T. Katsila¹, E. Papageorgiou², I. Leontari¹, A. Armakolas², M. Koutsilieris², G.Sivolapenko¹

¹University of Patras, Patras, Greece

²National and Kapodistrian University of Athens, Athens, Greece

*Corresponding author: email: mpampouri@gmail.com

PSP94, protein is known to have specific implications with prostate cancer where a down-regulation of PSP94 levels is associated with advanced metastatic prostate cancer⁽¹⁾. Tigapotide(PCK3145) is a synthetic 15-mer peptide that matches the natural sequence of amino acids 31 to 45 of PSP94 and was selected from other peptides derived from PSP94 as it exhibited the best *in vitro* and animal *in vivo* properties similar to PSP94⁽²⁾. However pharmacokinetics studies in animals and in patients with prostate cancer showed **rapid** clearance and a **short half-life**. **In order to** alter the pharmacokinetic profile of the peptide, and thereby to improve its pharmacodynamic potential PCK3145 was chemically modified with polyethylene glycol (PEG). This experimental work presents the results of a systematic study on the influence of the PEGylation of PCK3145 peptides on the proteolytic stability and biological activity of these conjugates compared to the wild-type peptide.

For the quantification and stability assays an HPLC-UV system was used. Proliferation of PC3 cancer cell line was measured using the MTT test. The cells were plated in 96-well plates and grown in media supplemented with 10% FBS and treated for 96h with the appropriate molecule at increasing concentrations (0µg/ml up to 10µg/ml).

A validated HPLC method development for the determination of the PEG-peptide conjugates was assessed for the first time. The proteolytic stability of the PEG-peptide conjugates in human plasma revealed a significant decrease in the degradation (table 1). A 50% inhibition of the cell metabolism/growth was achieved by the concentrations of 10 µg/ml of the three peptides (figure 1). However, at lower concentrations stronger growth inhibitory effect was observed for the PEG-peptides.

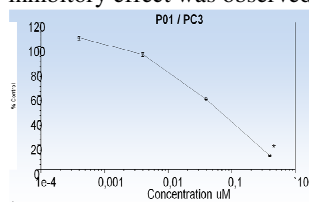


Figure 1

DEGRADATION %	PCK3145	PO1	PO2	PCK3145 +HALT	PO1+HALT	PO2+HALT
15 min	12	10	12	11	3	9
30 min	29	23	22	17	16	21
60 min	41	44	46	32	41	41
120 min	91	59	61	81	54	54

Table 1

The results of this study emphasize the ability of PEGylation to improve the stability of PCK3145 and to enhance the biological activity.

1. Garde SV, Basrur VS, Li L, Finkelman MA, Krishan A, Wellham L, Ben-Josef E, Haddad M, Taylor JD, Porter AT, Tang DG. Prostate secretory protein (PSP94) suppresses the growth of androgen-independent prostate cancer cell line (PC3) and xenografts by inducing apoptosis. *Prostate*. 1999 Feb 1;38(2):118-25.

2. Shukeir N, Arakelian A, Chen G, Garde S, Ruiz M, Panchal C, Rabbani SA. A synthetic 15-mer peptide (PCK3145) derived from prostate secretory protein can reduce tumor growth, experimental skeletal metastases, and malignancy-associated hypercalcemia. *Cancer Res*. 2004 Aug 1;64(15):5370-7.

PP177

Beneficial effects of adjunctive therapy with bioavailability-enhanced curcumin in subjects with metabolic syndrome receiving low-dose atorvastatin: A randomized parallel-group trial

Amirhossein Sahebkar,^{a*} Yunes Panahi,^b Nahid Khalili^c

^a*Biotechnology Research Center, Mashhad University of Medical Sciences, Mashhad, Iran*

^b*Chemical Injuries Research Center, Baqiyatallah University of Medical Sciences, Tehran, Iran*

^c*Department of Internal Medicine, Baqiyatallah University of Medical Sciences, Tehran, Iran*

***Correspondence to:** Amirhossein Sahebkar, PharmD, PhD, Cardiovascular Research Center, Mashhad University of Medical Sciences, Mashhad, Iran. E-mail:

sahebkar@mums.ac.ir; amir_saheb2000@yahoo.com

Patients with metabolic syndrome are at very increased risk of cardiovascular complications. Curcumin is a multifunctional natural product with a multitude of cardiovascular benefits. The present study aimed to investigate the benefits of supplementation with curcumin in patients with metabolic syndrome. This study was designed as a randomized double-blind placebo-controlled parallel-group trial among subjects with metabolic syndrome receiving low-dose atorvastatin (10 mg/day). Inclusion criteria were i) serum LDL-C > 130 mg/dL plus < cardiovascular risk factors, ii) serum LDL-C > 100 mg/dL plus ≥ 2 cardiovascular risk factors, or iii) triglycerides > 200 mg/dL. One-hundred subjects (age: 54 yrs, weight: 78 kg, 41% hypertensive, 39% smoker, 31% diabetic, 34% positive family history of CHD) were randomized to receive either bioavailability-enhanced curcumin (C3 complex[®]; Sami Labs Ltd., Bangalore, India; 1500 mg/day) or placebo for a period of 6 weeks. A full-fasted lipid profile comprising total cholesterol, LDL-C, HDL-C and triglycerides was determined at baseline and at the endpoint of study. The study protocol was approved by the Ethics Committee of the Baqiyatallah University of Medical Sciences, Tehran, Iran. Supplementation with curcumin C3 complex[®] was associated with a meaningful improvement of lipid profile. There were 21.6%, 32.75 and 8.7% reductions in serum total cholesterol, LDL-C and triglycerides concentrations whilst these indices remained statistically unchanged in the placebo group. Also, mean serum HDL-C levels were elevated by 37.5% in the curcumin group whereas there was no meaningful alteration in the placebo group. The present findings suggest an interesting clinically-relevant lipid-modulating effect of bioavailable curcumin in subjects with metabolic syndrome.

Keywords: Curcuminoids; Bioavailability; Cardiometabolic syndrome; Cholesterol; Cardiovascular disease

ⁱ poly(2-methyl-2-oxazoline)-grad-poly(2-phenyl-2-oxazoline)